High speed optical phase modulated signaling with offset filtering in a 50 GHz grid.

Olugbenga, Olubodun

High Speed Optical Phase Modulated Signaling with Offset Filtering in a 50 GHz Grid.

OLUBODUN OLUGBENGA

A thesis submitted to Swansea University in the fulfilment

of the requirement for the degree of

Doctor of Philosophy

Swansea University
Prifysgol Abertawe

College of Engineering

August 2011

ProQuest LLC.
789 East Eisenhower Parkway
P.O. Box 1346
Ann Arbor, MI 48106 – 1346

ABSTRACT

There are present employments of WDM systems with 40 Gb/s channel data rates, however ten years ago intensity modulated 10Gb/s channel rate (IM/DD) deployment was the prominent modulation format in installed capacities. The present commercial 40 Gb/s systems employment phase modulation formats in the available 50GHz grid spacing, through Partial DPSK (PDPSK) and DQPSK modulation formats. 100 Gb/s data rate deployments will readily be available in the nearest future, the choice modulation format to implement 100 Gb/s is Coherent QPSK via polarization multiplexing and digital signal processing.

This thesis presents the investigation of the performances of different phase modulation formats specifically in response to tight optical filtering appropriate to a 50 GHz grid channel separation with different strategies for compensating the inherent fibre impairment. The major contribution of this research is focussed on offset filtering strategy mainly at the receiver end of optical transmissions systems. Thus the impact of offset filtering on 42.7Gb/s DPSK, DQPSK, PSK and coherent QPSK in tightly filtered regime are comprehensively examined, results here show that performance penalty reductions inherent via the correlative coding formats that evolve from offset filtering of different phase modulated formats. These correlative coding formats that arises could be optimally exploited to realise >100 Gb/s data rate within a 50GHz grid channel spacing via polarization multiplexing of DPSK and PSK.

The impact of offset filtering on 42.7 Gb/s DPSK system is examined in a strongly filtered regime and performance improvement of ~1dB in calculated Q value was achieved over the symmetric filtered case for an OSNR of 15dB. Thus with additional optimization strategy based on the evolved spectral shaping at the constructive and destructive port of the MZI due to offset filtering, a 2.2 dB improvement was achieved over the symmetric filtered case. These offset filtering results show significant improvements over the symmetric filtered case, but PDPSK still out-performs this novel offset filtering design by ~0.8dB for the same OSNR. However by further exploiting the beneficial spectral shaping at the outputs of the MZI, PDPSK was also employed in conjunction with the novel offset filtering design to achieve a record 1.5dB improved performance over a conventional PDPSK deployment in a strongly filtered regime for an OSNR of 20dB.

The impact of offset filtering on a strongly filtered coherent homodyne PSK system is also comprehensively investigated and the performance improvement inherent over the conventional filtered case was around 5dB in calculated Q for an OSNR of 16dB.

The impacts of strongly filtered DQPSK/coherent-QPSK systems were also investigated

and the performance improvement of ~2.5dB was evident for QPSK over DQPSK systems; despite the inherent tolerance of DQPSK systems to narrow optical filtering. Also the performance penalty inherent with offset filtering was confirmed; however via the novel design introduced for DPSK receivers' significant performance penalty reductions of about 2dB was achieved with asymmetric filtering of DQPSK systems. Furthermore the considerations of ultra narrow filtering impact on DQPSK systems is also presented via offset filtering and the results shows a 100% performance recovery for half the filter bandwidth offsets.

The impact of offset filtering on strongly filtered advanced modulation systems, for future optical communications is also discussed in this thesis.

Declaration

This work has not been previously accepted in substance for any degree and is not being concurrently being submitted in candidature for any degree

Signed .....(OLUBODUN OLUGBENGA)

Date31/08/11

Statement1

This Thesis is the result of my own investigations, except where otherwise stated. Where corrections services have been used, the extent and nature of correction are clearly marked in footnotes.

Signed .....(OLUBODUN OLUGBENGA)

Date31/08/11

Statement2

I hereby give consent for my thesis to be available for photocopying and for interlibrary loan and for the title and summary made available to outside organisations

Signed .....(OLUBODUN OLUGBENGA)

Date31/08/11

I want to thank GOD for his Omnipotence, Grace and Mercy.

Acknowledgements.

I like to first and fore mostly thank my great supervisor Professor Nick Doran for his wonderful guidance, motivation, support and advice. Truly I have been privileged to work under a foremost manager that has made me believe that with hard work there is no limit to one`s achievement in any endeavour. The first statement he made to me comparing research to `squeezing the last drop of juice from an orange fruit` has always been my motto in believing i can always push the limits in my investigations. I have learned a lot and will continue learning from him. I will forever be grateful to him (SIR), Professor Nick Doran. I will also like to thank my co-supervisor Dr Donald Govan most especially for is contribution to the experimental investigation. The group was a very inspiring team.

I want to thank my father Dr JBO Olubodun and my mother Mrs O A Olubodun, for their financial and moral support. I deeply appreciate GOD for my loving and wonderful parents. Also i like to thank my wife Lisa Olubodun, my sisters Oluwayemisi Adewale, Oluwabanwo Ayo-Paul and Mojisola Fakeye.

I would not forget my wonderful kids Moyo, Christian, Joshua and Daniel and Alisha. Just as my father showed me his thesis in 1986, I hope someday they all will present their thesis to my future grand children.

I will also like to thank Professor Bonnet, Professor Marhic, Anjana, Abiodun Sholiyi, Mehdi Jamshidi and Dr Farsheed for helping me read my thesis.

Contents

List of Figures and Tables.

Patents and Publications

[1] O.A. Olubodun, D.S. Govan, N.J. Doran "Patent on Signal Recovery" (PCT/GB2011/050338, 2011).

[2] O.A Olubodun and N.J. Doran "Characterization of Asymmetric Filtered 40Gb/s RZDPSK System-Strong Filtering Considerations" Journal of Optical Communication July 2011.

[3] O.A Olubodun, M. Jamshidifar and N.J. Doran "Performance Impact of Offset Filtered 40Gb/s RZ-DPSK-Strong Filtering Considerations" IEEE/ICBEIA June 2011.

[4] O.A Olubodun and N.J. Doran "Performance Improvement of Asymmetrical Filtered 40GB/s RZ-DPSK Receiver Design -Strong Filtering Considerations" IEEE/NOC 2011.

[5] O.A. Olubodun, D.S. Govan, N.J. Doran "Performance Recovery of 42.7 GB/s DPSK System Due to Offset Filtering" OFMC Sept 2009.

[6] O.A Olubodun and N.J. Doran "Improved Performance of tightly filtered 40 Gb/s coherent RZ-PSK by filter offset" under review in Wiley/IJCS 2011.

[7] O.A Olubodun and N.J. Doran "Asymmetrical Filtered 54Gb/s Coherent RZ-BPSK Tolerant to 50GHz grid" under review of Photonics Technology Letters 2011.

[8] O.A Olubodun and N.J. Doran "Performance Enhancement of Offset Filtered 40Gb/s CSRZ-DPSK Receiver in a 50GHz grid" Under review of IET Journal of Optoelectronics

[9] O.A Olubodun and N.J. Doran "Coherent 40Gb/s RZ-PSK with Improved Chromatic Dispersion Performance" September 2011 submission to Optics Express Journal

[10] O.A Olubodun and N.J. Doran "Performance Enhancement of Partial-DPSK via a Novel Receiver design" September 2011 submission to Photonics Technology Letters 2011.

[11] O.A Olubodun and N.J. Doran "Novel 40Gb/s DPSK Asymmetrical Receiver design with significant Performance Revivification" September 2011 submission to IEEE Photonics Journal.

[12] O.A Olubodun and N.J. Doran "Performance Impact of Offset Filtered 40Gb/s RZ-DPSK-Srong Filtering Considerations" IEEE/MELECON 2012.

LIST OF ACRONYMS

ACRZ	Alternate-chirp return-to-zero
AMI	Alternate-mark inversion
ASE	Amplified spontaneous emission
BER	Bit-error ratio
CD	Chromatic dispersion
C-NRZ	Chirped nonreturn-to-zero
CRZ	Chirped return-to-zero
CSRZ	Carrier-suppressed return-to-zero
DB	Duobinary
DCF	Dispersion-compensating fibre
DCS	Duobinary carrier suppressed
DFB	Distributed feedback laser
DGD	Differential group delay
DI	Delay interferometer
DM	Data modulation
DMF	Data modulation format
DML	Directly modulated laser
DPSK	Differential phase shift keying
DQPSK	Differential quadrature phase shift keying
DST	Dispersion-supported transmission
EAM	Electroabsorption modulator
EML	Electroabsorption modulated laser
EPD	Electronic predistortion
FEC	Forward error correction
FM	Frequency modulation
FWM	Four-wave mixing
GVD	Group velocity dispersion
IFWM	Intrachannel four-wave mixing
ISD	Information spectral density

ISI	**Intersymbol interference**
ITU	**International telecommunication union**
MI	**Modulation instability**
MLSE	**Maximum-likelihood sequence estimator**
MZM	**Mach–Zehnder modulator**
MZI	**Mach–Zehnder Interferometer**
NL	**Nonlinearity**
NRD	**Net residual dispersion**
NRZ	**Nonreturn-to-zero**
NZDF	**Nonzero dispersion shifted fiber**
OA	**Optical amplifier**
OADM	**Optical add/drop multiplexer**
OBPF	**Optical band pass filter**
OOK	**On/off keying**
OSNR	**Optical signal-to-noise ratio**
OXC	**Optical crossconnect**
PASS	**Phased amplitude shift signalling.**
PSBT	**Phased Shaped Binary Transmission.**

Chapter 1

"Voracious Bandwidth Demand"

The present day demand for data (Internet Protocol) around the world is ever increasing at rates unprecedented, e.g. data traffic from YouTube, Skype, Twitter, Facebook etc has made the Internet much more of a global commodity than a service. The popularity and daily consumption of Internet services and applications has made Internet based services one of the most profitable global ventures. The Facebook establishment is estimated at around 50billion dollars worth with 750 million active users sharing about 4 billion files per day.

This demand just gives a tip of the iceberg in terms of overall world data consumption. Optical communications is the main source of this seemly infinite bandwidth. The bandwidth over which data can be transmitted in optical communication (from Ordinary band (O-band 1260-1360) to Ultra-long band (U-band 1625-1675) is over 50THz bandwidth. But the trend in demand for optical communications will still increase, in fact there are predictions of `EXAFLOODS` in the nearest future.

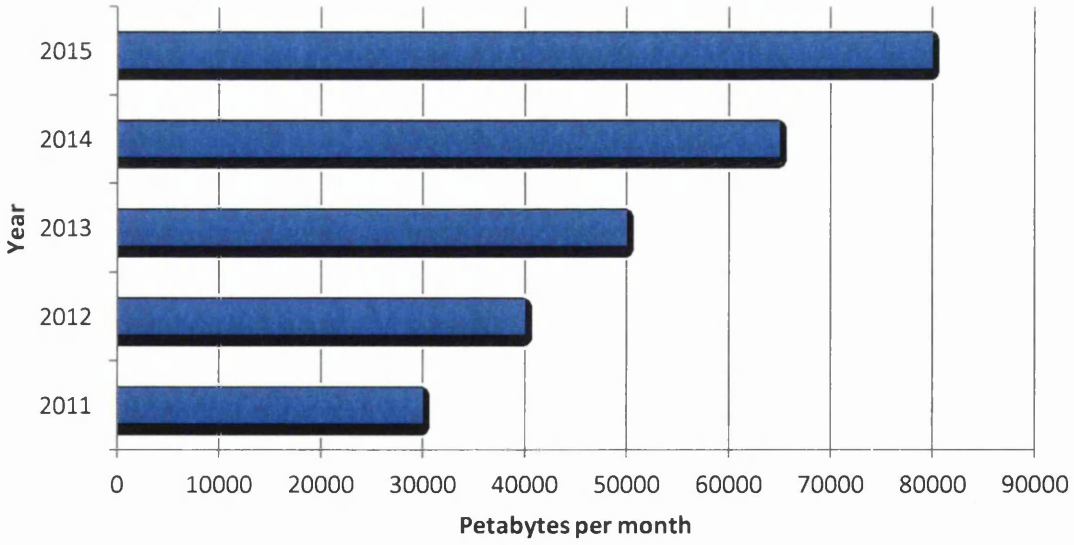

Fig 1.1: Global Internet traffic per month [1].

Figure 1.1 above shows the estimated Internet usage by the year 2015 [1], the monthly increase in consumption of Internet (trend) is expected to continue. These create a great challenge in terms of anticipated bandwidth supply by the service providers. The present 40 Gb/s data-rate employments is only adequate for a limited period and the proposed 100 Gb/s data rate via coherent QPSK will likely be exhausted before the end of the decade. Thus the need for intensified investigations to exceed the future global bandwidth demands.

The growth and progress in optical communications today could hardly have been envisaged centuries ago (405 BC), when the Greeks used heliographs for signalling in battles (this can be attributed to the genesis of optical communications), to the use of fire on mountains by Africans to communicate from one location to another, use of semaphore lines in 1790 AD [2] and signal lamps by mariners in Europe in 19^{th} century. In 1830, Samuel Morse invented the telegraph. This invention used coded messages transmitted by electrical pulses over copper wire. The process of matching words to electrical impulses was called Morse code keying technique [3]. In 1876 Alexander Graham Bell went further by showing that voice can be converted to electrical signal and transmitted over copper wire. The main limitation was that the connection could only be between two parties.

The invention of the switchboard made Bell's telephone invention more accessible and appreciated [2]. In 1940 coaxial cables replaced the wire pairs. Coaxial cables operated at 3MHz and were capable of operating 300 voice channels or 1 television channel. This system also had its demerits due to frequency dependent relationship that exist with the losses of the cable. The cable losses increased rapidly as the frequency went above 10MHz.

The introduction of microwave reduced the bandwidth problems of the coaxial system in 1948. But despite its advantages over coaxial system (extended carrier frequency to about 4GHz, bit-rates of about 100Mb/s) it soon became outpaced by the demand to transmit at faster data-rates. Thus research had to continue to find a better medium for telecommunications. The repeater spacing requirements of the microwave was ~1km, which was very costly, the losses of the medium was also an issue and the frequency limitations of microwave had to be combated.

These researches lead to the optical fibre as the successor, due to the optical fibre's inherent properties. After the invention of the laser in the 1960s, its attribute of providing coherent light sources with ability to modulate at high frequency (10,000 times greater than radio frequency capabilities) made optical communication very attractive [2]. In 1966,

joint research by Charles Kao and George Hockham proposed the use of fibre optics for long-distance communications. By 1970 Corning Glass Company produced the first set of low-loss fibres. These revolutionized the optic fibre in telecommunications [4]. There have been a lot of developments since the invention of the optical fibre, which was catalysed by the advancements in laser developments. These developments can be categorised into six major generations, which are detailed below.

First generation photonic networks utilized LED (Light emitting diodes) on Multimode fibres for about 10 km at 50Mb/s to 100Mb/s data rates. The first generation operated on a wavelength ~850nm. The 850nm range was attractive around 1980 due to the use of low cost silicon detectors at the receiving end. The 850nm fibre offered better performance over coaxial cable in terms of data-rate and bandwidth limitation.

The second generation photonic networks (early 1980s) used multi longitudinal mode lasers on 1300nm wavelength because of its low dispersion and less than 1 dB/km loss, initially on multimode fibre, using InGaAsP semi-conductors as lasers [5]. But the data-rate was limited to 100Mb/s due to modal dispersion. This prompted the introduction of single mode fibres by 1981, 2 Gb/s data rates were possible with repeater spacing of about 44km, around 1987, and data rates of about 1.7Gb/s became achievable with 50km repeater spacing.

The 3rd generation photonic networks operated at data rate of 2.5 Gb/s utilising silica fibres at 1550 nm wavelength, due to the minimum loss of the fibre at this wavelength. The chromatic dispersion at this wavelength constitutes a large impairment, thus development was delayed till single longitudinal mode lasers and dispersion shifted fibres (DSF) were developed. These developments and utilization of dispersion shifted fibre with single mode fibre, made the deployment of 10 Gb/s data rate possible over 100km. However impact of the DSF fibre was limited in long haul transmissions because the in the presence of fibre nonlinearity some dispersion is desirable to reduce its (nonlinear effects) impacts.

Thus the introduction of non zero dispersion shifted fibre (NZDSF). Another limiting condition was that the signal had to be electronically regenerated over 70 km.

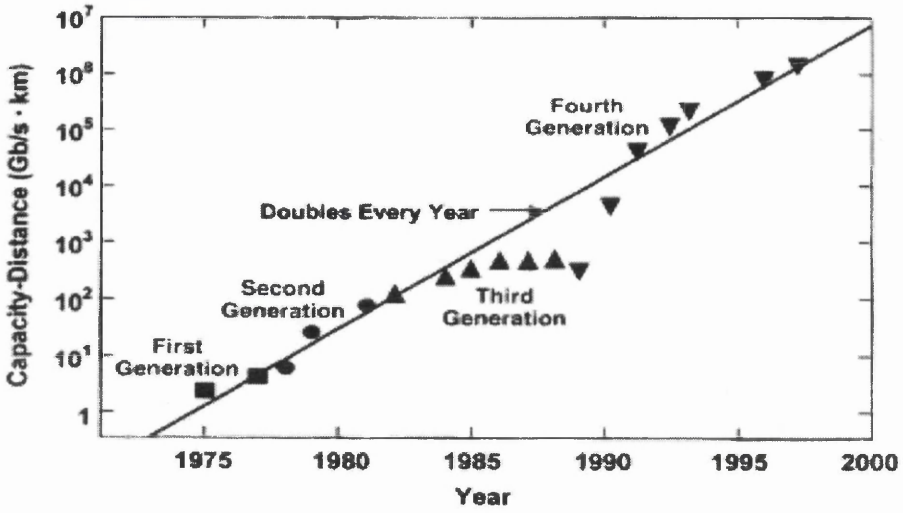

Figure 1.2: Increase in BL product over the developing lightwave systems. Different symbols are used to distinguish each generation. [2].

The 4th generation photonic networks introduced EDFA to amplify signals and thus became a landmark in photonic network evolution, because use of wavelength division multiplexing with EDFA enabled thousands of kilometres of transmission to be possible without electronic regenerators. By 1996, 5 Gb/s data rate was transmitted on several different wavelengths over 11,300 km, but dispersion was still a limiting issue [2].

The 5th generation was based on extending the wavelength range of WDM systems to S and L bands.

The present optical communication deployments are based on dense wavelength division multiplexing (DWDM) to achieve higher capacity for photonics network deployments via phase modulated formats. DWDM employs the simultaneous multiplexing of at least 8 different wavelengths in the same optical fibre. The sole aim is to reduce cost by efficient deployment of a combination of technologies, improving system tolerance to dispersion, fibre nonlinearities, improving the quality of the transmission and with multi-channel transmissions.

The recent reintroduction of coherent detection, via QPSK systems (due to its improved tolerance to polarization mode dispersion) is expected to enable 100 Gb/s data rates in installed capacities in the nearest future. The ever increasing Internet usage coupled with increasing demand for online entertainment and social networking is severely consuming the available bandwidth, and soon 1Tb/s (super-channels) data rates might be realized via OFDM with coherent detection [7].

1.1 The Motivation of the Research

The aim of these researches is to investigate the tolerance of 42.7 Gb/s optical phase modulated systems to tightly optical filtering regime (50 GHz grid) presented in a 50 GHz grid of the already installed intensity modulated systems which are transported at a 10 Gb/s data-rate. The investigation is implemented at the receiver by offset filtering of the optical bandpass filter. The choice of the optical bandpass filter in these investigations is a bandwidth that is representative of the net-filtering bandwidth that is available in 50GHz grid.

The impact of several concatenated optical filters inevitably results in narrow net optical filtering bandwidth at the receiver. Partial DPSK and differential quadrature phase shift keying formats have already been identified as main candidates for WDM 50 GHz grid deployments [8]. However there are several mitigations to the efficient deployment of these modulation formats, ranging from polarization performance of the MZI, limited electrical bandwidth for direct detection, OSNR penalties of the higher order modulation formats and sensitivity of the higher order modulation formats to laser detuning/filter frequency offsets.

Offset filtering in any modulation generally can enhance the spectral efficiency of the particular modulation format. Also very importantly is the fact that in a tightly filtered regime even the intensity modulated formats (i.e. OOK) vestigial/single sideband filtering has been shown to offer better performance than the symmetric filtered case [9]. Thus it will be interesting to investigate the impact of offset filtering on a 42.7 Gb/s DPSK/PSK system in a 50 GHz grid, based on the premise that the DPSK/PSK systems have better OSNR sensitivity and a better tolerance to nonlinear effects as compared to other higher order phase multi-level signalling.

Aside the impact of offset filtering the physical nature of the impact of the balanced detection will also be examined so that the knowledge of the spectral profile of the constructive and destructive ports of the DPSK demodulated signals can be used to improve the performance of a 42.7 Gb/s DPSK in a 50GHz grid. The impact of offset filtering at the receiver for 42.7 Gb/s BPSK/DQPSK/QPSK will also be characterized in the presence of an ASE-limited regime and dispersive regime.

The motivation behind this work is to explore an alternative strategy to the band-limited strategy which has been deployed in conjunction with 42.7 Gb/s

PDPSK/DQPSK/PSK/QPSK in a 50GHz grid. During this work, the optical transmission system at 40 Gb/s are modelled incorporating offset filtering at the receiver initially for a DPSK system and then extended to other phase modulated formats A novel receiver design is modelled based on the performance of offset filtering in a strongly filtered DPSK environment, via the performance of the two single ended detections. This concept is later extended to DQPSK, BPSK and QPSK modulation formats.

1.3 Objectives of thesis

The research presented in this thesis focuses on high-speed advanced phase modulated formats in a tightly optical filtered regime that might significantly impact the design of long-haul transmission systems in the nearest future. The success of the offset filtering of the phase modulated formats being investigated here could in principle enhance 100 Gb/s transmission systems with polarization multiplexing.

The success of the strategy deployed with phase modulations could be measured in terms of its tolerance to linear or nonlinear impairments, and most importantly the cost-effectiveness in deployment of the different modulation in the already existing channel spacing in 10-Gb/s intensity modulation direct detection (IMDD) systems.

The feasibility of phase modulated formats with this strategy in long-haul optical transmission is solely modelled with a strongly filtered 42.7 Gb/s DPSK system both with symmetric and asymmetric filtering, such that future work on other phase modulated formats could be reasonably envisaged.

1.4 Outline of thesis

This thesis is split into eight different chapters, which are as follows: Chapter 1 provides an introduction to the evolution of optical communications, motivation of the investigations, objective of thesis and thesis outline.

In Chapter 2 reviews of different forms optical phase modulation/ demodulation are presented. The 50 GHz grid channel spacing is also described in this chapter with the major optical components modelled in the simulations, and the algorithm used for all the simulation work was also described with some relevant diagnostic tools.

In Chapter 3 offset filtering results of strongly filtered 42.7 Gb/s DPSK system is presented, extensive examination of the physical origin of the performance trend is described, whilst also introducing a novelty in the receiver configuration that significantly improves the performance of a narrow filtered DPSK system.

Chapter 4 is focussed on offset filtering results of 42.7 Gb/s DQPSK system, extensive comparison of performance of the DQPSK system with an equivalent DPSK system is also undertaken. Lastly a novel asymmetric filtered DQPSK system is described with performance comparison with the conventional DQPSK system presented.

In Chapter 5 the impact of offset filtering on a strongly filtered 42.7 Gb/s BPSK system is modelled and the very exciting results are also presented. The impact of chromatic dispersion on a strongly filtered PSK system is modelled and presented, whilst also comparing the performance with an equivalent DPSK system.

In Chapter 6 the impact of offset filtering on a strongly filtered 42.7 Gb/s QPSK system is modelled and the results are also presented. The impact of chromatic dispersion on a strongly filtered QPSK system is modelled and presented, whilst also comparing the performance with an equivalent DQPSK system.

The Chapter 7, is based on the investigated results of strongly filtered DPSK in long haul transmission and preliminary experimental results on the impact of large filter offsets on a strongly filtered DPSK system. This is done to evaluate the impact of the offset filtered DPSK in a strongly filtered regime that is mostly presented in a linear regime, so as to envisage future work into the performance of the other phase modulated formats in long haul transmission. Then a conclusion is provided on the different contribution of these investigations to improving the performance of high speed phase modulated systems in tightly filtered regime.

The Chapter 8 is the conclusion and recommendations chapter on high speed phase modulated systems

1.5: Chapter 1- References.

[1] Cisco Systems Inc., "Cisco visual networking index: Forecast and methodology (white paper)," 2009. [Online]. Available: www.cisco.com/web/go/vni.

[2] A short history of fibre optics http:/www.sff.net/people/jeff.hechts/history.html. 1999

[3] G. P. Agrawal, "Fibre-optic communication systems", Third edition, 2002.

[4] www.mikeholt.com/technical.php?id=lowvoltage/unformatted/fiberoptics.

[5] K.C. Monham, R. Plastow, A.C. Carter and R.C. Goodfellow, "1.3 Gbps transmission over 107 km of dispersion-shifted mono-mode fibre using 1.55 μm multimode laser," *Electron Lett.* vol.21, pp 619-620, 1985.

[6] J.I. Yamada, S. Machida and T. Kimura, "2 Gbps Optical Transmission experiment at 1.3 μm with 44 km single mode fibre," *Electron Lett.* vol. 17, pp 479, 1981.

[7] J. Armstrong, "OFDM for Optical Communications" *J. Lightw. Technol*, vol. 27, no. 3, Feb 1, 2009.

[8] D.S. Govan and N.J. Doran "An RZ DPSK receiver design with significantly improved dispersion tolerance" *Optics Express*, vol. 15, Issue 25, pp. 16916-16921, 2007.

[9] T. Tsuritani, A. Agata, I. Morita, K. Tanaka, and N. Edagawa, "Performance comparison between DSB and VSB signals in 20Gbit/s – based ultra-long-haul WDM systems," in "*Proc*". *OFC 2001*, OSA paper MM5 2001.

Chapter 2

Limitations of Phase Modulation Formats in a 50GHz Grid channel spacing.

2.1 Introduction.

In order to make a qualitative study and evaluation of optical pulse propagation in a 50GHz grid imposed channel spacing in an already installed optical communication systems, it is important to describe the main optical fiber impairments that will be examined within the context of this investigations. The impact of fibre loss and chromatic dispersions impacts are the main optical communication impairments that would be investigated with different phase modulated formats in this research investigation. Fibre loss is occasioned by the attenuation coefficient of the different fibre types, that results in transmit power reductions as a function of the specific fibre attenuation. Thus the transmit power reductions can be adequately compensated by optical amplifiers. However an aftermath of the power compensations of the optical amplifier is a resulting amplified spontaneous emission (ASE) that inevitably degrades optical signal. Different signal formats are modeled in conjunction with the different variants of phase modulated formats in a tightly filtered regime. Next the demodulation processes of the different phase modulated formats are described in this chapter.

The 50GHz grid channel spacing is also described in details, while also describing the major optical components that are modeled in a back to back transmission. Lastly in this chapter the numerical model, justification for the choice of the detection statistics are also made and different diagnostic tools that are used in these investigations are also introduced. Then the techniques that have been deployed in improving performance of optical communications systems in the presence of specific impairments in a tight filtering regime are also described. The main contribution of these research investigations to optical communication is then introduced (offset filtering).

2.2 Optical Fibre Impairments

In this section the major effects that limit the effectiveness and performance of optical signals in optical fibres from source to reception are introduced. The major impairments are as follows, fibre loss (attenuation), chromatic Dispersion, fibre non-linearity and Polarization.

2.2.1 Fibre loss (attenuation loss).

Fibre loss is a linear impairment that affects optical transmission in photonic networks adversely. Fibre loss can be described as the single most important impairment in optical communication, the effect of fibre loss is not only degrading to optical systems performance, but the impact of compensating the effect of fibre loss gives rise to another major limiting factor that is virtually inevitable in optical communications systems (ASE-noise). As a signal launched into an optical fibre at transmitter; the effect of fibre loss starts to take place immediately. This is due to the fact that all fibre types that are available have their individual attenuation constant. Ranging from dispersion shifted fibre (DSF), dispersion compensating fibre (DCF), NZDSF to standard single mode fibre (SMF). Thus as an optical signal is transmitted with a given launch power at source into a fibre of a given length, the amplitude of the signal degrades as a function of the fibre attenuation constant. The table below gives the exact attenuation constant for several optical fibre types.

Fibre Types	Attenuation at 1550 nm in (dB/km)	Core Area (μm^2)	Dispersion at 1550 nm ps/nm/km
SSMF	0.2	70	17
NZDSF	0.25	60	3
DSF	0.3	50	0
DCF	0.5	30	-100

Table 2.1: Showing attenuation coefficient and core area for different fibre types.

Thus attenuation coefficient can be defined using the power loss after 1km in dB/km.

$$P_T = P_o \exp(-\alpha L) \qquad 2.0.1$$

Where α is called attenuation constant or coefficient; P_o is the optical signal power at the input of a fibre of length L; and P_T is the transmitted power or output power. The relationship between α and α_{dB} is as given below.

$$\alpha_{dB} = -\frac{10}{L}\log\frac{P_T}{P_o} = 4.343\alpha \qquad 2.0.2$$

It is the usual practice to express loss of optical fibres as α_{dB}. Loss is a prominent feature of all types of fibre, the fibre loss of single mode fibre as a function of signal wavelengths are as shown in the figure below:

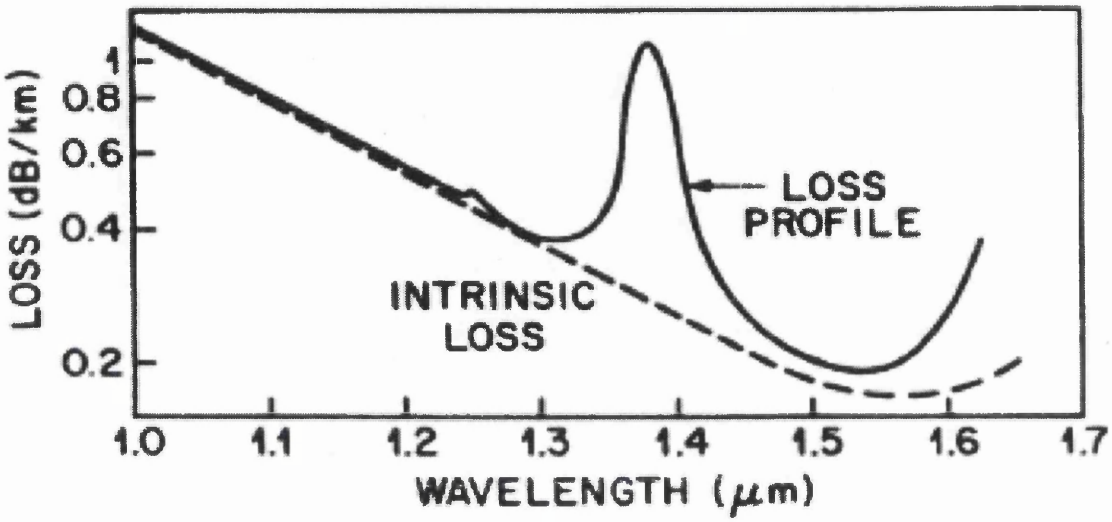

Fig 2.1: Measured loss spectrum of a single-mode silica fiber. Dashed lines show the contributions from Rayleigh scattering [1].

The plot above indicates that for a signal wavelength of around 1500nm, the loss accruable is 0.2dB/km which gives the best wavelength performance of the single mode fibre. Another wavelength that would have been of interest is the 1300nm wavelength due to its 0 dispersion performance and bending loss, but the attenuation loss for this wavelength is around a factor of 2 worse than 1550nm wavelength. However the bend loss for a 1300nm wavelength is lesser than at 1500nm wavelength.

Several factors contribute to loss profile of the optical fiber (SMF), absorption by hydroxyl ion (OH-), Rayleigh scattering and infra red electronic absorption [1]. The (OH-) absorption is caused by impurities (external factors), while Rayleigh scattering and infra red electronic absorption are due to intrinsic i.e physical properties of the optical fiber material. The importance of 1550nm also comes up by a coincidence of nature that the simultaneous amplification of signal wavelengths by EDFA is at its maximum gain and for about a 30nm bandwidth around 1550nm wavelengths.

2.2.2 Chromatic Dispersion

In this section the impact of optical fibre chromatic Dispersion properties will be described, its consideration within the context of tight optical filtering will also be analysed. This is in view of the fact that tight filtering degrades systems performance, but in

conjunction with chromatic dispersion further degradations will evolve. The good news is that just as there are several strategies to mitigating the impact of fibre loss, there are also many techniques to reduce or compensate the impact of chromatic dispersion.

Thus it will be of great interest to numerically model the impact of some techniques in the presence of combinations of tight optical filtering, ASE noise and chromatic dispersion. But before considering these combinations of impairments scenario, it is best to describe the impact of optical fibre chromatic dispersion on an optical pulse.

2.2.2.1 Group velocity dispersion

The impact of group velocity dispersion on an optical signal affects the signal on a time domain; essentially it is a linear impairment to optical pulse propagation in optical communications systems. Just as fiber loss and filtering induced penalties are linear impairments, so are the effects of GVD. Chromatic dispersion is an undesirable linear effect that affects the propagation of light waves in optical fibre (pulse broadening or compression depending on the sign of the GVD). Thus the propagation constant (β) and refractive index (n) depends on the signal wavelength in fibre. There are two major contributors to the chromatic dispersion; they are material dispersion and waveguide dispersion. Material dispersion is dispersion in which refractive index of material (silica) of the optical fibre is frequency dependent. Waveguide dispersion arises due to changes in wavelength that translate to changes in power distribution and will affect the (refractive indexes of core and cladding) effective index and propagation constant. The simple expression for chromatic dispersion will be described with some relevant parameters before the chromatic dispersion effect on an optical pulse (phase change on frequency domain) is described in details.

Simply these parameters are β_0 representing phase change, $V_g = {}^{1}/_{\beta_1}$ where V_g is the group velocity and β_1 is phase velocity and β_2 is the group velocity dispersion parameter and β_3 is the group velocity dispersion slope.

The dispersion parameter (D) is defined as the delay measured in picoseconds per nm (nanometre) separation of adjacent wavelength per km (ps/nm/km). D is ~16 ps/nm/km for standard single mode fibre (SSMF).

The effect of fibre dispersion is accounted for mathematically by expanding the propagation constant in a Taylor series about the signal centre frequency ω_0 at which the pulse is centred.

$$\beta(\omega) = n(\omega)\frac{\omega}{c} = \beta_0 + \beta_1(\omega - \omega_0) + \frac{1}{2}\beta_2(\omega - \omega_0)^2 \ ....$$

$$D = \frac{d\beta_1}{d\lambda_1} = -\frac{2\pi c\beta_2}{\lambda^2} \quad 2.1$$

where D is the dispersion parameter.

$$S = \left(\left(2\pi c/\lambda^2\right)^2 \beta_3 + \left(4\pi c/\lambda^3\right)^2 \beta_2\right) \quad 2.2$$

where S is the dispersion slope.

But the origin and physical effects of the three mentioned linear impairments are different. For GVD effects the regions of interest herein are explicitly GVD dominated regimes. Dispersion can simply be established as a direct relationship that exists between refractive index and wave frequency. The effect of dispersion cause the optical pulse to broaden or compress as a function of the sign of the group velocity dispersion, this broaden or compression is as a result different frequency component of the pulse travelling with different speed and thus results in pulse width broaden. A dispersive regime can generally be described as a regime where the effects of GVD largely exceed the effects of the fiber non linearity [2].

$$\frac{i\partial A}{\partial Z} = -\frac{i\alpha A}{2} + \frac{\partial^2 A\,\beta_2}{2\partial T^2} - \gamma|A|^2 A. \quad 2.3$$

The three terms on the right hand of the equation above govern the effects of fiber loss, dispersion and non linearity. Where A is the slowly varying amplitude of the optical pulse envelope and T is measured relative to a pulse with a given group velocity v_g that is T is normalized to the z axis for the group velocity $(T = t - z/v_g)$. (2.4)

The time frame normalized to the z axis t can also be normalized to the initial pulse width T_o

$$\tau = \frac{T}{T_o} = \frac{t - Z/v_g}{T_o} \quad 2.5$$

Just as the time frame has been normalized it important to normalize the amplitude of the pulse U as shown below with $\gamma = 0$ such that the non linearity is isolated.

$$A(z,\tau) = \sqrt{P_o}\exp(-\alpha z/2)\,U(z,\tau) \quad 2.6$$

P_o represents the peak power of the initial pulse, the fibre loss is represented by the exponential part of the above equation. Thus to simplify the equations for the purpose of analysis $U(z,\tau)$ is found to satisfy

$$i\frac{\partial U}{\partial z} = \frac{sgn(\beta_2)}{2L_D}\frac{\partial^2 U}{\partial \tau^2} - \frac{\exp(-\alpha z)}{L_{NL}}|U|^2 U \qquad 2.7$$

If the non linear and fibre loss of the NLSE are eliminated and equation 2.3 satisfies

$$\frac{i\partial U}{\partial z} = \frac{\beta_2}{2}\frac{\partial^2 U}{\partial T^2}$$

thus the dispersive and non linear lengths are given below

$$L_D = \frac{{T_0}^2}{\beta_2} \qquad L_{NL} = \frac{1}{\gamma P_0} \qquad 2.8$$

Where T_0 represents the initial pulse width, γ is non-linear parameter and P_0 is the peak power. Thus are three important lengths that are important to consider in determining the dominant impairment. i.e. either linear or non linear dominated regimes in optical fibre, $L, L_D \; and \; L_{NL}$ given as fiber length, dispersive length and nonlinear lengths. The evolution of optical pulses in an optical fiber is largely dependent on the magnitude of these three lengths. Thus the regime we are considering here is such that the $L \geq L_D,\ L \ll L_{nl}$.

and the dispersive part of the equation (2.8) normalized above can be solved by Fourier transform [3], such that $U(z,\omega)$ is the Fourier transform of $U(z,\tau)$ and is given below as

$$U(z,\tau) = \frac{1}{2\pi}\int_{-\infty}^{\infty} U(z,\omega)\exp(i\omega T)d\omega \qquad 2.9$$

This equation satisfies the ordinary partial differential equation

$$\frac{\partial U}{\partial z} = -\frac{1}{2}\beta_2\omega^2\breve{U}. \qquad 2.10$$

The equation 2.10 can be integrated to give

$$\breve{U}(z,\omega) = \breve{U}(0,\omega)\exp -(\frac{i}{2}\beta_2\omega^2 z). \qquad 2.11$$

Where $\breve{U}(0,\omega)$ is the Fourier transform at $z = 0$.

$$\breve{U}(0,\omega) = \int_{-\infty}^{\infty} U(0,T)\exp(i\omega T)\,dT. \qquad 2.12$$

By combining equations (2.9) and (2.11)

$$U(z,T) = \frac{1}{2\pi}\int_{-\infty}^{\infty} U(0,\omega)\exp(\frac{i\beta_2\omega^2}{2} - i\omega T)d\omega\,. \qquad 2.13$$

The above equation shows that the spectrum of the pulse remains unchanged in the presence of dispersion ,but that pulse width and shape are affected as a result of dispersion due to change in phase of the different spectral components.

$$U(0,T) = \exp(-\frac{T^2}{2T_0{}^2}) \qquad 2.14$$

Assume $U(0,T)$ is taken as the input Gaussian pulse with a GVD of β_2 after a distance Z

$$U(z,T) = \frac{T_0}{(T_0{}^2 - i\beta_2 z)^{1/2}}\exp\left[\frac{T^2}{2(T_0{}^2 - i\beta_2 z)}\right] \qquad 2.15$$

Thus a Gaussian pulse maintains its shape on propagation through z distance but the pulse width increase as shown below

$$T_1(z) = T_0{}^2\sqrt{(1 + (z/L_D)^2)} \qquad 2.16$$

$$U(z,T) = |U(z,T)|\exp[i\varphi(z,T)] \qquad 2.17$$

$$\varphi(z,T) = \frac{-sgn\beta_2\,(z/L_D)}{1+(z/L_D)^2}\frac{T^2}{2T_0{}^2} + tan^{-1}\left(\frac{z}{L_D}\right) \qquad 2.18$$

The first part of the right hand side of the above equation corresponds to the frequency chirp and the other part is the (constant phase shift) distance dependent phase shift. Thus there two phase shifts in the above equation; the time dependent and the constant phase shifts. The time dependent phase shift also depends on the sign of the β_2. For normal dispersion regime the sign of the chirp is negative and in an anomalous dispersion regime the sign of the chirp is positive. The dispersion induced pulse broaden can be understood from the point of view of the phase change in spectra domain leading to different parts of the signal spectrum travelling with different speed and arriving with a relative delay to their initial positions

2.3 Optical Modulation

The focus of this section is to describe different modulation techniques that are available in optical communication. As data rates increases one if the major limitations to practical deployment of higher data rate is the limited electronics bandwidth that are available for real systems. There are several types of optical modulators, range from direct modulated lasers, Electroabsorption and Mach Zehnder Modulators (MZM). However in this Thesis generation of the different signal format and modulation formats shall be concentrated through the MZM. As the operational understanding of most optical communications technologies are essential in the modeling of optical communications, the MZM operational process shall be described here and the different signal formats and modulation formats that are applicable to advanced modulation formats will also be described.

2.3.1 Mach-Zehnder modulator

The Mach-Zehnder modulator works on the principle of interference, controlled by modulating the optical phase. Incoming light is split into two at the input coupler; one or both arms of the modulator are equipped with phase modulators such that the two optical fields acquire some phase difference relative to each other, controlled by phase modulation voltages. Finally the two fields interfere at the output coupler. The interference is either destructive or constructive, thereby producing intensity modulation [12]. The optical field transfer function of the Mach Zehnder modulator is given below

MZM Optical field transfer function

$$T_{E(V_1,V_2)} = e^{i\frac{(\emptyset(V_1)+\emptyset(V_2)+\varphi)}{2}} COS\left[\frac{\left(\emptyset(V_1)+\emptyset(V_2)\right)-\varphi}{2}\right]$$

The square of the field transfer function is the power transfer function

$$\left|T_{E(V_1,V_2)}\right|^2 = T_{P(\nabla V)}.$$

MZM Optical power transfer function

$$T_{P(\nabla V)} = COS^2\left(\frac{k}{2}\left(\nabla V - V_{bias}\right)\right)$$

$\nabla V = voltage\ difference\ between\ V_1\ and\ V_2,$
$V_{bias} = voltage\ for\ additional, temporal\ constant\ phase\ shift\ (\varphi).$

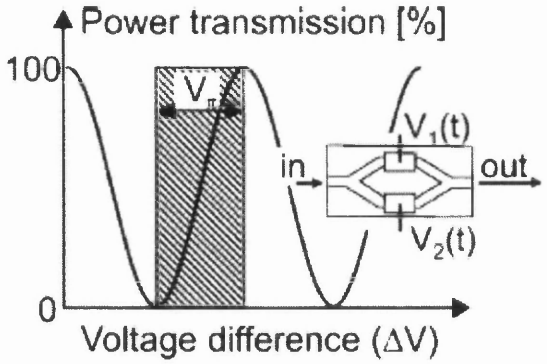

Fig 2.2 Schematic of Mach-Zehnder interferometer and output path optical intensity [25].

Overview of different ways to drive an MZM

In the Mach Zehnder modulator, $\emptyset(V_1, V_2)$ are the voltage modulated optical phases of the two arms. φ is additional temporally constant phase shift. If phase modulation is linearly dependent on drive voltage $\emptyset = KV$, then the power transfer function depends on drive voltage difference. The Mach Zehnder modulator has excellent extinction ratio. The required peak to peak drive voltages of around 6V require broadband driver amplifiers which can be a major challenge at data rates in excess of 10 GB/s. Today $LiNbo_3$ based MZM are widely available for modulation up to 40 GB/s. MZM forms the basis of many advanced modulation formats due to its independence in generating phase and intensity modulation formats.

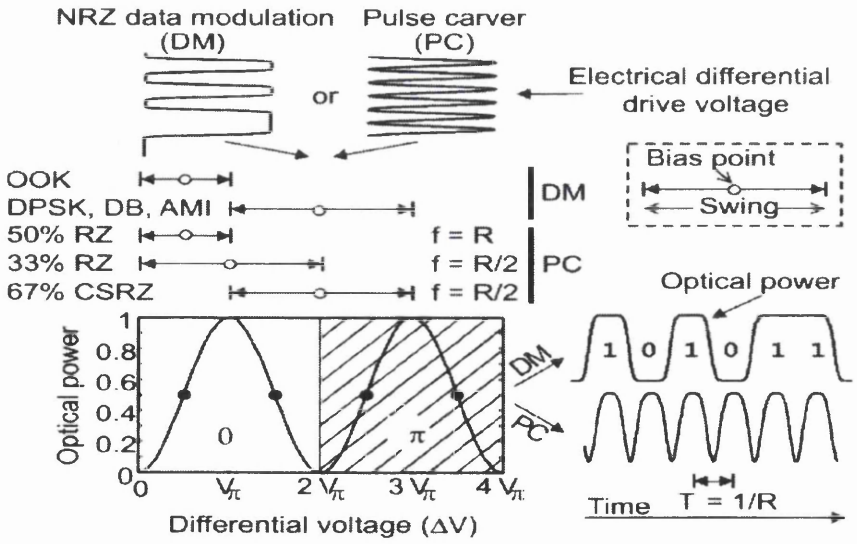

Figure 2.3: Overview of different ways to drive an MZM, resulting in different optical modulation formats (black circles: MZM quadrature points). PC: Pulse carver. [12]

2.3.2 Different Signal formats.

There are two main sub-divisions of signal formats namely non return to zero (NRZ) and return to zero signal (RZ) formats. The RZ signal can also be divided into three variants namely 33%, 50% and 67% [13]. The choice of any of these signal formats is largely dependent on application scenario, because of their different performances in presence of chromatic dispersion, tolerance to fiber non linearity and polarization mode dispersion. The sections 2.3.2.1 and 2.3.2.2 further explains the different relative performances of the different signal formats. This is occasioned by the three signal formats having different pulse widths and therefore different spectra widths. Also importantly at data rates of ~10 Gb/s pulse carving is not essential in tightly filtered regimes.

2.3.2.1 Non Return to Zero (NRZ) Signal formats

Different modulation format can be transmitted with several signal format (Duty cycles, is the ratio of pulsewidth to bit period), but the most common ones in optical communication are Non Return to Zero and Return to Zero (NRZ and RZ) The NRZ spectrum is shown below:

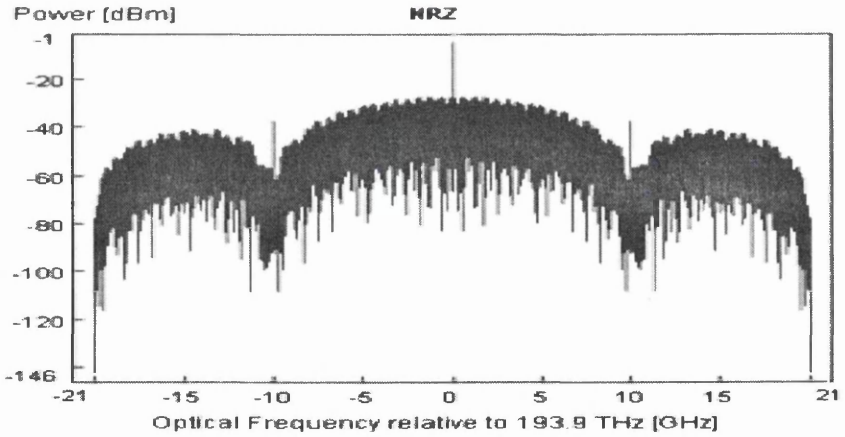

Fig. 2.4 Optical spectrum of NRZ signal with 10 Gbps data rate.

The NRZ signal format occupies the whole bit interval for a given transmitted signal, thus having a very narrow spectrum. For an NRZ pulse a 1bit occupies the whole length of the bit interval while for a 0 bit there is complete absence of pulse in the interval. Aside the Duobinary (DB) spectrum, NRZ spectrum is next to DB spectrum in terms of narrowness of the spectrum compared to all available signal format`s spectrum, i.e compared to the three different RZ signal format.

The NRZ has its inherent advantages over the return to Zero (RZ), in terms of cost; the NRZ signal format to be deployed in with any modulation format does not require an additional Mach Zehneder modulator in carving the transmitted pulse. This can be also be advantageous from the perspective of no extra insertion loss is been incurred in the generation of NRZ.

2.3.2.2 Return to Zero Signal Format:

Return to Zero (RZ), herein the pulse width of the optical signal is smaller than the bit period. Usually a clock signal with the same data rate as electrical signal is used to generate RZ shape of optical signals. For the RZ pulse a 1 bit is represented by partial occupation of the bit interval while for 0 bit, no pulse is used for the bit interval. These signal formats (RZ) in its different variants (33%, 50% and 67%) have their individual merits and demerits compared to NRZ. While 67%RZ is more tolerant to fiber non linearity, the lesser duty cycles are more tolerant to polarization mode dispersion (PMD).

The most notable merit of the RZ over the NRZ is improved sensitivity over non linear regimes (transmission distances). There is about 3dB improved sensitivity of RZ over the NRZ, the reason is largely due to higher peak power of the narrower pulse width of the RZ (in the presence of chromatic dispersion and fiber non linearity). The higher peak power of the RZ signal results in better eye diagram opening, this leads to improved receiver sensitivities for the same average power for the NRZ. Thus the improved receiver sensitivity of the RZ leads to increased transmission distances as opposed to NRZ signal for the same average power [12].

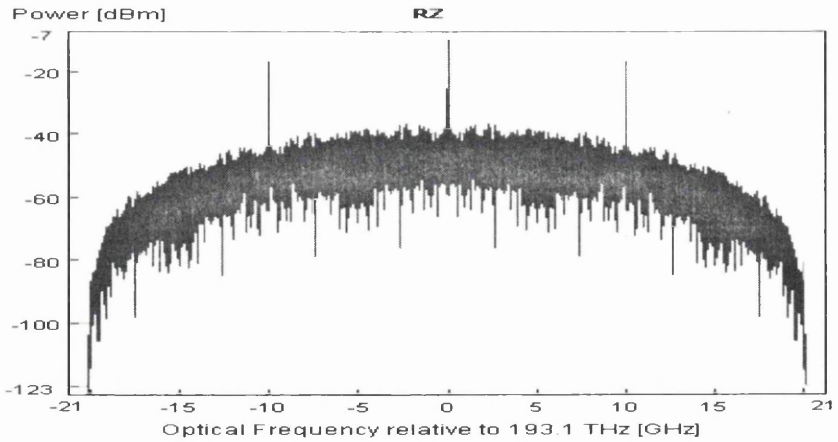

Fig 2.5 Optical spectrums of RZ signal with 10 Gb/s of data rate.

The absence of a pulse carver in the NRZ signal format is translated to weaker bit transitions and thus affecting its sensitivity in the clocking transition (eye diagram) as compared to the RZ format. The RZ signal formats, when the RZ pulses are chirped, the resultant pulses are more robust to the combined effect of fiber non linearity and dispersion. Thus the choice of the particular duty cycle to be deployed in conjunction with the DPSK or any modulation format is largely dependent on application scenario [14], cost of the extra pulse carving modulator and the corresponding optical fiber limiting impairments. The RZ format requires lesser OSNR for the same BER as compared to NRZ i.e around 1 to 3dB lesser OSNR [12].

2.3.2.2: Carrier Suppressed Return to Zero (CSRZ) signal format.

This is a special case of RZ signal format with a 67%duty cycle, special in the sense that it has inherent attributes of intensity and phase modulated format. CSRZ is a pseudo-multilevel modulation format, where the extra degree of freedom from the multi-level symbol is not utilized in increasing the bit rate as compared to multilevel signal format where symbol assignment does not depend on the previous or later symbol (i.e. DQPSK). The intensity modulation of the CSRZ is active while the phase modulation is passive, passive because the phase change is data independent.

CSRZ belongs to a sub class of memory modulation formats. Memory due to the symbol correlation that is inherent between the intensity and phase symbols. Thus for every bit transition there is optical field sign reversal (an alternate phase change), and this sequence of phase inversion leads to a null (0) carrier at centre frequency of the CSRZ spectrum. The alternating phase change leads to a net 0 power for the transmitted 1 bit data. This attribute ensures that the CSRZ has a better tolerance to fiber non linearity as compared to other signal formats [12]. The CSRZ signal format can be generated by sinusoidally driving a MZM at half data rate between two transmission maximum points and biasing at transmission minimum point between the two peaks. The memory nature of this type of duty cycle makes a particularly interesting signal format for deployment in a tight filtering environment [14].

2.3.2.3 RZ over NRZ

As with most optical modulation techniques, there are inherent advantages from deploying a specific modulation strategy just as there are drawbacks for deploying the same

strategy. I.e. the NRZ has its advantages in terms of its lesser cost for its employment relative to the RZ, because the RZ signal format requires an additional modulator. The narrower spectrum of NRZ is also better suited for WDM transmissions, where channels spacing are limited. Also of great importance is that tolerance of NRZ signal to linear cross talk is better than RZ, due to the smaller spectrum of the NRZ.

Although with appropriate filtering the performance of RZ signal within linear cross talk regimes can be greatly improved by minimizing its effect within channels using an RZ signal format. But within the context of advanced modulation formats, where data rates exceeds 40Gb/s data rate; thus impact of chromatic dispersion becomes comparable to the impact of fiber non linearity ($L_d \approx L_{NL}$) due to the decreases in signal pulse width, RZ performance becomes superior to performance the NRZ as the data rates increases.

The OSNR figure requirement for RZ is 1-3dB lesser than requirement for NRZ, because of the higher peak power of the narrower RZ pulse widths. When long strings of 1 bit are transmitted to the receiver with a RZ format the receiver can recover the 1 bits but it can't do the same for the NRZ and long 0 bit strings of the RZ because of the absence of transition makes it difficult for receiver to acquire a bit clock. In terms of most non linear induced penalties, RZ signal format has better tolerance compared to the NRZ. With self phase modulation (SPM) the irregular pattern of the NRZ signal from the absence of all pulses returning to zero for every bit slot, will result in SPM induced pattern dependence waveform distortions in the presence of dispersion. But due to the more constant patterning of the RZ signal, this SPM induced distortion is not inherent.

Also a chirped RZ has better tolerance to dispersion and non linear effects [12] than the chirped NRZ, when used in conjunction with dispersion compensating fiber (DCF). The chirped RZ can also be derived by deploying an additional MZM at the transmitter. This MZM is actually phase modulated, to introduce frequency chirping to the modulated RZ signals. The chirped NRZ [12] can be achieved by properly imbalancing a dual-driven MZM for NRZ signal, such that additional frequency chirp are introduced, this is done to improve the dispersion performance of NRZ system.

2.3.2.4 Duobinary or Partial response signaling.

Duobinary signaling being a member of correlative coding family is also identified as Phase Shaped Binary Transmission (PSBT) [15], and Phase Amplitude Shift Signaling

(PASS) [16]. Duobinary signal thus has an inherent mix of intensity and phase modulated signaling, where more than two symbols are used to represent a bit (modulation with memory). The distinction between the duobinary and the CSRZ is that there is a phase change for every bit transition as opposed to phase change in duobinary format being as a result of an odd 0 bit between successive 1 bits from the original data.

In this research duobinary demodulation is very important because most of the conversion of the phase modulated signaling at the receiver to electrical is implemented with at least one variant of correlative code or partial response signaling. Duobinary format being a memory modulation format (intensity and phase modulation) is a very unique modulation due to its narrow spectra profile, tolerance to chromatic dispersion and will be described in more details in section 2.3.6.3 (DPSK demodulation). It is important to consider that modulation formats with memory mostly benefit from using three optical symbols set {+1, 0, -1} in tight optical filtering regimes or dispersive regimes, because optical receivers use square law detection, (power = $|E|^2$), thus optical receivers map {+1, 0, -1} [+$|E|$, 0, -$|E|$] to a binary set {0, $|E|^2$}.

Thus employing 3 optical symbol levels for detecting two electrical symbol levels has enormous advantages in optical communications most especially within tight filtering regimes and for managing the effects of chromatic dispersions which is inevitable in optical signal propagation in optical fiber links. The duobinary modulation format can be generated electrically or optically. Generating the duobinary electrically requires a delay and add filtering or low pass filtering in generating a differential encoded data. This precoded data exhibits a phase change for every 0 bit in the original data sequence.

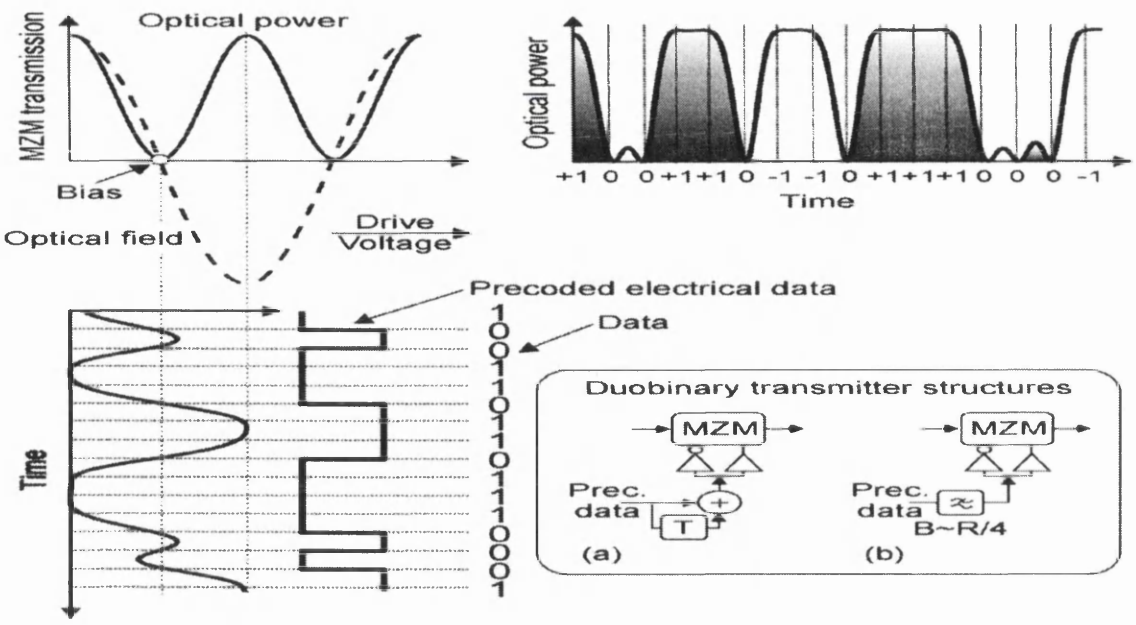

Fig 2.6 Duobinary signals are generated by driving a MZM around its transmission minimum using a three-level electrical drive signal, generated from the precoded data signal by either: (a) a delay-and-add circuit or (b) some other appropriate low-pass filter.

The low pass electrical filtering is employed with a 3dB bandwidth that is equivalent to 25% of the data rate. The delay and add, as the name denotes is an original data signal that is delayed then added to the un-delayed signal and thus generating a differential data. The precoded data drives a MZM with 3 level electrical drive signal around its transmission minimum. More importantly in this investigations duobinary signal generated at the demodulation of {+1, -1} PSK modulation is of more interest than the electrically generated duobinary [12].

Alternatively duobinary signal format can also be generated by severely optically filtering a PSK modulation format [14]. Compared to NRZ signal format that also has a narrow spectrum, the duobinary spectrum is narrower and thus outperforms NRZ in the presence of chromatic dispersion or strong filtering [12] due to its narrower spectra extent. The uniqueness of duobinary and other correlative coding techniques is largely due to their memory nature of (CSRZ, VSB, DB and AMI) etc.

The performance of phase modulation formats in tight filtering and in the chromatic dispersion is more driven by the memory nature of the DB signal as opposed to its memory-less modulation nature. Further insights into this distinct memory modulation behavior will be explained in chapter three and four.

2.3.2.5 Alternate Mark Inversion

In this research investigation Alternate Mark Inversion (AMI) is relevant due to the fact that the destructive output of a DPSK demodulation set up consists of an AMI spectrum. The AMI signaling is an intensity modulation format, with correlative coding characteristics. It is a line coding modulation format or memory coding modulation format due to the deployment of two symbols (intensity and phase) in modulating a single bit.

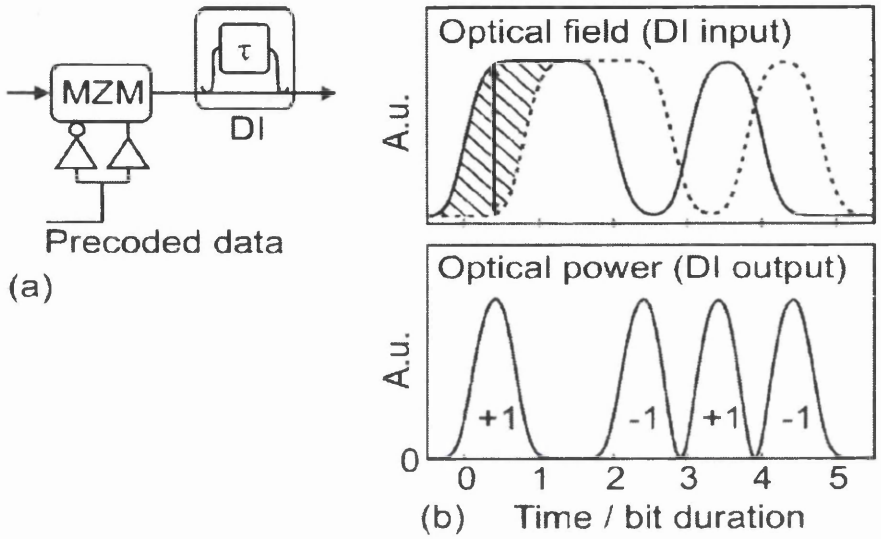

Fig 2.7 (a) Possible structure of a variable duty cycle RZ-AMI transmitter. (b) A signal in NRZ format interferes with its-delayed replica (dashed) in a DI, producing pulses of alternating phase.

But unlike other intensity -memory modulation format there is alternating phase change for each 1 bit data, even with a 0 bit between two 1bits. The additional phase modulation of the AMI can reduce the effect of fiber nonlinearity due [12] to net reduction in PSD due to alternating phase changes. AMI can be generated by passing a duobinary signal through a CSRZ signal, by employing delay and subtract circuits either electrically or optically.

Electrically the generation is similar to DB but the difference here is that AMI does not share bandwidth limitation with DB, thus the low pass electrical filtering as deployed with DB is replaced with high pass filtering. Thus the spectrum of the AMI is a double peaked spectrum and has a wider spectrum than the spectrum of the DB signal. The main condition in generating a delay and subtract filtering is that the interference of the optical MZI is set to a destructive interference which leads to a signal spectrum that is a complement inverse of the duobinary spectrum (DB).

2.3.2.6 Vestigial side band modulation.

Vestigial sideband modulation (VSB) is a form of modulation that is based on filtering out much of either of the sidebands, unlike other modulation formats where both sidebands are present. It is a particular modulation strategy that can be deployed to improve spectral efficiency of different modulation formats. Although very similar to single single side band modulation (SSB), but the prominence of VSB over SSB is largely due to the difficulty in optically or electrically achieving the SSB modulation formats.

VSB modulation deployed with different modulation formats has been shown to improve the system performance over certain fibre impairments relative to double side band modulation most especially in a narrow filtering regime, which is the area of concentration of this research [13, 14, 15]. However despite the inherent advantages of the VSB in an ASE noise limited regime, dispersive regime (except the duobinary that has a better performance) and similar performance to DSB modulation`s in non linear regimes, the main mitigation to the VSB modulation in tight optical filtering regime is crosstalk from WDM channels.

Except specific strategies such as polarization multiplexing, unequal channel spacing or digital signal processing technique such as MLSE or MAP are deployed to mitigate the impact of crosstalk that could potentially degrade the performance of VSB modulation severely [16, 17,18]

2.3.2.6: DPSK modulation.

There are two major ways of encoding phase modulated signals, i.e. straight-line phase modulators and Mach-Zehnder Modulator (MZM) [4]. The straight line phase modulator just modulates the phase of the optical wave while the intensity remains constant. The draw back from this straight-line modulator is the fact that the phase of a signal is not instantaneous, thus exact phase modulation is difficult to achieve. Thus chirp will be introduced in the process of this direct phase modulation [17].

The MZM introduces an intensity modulation while the phase of the optical wave is modulated. The MZM is based on the electro-optic process, where the refractive index of the material i.e. $LiNbO_3$ Lithium niobate is a function of the applied electric field. The exposure of the $LiNbO_3$ element to an optical field results in the optical light slowly moving through the element and the time it takes to travel through is a function of the optical phase of the optical signal. Thus the applied electric field is directly proportional to the resulting phase

change. If the MZM is biased at null point and driven with an exact voltage (twice the voltage for OOK) between 2 maximums point of the optical signal then an exact Π phase change results in the phase of the resulting optical signal at the output of the MZM. The accuracy of the phase modulation comes at the expense of the intensity dips depending on drive signal bandwidth and voltage. But the information bearing path of the signal is in the optical phase not the optical intensity. The dual sinusoidal curves of the optical phase and intensity of the MZM reduces the impact of drive wave imperfection, unlike the Phase modulated where any imperfection is transcended to the optical phase only.

2.3.2.6.1 Optical Phase modulation and generation.

The electric field of a typical laser source in optical communication can be represented in its real form as the equation below:

$$\vec{\epsilon}=A(\tau)\vec{e}cos(\omega\tau+\theta) \qquad 2.20$$

Where $\vec{\epsilon}$ is the magnitude of the optical field vector, $A(\tau)$ is the amplitude of the laser source, ω is the angular frequency, θ is the optical phase and $\vec{e}$ is the polarization of the laser source. The four different variables amplitude, frequency, phase and polarization can be used to optically modulated information unto the carrier signal. When a DPSK signal is considered over two bits intervals, the transmitted DPSK signals can be assumed equals $\sqrt{E_b/2T_b}\ \cos(2\pi f_c t)$ for $0 \leq t \geq T_b$, T_b is the bit duration and E_b represents the signal energy per bit. $s_1(t)$ represents the transmitted DPSK signal for $0 \leq t \geq 2T_b$ when we have a binary symbol 1 transmitted at the source and the second part of the interval is $T_b \leq t \geq 2T_b$. The transmission of a 1 bit symbol leaves the phase of the carrier constant over the interval $0 \leq t \geq 2T_b$, thus we can represent the 1 bit symbol of the DPSK modulation with the equation given below.

$$s_{1a}(t) = \sqrt{\frac{E_b}{2T_b}}\cos(2\pi f_c t), \quad \{0 \leq t \geq T_b\}$$

$$s_{1b}(t) = \sqrt{\frac{E_b}{2T_b}}\cos(2\pi f_c t), \quad \{T_b \leq t \geq 2T_b\} \qquad 2.21$$

Then let $s_2(t)$ represent the transmitted DPSK signal for $0 \leq t \geq 2T_b$, when we have a binary 0 bit symbol at the source for $T_b \leq t \geq 2T_b$. The transmission of a 0 bit symbol leads to a phase change of 180 degrees, we can represent $s_2(t)$ by the equations given below.

$$s_{2a}(t)=\sqrt{\frac{E_b}{2T_b}}\cos(2\pi f_c t),\{0 \leq t \geq T_b\},\ s_{2b}(t)=\sqrt{\frac{E_b}{2T_b}}\cos(2\pi f_c t+\pi),\{T_b \leq t \geq 2T_b\} \qquad 2.22$$

It can be seen that from equations 2.21 and 2.22 that DPSK is orthogonal over the 1bit symbol and 0 bit symbol intervals $0 \leq t \geq 2T_b$. The DPSK modulation is a modulation with T $= 2T_b$ and $E=2E_b$, without going into extensive mathematical derivations the probability of error for a DPSK modulation is given summarily as:

$$P_e = \frac{1}{2}\exp(-\frac{E_b}{N_0}) \qquad 2.23$$

However direct error counting is complicated to implement using the above closed form expression (above) most especially when the OSNR is higher. Thus Gaussian approximation is used to compute the Q values and the Q values are employed in estimating the Bit Error Rates of the DPSK modulation as opposed to the exact solution. However direct error counting using the close form expressions are very time consuming and under the conditions of a high OSNRs (DPSK system), error counting is very difficult to implement, because the BER is low. Thus (Gaussian approximation) is employed with fairly high OSNR, because it provides an accurate estimation of the systems BER. Several other parameter adjustments are also employed to improve the accuracy of the BER estimations of DPSK systems using Gaussian approximations and these conditions are further elaborated in section 2.7.1.

2.3.2.6.2: DPSK signal generation.

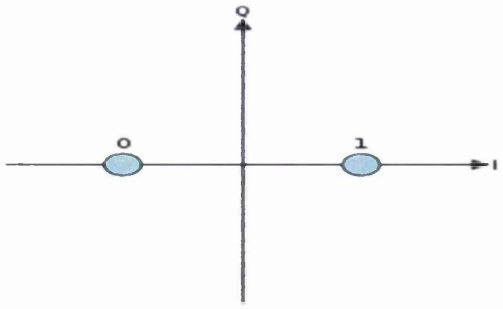

Fig 2.7 DPSK constellation diagram

The DPSK works as follows, the phase has two states of 0 and pi, thus for every 1 bit there is a phase change and for every 0 bit there is no phase change. The differential nature is show below in which data is encoded by via a change in the phase state of the optical signal

Data	1	1	0	0	1	1	0	1	0	1
Phase	0	π	π	π	0	π	π	0	0	π

Fig 2.8: Representation of DPSK signals generation.

2.3.6.3 DPSK demodulation.

In this section the demodulation of 42.7 Gb/s DPSK systems will be described, this is important because the performance of a strongly filtered DPSK system with a 50GHz grid; cannot be evaluated in isolation without relating the performance at narrow filtering regimes to wide filtering regime. Thus it is important to analyse the demodulation of a DPSK system as whole, such that better understanding of the demodulation process can enhance techniques that could improve the strongly filtered DPSK performance in a 50GHz grid. Just as will be seen in later parts of this chapter.

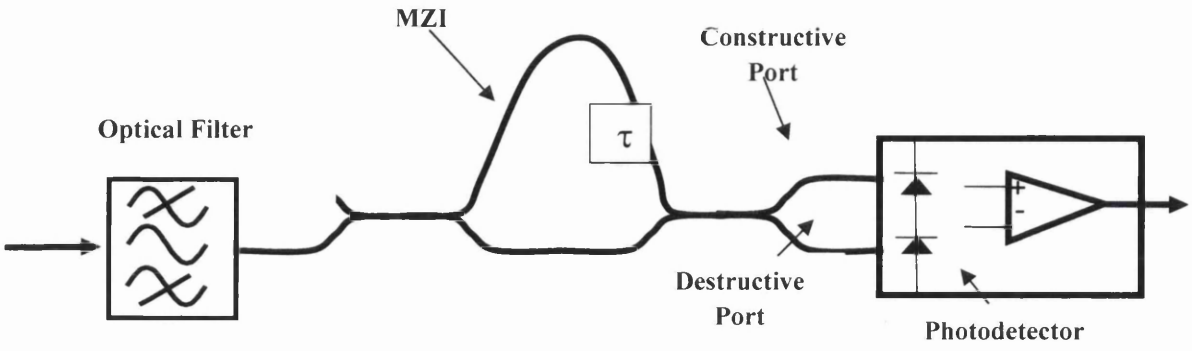

Figure 2.9: Diagram of a typical DPSK Demodulator diagram.

The DPSK demodulation is implemented by converting optical phase to optical intensity via electro-absorption or interferometric process (electro-optic process), because photo-detectors only respond to intensity of a signal rather than phase of a signal. As compared to Amplitude Shift Keying modulation where the intensity of the carrier signal is used to modulated 0 and 1 bits (i.e. 0 bit is modulated with absence of intensity of the carrier and 1 bit is modulated by the presence of intensity of the carrier signal). The separation between optical symbols used in encoding 0 bit and 1 bit for OOK format has a $\sqrt{2}$ less difference as compared to DPSK modulation format.

The main edge in the deployment of DPSK over OOK is the 3dB OSNR sensitivity for the same average power to achieve same BER (Bit error rate), is due to balance detection of DPSK signals and the phase symbol representation of DSPK has a larger separation in between the 1 bit symbol and 0 bit symbol than OOK (amplitude) symbols [14, 19]. These enhances DPSK systems in accepting more standard deviation of noise signal compared to OOK systems. Also of great importance is the improved tolerance of DPSK modulation format to fiber non linearity over OOK modulation, this is accounted for by the increased peak power of the spectrum of OOK format.

The spectra profile of DPSK and OOK modulation format are both similar, but for the presences of carrier tones on OOK modulation formats. Thus the impact of the 3dB OSNR sensitivity of the DPSK formats over OOK will also be reflected in the lower transmitted power which invariably translates to lesser non linear effects [19]. It has also been shown in [20] that in presence of serious fiber kerr non linearity that optimization of the DPSK delay in the Mach Zehneder Interferometer (MZI) and optimizing optical filtering bandwidth can improve the performance of DPSK modulation format. The effects of chromatic dispersion and polarized mode dispersion on DPSK and OOK modulation formats are relatively the same. But the process of the demodulation of encoded DPSK modulation, via conversion to partial response formats (duobinary {DB} and alternate mark inversion formats {AMI}) can enhance the improved tolerance to chromatic dispersion.

These improved tolerance to chromatic dispersion can be accomplished by exploring the inherent attribute of DB signal's narrow spectra profile and its 3 optical symbol levels {E, 0, –E} in conversion to 2 electrical symbols $\{0, E^2\}$. Thus in the presence of chromatic dispersion, a transmit data stream of 1, 0, 1 will be encoded by the DB signal as 1, 0, -1. The significance of the 3 optical symbols lies in the fact that chromatic dispersion will lead to the 1 bit pulses spreading to the 0 bit pulses, this will lead to a destructive interference

thus lowering the level of the 0 bit level, while for OOK there will be constructive interference leading to higher 0 bit levels and results in eye diagram closure.

This will lead to an improved sensitivity of the constructive port (with the duobinary spectrum) and eventually a better performance from balanced detection. Also an optimized increase in the free spectra range of MZI and commensurate optimization of the filtering bandwidth of the receiver can also increase the performance of DPSK system in the presence of chromatic dispersion [26, 27]. The major contribution of this work to DPSK modulation format is in the mitigation of optical filtering penalties induced in strong filtering regimes [18, 30].

2.3.3 DQPSK Modulation.

The aim of this section is to introduce the symbol modulation and demodulation of a DQPSK system, as DPSK modulation has been described in the previous section. It is important to introduce the similarity and differences between both systems most especially considering tight optical filtering (50 GHz). For a 42.7Gb/s DPSK system in a 50 GHz grid, the inherent optical bandwidth of DQPSK been half of the optical bandwidth of an equivalent DPSK system, thus the tolerance to narrow filtering is more enhanced with a DQPSK system.

Thus the representation of a DQPSK signal is the same as shown in equations 2.20 to 2.23, but the difference is that there is an additional symbol representation at ninety degree phase offset to the initial DPSK signal (DQPSK = 2DPSK), thus both have the same probability for bit error rate BER.

Nevertheless in order to achieve the same BER the QPSK requires twice the amount of power for DPSK, the number of bits for DQPSK is twice that of DPSK [12].

The symbol error rate of the DQPSK is given below

$$P_s = 1 - (1 - P_e) = 2Q\sqrt{\frac{E_b}{N_o}} \qquad 2.24$$

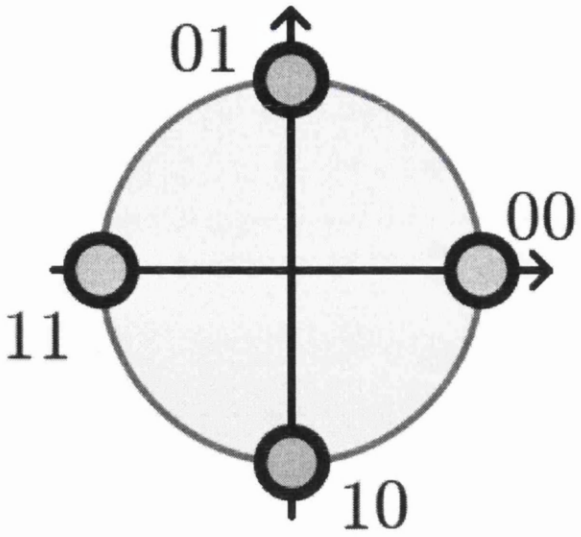

Figure 2.10; Signal constellation for DQPSK modulation format.

The diagram above is the constellation diagram for QPSK, the horizontal line represents the real part of the phase-optical equation and the vertical represents the imaginary part of the equation. The symbol representation on the constellation diagram is in the following other 00, 10, 01 and 11 $(0, \pi/2, \pi, 3\pi/2)$ for the DQPSK phase different phase states of the modulating optical carrier, where two bits are mapped to 1 symbol. Such that In-phase component (I) has a phase difference of 180 (π) between the two modulating symbols and the Quadrature component has the same phase difference but a different initial reference point $\pi/2$.

2.4: Optical PSK modulation

In the DPSK modulation phase is differentially encoded, while BPSK modulation is direct phase modulation. The DPSK demodulation is quite simple compared to the PSK demodulation where a local oscillator signal is needed to demodulate PSK signal. Also DPSK formats are less stringent to laser linewidth unlike PSK formats.

Data	1	0	0	1	1	0	1	0	1
PSK	π	0	0	π	π	0	π	0	π
DPSK	0	0	0	π	0	0	π	π	0

The symbol representation of the 0 and 1 bits at the transmitter is given below: When a PSK signal is considered over two bits intervals, the transmitted PSK signals can be assumed

equals $\sqrt{2E_b/T_b}\cos(2\pi f_c t)$ for $0 \leq t \geq T_b$, T_b is the bit duration and E_b represents the signal energy per bit. $s_1(t)$ represents the transmitted PSK signal for $0 \leq t \geq 2T_b$ when we have a binary symbol 1 transmitted at the source and the second part of the interval is $T_b \leq t \geq 2T_b$. The transmission of a 1 bit symbol leaves the phase of the carrier constant over the interval $0 \leq t \geq 2T_b$, thus we can represent the 1 bit symbol of the PSK modulation with the equation given below.

$$s_{1a}(t) = \sqrt{\frac{2E_b}{T_b}}\cos(2\pi f_c t), \quad \{0 \leq t \leq T_b\} \qquad 2.25$$

Then let $s_2(t)$ represent the transmitted PSK signal for $0 \leq t \geq 2T_b$. The transmission of a 0 bit symbol leads to a phase change of 180 degrees, we can represent $s_2(t)$ by the equations given below.

$$s_{2a}(t) = -\sqrt{\frac{2E_b}{T_b}}\cos(2\pi f_c t), \quad \{0 \leq t \leq T_b\} \qquad 2.26$$

The equations can be expressed as a basis function for a unit energy with the expression

$$\varphi_1(t) = \sqrt{\frac{2}{T_b}}\cos(2\pi f_c t) \qquad 2.27$$

Where $s_1(t) = \sqrt{E_b}\varphi_1(t)$ 2.28

$$s_2(t) = -\sqrt{E_b}\varphi_1(t) \qquad 2.29$$

Thus for a BPSK signal the signal has a one dimensional space and two data points on the constellation diagram represented by $\sqrt{E_b}$ and $-\sqrt{E_b}$

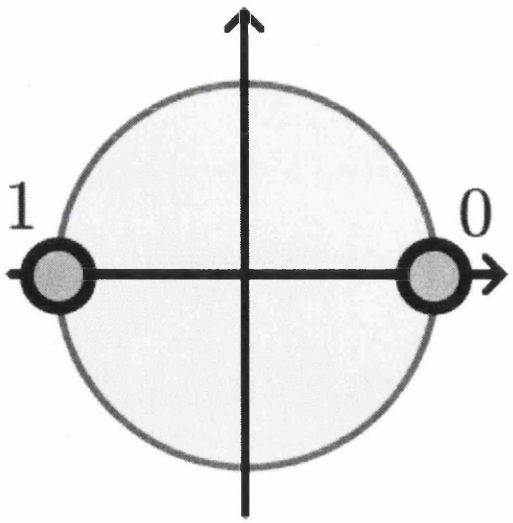

Figure 2.11: Signal constellation for PSK modulation formats

The probability of error for a BPSK modulation format (for case of transmitting 1 or 0 bit and receiving a 0 or 1 bit) is given as

$$\rho_e = \frac{1}{2} erfc \sqrt{\frac{E_b}{N_0}} \qquad 2.30$$

2.4.1 Optical Coherent Binary Phase Shift Keying (BPSK) Modulation.

Optical coherent modulation can be implemented via the amplitude, frequency (phase) and polarization of the carrier wave. Coherent Detection of (frequency)phase, amplitude modulated signalling is enhanced by the fact that that the optoelectronic conversion is over a linear scale, thereby introducing better phase, frequency and amplitude extraction of the modulated formats. The impact of the improved sensitivity of coherent detection can be highlighted by making a comparison of the sensitivity of DPSK and PSK modulation. It has been identified that PSK modulation performance is better in the context of lesser photons per bit [1] and in terms of OSNR performance. In fact amongst the several binary modulation formats coherent PSK offers the best sensitivity.

The recent resurgence in the demand of coherent modulation format is largely occasioned by the inherent multiple wavelengths amplification benefit of EDFA almost reaching its climax; the advent of EDFA in optical communication reduced the impact of coherent system due to associated cost and complexities in deploying coherent optical modulation formats. These is because in optical transmission the impact of ASE noise generated from the signal amplification over shadows the shot noise limited reception (where

the coherent detection offers improved sensitivity) because the OSNR at the receiver is largely determined by the ASE contributions.

The recent increase in demand coherent binary and multi level modulation is due to astronomical increase in demand for optical communication, which has moved from been a service to a commodity. The desire to increase performance (higher data rate) via already installed capacities and cost minimization for the service provider necessitates the recent researches in coherent optical communication.

The employment of coherent detection with any modulation is largely due to the performance impact of the local oscillator`s signal mixing with the received modulated, which is encompassed on a linear regime. Therefore no non linearity is introduced by the optoelectronic conversion process.

The conservation of modulated information and signal characteristics with coherent detection has enhanced the deployment of DSP for post processing of optical transmitted signal thereby offering improved tolerance to optical impairments. In terms of receiver performance with binary modulation formats coherent optical phase shift keying modulation schemed has been reported via simulation and experimentation to offer the best sensitivity of all the different binary modulation schemes (ASK, FSK and DPSK) [24, 25].

2.4.2: BPSK Demodulation

The demodulation of a PSK modulation format is described in this section. The demodulation in a PSK modulation format is implemented via mixing of the transmitted PSK at the output of the optical bandpass filter with a local oscillator signal. This mixing is implemented on a linear regime thereby enhancing an exact phase extraction unlike the DPSK modulation where a MZI is deployed in realising self phase referencing between the delayed signal at one arm of the MZI with the un-delayed signal at the other arm of the MZI.

Thus phase difference between successive bits actualized at the outputs of the MZI. The simplicity of the DPSK demodulation is an advantage in terms of cost of the MZI but the drawback is that the phase extraction of the process is not as precise as compared to the PSK demodulation. The PSK demodulator deploys a coupler $3dB/180^0$ after the OBPF in mixing the local oscillator`s signal with PSK signal. Thereby mixing of the inphase signal of the PSK signal with the inphase signal of the local oscillator on one output port. Also the out of Phase component of the PSK signal is mixed with the out of component of the local

oscillator. Thereby realising a balanced detection, although two single ended detections can be deployed at both the constructive and destructive port of the coupler after the mixing.

The local oscillator employed in the mixing with the PSK signal is a perfect local oscillator with zero linewith and phase locking is not implemented in any of the simulations. But actual phase displacement of the LO's signal is implemented to align the phase of the received signal. This is of course difficult to implement in practice because the phase matching in the field is subject to a time variant. For all cases of coherent detection in this thesis homodyne detection was employed in the simulation.

Thus the frequency of the local oscillator signal is assumed to be the same as the frequency the BPSK signal. The focus of the coherent BPSK investigation here is based on homodyne rather heterodyne due to the performance improvement (lesser photon per bit requirement for detection) and smaller receiver optical bandwidth as compared to heterodyne coherent detection (larger bandwidth) [5, 7]. Although an homodyne coherent system requires Optical Phase lock loop, the phase locking by an heterodyne system is implemented at the electrical stage. Also the line width requirement of the heterodyne coherent system is more tolerant to increase in linewidth of the local oscillator laser [7,8,9] than to requirements for homodyne. The optical field of the received BPSK signal and the local oscillator signal for the coherent mixing are shown in the equations below.

$$E_s = \frac{1}{\sqrt{2}} A_s[COS(\omega t + \emptyset_s) - iSin(\omega t + \emptyset_s)] \quad 2.31$$

$$E_{lo} = \frac{1}{\sqrt{2}} A_{lo} COS(\omega t + \emptyset_{lo}) - iSin(\omega t + \emptyset_{lo}) \quad 2.32$$

$$E_s = \frac{1}{\sqrt{2}} A_s[COS(\omega t + \emptyset_s + \pi) - iSin(\omega t + \emptyset_s + \pi)] \quad 2.33$$

$$E_{lo} = \frac{1}{\sqrt{2}} A_{lo}[COS(\omega t + \emptyset_{lo} + \pi) - iSin(\omega t + \emptyset_{lo} + \pi)] \quad 2.34$$

The equations 2.31 and 2.33 represents the received PSK signals at the outputs of the coupler i.e the former for the in-phase and the later for the out of phase. Also 2.32 and 2.34 represents the local oscillator signals (in-phase and out of phase) at the outputs of the coupler (3dB) coupler. Balanced detection is deployed by mixing of the PSK signal (in-phase) and the local oscillator`s signal (in-phase) at the constructive port and the destructive port has the interference of the out of phase signal of both the received BPSK`s signal and the local oscillator`s signal.

At the photodetector the difference between in-phase component (sum of the two in phase signals (PSK and local oscillator)) and out of phase component (sum of the two out of phase signals (PSK and local oscillator)) is used in obtaining an electrical decision variable.

$$P_s = kA_s{}^2 \qquad 2.35$$

$$P_{lo} = kA_{lo}{}^2 \qquad 2.36$$

$$P_t = k|E_s + E_{lo}|^2 \qquad 2.37$$

$$P_t = P_s + P_{lo} + 2\sqrt{P_s P_{lo}}\cos(\theta_s - \theta_{lo}) \qquad 2.38$$

$$P_t = P_s + P_{lo} + 2\sqrt{P_s P_{lo}}\cos((\omega_s - \omega_{lo}) + (\theta_s - \theta_{lo})) \qquad 2.39$$

The equations 2.35 and 2.36 represents the optical powers for the PSK and local oscillator signals, where K is the constant of proportionality and equation 2.37 represents the power incident at the photodetector, which responds to changes in optical intensity. The equation 2.38 and 2.39 represents the total optical power incident at the photodetector for both homodyne and heterodyne PSK detection. The difference in the equations is that of the change in angular frequency which for an homodyne detection is null and for heterodyne detection is in the range of some few Giga Hertz bandwidth.

$$\omega_{IF} = \omega_s - \omega_{lo} \qquad 2.40$$

Where ω_{IF} is the intermediate frequency, ω_s is the PSK signal`s angular frequency and $\omega_{lo}$ is the local oscillator`s angular frequency where ω_s *and* ω_{lo} are given as $2\pi f_s$ and $2\pi f_{lo}$, thus for an heterodyne detection the intermediate frequency is in the range of 0.08 to 6GHz. Within the context of this investigation in offset filtering of Phase modulated format in narrow filtering regimes the extra demand of the heterodyne detection in its inhert extra bandwidth is excessive and detrimental to basis of our investigation. Thus in

this research concentration of the impact of offset filtering in a TOF regime is investigated via homodyne PSK detection.

The photocurrent at the detector is given as a product of responsivity and sum of the powers of the local oscillator and PSK signals.

$$I_t = R(P_s + P_{lo}) + 2R\sqrt{P_s P_{lo} cos(\varphi_s - \varphi_{lo})} \quad 2.41$$

Thus for an homodyne detection the transmitted data is contained in the last term of the above equation (phased dc component) which implies for a perfect homodyne detection where PLL is deployed the last terms will be $2R\sqrt{P_s P_{lo} cos(\varphi_s - \varphi_{lo})}$ where $P_{lo} \gg P_s$. Having amplitude and phase components. Unlike the heterodyne detection which has amplitude, phase and frequency components in the resultant photocurrent generated at the detector

$$I_t = R(P_s + P_{lo}) + 2R\sqrt{P_s P_{lo} cos(\omega_{If} + \varphi_s - \varphi_{lo})} \quad 2.42$$

Although the difference in equations 5.1.17 and 5.1.18 are the intermediate frequency components of the heterodyne, the first part of both equations can be eliminated with bandpass filters, thus the remaining part of the (last part) of both equations where the difference in intermediate frequency component make the heterodyne part ac but the homodyne is dc.

There is a 3dB penalty inherent in the square of the photocurrent (heterodyne) dependency on the last past of the equation due to the mean of $cos^2\varphi = \frac{1}{2}$ over a period of φ. Thus in comparison of ideal homodyne and heterodyne detected PSK there is a factor of 2 improvements in homodyne detection. The realization of ideal homodyne PSK detection as compared to heterodyne PSK detection is more difficult due to stricter phase locking and linewidth concerns.

2.5: QPSK modulation format.

The QPSK system is essentially a 2 PSK system with phase shift in the carrier signal of one of the tributaries of ninety degrees with respect to the other. The transmitter structure is similar to DQPSK but the difference between QPSK and DQPSK is the demodulation. QPSK system deploys a synchronous receiver while the DQPSK system deploys an asynchronous receiver. The symbols for QPSK can be represented by the below equation for the symbol constellation in terms of the carrier wave used to generate the four different phases,

$$s_n = \sqrt{2E_b/T_b}\cos((2\pi f_c t) + \frac{\pi}{4}(2n-1)), \text{ where } n = 1, 2, 3 \text{ and } 4 \qquad 2.43$$

Thereby giving rise to 4 different phases with $\pi/2$ phase difference between each tributaries and a π phase difference within each tributaries i.e. the Inphase and the Out of Phase.

$$(\pm\sqrt{E_s}/2, \pm\sqrt{E_s}/2). \qquad 2.44$$

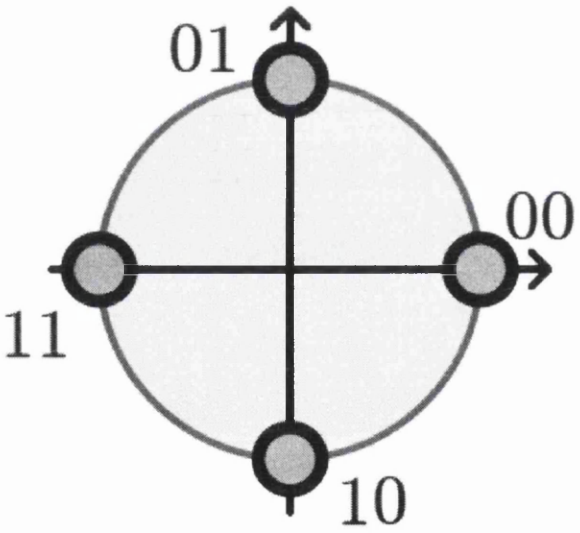

Figure 2.12: Signal constellation for QPSK modulation format.

The probability of error for a QPSK modulation format, is the same with PSK (for case of transmitting 1 or 0 bit and receiving a 0 or 1 bit) is given as

$$\rho_e = \frac{1}{2}\, erfc\sqrt{\frac{E_b}{N_0}} \text{ or } Q\sqrt{\frac{2E_b}{N_o}}. \qquad 2.44$$

The symbol error rate for QPSK is worse than PSK due to the increased number of symbols inherent in QPSK.

$$p_s = 1 - (1 - p_b) \text{ or} \approx 2Q\sqrt{\frac{2E_b}{N_o}}. \qquad 2.45$$

2.5.1 QPSK modulation and demodulation

The modulation and demodulation of QPSK is similar to PSK as shown in the previous section but for the additional phase modulation at the transmitter. This additional phase modulation is at an offset of ninety degree to the initial phase modulation and both tributaries are transmitted at half the data rate of an equivalent PSK system. In comparison to DQPSK systems the main difference in the modulation of QPSK system is that the an exact phase difference is deployed for QPSK systems, while phase difference between successive bits are deployed for the DQPSK systems.

Just has PSK systems have difference forms via homogenous and heterogeneous, same is applicable to QPSK systems.

2.6: 50GHz grid Channel Spacing.

WDM systems mainly use 1550nm wavelength region for two main reasons; low loss window (0.2dB/km for SMF) and by co-incidence of nature the excellent amplification window of the EDFA exists with region. ITU standardize WDM systems on a frequency grid centred around 193.1 THz as seen in the figure below illustrating the 100GHz and 50GHz equal channel spacing. WDM systems are centred on a convention band (C-band) 1530nm to 1565nm, also interestingly with the advancements in optical amplifications at 1565nm to 1625nm the L band is becoming prominent, and thus increasing the range for WDM channel deployments'.

The impact of this standardization by the ITU is that it has enhanced components manufacturing suited for specific frequency grids. As WDM systems increases the data capacities, the flexibility of installed/upgraded systems can also be increased by Optical Add/Drop Multiplexers (OADM) using WDM to split and combine specific optical wavelengths. The consequence of reconfigurable optical add-drop multiplex ROADM at optical nodes is that as more optical filters are deployed the net-optical bandwidth at the receiver becomes more narrowed.

This narrow effect especially within a 50GHz grid that is situated with the channel spacing available in a 50GHz grid with a 10Gb/s data rate leads to signal degradation due to the tight optical filtering imposed penalty. The net filtering bandwidth at the receiver is typically within the neighborhood of 32 to 37GHz optical bandpass depending on the number

of concatenated filters or cascaded WSS. Thus with 5 cascaded WSS the net bandwidth is around 35GHz for a 3rd order Gaussian filter [19].

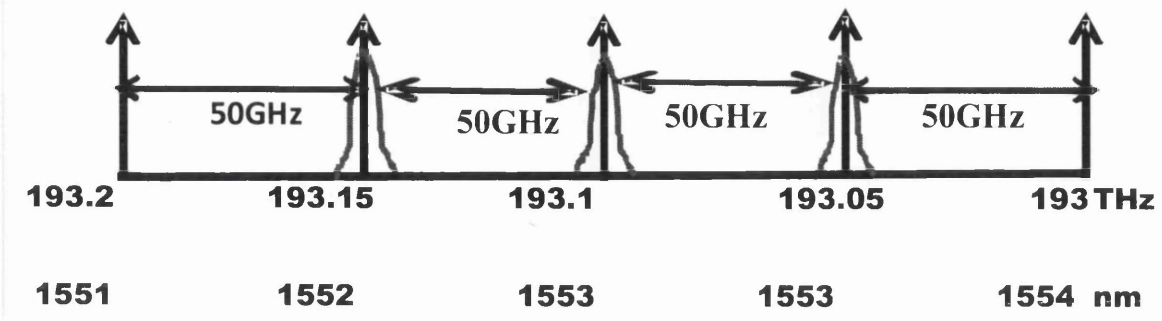

Figure 2.13; The 50GHz ITU frequency grid based on reference 193.1THz.

2.6.1: Optical Filters

Optical filters are vital components of optical transmission systems, in that they are the basis on which multiplexers (MUX) and demultiplexers (DeMUX) are built in achieving a wavelength division multiplex (WDM) channel transmission. The important functions of an optical filter are selection of specific transmission wavelengths/desirable wavelengths at the receiver, optical noise filtering (amplified spontaneous emission-ASE) and equalization of gain. The following attributes are vital for the effectiveness an optical filter in DWDM systems.

1 low insertion loss.

2 High tolerances to temperature, humidity and vibrations.

3 Polarization insensitivity.

4 Flat bandpass, to guarantee wide tuning range.

5 Low cost.

6 Negligible crosstalk to prevent interference from adjacent channels, this can be accomplished by deploying sharp (steep) filter edges (skirts).

7 fast tuning response of the filter to minimize the access time

There are several types of optical bandpass filters; either having their operational physical mechanism based on optical interference or diffraction or dispersion.

2.6.2: Narrowband-optical filtering

This section discusses the impact of optical narrowband filtering, i.e. a transmission impairment that typically occurs in an optical transmission network. An optical network requires that the transmitted optical signals travelling through the network has the flexibility to pass multiple optical add-drop multiplexer (OADM) and photonic cross connects (PXC) nodes along the transmission link [38]. An OADM compromises different optical sub-systems to realize wavelength switching. Generally, the WDM spectrum is de-multiplexed in order to stop specific WDM channels and allow other WDM channels pass through. This can either be achieved with via a wavelength selective switch (WSS), which can be a *AxB* switch, with *A* and *B* are the number of input and output ports, respectively. Typical examples are *1x4* or *1x9* WSS. A WSS is generally realized using micro-electro mechanical system (MEMS) technology [39].

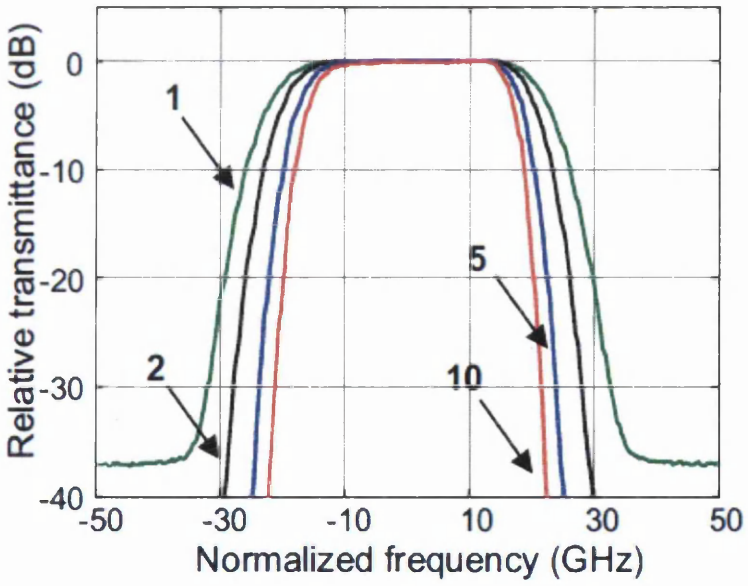

WIDTH OF A CASCADED 50-GHz WSS.

cascaded filters	3-dB bandwidth (GHz)	20-dB bandwidth (GHz)
1	43	59
2	39	52
5	35	45
10	32	40

Figure 2.14: Transmittance of a 50GHz WSS with 3dB bandwidth of 43GHz (20dB bandwidth of 59GHz) and the narrowing effect of several filters [37].

The wavelength de-multiplexing that occurs in via OADM gives rise to spectral filtering of the WDM channels. Importantly in optical networks where several concatenation of

OADMs occurs this can lead to the effective bandwidth at signal receptions been narrowed to percentages of the original deployed spectral spacing's.

.

The figure 2.14 above shows the measured transmittance of a state-of-the-art WSS, which has a (single-pass) 3-dB bandwidth of 43-GHz on a 50-GHz ITU grid. When the measured transmittance is cascaded several times to replicate cascaded filtering, the 3-dB bandwidth is reduced significantly, as depicted in figure 2.14. This indication that on a 50-GHz ITU grid, the available 3-dB bandwidth is approximately 35-GHz when a realistic number of 3-4 ROADM/PXCs are passed through along the transmission link. This bandwidth 35 GHz is therefore a realistic bench-marking in determining if a given modulation format can be deployed within 50-GHz grid channel spacing.

2.6.3: Wavelength Division Multiplexing (WDM).

To characterize a WDM signal, the signal wavelength or frequency can be used interchangeably. The wavelength ($\boldsymbol{\lambda}$) and frequency (f) are related by the equation

$$c = f\lambda \qquad 2.46$$

Where c denotes the speed of light in space, which is $3 \times 10^8\ m/s$. However the speed of light in fiber is actually lower than the above but closer to$2 \times 10^8\ m/s$. Wavelength is measured in units of nanometer ($nm, 1nm = 10^{-9}$) or micrometer(μm $1\mu m = 10^{-6}$). Frequency is measured in hertz (Hz, cycles per second) and prominently megahertz(MHz), gigahertz (GHz), and terahertz (THz), are used in optical communication. Thus using equation 2.46, $1.55\mu m$ corresponds to a 193.1 THz.

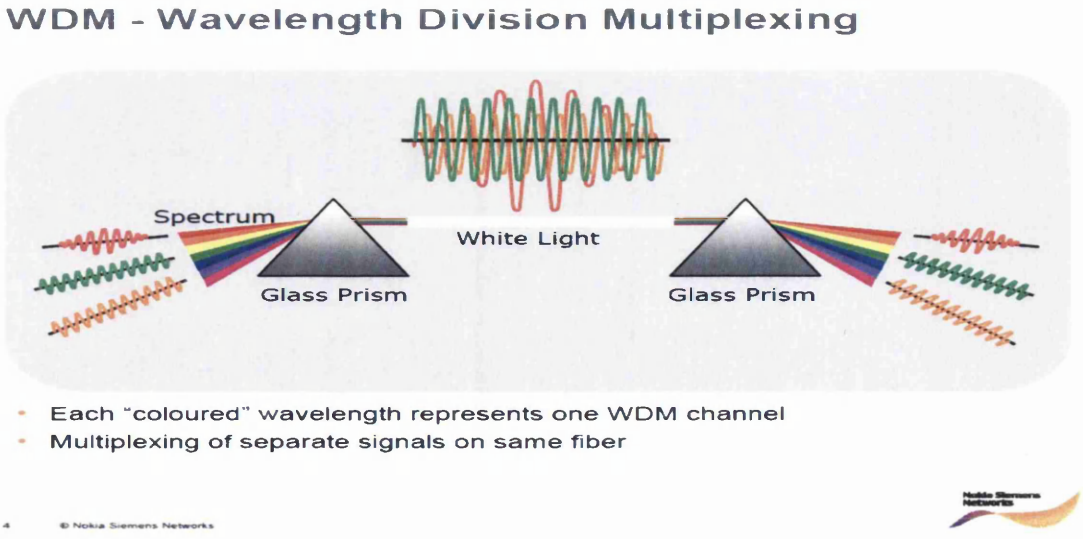

Figure 2.15: Illustration of optical wavelength division demultiplexing and multiplexing [35].

Channel spacing which is essentially the separation between two wavelengths or

frequencies in a WDM system is also very important. The channel spacing of a WDM system can be derived by differentiating the equation 2.11 to get a relationship between change in frequency Δf and change in wavelength $\Delta\lambda$ which is given below as

$$\Delta f = \frac{-c\Delta\lambda}{\lambda^2} \qquad 2.47$$

At a wavelength of 1550 nm channel spacing's of 0.8, 0.4, 0.2 and 0.1 nm corresponds to 100, 50, 25 and 12.5 GHz. These are typical spacing's specified on the ITU grid for WDM systems.

However with the advancements in the technology of optical fiber amplification via EDFA (Erbium Doped Fiber Amplifiers) which by coincidence of nature had an almost flat gain bandwidth of about 32 nm within the C band wavelength which also coincides with the low loss fiber window. Thus enhancing prominence of WDM systems, in that with 100GHz channel spacing in the 32nm gain window of the EDFA simultaneous transmission of 40 channels is possible via the bandwidth gain flatness of the EDFA.

WDM technique is an effective and economic way of increasing system capacity in optical fibers. In that several signal wavelengths are transported in a single fiber without the added cost of additional optical fibers. This thus gives rise to techniques for combining several carrier wavelengths in one fiber at the transmitting point and separating these different wavelengths at the reception points.

There are several optical components available in practical systems for implementing carrier wavelength multiplexing and demultiplexing, Ranging from reconfigurable optical add/drop multiplexers (ROADM), optical crossconnects (OXCs), arrayed waveguide gratings (AWG), to wavelength selective switches (WSS). These multiplexing and demultipexing technology are based on the principle of interference and dispersion i.e. different wavelengths travels with different speeds that enhances the separation of the different carrier wavelengths as WDM channels are transported via a medium which has a change in refractive index, as seen from the figure 2.15 above.

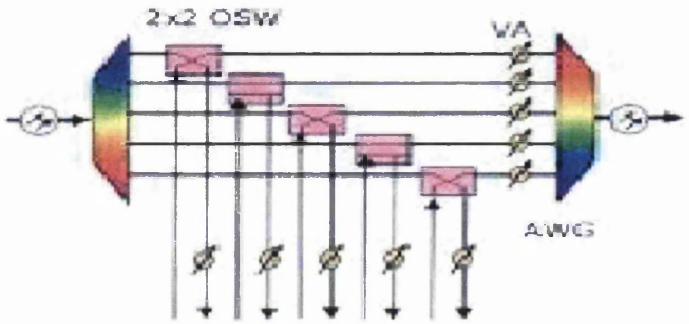

Figure 2.16: Schematic diagram of a reconfigurable add-or drop multiplexer based on optical switches [35].

The figure 2.16 above shows the schematic diagram of a ROADM An ROADM takes in an input signal at multiple wavelengths and specifically drops some of these wavelengths while it passes other wavelengths. Also an ROADM adds wavelengths to the outgoing signal. OXCs essentially perform the function same as an ROADM but they are larger in sizes and have larger numbers of ports compared to ROADM

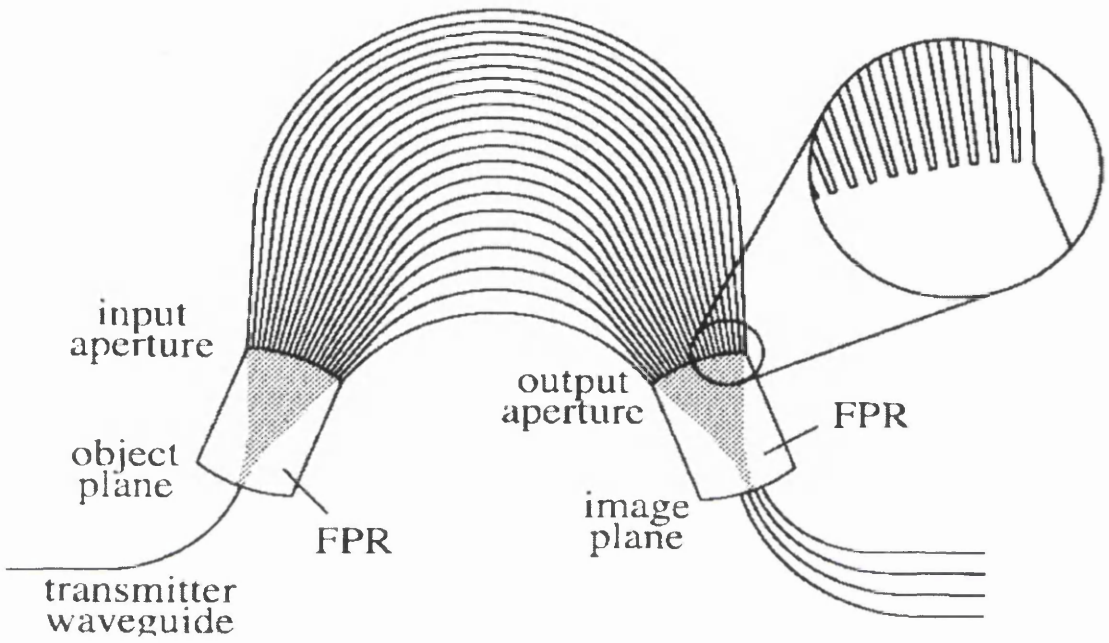

Figure 2.17: Schematic diagram of a waveguide-grating demultiplexer [36].

The figure 2.17 above showing the schematic diagram of a typical AWG that is employed in a WDM network. The Arrayed-waveguide Grating is an optical de -/multiplexer that can be used for both combining and separating (filtering) WDM channels. The incoming light at the transmitter waveguide transverses a free space and enters a bundle of optical fibers, with different lengths and thus different phase shifts are applicable to the different gratings (periodic structures). Phase shifts in an optical signal are wavelength dependent, because the different frequencies of the WDM channels travel with different speeds (frequency dependence on propagation constant). The separated wavelengths converge at the output aperture and are separated into different fibers at different wavelengths. The reverse process from the image plane to the transmitter also represents a multiplexing process. The main characteristic of a practical AWG are low insertion loss (<6dB), good extinction ratio (>20dB), compatibility, can combine channels at 200, 100, 50GHz and can split/combine up to 80 channels at a 50GHz channels spacing.

For modeling purposes in these investigations the optical filtering shall be based on Gaussian filters. The objective of each of the listed filters is to pass selected frequencies while attenuating other frequencies simultaneously, flat bandpass and good stop bands. Another inherent attribute of some frequency period filters are also to shape the spectrum of the signal to achieve a specific shape that are tolerant to certain impairments by controlling the bandwidth and filter orders (Gaussian filters). i.e. In the presence of dispersion in optical modulated systems, optical filtering can be used to achieve a duobinary spectrum: which is known for its very narrow spectrum relative to other modulation formats or signal formats. By delaying a DPSK signal that is fed to 3dB coupler and then constructively interfering the in-phase signal with the delayed signal at the constructive port. Vice versa is implemented at the destructive port to achieve an alternate inversion spectrum. Both the duobinary and the alternate mark inversion spectrum have their different performance sensitivities under different optical fiber mitigating conditions.

Just as band-limiting filtering can be used in optical communications systems to increase the spectral efficiency of the system, offset filtering can also be deployed to improve SE. Unlike band-limited filtering where the carrier wavelength is maintained on the channel , offset filtering is implemented by displacing the carrier wavelength from the channel center. The impact of offset filtering becomes very significant as the channel spacing reduces.

While duobinary is known for its improved tolerance to dispersion [12] due to its narrow spectra extent and the AMI has improved tolerance to fiber non linearity induced distortions [12] due to its inherent alternating phase reversal which enhances suppression of power. Most importantly Gaussian filters are modeled in these investigations, due to its versatility in the different shaping derived from 1st order to higher order Gaussian filters. The transfer function of Gaussian filter is as defined below:

$$f(v) = \exp\left(-\frac{Ln2}{2}\left(\frac{2(v-cf)}{bw}\right)^{2n}\right). \qquad 2.48$$

Where the cf represents the centre frequency of the filter, v represents the frequency offset of the filter, bw represents the3dB bandwidth and n is the order of the Guassian filter.

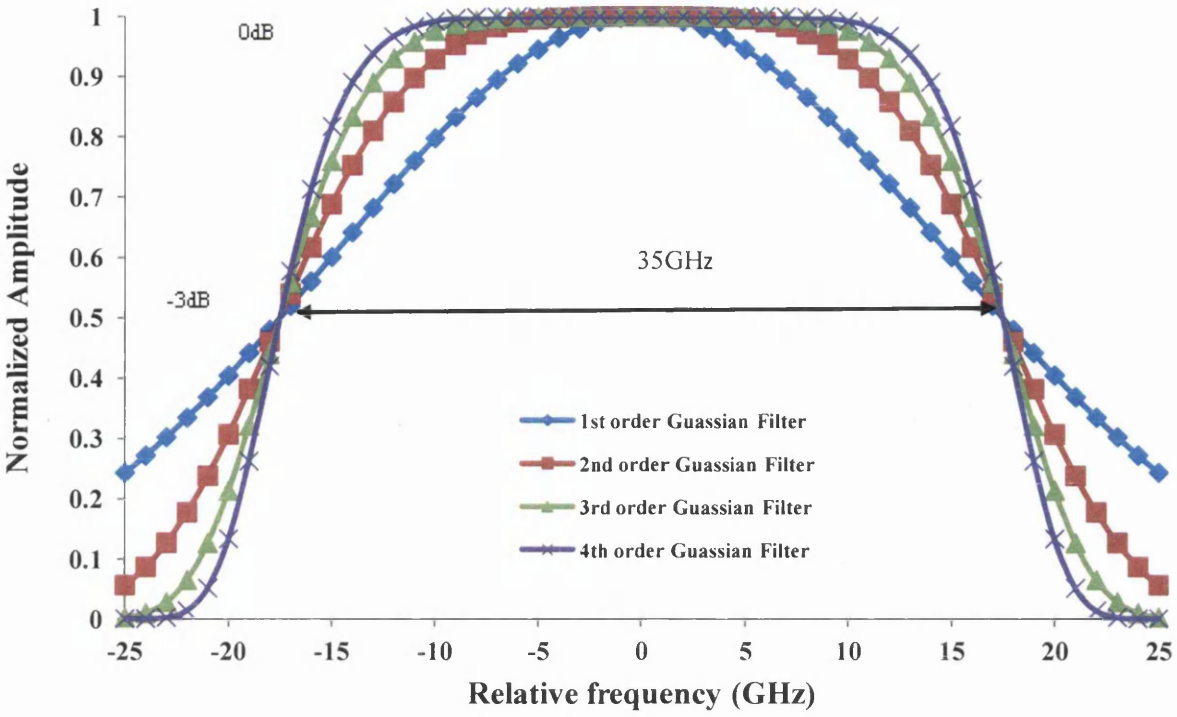

Figure 2.18: Plot of the normalized amplitude for a 35GHz 3dB bandpass against relative frequency (THz), for different orders of Gaussian filters. 1st order – blue line, 2nd order-red line, 3rd order-green line and 4th order-purple line. .

The order of the filter depends on the steepness of the filter skirts, where $n \geq 2$ is for higher order Gaussian filters. From simulation perspective it is more comprehensive to deploy several orders of Gaussian filters on different modulation format so as to understand the impact of different multiplexers/demultiplexers, interleavers or array waveguide grating on real systems. First order Gaussian filters due to its gentle edges have better performance than higher other Gaussian filters in scenarios where dispersion is absence and for single channel transmission. But for (WDM) channels the higher order Gaussians filters have better tolerance to cross talk from adjacent channels, its steeper edges also induces better noise rejection than the first order Gaussian filters.

However recent advancements in the developing optical filters has been reported in [39], such that the signal shaping is much more flexible as compared to the former scenario where the limitations imposed on simulation process only permits that 3rd to 4th order Gaussian filters are modelled to emulate OBPF that are available in practical system.

2.6.4: Mach Zehnder Interferometer.

A MZI is made by connecting two 3dB couplers together, such that the two output of the first coupler feeds the two inputs of the second coupler. An incoming light is split into two paths by the first coupler such that one path has the in-phase signal and the other path has the out-of signal, subject to the difference in path length of the coupler's output arm. Thus the incoming signal is divided into parts as a function of the coupler's coupling ratio. Thus for 50/50 coupler the intensity of the signal is split into two equal parts.

But the phase difference and original phase difference of $\pi/2$ between the two split signals. There is a further phase lag of $\beta\nabla L$ between the two arms of the MZI. This phase lag is a function of the difference in path length. If the path length is the same then the phase of the signal at the arms of the MZI are exactly the same (in phase). But for the design of the MZI which is needed in phase modulation to convert phase to intensity, filtering purposes and in some special cases signal equalization; the path length of both arms of the MZI are different. Such that the signal at the output port 1 (constructive port) of the MZI has a signal with a phase of $\beta\nabla L + \pi$ and a signal phase of $\beta\nabla L$ at the (destructive port) output port 2. Thus the phase difference between the two output ports 1 and 2 is a π.

Thus if $\beta\nabla L = k\pi$, where k is an odd number then the signals at the output port 1 of the MZI interfere constructively (added together). Then for k been an even number the signals at the output port 2 of the MZI interfere destructively (subtraction). Since the relative phase shift been the two arms is wavelength dependent, then the transmitivity is also wavelength dependent: the transfer function of the MZI can be expressed as

$$T_{f(MZI)} = |H(v)|^2 = cos^2(\pi v\tau).$$

Where $T_{f(MZI)}$ is the MZI transfer function, v is frequency of the signal and τ is the time delay (relative) between the two arms of the MZI. The interferences at the constructive and destructive ports of the MZI converts phase modulation to intensity modulation, this is important as the 2 photodetectors located after the MZI do not respond to phase modulation but to intensity modulations.

The significance of the correlative coding formats that are located at the outputs of the MZI, PS-AMI and PS-DB. Aside the conversion from phase to intensity modulation, the MZI actually acts as a band pass filter, due to its frequency dependent transmission characteristics. The relative delay introduced by the longer arm of the MZI, can also be utilized in partially compensating for GVD, this is due to the fact that this delay is opposite to the delay introduced by the optical fiber (smf) anomalous-dispersion (13). Thus unlike the optical

bandpass filter the MZI is signal Amplitude, frequency and phase dependent (complex).

2.7: GNLSE.

The optical transmissions in these research investigations are modeled by the generalized non linear Schrödinger equations GNLSE [20].

$$i\frac{\partial A}{\partial z} + \frac{i}{2}\beta_2\frac{\partial^2 A}{2\partial t^2} - \frac{i\alpha}{2}A = y|A|^2A \qquad 2.49$$

The numeric integration of the NLS is done by estimating the impact of the linear (chromatic dispersion) and non linear (self phase modulation–SPM) fiber impairments on the propagated optical signal, which is solved by deploying the symmetrized split step Fourier method.

Most of the works in this investigation were based on the linear fiber impairments, although in the concluding chapter (7), some investigations is done to evaluate the impact of the contributions of these researches on long haul transmission solely from the DPSK perspective while envisaging the impact of the research on other phase modulated formats. The calculated Q factor, eye diagrams, signal spectrum were deployed in evaluating the performance of high speed offset filtered phase modulated systems.

2.7.1 Optical Signal to Noise Ratio (OSNR)

OSNR is one of the several performance monitoring tools that are essential for evaluating the performance an optical communication transmission system. The Q factor, BER and eye opening of the eye diagram are some of the other important performance indicators. OSNR can simply be defined as ratio of optical signal power to (ASE) noise power.

In a WDM system BER and Q factors cannot be measured without actually demultiplexing all the individual (desirable) channels to make a realistic evaluation. However the OSNR can be derived from each channel of a WDM system via the optical signal spectrum. Thus OSNR offer a simple and indirect performance evaluating tool for optical signal transmission.

Although the OSNR does not give a perfect indication as to the performance of an optical transport system, however it can be directly correlated to the BER performance of a system, using the equation below

$$BER(OSNR) = \frac{1}{\sqrt{2\pi}} \int_{OSNR}^{\infty} \exp\left(-t^2/2\right) dt \qquad 2.50$$

Also OSNR is related to Q factor by the relationship below which can further provide an indicator as to the BER performance of the system.

$$Q_{dB} = 20\log\left(\sqrt{OSNR}\sqrt{\frac{B_o}{B_e}}\right) \qquad 2.51$$

It must be noted that in all the Q calculations employed in this thesis a fixed ratio of 70% of the optical bandwidth is maintained for the choice of the electrical bandwidth.

Where Q_{dB} represents Q factor in dB, B_o represents signal optical bandwidth and B_e represents the electrical bandwidth. OSNR somewhat gives an estimate of the Q factor performance, Q factor and BER are directly proportional as will be shown in the next section. A low OSNR is indicative of high BER and high OSNR translates to low BER, but still the OSNR does not account for the impact of the temporal impairments. However the value of OSNR offers a preliminary performance diagnosis of a multichannel system or initial indication of BER degradation [6]. Also the use of the OSNR in conjunction with Q factor, eye diagram and BER calculation enhance comprehensive evaluating tools for the performance of optical communication systems in the presence of both linear and non linear impairment.

The ASE added via the optical amplifiers in an optical transmission link invariably ultimately limits the reach of the system. The OSNR of an optical communication transmission system can be expressed as shown below.

$$OSNR = \frac{P_{signal}}{P_{ASE}} \qquad 2.52$$

Where P_{signal} represents the power of the optical and P_{ASE} represents the ASE noise power. The P_{ASE} is also given as $2n_{sp}(G-1)hv\nabla f$

Where n_{sp} is the amplifier spontaneous emission factor (population inversion) that is given by $0.5 \times 10^{-\frac{NF}{10}}$, G is the gain of the amplifier (The amplifier gain G is substituted with the fiber span loss $\alpha Lspan$ under the assumption that the gain of each amplifier is equal to the span loss), h is Planck's constant given by 6.626×10^{-34} , v is the optical frequency 193 THz, and ∇f is the bandwidth that measures the NF (it is usually 0.1 nm)

2.7.1 Q factor and Bit Error Rate (BER).

The Q factor can be defined as the measure of fidelity of the optical system transmission or simply measure of eye diagram opening. The eye diagram for optical communication system is the superposition of the individual bit boundaries of the transmitted signal (time domain), thus giving an overall view of the system performance as seen in the opening (or closing) of the eye, or the contribution of the ASE noise as evident with the standard deviation from the mean of the respective intensities of 1`s and 0`s

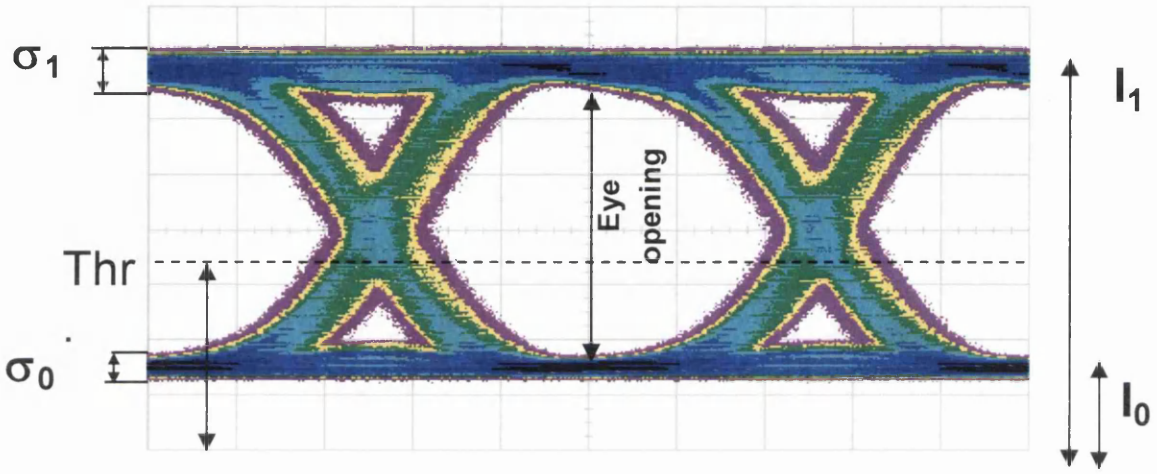

Figure 2.19: Schematic diagram of an eye diagram [39].

The eye diagram allows very long data patterns to be easily visualised and can thus aid in determination of the quality of the transmitted signal. Importantly the Q factor (Q value) also gives a good estimation of the BER using Gaussian statistics.

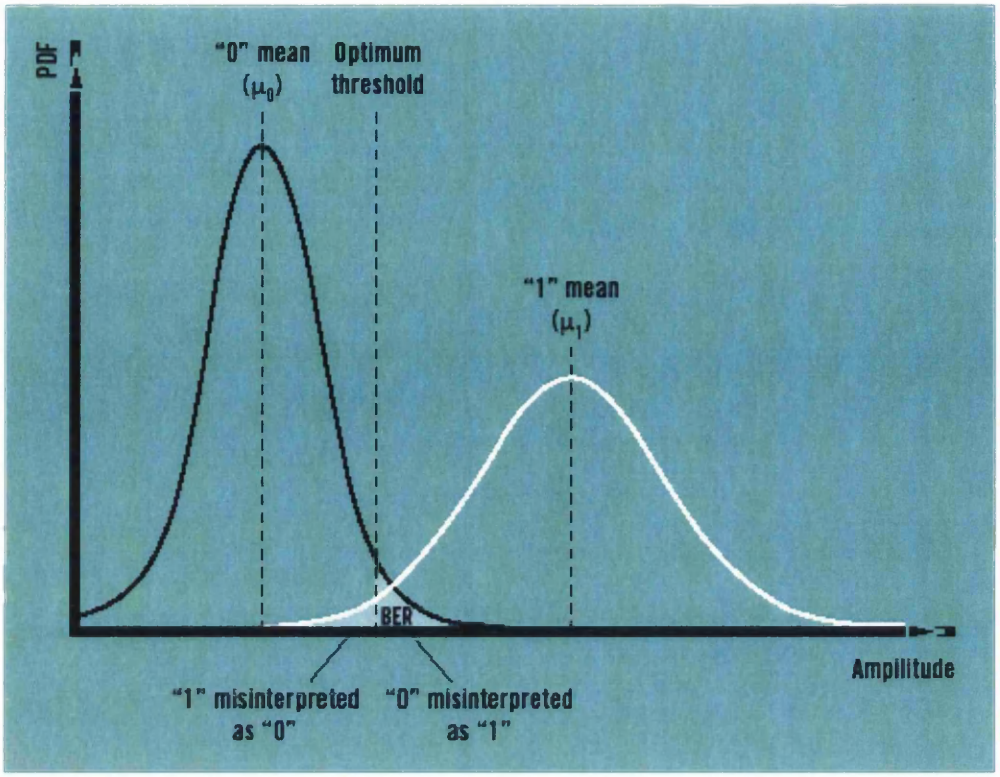

Figure 2.20: PDF with Gaussian distributions [40].

The relevance of the threshold (decision) level as shown in figure 2.19 is to determine whether a "1" or "0" bit has been transmitted. The decision level is a region between the points of intersection of the two PDF shapes, the exact point for the optimum is determined by symmetricity (identical) or asymmetricity (dissimilar) of the two PDF, i.e. for similar PDF shapes for "0" and "1" the optimum decision level will be exactly at the intersections of the two PDFs. Thus the need to vary the decision levels for every simulation investigations so as to increase the degree of accuracy in the calculated "Q factor"

There are certain conditions where "0" can be detected as "1" or"1" is detected as "0", the probability of misinterpretation is shown in figure 2.20.

The probability of error = $P[0]P[1|0] + P[1]P[0|1]$ 2.53

$P[0]$ = Probability a 0 was transmitted

$P[1]$ = Probability a 1 was transmitted

$P[1|0]$ = Probability a 1 was received when a 0 was transmitted

$P[0|1]$ = Probability a 0 was received when a 1 was transmitted

$$Q_0 = \frac{I_D - \{I_0\}}{\sigma_0} \qquad 2.54$$

$$Q_1 = \frac{I_D - \{I_1\}}{\sigma_1} \qquad 2.55$$

$$\text{Q factor } Q = \frac{I_1 - I_0}{\sigma_1 + \sigma_0} \qquad 2.56$$

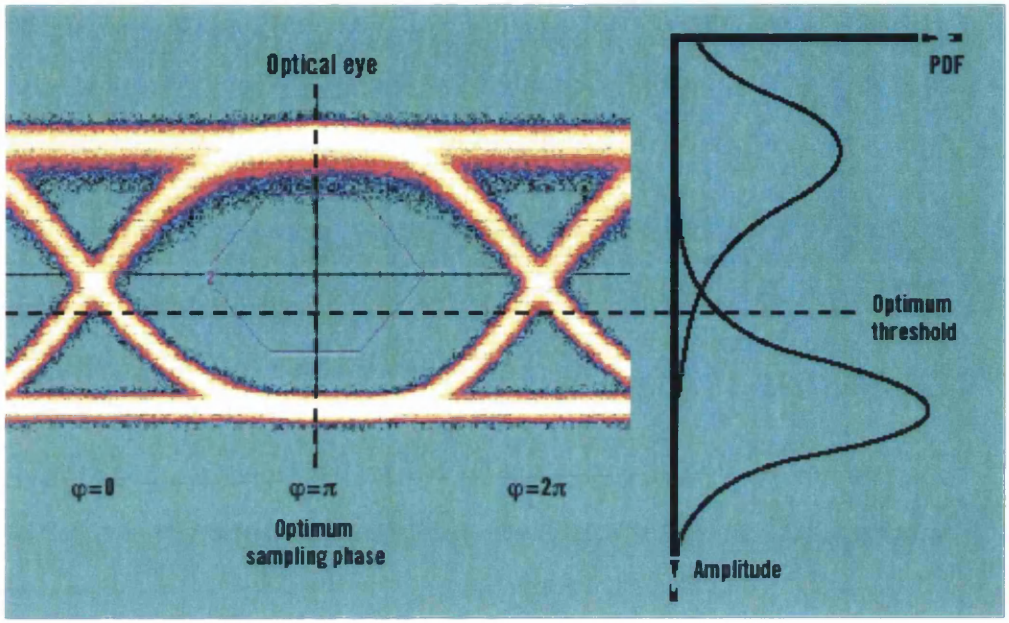

Figure 2.21: Optical eye diagram and PDF with Gaussian distributions [40].

Assuming that the signal distributions are Gaussian, the Q-factor can also be expressed in terms of BER and vice versa. Going back to the definition of the Q-factor to understand how it relates to the BER. The difference in the mean values produces the vertical eye opening. The higher the difference (eye opening), the better the BER will be as the two bell curves drift away from each other and have less overlap. This difference is divided by the sum of the noise distributions (standard deviation) which are illustrated by the width of the bell curves. Increases in noise result in more overlap in the two bell curves resulting in a higher BER.

Importantly when OSNR is high (i.e.) 20dB BER is very low, but Q value calculations is more reliable than BER estimations using the exact detection statistics from the Karhunen-Loeve series expansion (KLSE) or the error counting model (Monte Carlo) calculated in a simulation with high OSNR. In a low OSNR regime Q factor are more qualitative than quantitative, but overall despite the excellent agreement from the Q factor modelled with

Gaussian approximation in these research investigations and reported simulation , experimental investigations on DPSK systems [18, 21, 23] , DQPSK systems in [30, 31, 32]. It must be noted that the absolute value of the Q values are not important rather the change in Q values is much more significant in the simulation investigations implemented with Gaussian approximation. This is because the error becomes very high and Q values are more qualitative than quantitative, the Q values overestimate the BER performance of DPSK systems.

The BER assuming Gaussian noise can be written as $BER \cong \frac{1}{Q\sqrt{2\pi}} exp\left[\frac{-Q^2}{2}\right]$ 2.57

Thus a Q value of 6 and 7 are equivalent to a BER of 10^{-9} and 10^{-12} . It is conventional in most optical communication systems to operate around the forward error correction (FEC) limit which is around 3.8×10^{-3} which is around a Q value of 2.7 (8.5dB). Most optical communications systems employ a FEC overhead of 7%, in this research a 7% overhead is always deployed for the investigations of 40Gb/s data rate. Thus 42.7Gb/s data rates are used in majority of these research investigations.

The Q factor calculated with the Gaussian approach [21] has been widely criticized has been qualitative in evaluating the performance of phase modulated formats [22], while the exact approach has been more quantitative. However in view this observation it must be noted that Gaussian approximation provides very good estimates of the calculated Q factor derived from the exact approach [23, 24, 25] provided certain configuration measures are enshrined i.e. the ratio of optical bandwidth to electrical bandwidth must be keep within the neighborhood

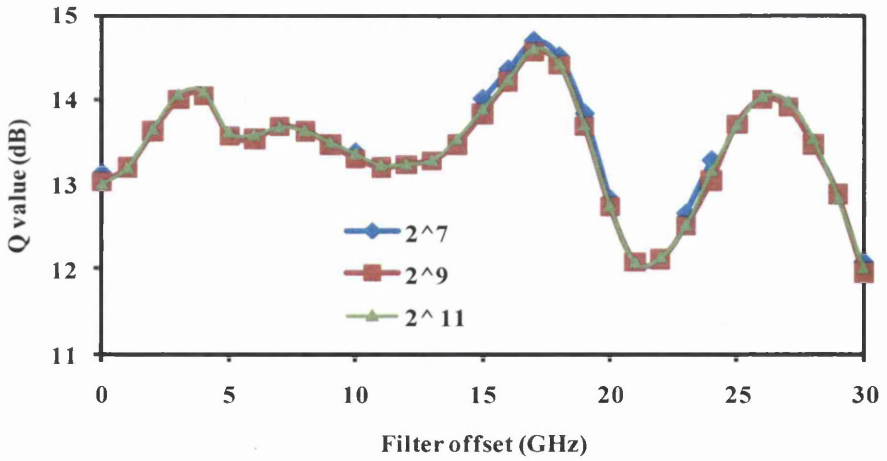

2.22: Q values (dB) plotted against filter offset (GHz) of 35GHz OBPF 42.7Gb/s RZ-DPSK with different PRBSs 2^7 is represented as blue line, 2^9 is represented as red line and 2^{11} is represented as the green line.

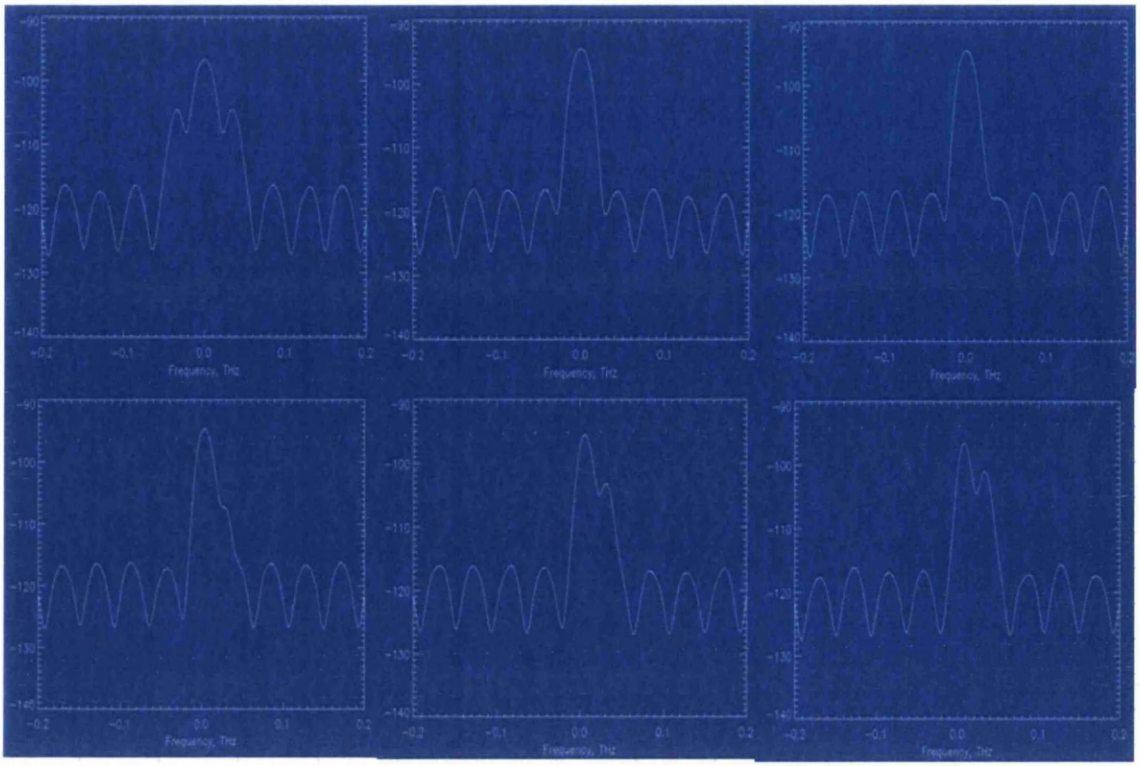

of 70%, the decision level must be varied for all the calculations to derive the best Q performance, pattern dependency must be avoided by implementing several bit sequence, to confirm convergence, varied decision levels for optimum performance, the number of points per bits should be as large as possible. In all the simulations in this investigations 128 points per bit and 100 runs to average the calculated Q was deployed. Both 2^9 and 2^{11} PRBS were employed separately, also 2^7 PRBS with 256 points per bits, 1000 runs to average the calculated Q values were deployed as a measure of confidence to confirm random points on each plots as shown in figure 2.22 .

Thus in all the numerical investigations in these research the above guidelines were conformed to and the resulting performance of the calculated Q were in excellent agreement with similar numerical investigations that have been published [18, 30]. It is important to consider that the absolute value of the Q value is not important performance measure but the change relative change in Q values as different parameters are measured (i.e. chromatic dispersion, filtering penalty etc).

2.8: Chapter 2 Summary.

In this chapter the impact of fiber loss (ASE-noise), chromatic dispersion and narrow filtering performance penalty has been reviewed. Different optical phase modulation formats were also described in this chapter. The advantages and disadvantages of these different modulation schemes were also reviewed. Also different demodulation strategies and components were presented. The GNLSE software deployed for this research investigations was also introduced, whilst analysing the pros and cons of using Q-values calculated via Gaussian approximations.

The review of the linear impairments, different phase modulated formats, demodulation techniques and introduction of the numerical modelling tools in this chapter were to enhance the understanding of performance of optical phase modulated formats in a strongly filtered regime, such that the performances of phase modulated formats can be accurately estimated in the presence of different impairments and comparative advantages of different demodulation techniques can be deployed to reduce the inherent performance penalty in a strongly filtered regimed. Thus the impact of the different phase modulation variants and impact of optimized offset filtering stratagies will be deployed in a strongly filtered regime in subsequent chapters.

2.9: Chapter 2 References

[1] C.R. Menyuk. "Stability of solitons in birefringent optical fibers: Equal propagation amplitudes". *Opt. Lett.*, 12(8):614–616, 1987.

[2] G. P. Agrawal. Nonlinear Fibre Optics, chapter 2, page 37. *Academic Press, San Diego*, 1995.

[3] G. P. Agrawal. Nonlinear Fibre Optics, chapter 2, page 38. *Academic Press, San Diego*, 1995.

[4] G. P. Agrawal. Nonlinear Fibre Optics, chapter 2, page 41. *Academic Press, San Diego*, 1995.

[5] G. P. Agrawal. Nonlinear Fibre Optics, chapter 2, page 43. *Academic Press, San Diego*, 1995.

[6] G. P. Agrawal. Nonlinear Fibre Optics, chapter 3, page 61. Academic *Press, San Diego*, 1995.

[7] G. P. Agrawal. Nonlinear Fibre Optics, chapter 3, pages 63–70. *Academic Press, San Diego,* 1995.

[8] G. P. Agrawal. Nonlinear Fibre Optics, chapter 3, page 63. *Academic Press, San Diego*, 1995.

[9] G. P. Agrawal. "Nonlinear Fibre Optics", chap3, pp 76. *Academic Press, San Diego*, 1995.

[10] T. L. Koch, "Laser sources for amplified and WDM lightwave systems", *in Optical Fiber Telecommunications III*, Eds. New York: Academic, pp. 115–162 1997.

[11] T. Li (ed.), "Optical Fiber Communications: Fiber Fabrication", vol. 1, *Academic Press, San Diego, 1985.*

[12] P.J. Winzer, and R.J Essiambre: 'Advanced modulation format for high-capacity optical transport network', *J. Lightwave Technol*, vol 24, pp. 4711–4728, 2006.

[13] R. Ramaswami, K. Sivarajan, "Optical Networks: A Practical Perspective", 3rd Edition ISBN: 0123740924.

[14] I. Lyubomirsky and C. Chien "Tailoring the Duobinary Pulse Shape for Optimum Performance" *J. of Lightwave Technol*, Vol. 23, Issue 11, pp. 3732- 2005.

[15] T. Tsuritani, A. Agata, I. Morita, K. Tanaka, , and N. Edagawa, "Performance comparison between DSB and VSB signals in 20Gbit/s – based ultra-long-haul WDM systems," in "Proc" *OFC 2001*, OSA paper MM5, 2001.

[16] M.G. Joan, P. J. Winzer, R. Essiambre, S. Chandrasekhar, Y. Painchaud, and M.

Guy "Experimental Study of MLSE Receivers in the Presence of Narrowband and Vestigial Sideband Optical Filtering" *IEEE Photon. Technol. Lett*, vol. 19, no. 16, Aug 15, 2007.

[17] W. Idler, S. Bigo, Y. Frignac, B. Franz, G. Veith "Vestigial Side Band Demultiplexing for Ultra High Capacity (0.64 bit/s/Hz) Transmission of 128x40 Gb/s Channels" in "Proc" *OFC 2001*, Page MM3 May 2001.

[18] K. Tanaka, I Morita and N. Edagawa, "Study on optimum pre-filtering condition for 42.7Gbit/s CS-RZ DPSK signal" in proc *OFC 2001*, May 2001.

[19] F. Heismann "System Requirements for WSS Filter Shape in Cascaded ROADM Networks" in "Proc" of *OFC 2010*, 18 May 2010

[20] G. P. Agrawal. Nonlinear Fibre Optics, chapter 2, page 41. *Academic Press, San Diego*, 2007.

[21] J. L. Rebola and A. V. T. Cartaxo, "Gaussian approach for performance evaluation of optically preamplified receivers with arbitrary optical and electrical filters," *IEE Proc.-Optoelectron.*, vol. 148, no. 3, pp.135–142, Jun. 2001.

[22] P.J. Winzer, "Impact of Filtering on RZ-DPSK Reception" *IEEE Photon. Technol. Lett* , vol. 15, no. 6, June 2003.

[23] N.B. Pavlovic, N.M.S Costa., A.V.T Cartaxo, "Single-Sideband Differential Phase-Shift Keying Asynchronous Carrier-Suppressed Return-to-Zero – A Novel Signaling Format Optimized for Long-Haul UDWDM Systems", *J. Lightw. Technol.*, vol. 27, no. 12, June 15 2009.

[22] E. Forestieri, "Evaluating the error probability in lightwave systems with chromatic dispersion, arbitrary pulse shape and pre-, and postdetection filtering," *J. Lightw. Technol.*, vol. 18, no. 11, pp. 1493–1503, Nov. 2000.

[23] N. Costa and A. Cartaxo, "BER estimation in DPSK systems using the differential phase taking into account the electrical filtering influence," in "Proc". *IMOC 2007*, Salvador, Brazil, pp. 337–340, Oct.2007.

[24] J.M. Kahn and K.-P. Ho, "Spectral efficiency limits and modulation/detection techniques for DWDM systems," *IEEE J. Select. Topics Quantum Electron,* vol. 10, no. 2, pp. 259–272, Mar.-Apr. 2004.

[25] K. Kikuchi, "Phase-diversity homodyne detection of multilevel optical modulation with digital carrier phase estimation," *IEEE J. Select. Topics Quantum Electron,* vol. 12, no. 4, pp. 563–570, July-Aug. 2006.

[26] A H. Gnauck and P. J Winzer, "Optical phase-shift-keyed transmission," *J.*

Lightwave Technol., vol. 23, pp. 115-130 (2005).

[27] D. S. Govan and N. J. Doran, "An RZ DPSK receiver design with significantly improved dispersion tolerance," *Opt. Express,* vol. 15, no 25, pp. 16916-16921 (2007).

[28] O. A. Olubodun and N. J Doran, "Characterization of Asymmetric Filtered 40Gb/s RZ-DPSK System-Strong Filtering Considerations", *Optics Communication Journal,* July 2011.

[29] O.A. Olubodun and N. J. Doran "Performance Improvement of Asymmetrical Filtered 40Gb/s RZ-DPSK Receiver Design-Strong Filtering Considerations" *IEEE/NOC* July 2011.

[30] M. Serbay, J. Leibrich, W. Rosenkranz, T. Wuth, and C. Schulien, "Experimental Investigation of Asymmetrical filtered 43 Gb/s RZDQPSK" *IEEE/LEOS annual meeting* 2006, paper WH5

[31] D. van den Borne, S. L. Jansen, E. Gottwald, G. D. Khoe, H. de Waardt, "Optical Filtering tolerances of 42.8-Gbit/s RZ-DQPSK Modulation" in proc. *OFC* (2006).

[32] L. Zong, J. Veselka, H. Sardesai, and M. Frankel "Influence of Filter Shape and Bandwidth on 44 Gb/s DQPSK Systems" in proc *OFC 2009* post deadline papers, 2009.

[33] G. P. Agrawal, "*Fibre-Optics Communication Systems*", chapter 7, page 291. John Wiley & Sons, Inc., New York, 2002.

[34] M. Finkenzeller (Nokia Siemens Networks) "Delivering 100G per wavelength with today's DWDM infrastructure" M2 Presswire 25 Jun 2007.

[35] www.google.com/oadm+WSS.

[36] M. K. Smit and C. van Dam, "PHASAR-Based WDM-Devices: Principles, Design and Applications" *IEEE J. Select. Topics Quantum Electron*, vol. 2, no. 2, June 1996.

[37] F. Heisman et. al, "43-Gb/s NRZ-PDPSK WDM transmission with 50-GHz channel spacing in systems with cascaded wavelength selective switches" in proc *OFC* (2009), paper OThC1.

[38] R. Shankar et al., "Multi-degree ROADM based on wavelength selective switches: architectures and scalability," *Opt. Comm.* 279, 94-100 (2007).

[39] D. Gariépy and G. Hen "Measuring OSNR in WDM system-effect of resolution bandwidth and optical rejection ratio" documents.exfo.com/appnotes/anote098-ang.pdf

[40] T. Antony and A. Gumaste "WDM Network Design" Cisco Press. Date: Feb 7, 2003.

Chapter 3

Tight Optical Filtering of 40Gb/s DPSK modulation format in a 50GHz Grid

3.1 Introduction:

The main objective of this chapter is to present modelled results on the impact of offset filtering on a 40 Gb/s DPSK system within a tight optical filtering (TOF) regime. A tight (strong) optical filtering regime for 40 Gb/s DPSK system is encountered in a 50 GHz grid. Alternative strategies that can improve performance of the transmitted 40 Gb/s DPSK signals at the receiver i.e. offset filtering (vestigial sideband filtering (VSB) or single sideband (SSB) filtering) in a 50 GHz grid will be explored in this chapter. Why 50GHz grid? This is the available channel spacing in already deployed optical communication systems (10 Gb/s OOK channels in a 50 GHz grid).

There is evidently a need to employ higher wavelength division multiplexing (WDM) data rates ($\geq$ 40 Gb/s) within this available channel spacing i.e. partial DPSK (PDPSK) [1,2,3] and differential quadrature phase shift keying (DQPSK) modulation formats via polarized division multiplexing (PDM) [4,5,6,7]. These already deployed techniques despite their individual merits still have their reasonable limitations in terms of polarize division multiplexing for 100 Gb/s (PDPSK) and OSNR penalty (PDM-DQPSK).

Most modulation formats suffer performance penalties in the presence of tight optical filtering due to narrow-band filtering induced inter symbol interferences (ISI) [8]. However it is important to recall from chapter 2 that RZ signal formats has been shown to have better tolerance to fibre nonlinearity as compared to NRZ signal formats as data rates increase. Thus RZ- signal format with balanced detection will be used in parts of the investigations on the impact of offset filtering on 42.7 Gb/s DPSK system in 50GHz grid.

There are two important ways to execute tight optical filtering: band-limited (BL) filtering and offset filtering. The essential difference between the two TOF strategies is that for the BL filtering the two side bands of the signal are present and for the offset filtering less than two side bands are present and could be vestigial side band (VSB) or single side band (SSB).

Herein the focus will be on the latter variety of TOF, where the centre frequency of the filter is displaced away from the carrier frequency of the channel. It is important to note

that in TOF regimes that the VSB or SSB have shown better performances as compared to double side band (DSB). However with a DPSK signal, there are no well defined sidebands as compared to OOK. Offset filtering of 42.7Gb/s DPSK system, will be implemented mostly with a 3rd order Gaussian filter unless otherwise stated.

This chapter is organised as follows: section 3.1 is based on the chapter introduction. The section 3.2 is based on Partial-DPSK results generated specifically in a 50GHz grid as a benchmark for the numerical model deployed in these investigations and also for basis of comparison with other demodulation techniques.

The section 3.3 is based on the initial contribution of this research via impact of offset filtering on the performance of 40Gb/s 50%RZ-DPSK system in a tight filtering regime. In (section 3.4) impact of offset filtering on 40Gb/s 50%RZ-DPSK system in the presence of chromatic dispersion results are presented.

Section 3.4 presents the impact of a Novel filtering design based on the results generated in section 3.4, introducing OBPFs at the constructive and destructive port of MZI. Although the performance improvement results generated in section 3.4 were marginal as compared to PDPSK, the results for the Novel filtering design were comparable to PDPSK results. Section 3.5 also focuses on modifications to the novel model, to a more practicable model that could be implemented in real systems by detuning the laser.

The section 3.6 presents results based on the performance of Offset filtering at the destructive port in conjunction with PDPSK in a strong filtering regime The section 3.7 presents the summary of the chapter 3 and section 3.8 references for the chapter 3.

Thus faced within a scenario (TOF) where the need to deploy and improve higher data rates (> 40 Gb/s) within a limited channel spacing (50GHz grid) and limited electrical bandwidth there is a need to explore the inherent induced modulation formats (AMI or DB) techniques available at the receiver due to symbol correlations. Thus the induced modulation formats could possibly be further exploited to improve the DPSK systems' tolerance to polarization multiplexing thereby ensuring > 100 Gb/s deployment in a 50GHz grid from the receiver perspective. The DPSK modulation format due to its increased symbol spacing has a 3dB OSNR advantage as compared to OOK modulation format [9,10]; this is largely due to the balanced detection advantage of the DPSK modulation format over the OOK modulation. The 3dB lower OSNR requirement of the DPSK modulation over the OOK modulation for the same average power for same bit error rate (BER), enhances better tolerance to fibre nonlinearity and eventually extend transmission reach by a factor of 2. Most importantly cost

of demodulating encoded DPSK signals is relatively cheap as compared to coherent PSK where a local oscillator (LO) is needed to demodulate the encoded PSK signals.

The simplicity of the DPSK is a major strong point as opposed to the complex and difficult to realise phase tracking (in practical systems) of the Homodyne PSK, also the laser linewidth requirement of DPSK is much more relaxed as compared to Homodyne or Heterodyne PSK detection [11]. The less stringent laser linewidth requirement of DPSK is not just an added advantage, but also the fact that there is no need for an additional laser source at the demodulating stage, which would have required that stability is maintained between the transmitter and receiver (LO) laser linewidths. Thus DPSK offers a cheap and performance sensitive solution for demodulation (phase referencing between two adjacent transmitted bits) of phase encoded modulation format.

Although the performance of DPSK systems is less than BPSK systems [12,13], the relative ease and cost in demodulating DPSK systems makes it more prominent. The improved sensitivity of the DPSK modulation format that can be derived at the receiver for strongly filtered regime PDPSK or by replacing the MZI with a single narrowband optical filter [14,15] make DPSK reception very important in the sense that by carefully managing and optimizing the inherent phase attribute of the DPSK signal (3dB OSNR advantage) and the inherent correlative coding format (memory subdivision of intensity modulation format – enhanced spectral shaping) attribute AMI and DB format that are characterized at output ports of MZI;

The DPSK performance penalty incurred in tight optical filtering regimes and chromatic dispersion limitations can be alleviated [1, 2, 3]. Also alternative strategies that can improve performance of transmitted DPSK signals at the receiver i.e. offset filtering and SSB filtering will be examined .

3.2 Impact of Partial DPSK on a Strongly Filtered 40Gb/s RZ-DPSK system

In this section PDPSK demodulation process will be described, while the impact of free spectral range optimization will also be modelled in a typical 50GHz grid scenario. The generated results will be compared with published numerical and experimental investigations. It is important to understand the physical reasons behind the performance improvement of PDPSK over conventional DPSK systems. Understanding the performance impact of PDPSK most especially in the presence of ASE noise dominated regime, presence of strong filtering

and chromatic dispersion can enhance the design of an alternative demodulation strategy to PDPSK.

DPSK modulation format is conventionally demodulated via an optical bandpass filter, which can also serve as demultiplexer and with a one-bit delay at the MZI. The MZI is based on interferometric application where an incoming signal (phase modulated) is split with a 3dB coupler into two parts. The splitting ratio can also be varied subject to a predetermined aim. In these investigations a conventional splitting ratio will be modelled. The conventional model is a 50/50 coupling process. Thereby each split signal loses half its amplitude, but herein data is not modulated in intensity so it does not affect the performance of the system.

The MZI is inserted between the optical bandpass filter (demultiplexer) and two photodetectors. The relevance of the MZI is that a DPSK signal being a phase modulated signal cannot be detected by the photodector, since photodetector can only respond to optical intensity (intensity modulation). Thus an MZI converts phase modulation to intensity modulation. At the MZI the splitting ensures that the in-phase and out-of-phase signals are at the two different ports via interference of neighbouring bits, such that the delay in between the two ports of the MZI is exactly a one-bit delay (23.42ps).

The bit delay being exactly a bit period leads to two different forms of interferences; constructive and destructive interference at the two output ports of the MZI. A reduction in the period is translated to an increase in spectral range of the signal spectrum and an increase in bit period is a decreased spectral range. But the positive impact of PDPSK is felt more with reduced bit period in the MZI. When there is a less than a 1-bit period delay in the MZI, the interference between successive bits results in a partial interference at the constructive and destructive ports and thus improves the dispersion performance of a band-limited DPSK system [3, 23].

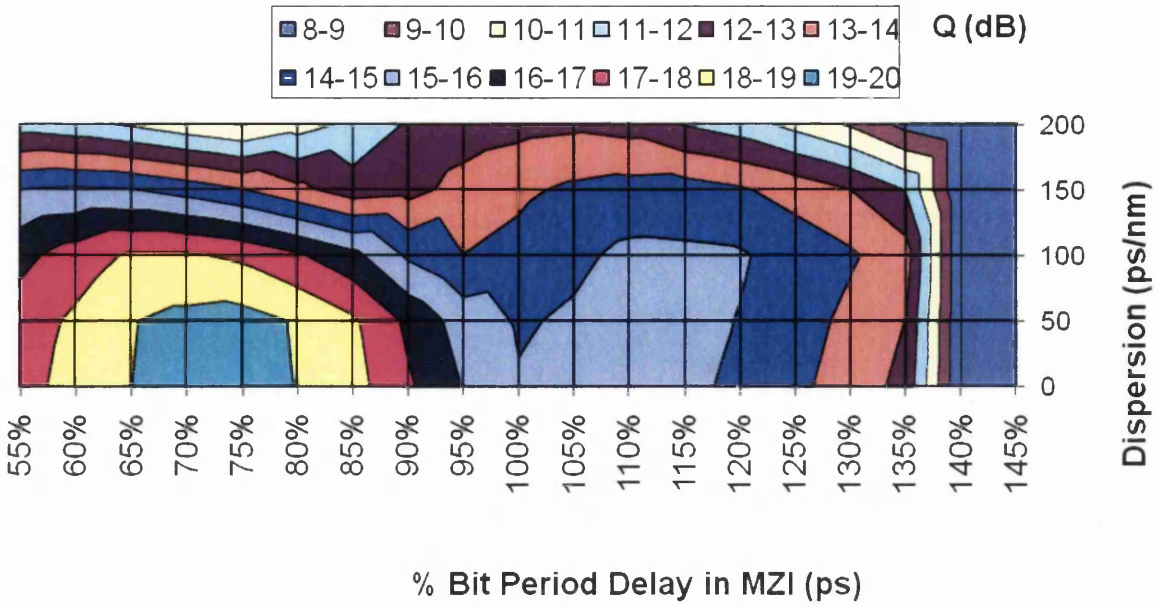

Figure 3.1: Contour plot of Q value in (dB) for % Bit period delay in MZI (ps) on x axis and dispersion (ps/nm) on the y axis for 35GHz OBPF 42.7Gb/s RZ-DPSK system.

The interference of the delayed (< 1 bit period) and un-delayed neighbouring bit results in a net bit period reduction at the output of the MZI. Thus reduction of the net bit period gives rise to smaller pulse-width (increase in FSR) and this leads to better tolerance to chromatic dispersion. Better tolerance to chromatic dispersion in the sense that dispersion leads to pulse broadening, and the pulse-width reduction from the optimized delay of the MZI compensates for this undesirable broadening [1,2,3]. Thus PDPSK leads to reduction in ISI.

The contour plots in figure 3.1 gives an illustration of the performance of a DPSK and PDPSK for a 42.7 Gb/s 50%RZ-DPSK system. The Q-values in (dB) are plotted for dispersion (ps/nm) against a percentage delay in MZI. The plot shows that in the absence of dispersion for a 35GHz OBPF, that PDPSK can improve performance by about 4dB (15-16dB to 19-20dB) in calculated Q, by decreasing the delay in the MZI from 100% to ~70%. The performance of PDPSK in the presence of dispersion can also be seen (figure 3.1) from the 100ps/nm dispersion in which a one-bit delay (100% delays) which has a Q (dB) of 14 to 15dB is improved to 18 to 19dB with bit delay of ~65 to 70% (15.233 to 16.394ps).

The plot (figure 3.1) also shows the performance of having more than a bit delay in the MZI. This (>100% delay) does not lead to any benefit in the absence of dispersion, but for example in the presence of dispersion of 100ps/nm there is a marginal improvement of 1dB for bit delays of 110 to 120%. The results here (figure 3.1) are for a 2^{nd} order Gaussian

filter and for a 20dB OSNR, the results are consistent with simulation and experimental investigations presented in [1, 2, 3, 23].

The most important abstraction from the contour plot above is that deploying PDPSK in a narrow-band filtering regime can result in OSNR recovery as seen in the maximum point of the contour plot which is equal to (19-20dB), which is almost equal to the OSNR of the modelled DPSK system.

In some related papers it has been shown that with PDPSK [1,2,3,21] the performance of the receiver within a strong filtering regime, can be improved significantly both in the presence and absence of dispersion. The impact of PDPSK [22] in presence of dispersion was reported with an RZ-DPSK, resulting in a 12.5% increase in dispersion tolerance. Also in [3] PDPSK was reported with 100% increase in dispersion via optimization of optical filtering bandwidth.

The context of this research is improving DPSK performance within a 50GHz grid. So the results reported in [1,2,3,21,22] are of great important (bench-mark) in designing an alternative technique to improving the performance of a DPSK system in the presence of a combination of ASE noise, dispersion and [20] fibre nonlinearity limited regime. The benefit of PDPSK is derived mainly from optimizing the delay in the MZI and the optical filtering bandwidth. PDPSK without narrow band-limited filtering will result in improved dispersion tolerance but an OSNR penalty. The band-limitation imposed by optical filtering can enhance ASE rejection of DPSK system, and thus reduce performance penalty.

The results achieved in [20] with PDPSK alone in the presence of fibre non linearity was marginal, but the performance improvement was significant in the presence of narrow filtering. Analysing the constructive and destructive port of the MZI in a balanced detected DPSK system in the presence of impairments is essential to get a better understanding of the impact of PDPSK. When a PSK signal is received with a bit delay the spectrum at the constructive port is a duobinary signal and the spectrum at the destructive port is an alternate mark inversion AMI spectrum. The duobinary signal is known for its tolerance to chromatic dispersion and tolerance to tight optical filtering [3,19]. The AMI signal is known for its tolerance to fibre nonlinearity due to the constant phase (π) changes that results in suppression of pulse to pulse interaction [24], unlike the scenario with a duobinary where an odd 0 bit has to be in between the 1 bit for a phase change to occur.

The constant phase change of the AMI results in nonlinear phase compensation due to the net power cancellation at the carrier of the +1 phase change and -1 phase change of the AMI. Since the constructive port alone has an inherent duobinary spectrum which is tolerant

to chromatic dispersion, PDPSK with a balanced detection reduces the pulse width of the delayed signal (increase in spectral range) which translates to a wider spectrum at the outputs of the MZI if the impact of the optical bandpass filter is isolated. But in the presence of narrow filtering, there is a resultant net filtering impact of the MZI and OBPF which is also dependent on the roll-off of the optical filter and results in more ASE noise rejection.

This results in narrowed spectra of the duobinary and AMI. The 3dB advantage of the DPSK can eventually be obtained by optimised filtering and delay of the MZI with a balanced detection. The plot in figure 3.2 shows the Q-value (dB) plotted against chromatic dispersion (ps/nm) for different filter shapes and a fixed bandwidth (35GHz OBPF). The impact of a strongly filtered DPSK system can be seen (i.e. without PDPSK in the absence and presence of dispersion). The different filter shapes i.e. 1st order Gaussian filters and super Gaussians filters (2nd to 4th order), and their different performances are illustrated. The plot indicates that the steeper filters are less tolerant in an ASE noise dominated regime.

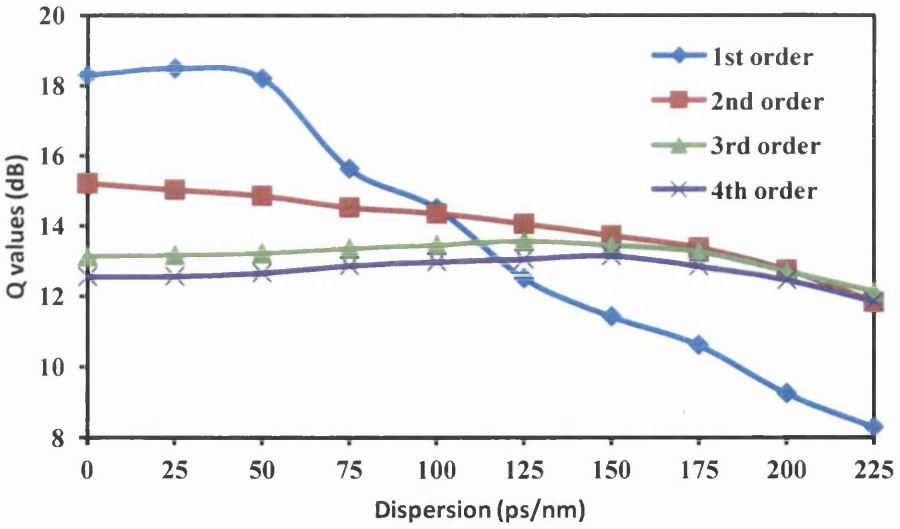

Figure 3.2: Q value (dB) plot as a function of dispersion (ps/nm) for different orders of Gaussian filters for a 35GHz OBPF, 1st order is blue line, 2nd order is red line, 3rd order is green line and 4th order is purple line.

It is particularly obvious that the best performance of the different Gaussian OBPF is that of order 1 having a performance of ~18dB and the same filter has a penalty of ~2.5dB in the presence of 75ps/nm dispersion. The super Gaussian filters, although having a lesser sensitivity in the absence of dispersion, however do offer better tolerance to dispersion than the 1st order Gaussian OBPF. The plot above thus shows the significance of spectral shaping

to the tolerance of some linear impairment. Also comparing figure 3.1 and 3.2, gives an insight to performance of a DPSK signal with optimized filtering and delay in the MZI to dispersion tolerance and OSNR recovery.

3.3: Impact of Asymmetrical Filtering on 42.7Gb/s DPSK systems

Strong Filtering considerations

In this section the performance of an offset filtered 40Gb/s DPSK system will be analysed via numerical simulations in the presence of a dominant ASE noise regime. The offset filtering would be implemented at the receiver. This filtering (offset filtering) has the same performance with pre-filtering at the transmitter. Just as band-limited filtering has been deployed in several investigations [1,2,3] to improve the performance of 40Gb/s DPSK systems. Herein offset filtering will be deployed to reduce the spectrum of the DPSK system at receiver. These offset filtering will be implemented via balanced and two complementary single ended detections, so as to analyse the spectral profiles at the constructive and destructive ports of the MZI.

The demand for 40Gb/s has led to the introduction of phase modulation techniques in optical communications. The simplest of these formats, differential phase shift keying (DPSK), is attractive due to its intrinsic improved OSNR performance and tolerance to fiber nonlinearity. However one of the key requirements is that the 40Gb/s channels must be compatible with the 50GHz channel spacing used in 10Gb/s systems. With DPSK the required filtering robustness can be accomplished using partial DPSK i.e. optimising the delay used in the receiver Mach-Zehnder demodulator [3, 9, 25].

It is however important to investigate other methods to improve DPSK performance with the narrow filter bandwidths encountered in 50GHz WDM systems. In this section a 42.7 Gb/s DPSK system is numerically modelled with a single optical bandpass filter (OBPF) at the receiver. In the majority of the work presented here 35GHz was chosen as the filter bandwidth since this is more representative of the typical overall bandwidth [26] which would be encountered in a 50GHz grid system.

In this work the centre frequency of the OBPF was offset from the carrier frequency of the channel in order to examine the impact on performance of this offset. Offsetting the central frequency of the filter normally results in a performance penalty [27,28], however these investigations found that an improved performance can be obtained for filter offsets which are a large fraction of the bit (symbol) rate. This section focuses on this improvement

which suggests that detuning of the transmit laser could result in significant performance improvement in the narrow optical filtering experienced in 50GHz spaced DPSK systems.

3.3.1 DPSK Asymmetric Filtering Model.

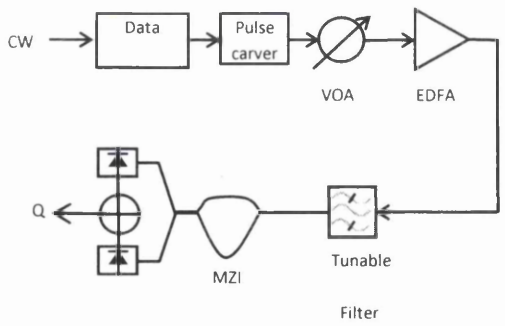

Fig.3.3: 42.7Gb/s DPSK Asymmetric filtering modeled.

The system used in the simulations is illustrated in Fig. 3.3. A 2^9 PRBS is used to drive a Mach-Zehnder modulator (MZM) to produce a 42.7 Gb/s DPSK optical signal, which is followed by a pulse carving MZM generating a 50% RZ signal. By modeling a longer bit sequence or a 2^7 bit sequence leads to practically the same results as with the 2^9 used in the below figures. Noise is added using the VOA/amplifier combination.

At the receiver, the DPSK signal is first filtered by the tunable OBPF, the central frequency of which is initially centred on the signal wavelength and moved by up to 30 GHz. The signal is demodulated by a Mach-Zehnder interferometer (MZI) with a one-bit delay and detected by a balanced receiver. Single ended detection was also investigated in our simulations to identify the effect of offset filtering on the two received signals. The OSNR at the receiver was varied from 14 to 22dB. The filter was generally taken as a 35GHz bandwidth 3rd order Gaussian filter and a 30GHz bandwidth 5th order Bessel electrical filter was used following the receiver. In the following the Q-values were calculated assuming Gaussian statistics.

3.3.2 Results on Asymmetric Filtered 50% RZ-42.7Gb/s DPSK system (Modelled).

In this section the offset filtering results generated from the numerical model will be presented for both balanced and two single ended detection. These results will enable a better understanding of the performance improvement potentials that are inherent at the constructive and destructive port of the MZI for a 35GHz OBPF DPSK system. AMI and DB signal format being both a memory intensity modulation format can both be optimised to enhance the performance of phase modulated signalling. Figure 3.4 below shows the calculated Q plotted against filter offset for three values of OSNR. In all three cases the Q-value initially rises, and then the performance declines as would be expected, however as the offset approaches 20GHz a recovery is observed with a peak value which exceeds the centre filtered value. With all three OSNRs the best performance is found with an offset of 17GHz which is half the filter bandwidth which is in turn a large fraction of the symbol rate. A pronounced minimum is found at 22GHz which is about half the symbol rate and a further peak is obtained at around 27GHz.

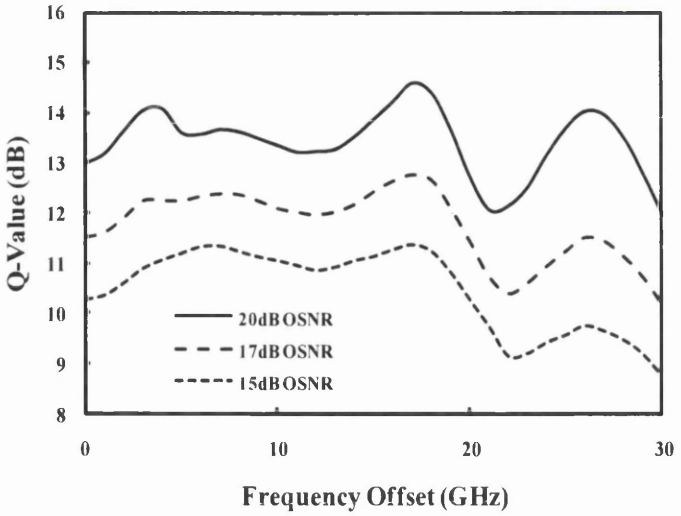

Fig. 3.4: Q as a function of offset for a 35GHz filter for three values of OSNR.

In Figure 3.5 the filter bandwidth is varied for a fixed OSNR. This figure shows that there is a range of filter bandwidth for which improvement for offsetting is observed in DPSK modulation format and that for ~40GHz optical bandwidth the performance improvements are observed around 7GHz offset, which is comparable to the result achieved with a 45GHz OBPF for 42.7GHz, 67%RZ-DPSK in [29]. In another related paper [30] pre-filtering was deployed in a CSRZ (intensity modulation format) and a similar pattern as seen in the graph above was observed.

Further results as will be seen in the later part of this section will reveal a better understanding of the underlining physical background for this intriguing performance with offset filtering of a 42.7Gb/s DPSK system. The peak at half the filter bandwidth is particularly clearer for filter bandwidths around 35GHz. Moreover the peak at around 5GHz becomes more pronounced for narrower filtering and specific filter bandwidths can exceed the larger offset peak. A third peak is observed which is only present at large OSNRs.

Thus the advantage of offsetting identified here should be understood to be filter bandwidth dependent.

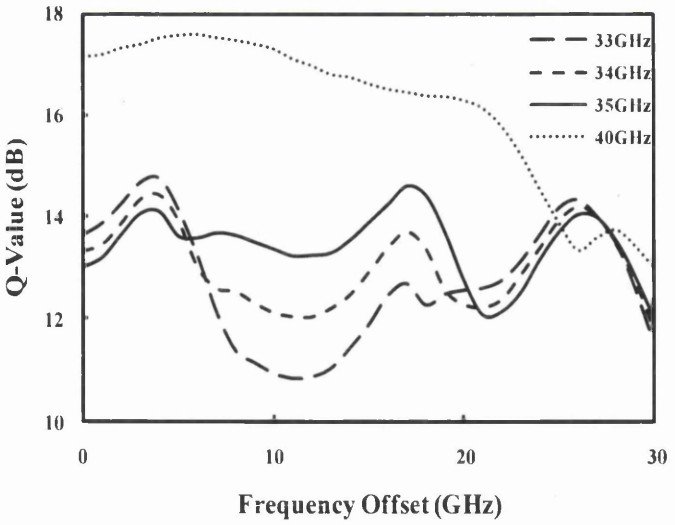

Fig. 3.5: . Q value (dB) against Frequency offset (GHz) for 33 (dashed line), 34 (small dash), 35 (continuous) and 40GHz (dotted), 3 dB filter bandwidth for OSNR of 20dB.

Fig. 3.6 compares balanced detection performance with single ended performance at the constructive and destructive ports for an OSNR of 20dB. This figure illustrates that, as has been noted previously [14], for this strong filter, single ended detection (at zero offset) is slightly better than balanced detection under certain conditions [31]. The particular condition here is the filter shape, which is a 3rd order Gaussian filter. For a 1st and 2nd order Gaussian filter the balanced detection performs better than the single ended detections in a strong filtering regime.

However it is clear that the destructive port performance rapidly increases with offset so that balanced detection is generally superior to single ended performance. There is an exception around 10GHz offset where the destructive port alone gives the best Q. The peak around 17GHz (half filter bandwidth) is only present at the constructive port. It is clear that the improved performance at 17GHz offset is largely due to the signal quality at the destructive port where the Q-value has increased by >5dB compared to the centred filtered case. The constructive port shows a ~1.8dB penalty when the filter is offset 17GHz from the channel wavelength which declines still further for larger offsets. The trend in Fig. 3.4 is also obtained for other values of OSNR.

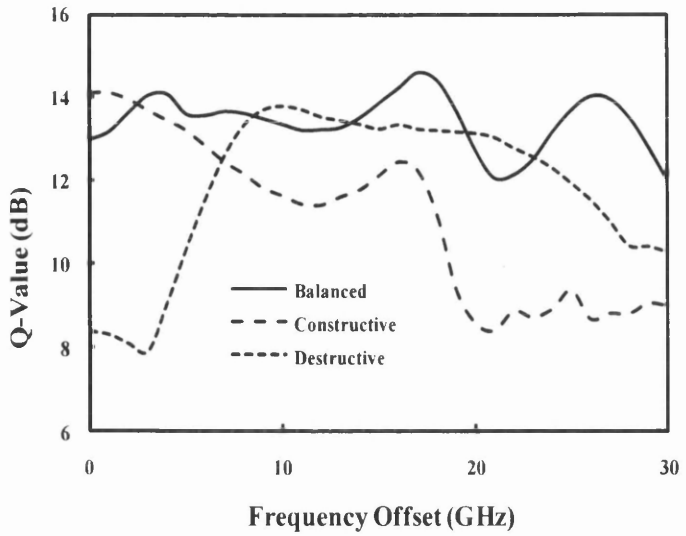

Fig. 3.6:. Q-value (dB) dependence on the filter offset (GHz) for balanced (continuous) , constructive (dashed) and destructive (dotted) single ended detections at both ports of the MZI for an OSNR of 20dB.

Fig. 3.7, which is a key result of this section, shows the Q value dependence on OSNR comparing the 17GHz offset with a centred filter. The difference in performance between the centred filter and 17GHz offset filter is as much as 1.8dB at large OSNR but reduces as the OSNR decreases.

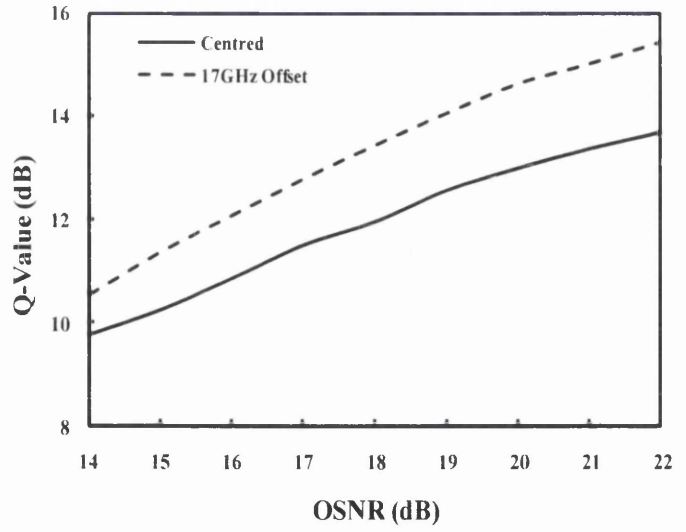

Fig. 3.7: Comparison of Q value (dB) for centred (solid line) and 17GHz offset (dash line) filter as a function of OSNR (dB) for a 35GHz 3dB OBPF 3rd Order Gaussian filter.

Nevertheless it is remarkable that a significant improvement (~1dB) can be observed even for low OSNR and the improvement seen here is in complete agreement with results in [30]. It is worth recalling that the results presented here could be obtained by detuning the CW laser source.

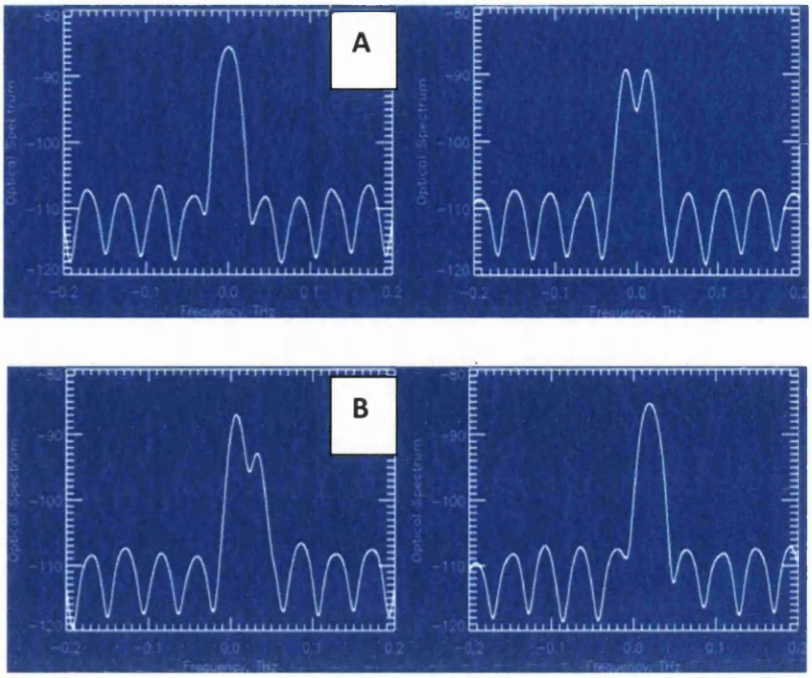

Fig. 3.8: Optical spectra at the constructive (left) and destructive (right) port of the centred (A) and 17GHz offset (B) filtered DPSK.

3.3.3: Discussions on simulation results for Asymmetrical Filtered 50% RZ-42.7Gb/s DPSK system.

In order to better understand the underlying reason for the improvements observed in Fig. 3.7, it is important to recall the effect of demodulation on DPSK signals. It is well established that the output of the constructive port is duobinary (DB) and the signal at the destructive port is alternate mark inversion (AMI) [19, 31, 32]. DB because of its narrower spectral width (narrower than AMI spectrum) has superior performance with respect to filtering whilst the AMI due to its wider spectral width has lower tolerance to narrow bandlimited filtering. The effect of offsetting is to greatly improve the AMI performance whereas the DB performance is degraded to a lesser extent. Thus as expected, there is an initial peak in performance as the AMI signal (destructive port) improves with detuning; this is observed in these calculations at around 5GHz.

The second and most important peak in performance is at an offset approximately half the filter bandwidth. At this offset the DB and AMI spectra can be considered to be reduced to something more like vestigial side band (VSB) signalling. It is known that DB may be derived from AMI by side band filtering [32]. This alteration is also evident in the spectra displayed in fig 3.8 where we see that the destructive port now has a single lobe which is

characteristic of DB. At this point the constructive port spectrum changes to display a side lobe [33].

The physical origin of the peak in performance at the half filter offset coincides with the optimum position for AMI to DB conversion, underlying the mechanism which leads to this peak. The tolerance of VSB signalling [34] to tight filtering is well known with corresponding good rejection of ASE and it is therefore not surprising that the best performance occurs near the optimum for producing such signals from either port.

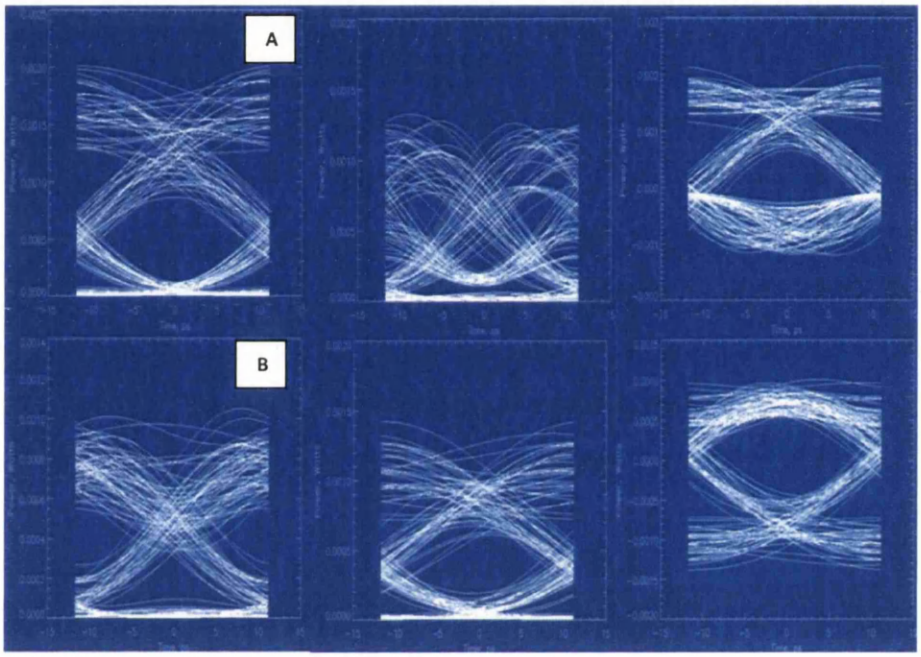

Fig. 3.9: Constructive (left), Destructive (middle) and Balanced detection (right) optical eye diagrams for the centre filtered DPSK (A) and the 17GHz offset filtered signal (B).

In Fig. 3.9 the eye diagrams for constructive, destructive, and balanced detections are compared for 20dB OSNR. This figure shows that the destructive port offset eye resembles the DB eye seen in the constructive port in the centre filtered case. The offset constructive port is no longer DB but has a more open eye than the contrasting centre filtered destructive eye. The balanced eye for the offset case is an inverted form of the centre filtered balanced eye reflecting the spectral change at the destructive port to a DB signal, confirming the logical inverse relationship that exists between the constructive and destructive port of the MZI.

The observed improvement in Q originates from the destructive port becoming DB and the constructive port remaining with a relatively good eye. It should be noted that the performance of DPSK modulation can in principle be improved at the demodulator due to the correlative coding format that are inherent at the output of the MZI. These correlative coding formats AMI and DB thus can with appropriate filtering strategies be spectrally shaped to

The desire to extend capacities of installed systems, different needs of the end users and cost saving drive by the service providers can be met if the tolerance of phase modulation formats to chromatic dispersion and polarization mode dispersion can be improved. In this section, via numerical investigations the performance of strongly filtered DPSK systems will be investigated in the presence of chromatic dispersion by offsetting the centre frequency of the OBPF at the receiver. Chromatic dispersion leads to pulse broadening on the time domain, due to different wavelengths travelling with different speeds. This leads to a linear phase shift on the spectral domain (frequency chirp) that leads to increased intersymbol interference and eventually degrades the sensitivity of DPSK systems. Thus reasonably the impact of offset filtering on DPSK systems in the presence of chromatic dispersion should result in increased performance penalty. The interesting scenario that evolves at the output of the demodulator (MZI) of a balanced detected DPSK, where DB and AMI (memory signal formats) are present might have implications in the presence of chromatic dispersion.

Most especially when offset filtering has been identified as a filtering strategy for converting AMI to DB [32]. The impact of offset filtering in a 35GHz OBPF DPSK system has been [39,40] and offset filtering has been reported to improve system performance largely due to a relative beneficial constructive and destructive ports of MZI . Optimizing the offset filtering at the receiver, in the presence of chromatic dispersion will be implemented numerically so as to characterize the performance. Of course this could have implications on transmission systems, as a balance between chromatic dispersion effects and fibre nonlinearity effects evolves as data rates increase beyond 40Gb/s.

$$L \geq L_D \approx L_{NL}$$

Where L is fiber length, L_D is the dispersive length and L_{NL} is the nonlinear length in km, recalling from chapter 2 that as the dispersive length becomes comparable to the nonlinear length then interplay between GVD and SPM will lead to a unique pulse behavior as compared to GVD or SPM alone. The balance or interplay between GVD and SPM becomes more rampant as data rate increases and for long haul transmissions. Thus keeping in view the interplay between the GVD and SPM in long haul transmissions it will be necessary to investigate the impact of offset filtering at the receiver on chromatic dispersion performance of $\geq$ 40 Gb/s data rates.

In section 3.4 it was shown that offset filtering can improve the performance of a conventional strongly filtered DPSK system in the presence of ASE noise [39, 40], the improvement seen in the last section was occasioned largely by the offset filtering of the AMI

signal [32, 33] at the destructive port of the MZI, thereby leading to ~5dB penalty reduction at the port. However the improved performance from offset filtering in section 3.3 was largely due to balanced detection of two sensitive ports of MZI having two-memory-intensity-modulation formats. Herein (context of chromatic dispersion) it will be interesting to characterize the impact of the memory (VSB-AMI and VSB-DB) inherent at the MZI outputs on the performance of 40Gb/s RZ DPSK systems in the presence of chromatic dispersion.

3.4.1 DPSK Asymmetric Filtering Model- Chromatic Dispersion considerations.

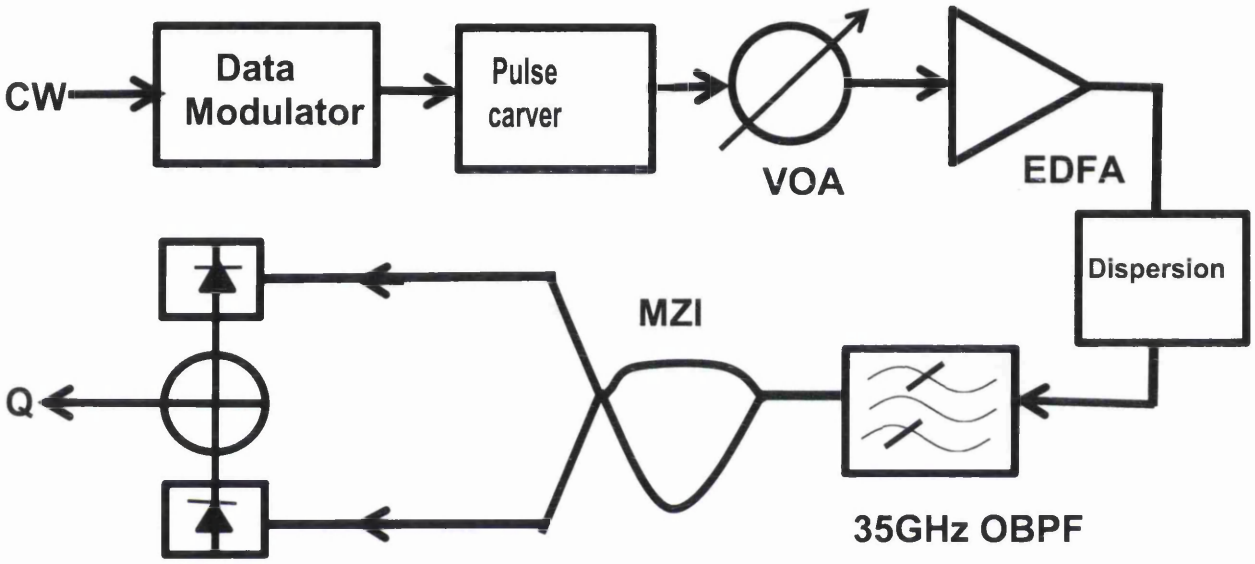

Figure 3.10: System model for offset filtering in the presence of Dispersion

3.4.2 42.7Gb/s 50%RZ-DPSK Asymmetric Filtering- Chromatic Dispersion considerations results.

In this section the modeled results for the impact of chromatic dispersion on the performance of an offset filtered 42.7 Gb/s 50%RZ-DPSK system as shown in the figure 3.10 above will be presented in other to analyze the impact of balanced detection and the two single ended detection in this scenario. The impact of the changes in the spectral profile at the constructive and destructive ports of the MZI as the filter is offset in the presence of some chromatic dispersion will also be presented so as to understand the physical reasons behind the performance evolutions as the filter is displaced away from carrier frequency.

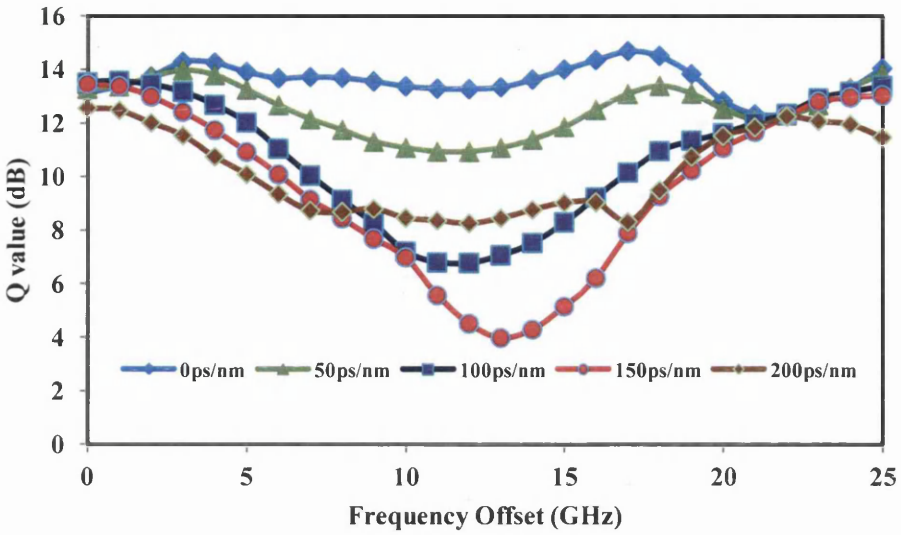

Fig. 3.11: Q-value (dB) against filter frequency offset (GHz) in the presence of some chromatic dispersions for balanced detected 35GHz OBPF-42.7Gb/s 50%RZ-DPSK system for an OSNR of 20dB.

The results in figure 3.11 show the Q-value in dB for 50%-RZ-DPSK signals filtered at the receiver with a 35GHz OBPF (OSNR of 20dB) with frequency displacements from 0 centre frequency to 25 GHz in the presence of 0, 50, 100 150 and 200ps/nm residual dispersion. The results shows that the Q values initially rises then falls and then starts to ascend again before it reaches an optimum value around 17GHz offset for the case in absence of chromatic dispersion.

The improvement for the 0 dispersion for the optimized ~17GHz offset is around 1.8dB improvement over the 0 offset [39, 40]. The improvement for the optimized offset in the presence of 50, 100 and 150ps/nm is ~1.5, 0.6 and a penalty of 0.16dB respectively over the 0 GHz offset. The results shows that for dispersions of 0 and 50ps/nm, the 19GHz offset showed the best performance and for higher residual dispersions the 20GHz offset showed the best performance till the dispersion increased to 150ps/nm. Despite the dispersions benefit of offsetting the OBPF from 0 to 100ps/nm, the benefit declines to a recovery in the presence of chromatic dispersion of 150 ps/nm. The impact of offset filtering in optical communication systems generally leads to performance penalty.

3.4.3: 42.7Gb/s 50%RZ-DPSK Asymmetric Filtering- Chromatic Dispersion considerations results.

The results shown in the previous section demands a spectral resolution in order to understand the chromatic dispersion performance of a strongly filtered DPSK system in a 50GHz grid. These spectral profiles will enable better understanding of an asymmetric filtered DPSK system in a more complicated regime that is dominated by the interplay between GVD and SPM. Fig. 3.12a below shows the contribution of the spectra of the two ports of Mach-Zehnder Interferometer MZI, constructive and destructive port.

The first two plots of figure 13a shows the presence of duobinary and alternate mark inversion (AMI) signal for the 0 centered filtered system. The spectra in figure 3.12b shows a reduction in one of the lobes of the AMI now transformed at the constructive port and a well vestige AMI signal at the destructive port now having a duobinary like shape.

The improved performance of the narrow filtered DPSK with optimized offset filtering is largely due to the smoother spectral profile of the spectra at the constructive and destructive ports of the MZI of the optimized offset filtered DPSK system [25]. The performance of strongly filtered DPSK system with the large offset is comparable to that of the symmetric filtering despite the massive reduction in the spectrum of the offset filtered DPSK system.

This performance in the presence of dispersion is attributed to spectra at the constructive port and destructive port of the offset filtered DPSK system. At the constructive port the initial duobinary spectrum has become vestige to an AMI spectrum. There has been reported improvements in sensitivity of SSB-DCS signaling [32] in the presence of dispersion, also the spectrum of the initial AMI at the destructive port has become reduced to a more sensitive duobinary spectrum [33] although the performance of the offset filtered DPSK in the presence of dispersion can generally be termed as comparatively equivalent to the symmetric filtered case for dispersions ranging from 0 to 100ps/nm, beyond which the performance of offset filtered DPSK is actually a recovery in performance.

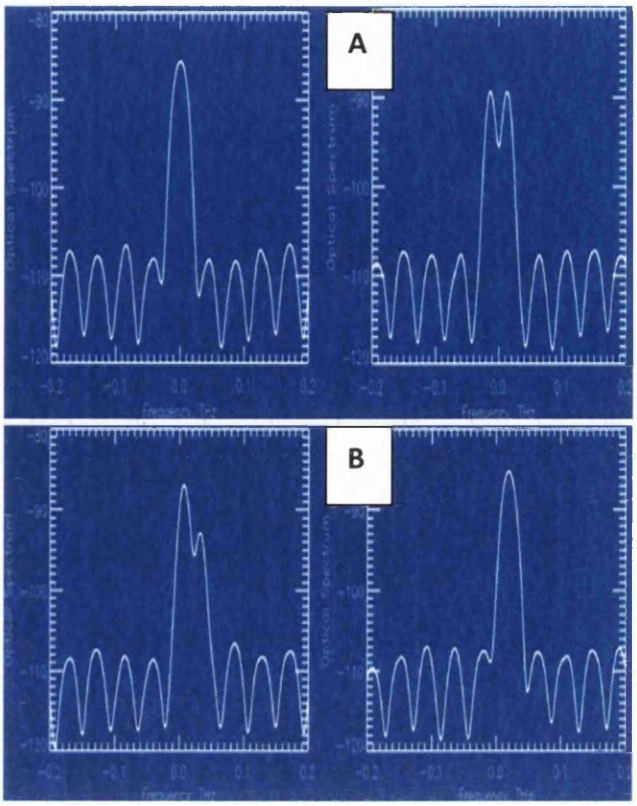

Figure 3.12: (a) Spectra of the constructive, destructive (conventional filtered) and (b) constructive and destructive of the (offset filtered DPSK system).

This is largely due to the spectrum of the duobinary which is the most sensitive signal format in terms of chromatic dispersion performance from its narrow spectrum. This is due to the duobinary signal's inherent 3 optical symbol levels (+1,0,-1) used in demodulating 2 electrical signals. These 3 symbols in a duobinary signal actually interfere; thus in the presence of dispersion, a 1 bit level interferes with a 0 bit level destructively and thus lowers the level of the 0 bit signal as opposed to constructive interference that will occur in other narrow spectrum signaling, i.e. NRZ.

It is however remarkable that the performance of a much vestige spectrum could have comparable performance to the band-limited duobinary signal (conventional filtering). Thus the chromatic dispersion performance of an offset filtered strongly filtered 35GHz OBPF 42.7Gb/s DPSK systems can recover with very large offsets due to relative sensitivity of VSB AMI and VSB DB that leads to further ASE noise suppression and better memory performance from the inherent partial response coding that evolves from offset filtering at the MZI output ports. Comparing the performance of offset filtered 42.7Gb/s DPSK in section 3.3 (ASE noise dominated regime) [39, 40] to the performance presented in this section in the presence of chromatic dispersion [41]; in the presence of chromatic dispersion the performance of offset filtered 42.7Gb/s DPSK system is at best a recovery performance

because the performance difference between the optimized offset and centred filtered case progressively decreases as chromatic dispersion increases. Also unlike the result in section 3.3 which showed that the optimized offset for a 35GHz OBPF filter is always around 17GHz offset (half the bandwidth), but the results in section 3.4.2 shows that the optimized offset filtering is a function of the chromatic dispersion present .

3.5 Novel offset filtering design on an 42.7Gb/s RZ-DPSK system

The impact of offset filtering on strongly filtered DPSK has been presented in section 3.4 [39,40] in the presence of ASE-noise dominated regime, however the different peak performance sensitivity of the constructive and destructive single ended detection with offset filtering has shown that despite the beneficial advantage of the balanced detection, that conventional Strongly filtered DPSK performance is not fully optimized because of the lesser performance of the AMI signal that is inherent at the destructive port in the presence of tight (narrow) filtering.

Having in mind that the constructive port has the data and the data-'bar', which is the logical inverse of the data, is located at the destructive port, and there are equal amount of information at both ports [25]. The duobinary signal is optimized by bandlimited filtering and AMI signal is optimized by offset filtering in the presence of tight optical filtering or chromatic dispersion. The investigations in section 3.4, although showing some marginal performance improvement, the inherent performance with the model in section 3.4 is not as pronounced as the improvements inherent with PDPSK (section 3.2). Thus in this section a novel filtering model that seeks to improve the performance of a strongly filtered 42.7Gb/s DPSK system in a tight filtering regime (50GHz grid) is introduced [39].

3.5.1 Novel filtering justification.

The novel offset filtering 42.7Gb/s 50%RZ-DPSK was modelled with two filters at the constructive and destructive ports of the MZI. The performance of the two models is essentially the same when symmetric filtering is deployed. The motivation for this novel design can be seen in these earlier papers [29,30], where the performance of asymmetric filtered CSRZ-40Gb/s DPSK system can be seen to improve over the symmetric filtered case.

The difference between the work investigated in that paper and this work was that emphasis of the paper was mainly on 3dB filter bandwidth of 45GHz. Although a particular plot in figure 2 of [30] gave some indications to the performance improvement of asymmetric filtering within narrow bandpass filters with CSRZ signal. This work is solely based on

filtering 3dB bandwidths between 33 to 40GHz bandpass filters. The choice of 3dB bandwidth of 35GHz is more representative of filtering bandwidth available for a DPSK modulation format in a 50GHz grid due to concatenation of several OBPFs in a link.

In the majority of the work presented here 35GHz was chosen as the filter bandwidth since this was more representative of the typical overall bandwidth which would be encountered in a 50GHz grid system. The degree of asymmetric filtering improvement recorded here is around half (50%) of the filter bandwidth, although the choice of offset filtering is largely dependent on filter bandwidths.

The detailed physical explanation for the penalty reduction of the asymmetric filtering in a strong filtered regime was reported [40]. In this work the center frequency of OBPFs (33 to 40GHz) were offset from the carrier frequency of the channel in order to examine comprehensively the nature of the performance impact of offset filtering in a 50GHz grid. Offsetting the central frequency of the filter normally results in a performance penalty [27, 28] however [40] found that an improved performance can be obtained for offsets which are a large fraction of the bit (symbol) rate. In this section further investigations into the nature of the improvement [29,30,39] (from demodulation perspective) which suggests that detuning of the transmit laser could result in significant performance improvement in the narrow optical filtering experienced in 50GHz spaced DPSK systems is carried out.

The focus of this section is thus mainly on performance improvement in a 42.7Gb/s DPSK system with a novel design based on the analysis of the nature of the performance of the conventional model's constructive and destructive port of the MZI under asymmetric filtering in a strong filtering regime.

3.5.2: Novel DPSK Asymmetric Filtering Model.

The model used in simulating the novel offset filtering design will be described in this section. The results achieved in section 3.4 that have been confirmed by numerical and experimental investigations in [29, 40] gave further insights as to performance potentials that are available at the output ports of MZI: the fact that the correlative coding formats that are inherent at the MZI output have a memory capacity that can be further induced by the pre-filtering [43]. Thus this model seeks to explore the advantages of the DB and AMI by deploying different levels of offset filtering to improve the sensitivity of the two correlative coding formats (memory-formats) located at the constructive and destructive ports of the MZI.

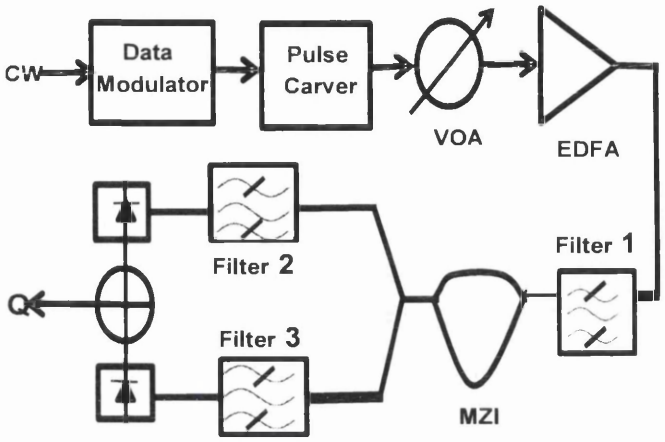

Fig 3.13: Novel DPSK model

The model illustrated in Fig 3.13, is same as the figure 3.3 but the extra filters are employed at the output of the MZI, thus the configurations and parameters used are same as in fig 3.3 section 3.4. then the signal at both output ports of the MZI is filtered by 2 identical tuneable 35GHz OBPF. The filtering arrangement of the novel design does not lead to any difference in performance compared with conventional model, when the two filters are symmetrical filtered.

The signal is followed by a balanced receiver. Single ended detection was also investigated in our simulations to identify the effect of offset filtering on the two received signals and confirm same performance for the single ended detections for both the conventional DPSK configuration and our novel configuration. This is necessary because any difference in performance between the single ended detections at both the destructive port and the constructive port for offset filtering of the conventional and novel will be indicative of an anomaly in the result so derived from the novel configuration. The OSNR at the receiver for the investigation was varied from 15 to 22dB for the novel configuration.

3.5.3. Results for Novel DPSK filtering design.

In this section simulation results generated from the novel model illustrated in section 3.5.2 will be presented. Firstly the novel DPSK offset filtered receiver design's results will be presented at an OSNR of 20dB, then the performance of the novel design will be compared to the performance of the conventional model via symmetric filtering. Thirdly the performance inherent from the model will be compared with the conventional model performance at different OSNRs. This will be done to quantify the performance improvement or penalty incurred from using the novel offset filtering design as compared to the conventional model.

Also in this section an initial result generated in section 3.3 will be presented for 42.7Gb/s 50%RZ-DPSK system by comparing the balanced and two single ended detections by using the performance of the conventional 35GHz OBPF 42.7Gb/s DPSK performance as reference.

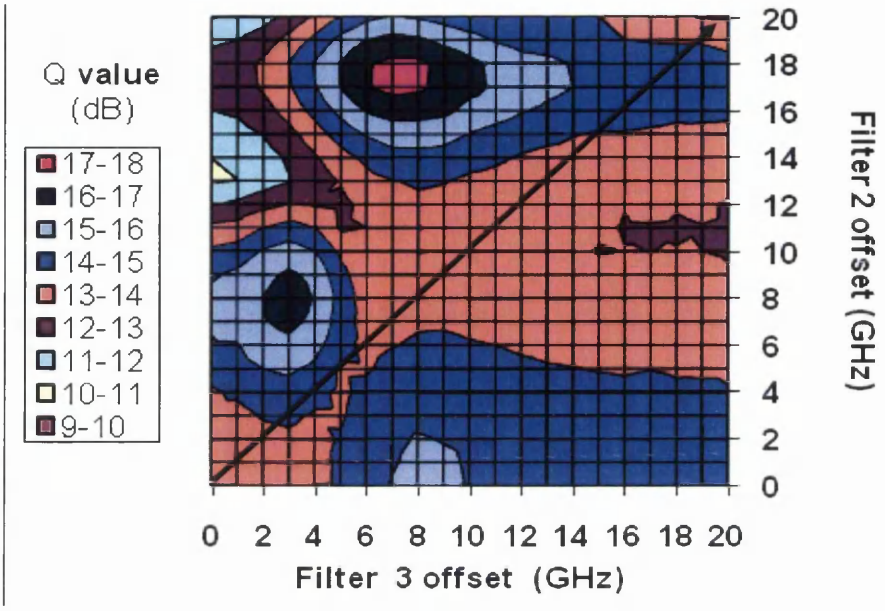

Figure 3.14: Q value (dB) contour plot for novel model with frequency offset of filter 1 and 2 (GHz) 20dB OSNR.

Fig 3.14 shows a plot contour on Q value in dB optimizing the frequency offset of the two 35GHz OBPF at the constructive and destructive. It can seen the Q value reaches a peak ~18dB which is the intersection of 8 GHz offset of the filter located at the constructive port and the ~18 GHz of the filter located at the destructive port, that the improved performance is due to large offset at destructive filter. These can be explained by the fact that offset filtering of an AMI spectrum actually leads to a spectrum that is more closely related to a DB signal, due to large reduction in either of the peaks of the AMI [9].

The improved performance from inserting narrow filters is rather surprising, in that deploying a narrow filter will generally lead to performance penalty. But in view of the performance of DPSK signal in the presence of strong optical filtering which is more due to the filtering tolerance of DB signal at the constructive rather than the double peaked AMI at the destructive port. Thus intentional frequency imbalance at the output of the MZI for a strongly filtered DPSK system enhances the performance of destructive port for an improved balanced detection.

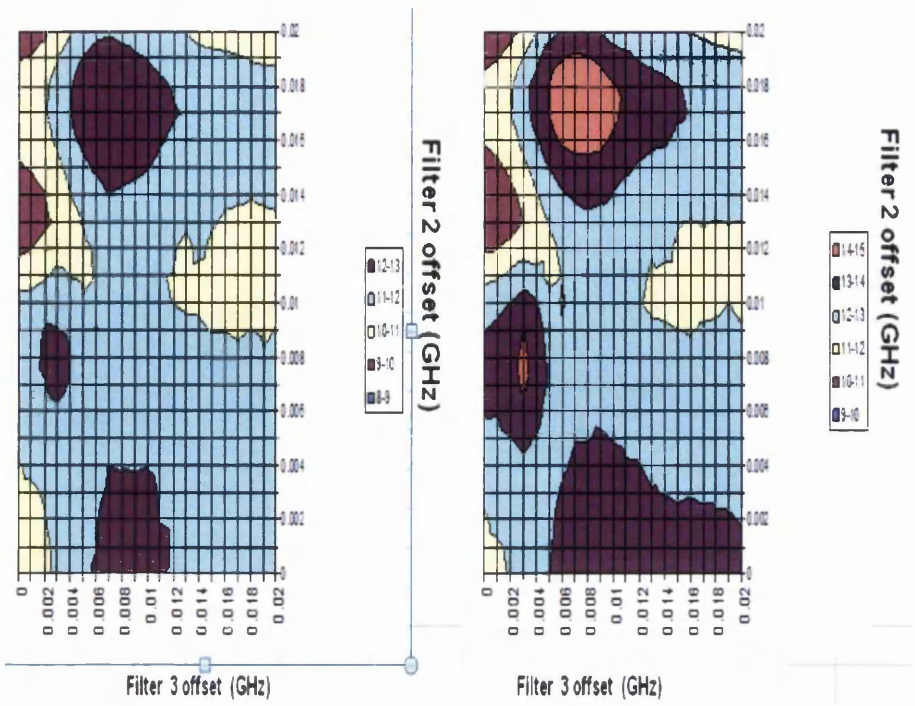

Figure 3.15: Q-value (dB) contour plot for novel model with frequency offset of filter 1 and 2 (GHz) both 15 and 17dB OSNR

The above contour plots illustrated above shows the performance for the same model used for the contour plot in figure 3.14 but the contour plot in figure 3.15 are both for 15dB and 17dB OSNR. Several of these contour plots were generated for different OSNRs, so that the performance trend of the novel filtering model can be established such that comparison with conventional model performance could be enhanced. Thus the figure below was generated from all the different contour plots that were generated for the investigations.

The graph shown in fig 3.16 is plot for Q-value improvement of 2.3 to 4.5 dB for the novel optimized offset filtering over the conventional model. The motivation for this work is the different performance peaks that are obtained from offsetting the centre frequency of a strongly filtered DPSK system with both constructive and destructive single ended detection. Offsetting the centre frequency of an optical filter would mostly lead to penalty alleviation in most modulation formats, but the DPSK demodulation via interferometric process can actually utilise the equal amount of information that is present at the outputs of the MZI

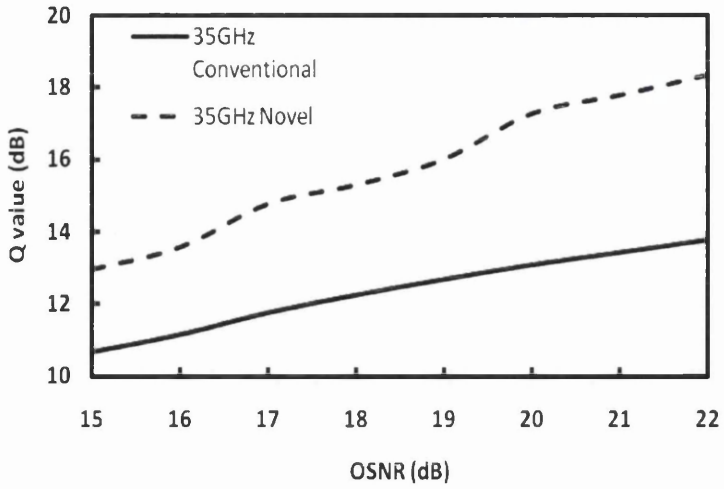

Figure 3.16: Q-value (dB) as function of OSNR (dB) for the conventional and the novel mode.

The different tight optical filtering performance of the duobinary (DB) and alternate mark inversion (AMI) signal within band limited filtering and offset filtering is explored in deriving better sensitivity with balanced detection. The duobinary signal in this case AM-PSK duobinary is well-known for its resilience to tight optical filtering and chromatic dispersion [31, 33], due to its narrow spectra extent.

The performance of the AMI spectrum can have a comparable performance to the DB signal in situations in which the AMI spectrum is vestige (SSB-filtering) i.e. by detuning the spectrum of AMI obtainable at the destructive output port of the MZI, this is similar to the behavior of the DCS-SSB and carrier suppressed AMI-SSB [32,33].

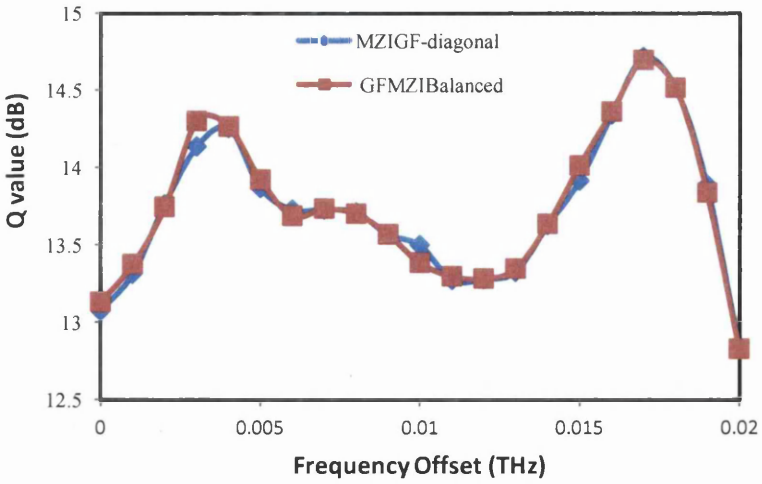

Figure 3.17: 3.17 Plots of Q values (dB) vs filter frequency offset (THz) for 42.7Gb/s 35GHz OBPF 50% RZ DPSK for the conventional balanced (red) model and the novel (blue) model (i.e. the diagonal of the contour plot in figure 3.14).

The figure 3.17 above illustrates the performance of 42.7Gb/s 50% RZ-DPSK under strong optical filtering of 35GHz OBPF with a balanced detection and the diagonal of contour plot in figure 3.14. This result confirms that the result shown in figure 3.14 is valid, since the optical band pass filter being deployed both before the MZI, or after the MZI both operate on a linear regime and no non linearity was included in the simulations. Thus the agreement of the two different models in terms of balanced detection as seen in the diagonal in figure 3.14 and balanced detected results of conventional model, thus gives a reassurance as to the practicability of the model.

This is further ensured with the two plots below that compare the performances of the two single ended detections with the horizontal and vertical axis of the contour plot in figure 3.14. These agreements between the two models (via symmetric filtering with the novel model and diagonal of the model) thus further show that better performance improvements can derived by inducing the correlative coding attributes of the two MZI output ports as seen in figure 3.14. The performance improvements inherent with novel model are comparable to performance improvements achieved with PDPSK over conventional filtered (35GHz OBPF) DPSK system at high OSNRs.

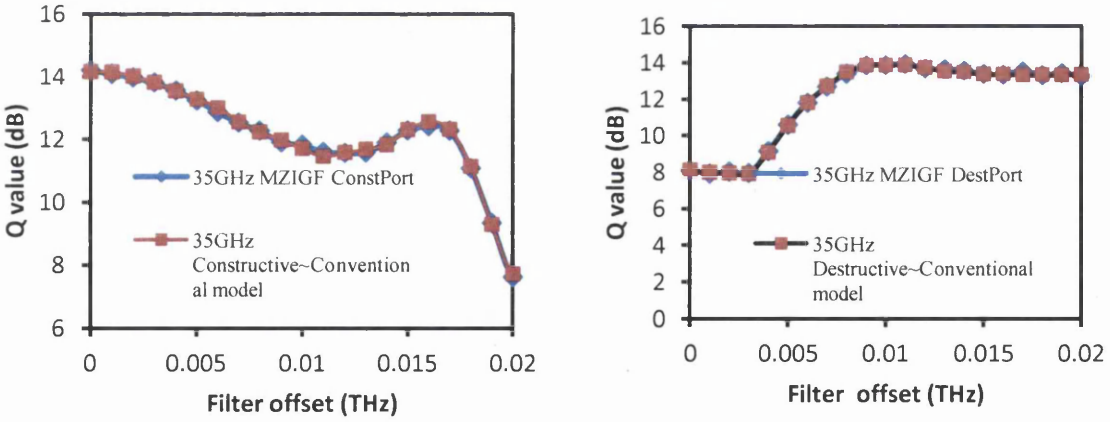

Figure 3.18:Plots for the single ended constructive detection (a) of 42.7Gb/s 35GHz OBPF 50% RZ DPSK from both conventional model and novel model Plots for single ended destructive detection (b) of 42.7Gb/s 35GHz OBPF 50% RZ DPSK from both conventional model and the novel model.

3.5.4:Discussions on the impact of the Novel Receiver Design.

In this section the discussions on the impact of the novel offset filtering design will be discussed, while detailed performance comparisons will be made with an equivalent performance of a conventional model. This is important in order to understand the origin of the performance improvement inherent with novel design. A better understanding of the

physical origin of the performance can enhance a better adaptability of the novel design in practical optical DWDM transport systems.

The precise offset required for improved performance in strongly filtered DPSK systems is filter bandwidth dependent. Thus this is the basis for further work as shown in our novel model, that utilizes the advantages inherent in offset filtering (SSB) of the AMI signal to a duobinary signal; the improve sensitivity of destructive port can lead to improvement in performance of a balanced detected strongly filtered DPSK system.

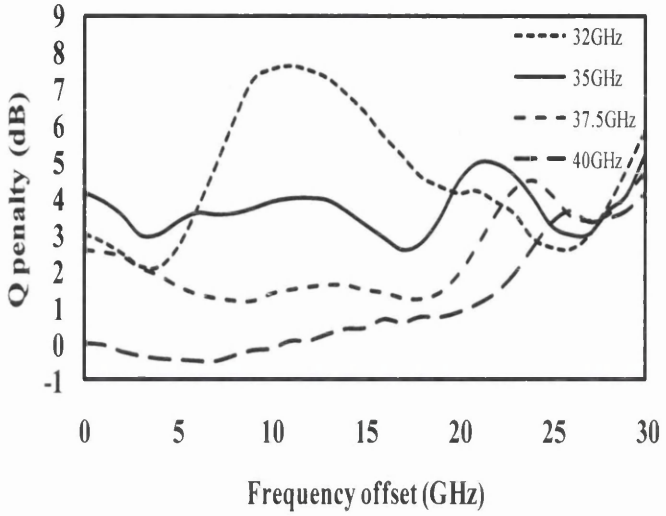

Figure 3.19: Q-penalty against offset for 33, 34 35 and 40GHz OBPF for 42.7Gb/s 50% RZ DPSK 20dB

Firstly a review of the performance penalty inherent with a 35GHz OBPF 42.7 Gb/s 50%RZ-DPSK (conventional) system is compared with the other bandpass filters in figure 3.19 above. The magnitude of the performance penalty is around 4.15dB for a conventional 35GHz filtered DPSK system compared to the performance of the 40GHz OBPF. Although offsetting the 35GHz OBPF filter to half the filter bandwidth (17GHz) can reduce the performance penalty to 2.5dB. This plot thus gives a better insight into the performance of the novel offset filtering design that can completely reduce the above performance penalty.

Thus the novel design presented here is based on exploring the inherent physical features of the correlative coding formats (AMI and DB) at the output ports of the MZI [31] in spectral shaping by the additional degree of freedom gained by having inherent intensity-phase modulated signals at the two ports. These modulation formats (AMI and DB) being memory modulation formats (line coding), thus can be both exploited to improve tolerance to specific fiber impairments (linear and nonlinear). The exploitation of the memory is further strengthened by offset filtering (prefiltering induced symbol correlation) that introduces memory even to memory-less modulation formats [43]. The DB signal is well-known for its

tolerance to chromatic dispersion and tight optical filtering [31], just as AMI is well-known for its nonlinear tolerance [44, 45]. The implication of this difference in tolerance by the DB and AMI, which are both located at the output ports of the MZI for a DPSK signal, is that by adequately optimizing the inherent memory properties of the two signals subject to dominating impairment at the receiver, the DPSK performance can be significantly improved most especially within a tight optical filtering regime.

Interestingly DB can be derived from an AMI by deploying offset filtering [32] and within the constraints of a tight optical filtering regime the induced performance penalty and chromatic dispersion tolerance of a strongly filtered 42.7Gb/s system can be improved by introducing band-limited filtering or offset filtering at the two output ports of the MZI. Further investigation to the performance of this novel filtering design in a nonlinear regime is envisaged in view of some reported investigations [46, 47] where memory modulation has been used to compensate for nonlinear propagation impairments.

The contour plot in figure 3.14 could reasonably be difficult to implement in real systems, thus a more practical model that would inevitably reproduce similar improvements as achieved in figure 3.16 is now presented. This improvised model now has the filter1 that was ignored in the figure 3.16 model. The improvised model has three identical OBPFs one before MZI (no detuning), the second OBPF at destructive port (detuned) and the third at the constructive port (detuned).

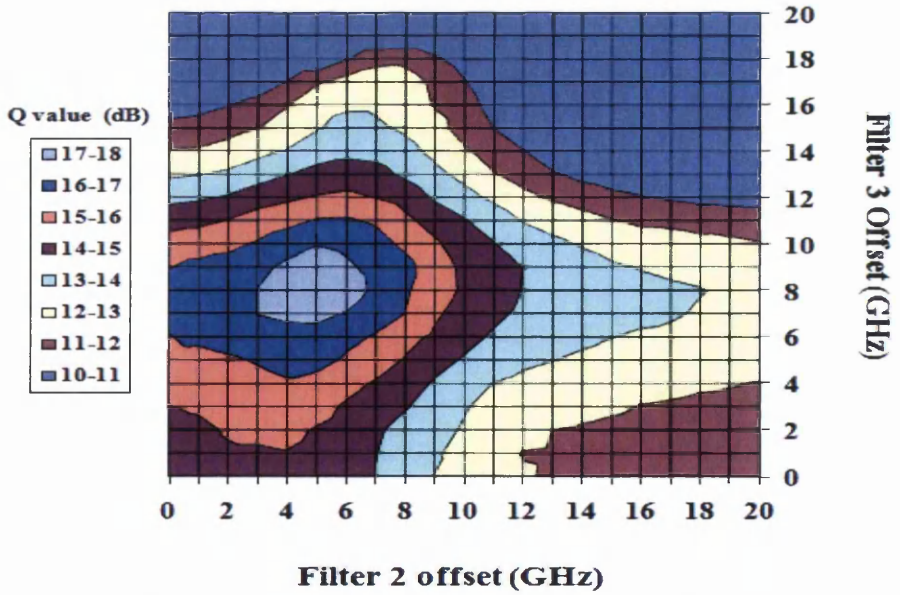

Figure 3.20: Q-value (dB) contour plot for novel model with 0 offset at filter 1, frequency offset of filter 2 and 3 (GHz)

An additional OBPF before the MZI results in net filtering narrowing effect, as seen in the zero filter offset of the contour plot in figure 3.20. The results here can be justified by the plot for the 33GHz OBPF in figure 3.19 where its penalty reduction for 0 and ~5GHz offset is more than 0 and 17GHz offset of the 35GHz OBPF.

The design in figure 3.14 would reasonably be costly to implement in practical systems, thus a 3rd model with two filters is proposed to simplify the model used in generating the contour plot with 3 filters. The third additional model does not have any OBPF at the constructive port because the performance of the DB signal is optimized with band-limited filtering. The new model has two identical OBPFs one before MZI and the other located at the destructive output port of the MZI. Having an OBPF at the destructive port is to essentially reduced the double lobe of the AMI spectrum to DB spectrum and thus improve the sensitivity of the destructive port. This invariably leads to more sensitivity of the balanced detection.

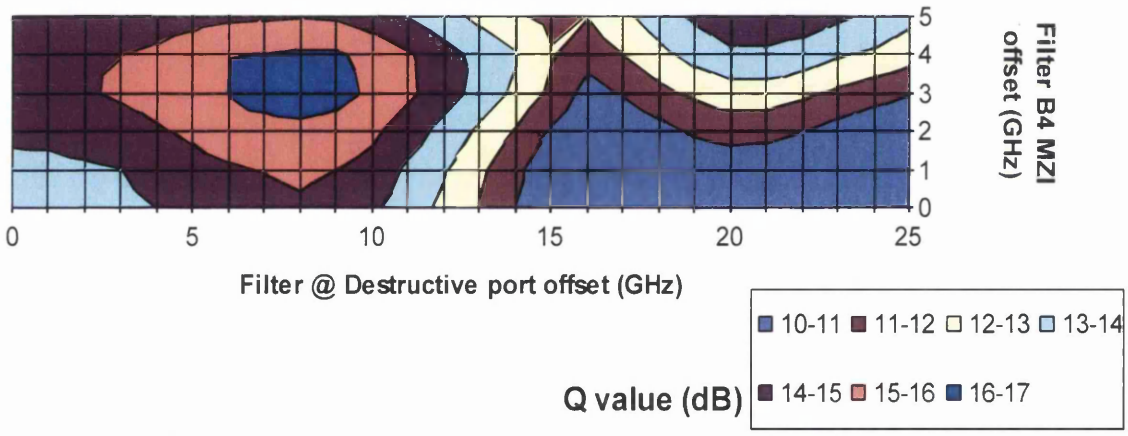

Figure 3.21: Q Contour plot of Q-value (dB) for offset filtering (GHz) at OBPF before the MZI and offset filtering at the Destructive port of MZI (GHz)

The results generated here shows that detuning the laser from 0 to 5GHz and offset filtering at the destructive port (from 0 to 25GHz) of the MZI could reasonably increase sensitivity within narrow filtering regime, which are occasioned in a 50GHz grid. The results for figure 3.21 are essentially a reproduction of the result in figure 3.20.

The improvement seen with these novel models are better appreciated within the context of performance recovery in the presence of strong filtering, i.e. the performance improvement of the narrow filtering regimes can be viewed as deriving the benefit of broader filters with a narrower filtering by biasing the demodulation favorably with two duobinary signals at the

output of the MZI, as opposed to the conventional duobinary and AMI signal at the outputs of the MZI.

3.6: Offset filtering in conjunction with PDPSK in a strong filtering regime.

In this section the performance of a strongly filtered 42.7 Gb/s RZ-DPSK systems (i.e. 35 GHz OBPF) will be examined with a combination of two strategies (1) the very prominent PDPSK (2) Offset filtering at the ports of the MZI. The performance of PDPSK is well known for its superiority over conventional DPSK systems in a strongly filtered regime in presence and absence of chromatic dispersion in section 3.2 [23]. However in this chapter performance of a strongly filtered DPSK system has been investigated with offset filtering at the OBPF both before and after the MZI.

It was importantly observed that the performance of 35 GHz OBPF for a 42.7 Gb/s DPSK system can be significantly improved via the novel offset filtering design. In the former sections the improved performances of the offset filtered systems were not quantified relative to the performance of PDPSK. Although it was stated that the novel filtering performance could approach the performance of the PDPSK, thus in this section the performance of a strongly filtered DPSK system is examined with a novel filtering design as shown in figure 3.13 but without the 1st filter, with band-limited filtering at the constructive port and offset filtering at the destructive port of the MZI and delay of the MZI is varied.

It is important to consider that the performance of a PDPSK system is essentially enhanced by the performance of the constructive port where a duobinary signal is inherent, while the performance of the destructive port`s AMI is largely a performance penalty.

3.6.1: Offset filtering-PDPSK results in a strong filtering regime.

The contour plot below in figure 3.22 shows the performance of PDPSK and offset filtering at the OBPF located at the destructive port of the MZI in an ASE noise dominated regime. The figure 3.22 show a contour plot of Q values in dB for percentage bit period delay in MZI against filter offsets in GHz for the OBPF at the destructive port.

The 0 offset performance shows that the optimized MZI delay can significantly improve the performance of the system by around 3 dB, but by deploying offset filtering at the destructive port that the performance of the system can be improved by around 5dB for an OSNR of 20dB.

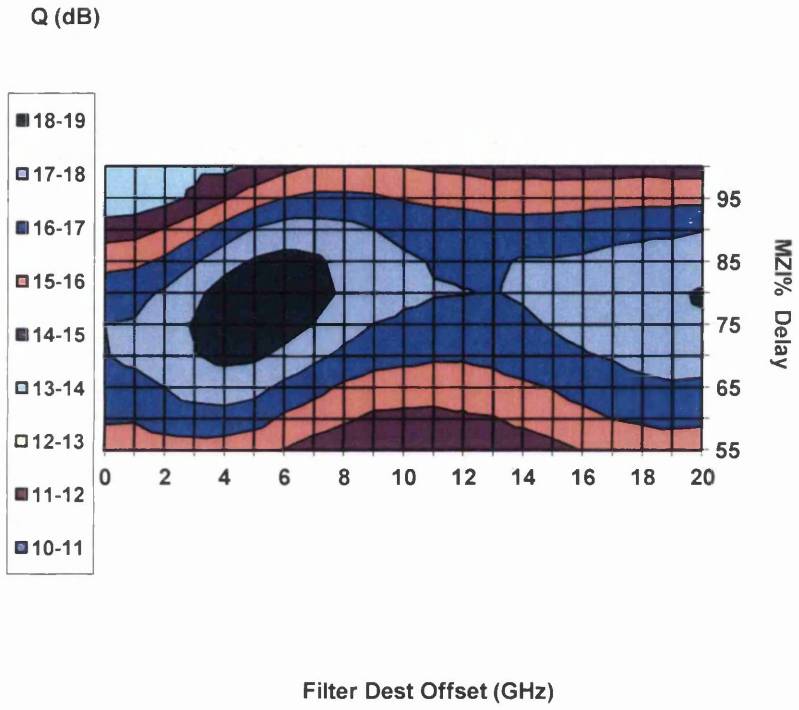

Figure 3.22: Q Contour plot of Q-value (dB) for % bit period delay in MZI against filter offsets in (GHz) of 3rd order 35 GHz OBPF at destructive port of the MZI (GHz).

The magnitude of the performance improvement inherent with this innovative receiver design can be appreciated in the figure 3.23 below. The figure 3.23 plots the Q value in dB against the optimized bit period delay (percentage) in the MZI for performance of the conventional PDPSK system and optimized delay in MZI/filter offsets at the destructive port of the MZI. The graph shows that with a 100% delay in MZI (23.42ps) that the offset filtered system (destructive port improvisation) has a performance improvement of ~2dB over the conventional DPSK system for a 35 GHz OBPF for an OSNR of 20 dB.

However as the MZI delay is varied the performances of both systems improves, while the offset filtering at the destructive port (novel-PDPSK) system reaches a peak performance with 80% bit period delay in the MZI, the conventional PDPSK system reaches a peak with 75% delay in MZI.

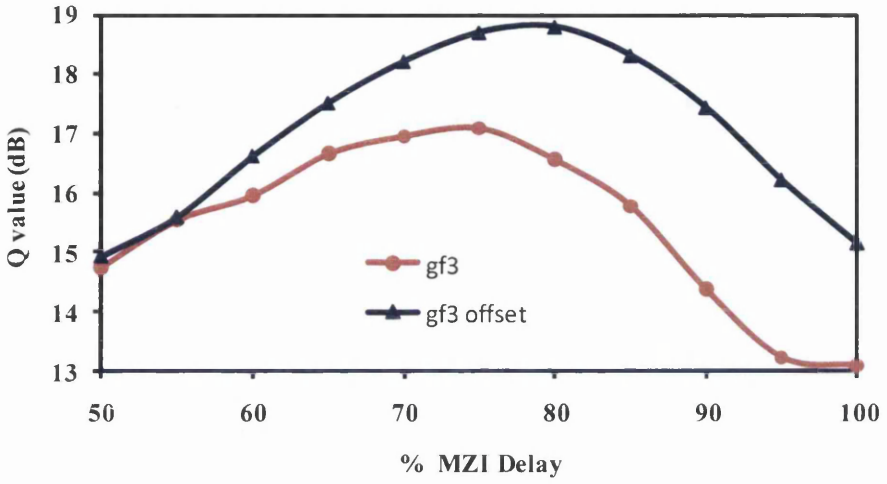

Figure 3.23: : Q-value in dB against % bit period delay in MZI 35GHz OBPF 42.7Gb/s 50% RZ DPSK 20dB, where the blue line represents the novel-PDPSK model and red line represents the conventional PDPSK model.

Interestingly the peak performance of the novel-PDPSK system has 1.7dB improvement over the peak performance of the conventional PDPSK system for an OSNR of 20dB in calculated Q values. The OSNR of the investigation was also varied from 18 to 15 dB to confirm the performance trend as shown in figure 3.23 above, the results showed 1.4 and 0.7dB improvements for the varied OSNRs.

In the presence of chromatic dispersion the novel-PDPSK still maintained an improved performance over the conventional case i.e. the performance improvements in the presence of chromatic dispersion of 50 and 100 ps/nm are 1.1 and 0.4dB over the conventional PDPSK.

3.6.2: Discussions on Offset filtering-PDPSK performance in a strong filtering regime.

The results as seen in this section with an inherent performance improvement of the PDPSK-offset filtering novel where a close to 1dB in calculated Q is observed over the conventional PDPSK system; can be better understood by analyzing the performance of a balanced PDPSK system in a strongly filtered regime. The performance of PDPSK system is enhanced in a balanced detection by the signal at the constructive port of MZI, where a duobinary signal is inherent. The performance (conventional PDPSK) of the destructive port is largely a performance penalty due to the wider spectrum of the double peaked AMI signal.

It must be noted that the two signals at the two outputs of the MZI are both memory modulation formats. Although the DB has a much narrow spectrum than the AMI, memory modulation format are very unique due to their multi-symbol nature (intensity and phase modulation). In the presence of specific impairments the memory modulation formats exploit their additional degree of freedom gained from the extra symbol modulation in shaping the signal spectrum subject to the impeding impairments [19].

The DB signal is well known for its tolerance to tight optical filtering and chromatic dispersion due to the narrow spectral extent and three level optical symbols used in detecting 2 electrical symbols at the photodetector as previous explained in chapter 2.

It has been shown in [32, 39, 40, 41, 48] that a DB spectrum can be derived from an AMI by offset filtering and the performance of the vestige AMI is significantly improved in the presence of ASE-noise noise and chromatic dispersion. It was also shown in [43] that pre-filtering (offset filtering) induces a beneficial memory modulation format in the presence of tight filtering on a memory-less modulation format.

Thus the physical reason for the performance improvements as seen with this novel-PDPSK system in a strongly filtered regime is largely due to further exploitation of the inherent attribute of the residing memory modulations of the outputs of the MZI. Whereby a balanced detection is deployed, but with induced performance improvements at the destructive port of the MZI.

3.7 Chapter 3-Summary:

1 We have investigated the effect of offset filtering of a 42.7Gb/s DPSK signal using typical filter bandwidths present in a 50GHz grid. The results show that the performance of the strongly filtered DPSK system can be improved by ~1dB at low OSNR (15dB) and by up to 1.5dB for an OSNR of 20dB by detuning the laser frequency. Three values for detuning are observed with the most effective found to be around half the filter bandwidth. The precise offset required for improved performance in strongly filtered DPSK systems is filter bandwidth dependent. This interesting result could reasonably be anticipated to also occur in coherent PSK/QPSK systems. The experimental results reported in [42] is a good indication as to the practicality of the performance improvement seen with offset filtering. There is still need for further experimental confirmation of the improvement (penalty reductions) seen here with a 35GHz OBPF, which is representative of typical bandwidths available in a 50GHz grid/net filtering resulting from concatenation of several filters as obtainable in real transmission systems.

2 We have investigated the impact of residual dispersion on displacing the centre frequency of a 35GHz OBPF at the receiver for a 42.7Gb/s DPSK system. The results show that the performance of the narrow filtered DPSK system is improved by largely offsetting the centre frequency of the filter in the presence of some dispersion. Thus optimized offset of carrier frequency of the filter in the presence of dispersion generally results in performance recovery as compared to symmetric filtering. The performance of offset filtered 35GHz OBPF 42.7Gb/s DPSK systems has improved performances over the symmetrical filtered system for dispersions ranging from 0 to 50ps/nm, but beyond this point the performance of offset filtered DPSK systems (35GHz OBPF) becomes a performance improvement. Offset filtering with 42.7Gb/s DPSK can provide a cheap alternative for managing the sensitivity DPSK systems in 50GHz grid and metro networks due to its better and comparable performance to the symmetric filtering in the presence of 0 to 50ps/nm and > 50ps/nm dispersion.

3 We have deployed a novel asymmetric filtering imbalance model with balanced detected 42.7 Gb/s DPSK signal in the presence of strong filtering. The results show that performance of strongly filtered DPSK system can be improved by 2.3dB at low OSNR (15dB) and by up to 4.5dB for an OSNR of 22dB. The novel configuration based on introduction of 2 additional OBPF to a conventional DPSK model and swapping the position of filter with the MZI. This result justifies the performance improvement shown here can be achieved at the output of MZI by virtue of the different spectral performance of the constructive and destructive port of the DPSK system. Thus within a strong filtering regime for a DPSK system this design could derive the benefit of partial DPSK with less cost and complexity. Further work is envisaged with asymmetrical filtering of coherent PSK/QPSK to thus provide a better alternative to 100Gb/s deployment in a 50GHz grid.

4 We have deployed a novel asymmetric filtering imbalance model with balanced detected 42.7 Gb/s PDPSK signal in the presence of strong filtering and chromatic dispersion. The results show that performance of strongly filtered PDPSK system can be improved by 1.7dB for an OSNR (20dB) The novel configuration based on introduction of 2 additional OBPF to a conventional DPSK model and swapping the position of filter with the MZI. This result further shows that the performance improvement can be achieved deploying offset filtering at the destructive port of MZI and in conjunction with PDPSK, (PDPSK) which is the most prominent technique for improved performance in a strongly filtered DPSK system. Thus within a strong filtering regime for a DPSK system this design could enhance the benefit of PDPSK by slightly offsetting the OBPF at the output of the MZI. Further work is envisaged with this model for different signal formats, different OBPF, at higher data rates (i.e. 50Gb/s PDPSK in a 50GHz grid and an intensive experimental investigation to confirm the performance trends as seen with this novel-PDPSK design.

3.8: Chapter 3-REFERENCES

[1] Y. K. Lize , X. Wu , L. Christen , M. Faucher A. E. Willner "Free Spectral Range and Optical Filtering Optimization in NRZ-, RZ- and CSRZ-DPSK demodulation" *IEEE/LEOS* 2007.

[2] Y. Ke. Lizé, X. Wu, M. Nazarathy, Y. Atzmon, L. Christen, S. Nuccio, M. Faucher, N. Godbout, A. E. Willner "Chromatic dispersion tolerance in optimized NRZ-, RZ- and CSRZ-DPSK demodulation" 17 March 2008 , vol. 16, no. 6 , *Opt Express* 4228, 2008.

[3] D. S. Govan and N. J. Doran, "An RZ DPSK receiver design with significantly improved dispersion tolerance," *Opt. Express*, vol. 15, no 25, pp. 16916-16921 (2007).

[4] S. Chandrasekhar, X. Liu, A. Konczykowska, F. Jorge, J.-Y. Dupuy, and J. Godin "Direct Detection of 107-Gb/s Polarization Multiplexed RZ-DQPSK Without Optical Polarization Demultiplexing" *IEEE Photon. Technol. Lett*, vol. 20, no. 22, Nov 15, 2008.

[5] D. van den Borne, S. L. Jansen, E. Gottwald, E. D. Schmidt, G. D.Khoe, and H. de Waardt, "DQPSK modulation for robust optical transmission," in "Proc", *OFC* 2008, San Diego, CA, Invited paper OMQ1, Feb. 2008.

[6] H. Masuda, A. Sano, T. Kobayashi, E. Yoshida, Y. Miyamoto, Y. Hibino, K. Hagimoto, T. Yamada, T. Furuta, and H. Fukuyama,"20.4-Tb/s (111 Gb/s) transmission over 240 km using hybrid Raman/EDFAs," in Proc. *OFC/NFOEC 2007*, Anaheim, CA, Mar.2007, Postdeadline Paper PDP20.

[7] S. Chandrasekhar, X. Liu, D. Kilper, C. R. Doerr, A. H. Gnauck, E. C. Burrows, and L. L. Buhl, "Hybrid 107-Gb/s polarization-multiplexed DQPSK and 42.7-Gb/s DQPSK transmission at 1.4-bits/s/Hz spectral efficiency over 1280 km of SSMF and 4 bandwidth-managed ROADMs," in "Proc". *ECOC2007*, Postdeadline paper PD1.92.

[8] G. Charlet, E. Corbel, J. Lazaro, A. Klekamp, W. Idler, R. Dischler, S. Bigo, P. Tran, T. Lopez, H. Mardoyan and J.-P. Thierry "Comparison of system performance at 50, 62.5 and 100 GHz channel spacing over transoceanic distances at 40 Gbit/s channel rate using RZ-DPSK" *Electronics Lett,* vol. 41 no. 3, Feb 2005.

[9] A. H. Gnauck and P. J. Winzer, "Optical phase-shift-keyed transmission", *J. Lightw. Technol.*, vol. 23, no. 1, pp. 115–130, Jan. 2005.

[10] P. A. Humblet and M. Azizoglu, "On the bit error rate of lightwave systems with optical amplifiers", *J. Lightw. Technol.*, vol. 9, no. 11, pp. 1576–1582, Nov. 1991.

[11] L. G. Kazovsky, G. Kalogerakis, W. T.Shaw, "Homodyne Phase-Shift-Keying Systems: Past Challenges and Future Opportunities" *J. Lightw. Technol.* vol: 24 , Issue: 12 , Page(s): 4876 – 4884, 2006.

[12] http://www.tf.uni-kiel.de/etit/NT/download/publications/apoc02.pdf.

[13] K. P. Ho and H.Cheng "Effects of Chromatic Dispersion on Optical Coherent-Detection Systems" *IEEE Transactions on Communications* vol. 56, no . 9, Sept 2008.

[14] D. Penninckx, H. Bissessur, P. Brindel, E. Gohin and F. Bakhti, "Optical Differential Phase Shift Keying direct detection considered as a duobinary signal, in "Proc" of *ECOC 2001*, 456-457 (2001).

[15] I. Lyubomirsky and C. Chien "DPSK Demodulator Based on Optical Discriminator Filter" *IEEE Photon. Technol Lett*, vol. 17, no. 2, Feb 2005

[16] P. J. Winzer and A. Kalmar, "Sensitivity enhancement of optical receivers by impulsive coding", *J. Lightw. Technol Lett.*,vol. 17, no. 2, pp. 171–177, Feb. 1999.

[17] P. J. Winzer, M. Pfennigbauer, M. M.Strasser, and W. R. Leeb, "Optimum filter bandwidths for optically preamplified RZ and NRZ receivers", *J. Lightw. Technol.*, vol. 19, no. 9, pp. 1263–1273, Sep. 2001.

[18] W. Idler, A. Klekamp, R. Dischler, J. Lazaro, and A. Konczykowska, "System performance and tolerances of 43 Gb/s ASK and DPSK modulation formats", in "Proc" *ECOC,* 2003, Paper Th2.6.3.

[19] P. J. Winzer and R. J. Essiambre, "Advanced modulation formats for high-capacity optical transport networks," *J. Lightwave Technol.*, vol. 24, pp. 4711-4728 (2006).

[20] X. Li, F. Zhang, X. Zhang, D. Zhang, Z. Chen, and A. Xu, "Free spectral range optimization of return-to-zero differential phase-shift keyed demodulation in 40 Gbit/s nonlinear transmission, " *Optics Express*, " Vol. 16, Issue 3, pp. 2056-2061 Jan 2008.

[21] B. Mikkelsen, P. Rasmussen, P. Mamyshev, F. Liu, "Partial DPSK with excellent filter tolerance and OSNR sensitivity", *Electron Lett.* 42, 1363-1364 (2006).

[22] Y. K. Lizé, L. Christen, X. Wu, J.-Y. Yang, S. Nuccio, T. Wu, A. E. Willner and R. Kashyap, "Free spectral range optimization of return-to-zero differential phase shift keyed demodulation in the presence of chromatic dispersion", *Opt. Express* **15**, 6817 (2007).

[23] P. Moreno-Gomez, D. S. Govan and N. J. Doran "Experimental Verification of the Dispersion Tolerance Improvement of Partial DPSK with Optimised Filtering" in "Proc" *ECOC* 2009.

[24] K. S. Cheng and J Conradi "Reduction of Pulse-to-Pulse Interaction Using Alternative RZ Formats in 40-Gb/s Systems" *IEEE Photon. Technol. Lett* , vol. 14, no. 1, Jan 2002.

[25] P. J. Winzer, S. Chandrasekhar and H. Kim, "Impact of filtering on RZ-DPSK Reception," *IEEE Photon. Technol. Lett.*, vol. 15, no. 6, pp. 840-842, Jun. 2003.

[26] C. Malouin, J. Bennike, T. Schmidt "DPSK Receiver Design – Optical Filtering Considerations" in "Proc" *OFC/NFOEC 2007*. Conference 2007.

[27] M. Serbay, et al. " Experimental Investigation of Asymmetrical filtered 43 Gb/s RZ-DQPSK" *IEEE/LEOS* annual meeting 2006, paper WH5

[28] K. Schuh, et al. "Tolerance Analysis of 107 Gbit/s ETDM ASK-NRZ VSB" in "Proc" *OFC 2008*, paper OWJ5.

[29] K. Tanaka, I Morita and N. Edagawa, "Study on optimum pre-filtering condition for 42.7Gbit/s CS-RZ DPSK signal" in "Proc" *OFC* 2001.

[30] A. Agata, I Morita, T. Tsuritani, and N. Edagawa, "Characteristic of Asymmetrically Filtered 40Gbit/s CS-RZ signals" *in "Proc"OFC 2001.*

[31] P.J. Winzer and R. J. Essiambre "Optical Receiver Design Trade-Offs" in proc *OFC*, Technical Digest (Optical Society of America, 2003), paper ThG1

[32] A. Hirano, Y. Miyamoto, K. Yonenaga, S. Kuwahara, H. Miyazawa, K. Murata, K. Sato and Y.Tada "SSB direct detection scheme in duobinary-carrier suppressed Rz transmission," *Elect Letters,* vol. 38 no. 12 pp 585 Jun 2002.

[33] N. B. Pavlovic′ and A. V. T. Cartaxo , "Influence of Tight Optical Filtering on Long-Haul Transmission Performance of Several Advanced Signaling Formats," *J. Lightwave Technol.*, vol 26, pp. 1339-1348 (2008).

[34] T. Tsuritani, A. Agata, I. Morita, K. Tanaka, , and N. Edagawa, "Performance comparison between DSB and VSB signals in 20Gbit/s – based ultra-long-haul WDM systems," in proc *OFC* 2001, OSA paper MM5.

[35] C. Xu, X. Liu, "Differential Phase-Shift Keying for High Spectral Efficiency Optical Transmissions," *IEEE J Sel Topics in Quantum Electron,* vol 10 Issue: 2 On page(s): 281 - 293 June 2004.

[36] S. Bigo, "Multiterabit DWDM terrestrial transmission with bandwidth-limiting optical filtering," *IEEE J. Sel. Topics Quantum Electron.*, vol. 10, no. 2, pp. 329-340, Mar./Apr. 2004.

[37] A. H Gnack et al., "2.5Tb/s (64x42.7Gb/s) Transmission over 40x100-km NZDSF using RZ-DPSK format and all-Raman–amplified spans", in "Proc" *OFC 2002*, Paper FC2, 2002.

[38] C. Rasmussen et al., "DWDM 4)G transmission over trans-pacific distance (10,000km) using CSRZ-DPSK, enhanced FEC and all-Raman amplified 100km Ultra Wave fiber spans," in "Proc" *OFC 2003*, Paper PD18,2003.

[39] O.A Olubodun and N.J. Doran "Performance Improvement of Asymmetrical Filtered 40GB/s RZ-DPSK Receiver Design -Strong Filtering Considerations" *IEEE/NOC* July 2011.

[40] O.A Olubodun, M. Jamshidifar and N.J. Doran "Performance Impact of Offset Filtered 40Gb/s RZ-DPSK-Strong Filtering Considerations" IEEE/ICBEIA June 2011.

[41] O.A. Olubodun, D.S. Govan, N.J. Doran "Performance Recovery of 42.7 Gb/s DPSK System Due to Offset Filtering" *OFMC* Sept 2009.

[42] Y. Cai, J. Cai, A. Pilipetskii, G. Mohs, and N. S. Bergano "Spectral efficiency limits of pre-filtered modulation formats" in "Proc" *Opt Express*. September 2010 / Vol. 18, No. 19 / 2010.

[43] J.-X. Cai *et al.*, "Transmission of 96/100 G pre-filtered PDM-RZQPSK channels with 300% spectral efficiency over 10 608 km and 400% spectral efficiency over 4 368 km," in "Proc". *OFC 2010*, Mar. 21–25, 2010, Post-deadline paper PDPB10.

[44] A.V. T. Cartaxo, N. B. Pavlović, and T. M. R. Dias "Nonlinearity and Dispersion Tolerances of SSB-DCS-RZ, SSB-AMI-RZ, and BL-PSBT in Long-Haul UDWDM Transmission Systems" *Telecommunications Symposium,* 2006 International Issue Date: 3-6 Sept. 2006.

[45] X. Wei Gnauck, A.H. X. L Leuthold, J. "Nonlinearity tolerance of RZ-AMI format in 42.7 Gbit/s long-haul transmission over standard SMF spans", *Electronics Lett* , Oct.2003 Volume: 39 Issue:20 PP: 1459 – 1461.

[46] S. Randel, B. Konrad, A. Hodz˘ic, and K. Petermann, "Influence of bitwise phase changes on the performance of 160 Gbit/s transmission systems", in "Proc", *ECOC*, 2002, Paper P3.31

[47] D. M. Gill, A. H. Gnauck, X. Liu, X. Wei, and Y. Su, "2 alternate-phase on/off keyed 42.7 Gb/s long-haul transmission over 1980 km of standard single-mode fiber", *IEEE Photon. Technol. Lett.*, vol. 16, no. 3, pp. 906–908, Mar. 2004.

[48] O. A Olubodun and N. J Doran., "Characterization of Asymmetric Filtered 40Gb/s RZ DPSK System-Strong Filtering Considerations", *Optics Communication Journal*, July 2011.

CHAPTER 4:

4.1 Optical Differential Quadrature Phase Shift Keying (DQPSK) modulation format in 50GHz Grid.

The aim of this chapter is to evaluate the impact of offset filtering on 42.7 Gb/s DQPSK systems within a tight optical filtering regime (50GHz grid). The impact of offset filtered DQPSK systems in regimes limited by ASE-noise dominance and in the presence of chromatic dispersion will be analyzed in this chapter.

Despite the benefits of inherent reduced bandwidth, tolerance to chromatic dispersion and polarization mode dispersion of the DQPSK modulation format, there are some drawbacks to its implementations i.e. OSNR penalty, tolerance to laser detuning (1-4). However the DQPSK modulation format's encoding and decoding process have presented in chapter 2, so that a better understanding of the modulation and demodulation processes can enhance better opportunities to improve the tolerance of 42.7 Gb/s DQPSK systems to specific mitigating impairments, most especially the tolerance of DQPSK systems to offset filtering or laser detuning in a 50GHz grid [4].

Increase in the demand for optical communications has given rise to research in advanced modulation formats. DPSK has been the simplest of the phase modulated formats and has its inherent limitations in terms of spectral efficiency, tolerance to optical filtering and chromatic dispersion. Optical differential quadrature phase shift keying (DQPSK) provides a better solution to the listed optical communication limiting impairments [5].

Although the BER of the DPSK modulation format and DQPSK modulation format are potentially the same, the symbol error rates are different [6]. The difference is occasioned by the DQPSK modulation format's inherent higher number of symbols per bit i.e. 2 symbols per bit ($log_2 M$) whereas DPSK has 1 symbol per bit. Where $log_2 M$ is the number of data bits per M symbols and R is data rate such that the symbol rate is $R/log_2 M$ [7]. Thus for the same data rate DQPSK requires half the optical bandwidth of DPSK modulation format. And for the same symbol rate DQPSK doubles the data rate of DPSK. The increased spectral efficiency of DQPSK relative to DPSK is at the expense of the complexity of the DQPSK transmitter and receiver. Conventionally DQPSK is transmitted with two data modulators in which a phase shift (offset) of $\pi/2$ is introduced to one of the data modulators.

The IN-phase signal of the DQPSK is driven at a 0 reference phase and the Quadrature signal is driven at 90^0 phase-shift from the in-phase signal. The complexity at the receiver relative to the simple DPSK is such that the DQPSK system has two data modulators, two

MZIs and 4 photodetectors. In terms of performance sensitivity DQPSK has a lower bit error rate for a given data rate as compared to ASK. But comparison with DPSK results in ~1.3dB BER penalty [5]. DQPSK is essentially a simultaneous transmission of 2DPSK with 4 different optical phases. There has been several reported investigations which have addressed the complexity of the DQPSK reception. One such attempt for less complex DQPSK receiver is based on polarization [8], where the two arms of the MZI are replaced by the fast and the slow axes of a polarization maintaining fiber, whose differential group delay (DGD) equals one symbol period and the output signals at the two axes are then combined before photodetection. The high level of precision needed in maintaining the polarizations of these axes thus eventually increases the complexity and eliminates the simplicity of implementation of the polarization based DQPSK receiver. The 3rd attempt at reducing the complexity of the DQPSK receiver was reported in [9, 10] where the 2 AMZI of the conventional DQPSK receiver was replaced with two narrow optical band pass filters.

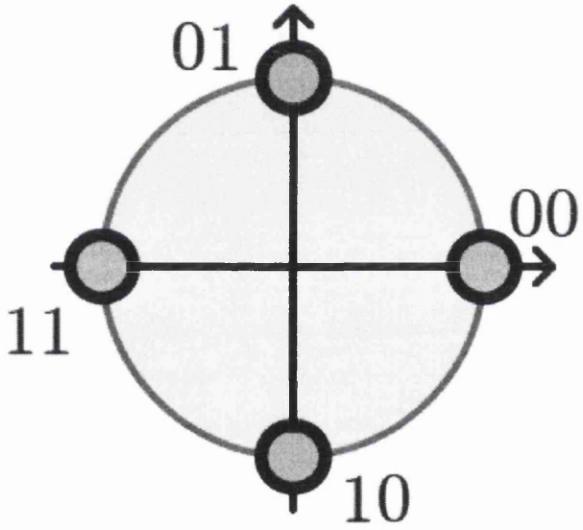

Figure 4.1: Signal constellation for DQPSK modulation format.

The DQPSK receiver design here explored the complementary cosine shaped transfer function of the conventional DQPSK receiver MZIs. The drawback for this novelty was in the OSNR penalty relative to the conventional model, although the novel receiver had a better tolerance to chromatic dispersion and frequency detuning of the laser. The fourth attempt at reduced complexity of the DQPSK receiver design was reported in [11] where only one of the MZI outputs was employed i.e. either the constructive or the destructive port for the I and Q. This eventually eliminates 2 photodetectors from the 4 detectors used in conventional DQPSK model. Thus multi-level phase modulation (DQPSK) provides an alternative for

increasing data rates without increasing the optical bandwidth. Implying that for the same data rate with DPSK and DQPSK, DQPSK modulation format can be employed with half the optical bandwidth of the corresponding data rate. Also true is the fact that for the same optical bandwidth DQPSK is transmitted with twice the DPSK's data rate.

4.2 Impact of DQPSK transmitter with a single Data Modulator on the performance of the opposite (tributary) receiver.

In this section the impact of one of the nested data modulator of the DQPSK transmitted will be investigated on the performance of the opposite tributary receiver performance. This configuration is implemented in order investigate the impact of the crosstalk of the two DQPSK signals from the two separate data modulators on the detections of either of the receivers (e.g inphase or quadrature receiver).

The symbol spacings between the DQPSK symbols which is half the bit spacings of the DPSK system has been attributed as the reason for the worse OSNR performance of the DQPSK relative to the DPSK system. Herein the investigation will be implemented by switching off the power of either of the data modulators (either the Inphase or the Quadrature), and reception will be carried out in the opposite receiver with different bandpass filters. This is done to establish the impact of crosstalk and interference from the two data modulators on either of the receiver`s performance.

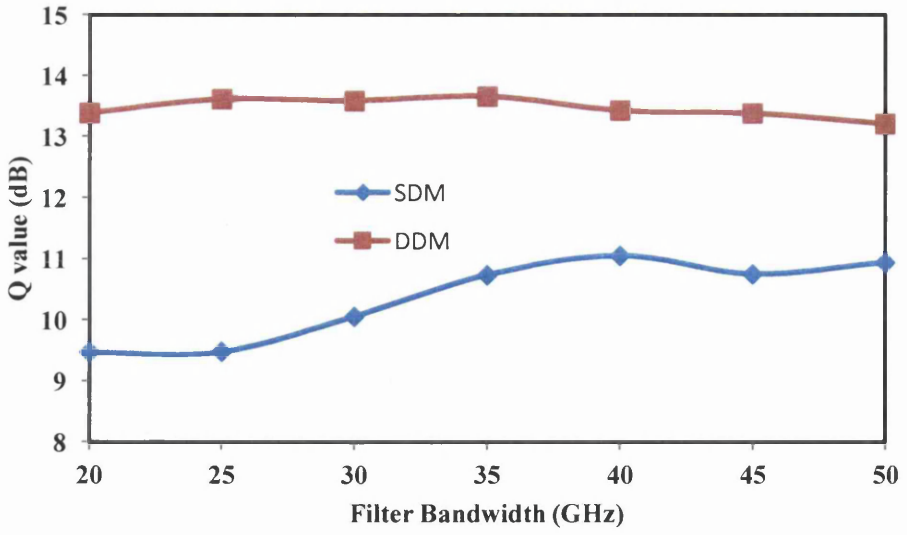

Figure 4.3: Q value in (dB) against different filter bandwidths in (GHz) for 1st order Gaussian filter for a 42.7Gb/s 50%RZ-DQPSK system 16dB OSNR, the red line represents the performance of a conventional

DQPSK system and the blue line represents the performance of a DQPSK system in which one of the powers of the two data modulator is switch-off (receiver is the opposite tributary to the powered data modulator).

The figure 4.3 above plots the Q values in (dB) against the filter bandwidth (GHz) for the conventional 50%RZ_DQPSK (1st order Gaussian filter) model, same as the model deployed in section 4.2 (labeled red in the figure 4.3). The blue line represents a special model where the power of either of the two data modulators is switch off, and the DQPSK system is received at the opposite receiver (the other out of phase receiver).

It can be seen that the impact of the opposite tributary on the order tributary is very significant although there is about 2.5dB performance penalty incurable from switching off the power of either of the data modulators. A 2.5dB performance penalty can be seen as the extent of the interference from the either of the two DQPSK data modulators on the detection of the two receivers. Thus the performance here gives some insights as to why the OSNR performance of 42.7Gb/s DQPSK system is penaltied relative to the performance of a 21.35Gb/s DQPSK system.

4.3: DQPSK Simulation Mode:

In this section a description of the back to back model that will used in the numerical investigations of the performance a 42.7Gb/s 50% RZ-DQPSK system under different conditions will be presented. Having described similarities/differences between the optical DQPSK/DPSK systems in section 4.2 and some of the factors that affects the performance of a DQPSK system in section 4.3. Here in this section the modulation and demodulation of an optical DQPSK will be captured in a conventional DQPSK model.

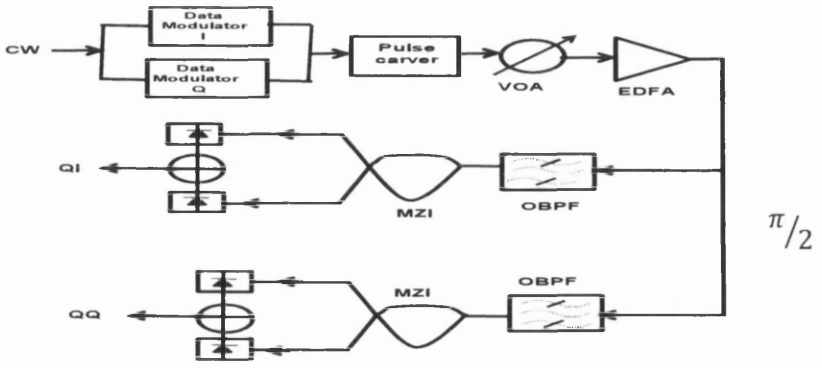

Figure 4.2: Conventional DQPSK modeled diagram.

The above diagram shows a DQPSK model which consist of two data modulators, 2 MZI and 4 photodetectors. The system used in the simulations, is illustrated in Fig. 2. A 2^9 PRBS is used to drive a Mach-Zehnder modulator (MZM) to produce two- 21.35 Gb/s DPSK optical signals, the difference between the data modulators i.e. the in-phase and the Quadrature is that the drive voltage of in-phase MZM is set (initialed) at a phase reference of 0 and the Quadrature is set at a phase reference of point of $\pi/2$ by adjusting the biasing point and drive voltage. The output of the Quadrature data MZM is such that the carrier phase is modulated at a $\pi/2$ offset to the carrier phase of the output of in-phase data MZM ($\pi/2$ phase shifted). The data modulator is driven to generate a π shifted phase modulation in MZM by a sinusoidal signal biased between two peaks at the data rate with an alternate phase change at the bias.

The IN-Phase and Quadrature data modulator are driven and biased in a similar way but the output 42.7Gb/s DPSK signals at output have a phase difference ($\pi/2$). This is followed by a pulse carving MZM generating a 33%, 50% or 67% RZ signal depending on the desired signal format. The NRZ-DQPSK is generated without the pulse carving MZM. We have confirmed that longer bit sequence leads to practically the same results as with the 2^9 used in the above model. Noise is added using the VOA/amplifier combination. At the receiver, the DQPSK signal is first filtered by the tunable OBPF, The signal is demodulated by a two Asymmetric Mach Zehnder interferometer (AMZI) with a one symbol period delay, $\pi/4$ phase difference (at the destructive arm) between the two arms and detected by a balanced receiver for the in-phase demodulator. The Quadrature demodulation is the same as the in – phase but for the $-\pi/4$ phase state of the destructive port of the AMZI. Single ended detection was also investigated in our simulations to identify the effect of offset filtering on the two received signals. The OSNR at the receiver was varied from 14 to 22dB. The filter was generally taken as 31 to 50GHz bandwidth to capture the scenario in a 50GHz grid, 1st to 4th order Gaussian filters were deployed to characterize the impact of the steepness of the filter skirt on performance of DQPSK systems. and a 30GHz bandwidth 5th order Bessel electrical filter was used following the receiver. In the following the Q-values were calculated assuming Gaussian statistics.

4.4: Performance of 42.7Gb/s DQPSK system in the presence of ASE-noise and Strong band-limited filtering.

The model above was used for the simulation of DQPSK results below, although this research focuses on high speed modelling, the simulations results here confirm an excellent agreement between the GNLSE model (with Gaussian statistics) and (KLSE or exact published results generated via simulation and experimentations [4, 14, 15]. However the elusive discrepancies between simulation and experimental results in [4] were due to filter shape that was deployed in the experiment which was not a replica of the Gaussian filter that was modelled. The shape, bandwidth of an optical filter, and electrical filter bandwidth greatly determine the performance of any modulation format [16].

ASE noise generated as a result of compensating for fibre loss is a very important impairment in optical communications, although other impairments have their individual mitigating effects, but in the context of multi level signalling, the foremost impairment to be investigated here is the ASE noise in a DQPSK system. DPSK offers a better OSNR sensitivity as opposed to DQPSK. This is largely due to the phase noise generated by transmitting 2 DPSK signals simultaneously [6] also our investigation confirmed in section (4.2), when either of the two data modulator's power for a 42.7Gb/s DQPSK transmit system is switched off the ASE performance is exactly the same for the 21.35Gb/s DPSK system. Also we confirmed that the opposing demodulator (receiver) in a DQPSK system in which the I or Q data modulator is switched off, still offers some sensitivity.

This investigation is of interest because it accounts for the interference of the calculated Q (in-phase) by the Quadrature Q value at the in-phase receiver, thus the imperfection of the DQPSK receiver in phase referencing for DQPSK detection. The situation with coherent QPSK will be reported as investigated in chapter 6. The DQPSK demodulation process utilizes the phase difference between two successive bits in determination of the bits phase change, the two bits used will be corrupted by ASE noise via transmission.

So in essence DQPSK deploys two error bound bits in phase referencing and this generally results in lesser sensitivity as opposed to exact phase extraction in coherent QPSK [17]. The relative lesser performance of DQPSK system notwithstanding its multi level phase modulation impact is of high prominence due to the better sensitivity of DQPSK as opposed to OOK. In a 50GHz deployment 42.7 Gb/s DQPSK systems have been deployed successively to increase spectral efficiency [18]. In 100 Gb/s systems sensitive polarization

multiplexing of DQPSK has been reported with simulations and experiments [19]. Also hybrid systems with simultaneous deployments of OOK and 40Gb/s DQPSK [20].

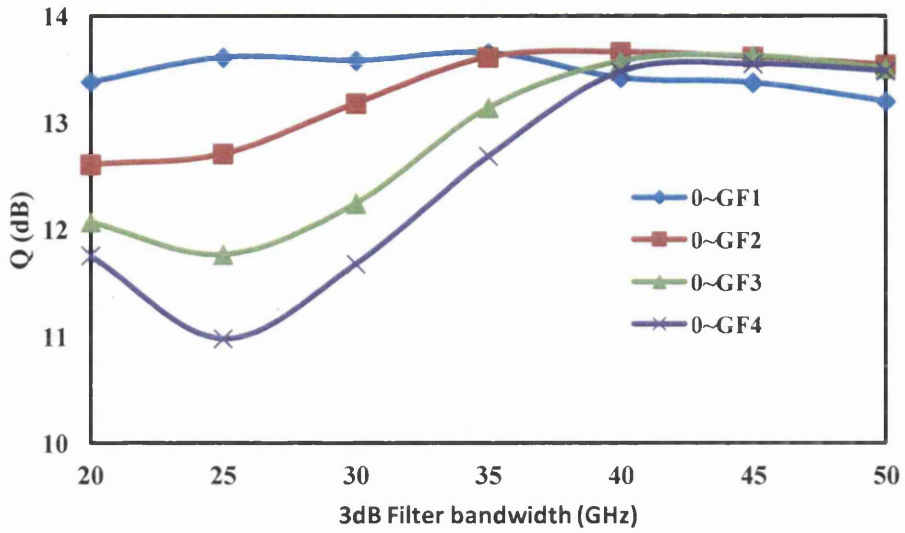

Figure 4.3: Simulated narrowband filtering performance of 42.7GB/s RZ-DQPSK system in an ASE-noise limited regime for an OSNR of 16dB, 1st order (blue), 2nd order (red), 3rd order (green) and 4th order Gaussian filters.

Figure 4.3 illustrates Q value (dB) as function of 3dB filter bandwidths ranging from 20GHz to 50GHz for different types of OBPF (Gaussian filters from order 1 to 4) for an OSNR of 16dB. The choice of 25 to 50GHz OBPF is influenced by the filtering bandwidth available in a 50GHz grid. With the concatenation of several filters in a transmission link the narrow effect of employing several filters results in net filtering bandwidth within the neighborhood of 34 to 40GHz, so one can evaluate the performance of the net narrow filtered DQPSK system (34 to 40GHz) OBPF in comparison to the available channel spacing. The performance shows that 1st and 2nd orders of Gaussian filters have the best tolerance to narrow optical filtering, which is consistent with [7]. Also, as seen from the plots the effect of filter shapes does not reflect in the performance of DQPSK systems >35GHz OBPF.

In the plot above an interesting trend can be seen with the performance of a 20GHz OBPF compared to the 25GHz OBPF, where the performance of the 25GHz is penaltied relative to the 20GHz OBPF. A similar trend was observed in [26], also the fact that 85.6Gb/s DQPSK system was deployed in 50GHz grid WDM system [27], further gives some insight to the tolerance of DQPSK system to strong optical filtering. However deploying wider optical band pass filters on phase modulated formats should not necessarily result in performance

improvements, based on the fact that the wider optical bandwidth could lead to lesser ASE – noise rejections.

The major point here is that using a 1st order or 2nd order Gaussian filter there is a marginal penalty from using extremely narrow filters (20GHz) compared to 50GHz OBPF. The implication of these reduced penalties from strongly filtering a 42.7 Gb/s DQPSK system could be translated to hybrid transmissions (ASK-DQPSK) in 50GHz. This might reduced the cross phase modulation impairments which are generated from hybrid deployments. As illustrated above the tolerance of DQPSK to narrow filtering is quite robust, except for the case of higher order Gaussian filters. Thus narrow filtered 42.7 GB/s DQPSK deployment in 50GHz 42.7 GB/s grid benefits from minimal penalties in the presence of ASE noise limitations as opposed to the penaltied performance of DPSK systems in narrow filtering regimes.

4.5: Chromatic Dispersion performance of 42.7 Gb/s DQPSK system.

In this section chromatic dispersion performance of a DQPSK system in a strongly filtered regime will be examined. Chromatic dispersion is one of the main inherent advantages of DQPSK modulation system in optical communication. As reported in the [21] the optimum filter width for DQPSK is around 37.5GHz and corresponding width for DPSK is 55GHz for the same BER, also in [21] the 42.7Gb/s RZ-DQPSK has quadruple filter width tolerance of 30GHz compared to ~7GHz filter width for 42.7Gb/s DPSK system for a 0.5dB penalty.

The fact that DQPSK is a multi level phase modulation (2 bits/4 levels per symbol) reduces the optical bandwidth whilst the pulse width is increased accounts for the increased dispersion tolerance of 42.7Gb/s DQPSK (46.84ps-bit period) over the same data rate for DPSK (23.42ps-bit period). The effect chromatic dispersion on a channel increases in quadruple with increase in data rate, thus considering the equation of chromatic dispersion below:

$$D = \left(\frac{2\pi c}{\lambda^2}\beta_2\right) = \frac{\lambda}{c}\frac{\partial^2 n}{\partial \lambda^2} \qquad 4.14$$

From the above equation it can be seen that chromatic dispersion is inversely proportional to the square of the wavelength of signal, which itself is inversely proportional to angular

frequency of the signal, $\frac{\lambda}{c}$ is equivalent to time, but symbol period of 42.7Gb/s DQPSK is half the symbol period of 42.7Gb/s DPSK, thus dispersion tolerance of 42.7Gb/s DQPSK is four times that of 42.7Gb/s DPSK system. The below equation illustrates the spectra domain representation of signal propagation in optical fiber [22].

$$B(z,\omega) = B(0,\omega)\exp\left[j\beta(\omega)z\right] \qquad 4.15$$

Where the $B(z,w)$ and $B(0,w)$ represents the low pass representation of a signal at distance z and 0. $B(w)$ is the propagation constant and can be expanded by a Taylor's series around the centre frequency ω_c thus yielding [22]

$$\beta(\omega) = n_r(\omega)\frac{\omega}{c} \approx \beta_0 + \beta_1(\omega-\omega_c) + \frac{1}{2}\beta_2(\omega-\omega_c)^2 + \frac{1}{6}\beta_3(\omega-\omega_c)^3 , \quad 4.16$$

$$v_g = \beta_1{}^{-1} = \left(\frac{\partial\beta}{\partial\omega}\right)^{-1}$$

$$\therefore \quad B(L,\omega) = B(0,w)exp\left[j\frac{1}{2}\beta_2\omega^2 L\right] \qquad 4.17$$

Conventional DQPSK model was employed in these investigations, although the narrow filtering DQPSK model [5] has been shown to exhibit a better dispersion tolerance than the conventional, the trade off of this narrow filtering model is the OSNR performance which is worse off compared to the conventional model. The impact of different signal format has observed in [10] and shows that different signal formats ranging from NRZ to 33%RZ to 50% and to 67%RZ can be deployed with DQPSK, although in a regime limited by chromatic dispersion 50%RZ has been experimentally shown to offer the best tolerance and 67%RZ comes closely next in performance. The figures below shows the back to back DQPSK model and the other illustrates the performance of 42.7Gb/s DQPSK system compared to a corresponding 42.7Gb/s DPSK system.

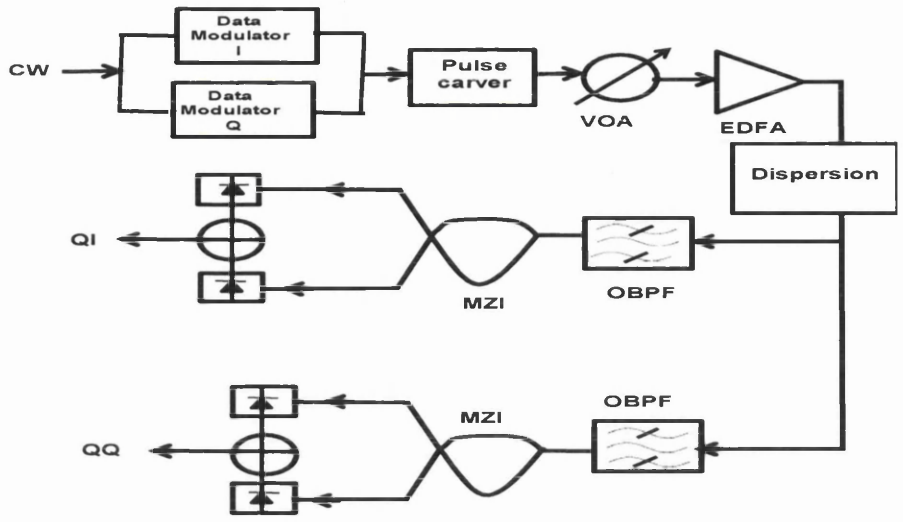

Figure 4.4: Conventional DQPSK in the presence of Dispersion (modeled diagram)

The figure 4.4 above shows a conventional model for a 42.7 Gb/s DQPSK system, in the presence of dispersion. The model is similar to the model in 4.2 but for the chromatic dispersion that is included in the figure 4.4. The chromatic dispersion parameter is a variable which is a function of the length of SMF fiber. The figure 4.5a below shows the Q value (dB) plotted against dispersion (ps/nm) from 0 to 150ps/nm for both 42.7Gb/s 50%RZ-DQPSK and 50%RZ-DPSK systems. The OSNR used in the figure 4.5a below is 20dB OSNR and the optical filtering bandwidth used for the investigation was a 35GHz OBPF, 2nd order Gaussian filter.

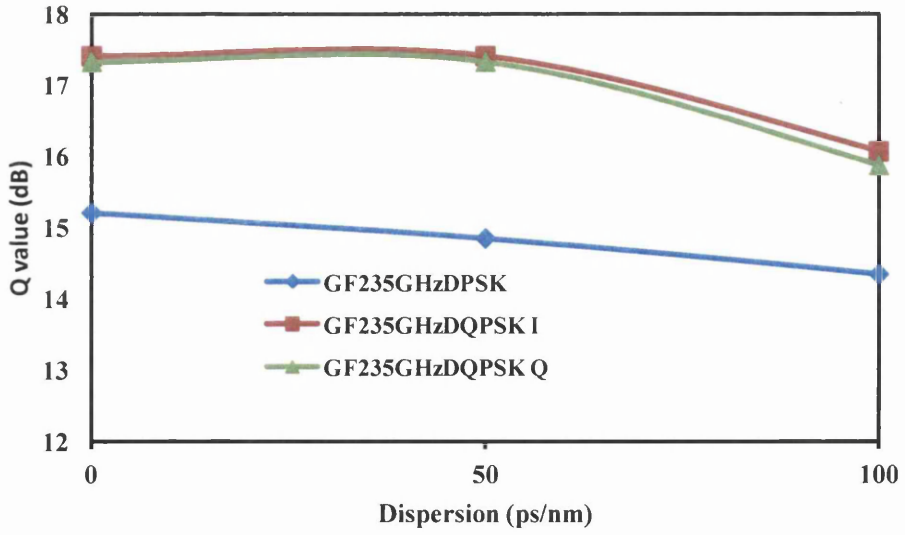

Figure 4.5a: Simulated narrowband filtering performance of (35GHz) 42.7GB/s RZ-DQPSK (In-Phase (red) and Quadrature Phase (green)) and RZ-DPSK (blue) system.

As seen in the figure 4.5a it is observed that at the same OSNR the calculated Q of the 42.7Gb/s 50%RZ DQPSK is ~ (2.5 and 1.5dB) better than the DPSK system for chromatic dispersions of (100 and 150ps/nm). The figure below shows the performance of a bandwidth-limited filtering on 42.7Gb/s DQPSK systems performance in the presence of dispersions of 200ps/nm.

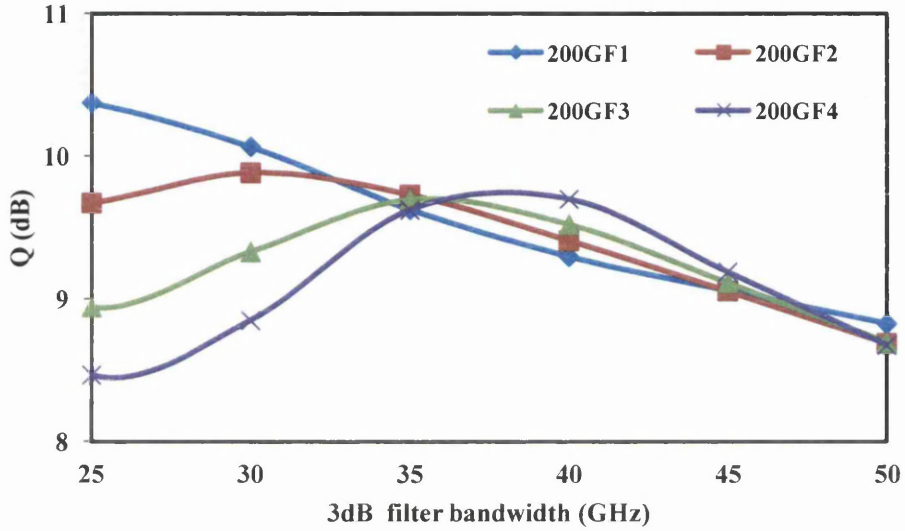

Figure 4.5b: 4.5b: Simulated band-limited filtering performance of 42.7GB/s RZ-DQPSK system with different filter shapes in presence of 200ps/nm chromatic dispersion, 1st order (blue), 2nd order (red), 3rd order (green) and 4th order (purple) in the presence of 200ps/nm chromatic dispersion.

The OBPF bandwidths were varied from 25GHz to 50GHz to characterize the performance of different filter shape with different:; Thus as illustrated below figure 4.5b the narrower filter widths ~30GHz performance better than the wider filters for the cases of 1st and 2nd order Gaussian filters in the presence of some dispersions. But with higher order Gaussian filters 3rd and 4th Gaussian filters out perform the lower order Gaussian filters for bandwidths close to the bit rate.

Thus subject to filter bandwidth and shape, the 42.7Gb/s DQPSK system can described as very tolerant to chromatic dispersion (linear impairments) in a strongly filtering regimes (50GHz grid).

4.6: Impact of Offset Filtering on the Performance of 42.7Gb/s DQPSK system.

In this section the impact of offset filtering on DQPSK systems in a tightly filtered regime will be presented. In chapter 3 performance improvement results with offset filtering of DPSK was presented in the context of 50GHz. The interesting spectra interplay within the constructive and destructive ports of the MZI for the DPSK was also presented. However

herein the impact of offset filtering on a 42.7Gb/s DQPSK system will be comprehensively investigated with different bandpass filters and filter shapes within a tightly filtered regime.

The inherent increased symbol alphabet size of the DQPSK compared to the DPSK system at the same data rate, enhances tolerances to linear impairments (chromatic dispersion, polarization mode dispersion and narrow optical filtering penalties). Despite all these advantages of DQPSK, the OSNR penalty and tolerance to laser drift or frequency offsets stands out as the major drawbacks of the this multi-level signalling.

The performance of asymmetric filtering on 43 Gb/s 50%RZ-DQPSK was investigated in [4] although the 50GHz OBPF that was employed gave some insights to the performance of DQPSK system via laser detuning in narrow filtering regimes. 50GHz OBPF does not give a complete representation of netfiltering bandwidths available in 50GHz grid, because as the number of ROADM/WSS increases the net (residual) bandwidth rapidly drops to around 35GHz OBPF. It is well known fact that choice of optical filter shape, bandwidth, signal format and electrical filtering can influence the performance of any modulation scheme. As was shown in section 4.4 figure 4.3, the performance difference between a 1st order Gaussian 50GHz OBPF that was used in [4] and a 3rd order 35GHz Gaussian OBPF is less than 0.5dB.

Thus showing the tolerance of DQPSK to tight optical filtering regimes as compared to a ~5dB performance penalty incurable with an equivalent DPSK systems. Offset filtering been the main context in these investigations, with a DQPSK system it has serious implications because unlike DPSK the MZI is asymmetric.

Thus frequency mismatch between transmit laser and the phase of AMZI generally leads to performance degradations. NRZ-DQPSK requires lesser optical equipment as compared to RZ-DQPSK (no pulse carving MZM) But RZ signal has been investigated by simulation and experimentation to offer better tolerance to linear and non linear impairments for DQPSK systems.

These research on the impact of offset filtering on DQPSK system seeks to further investigate the impact of different filter shapes and bandwidth (narrower than investigated in [4]) on an ASE limited regime and chromatic dispersion limited regime. Also the physical reasons for the lesser tolerance of the DQPSK to offset filtering is explained in other to provide basis for future investigations. The model used in the simulation was the same as the model in figure 4.4, the difference for the offset filtering model was that a tuneable OBPF was used instead of the fixed OBPF as deployed in figure 4.4.

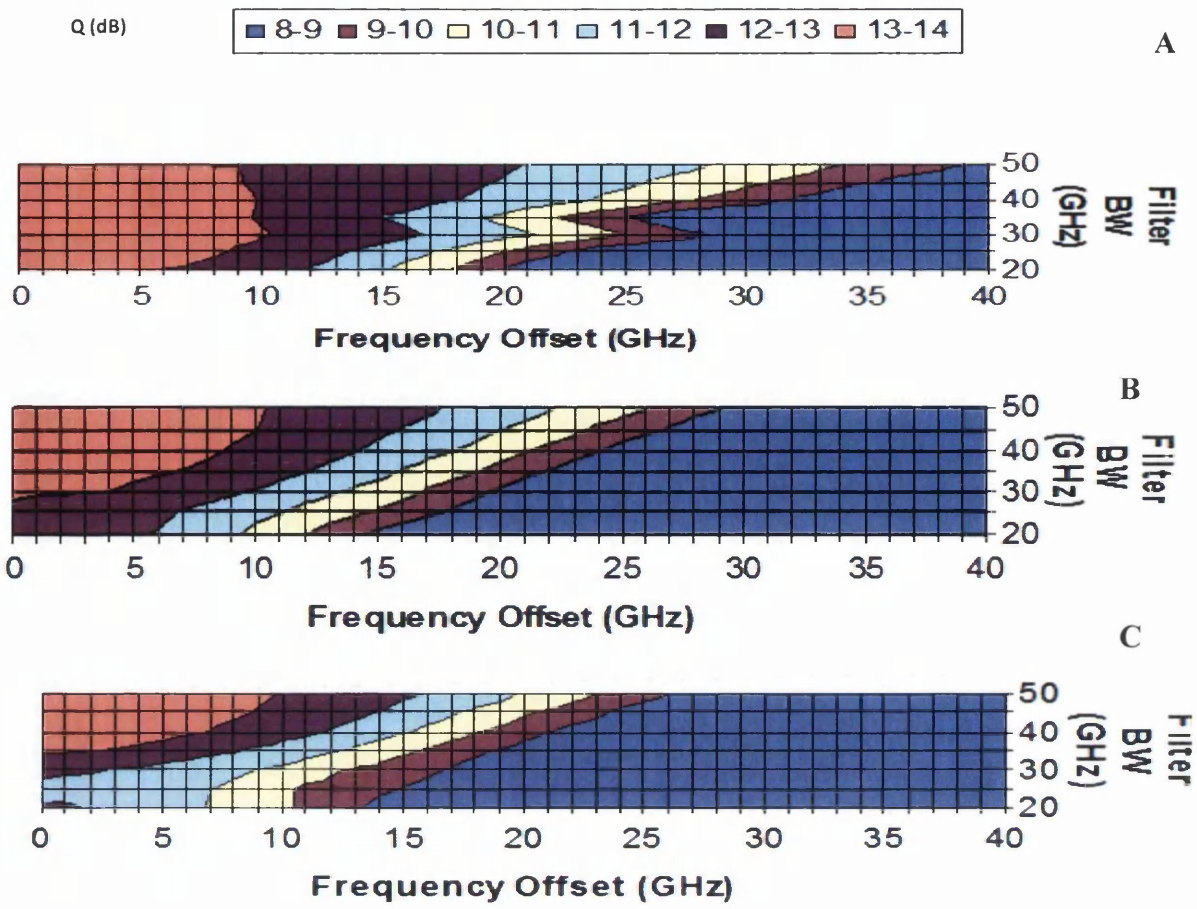

Figure 4.6 ; The contour plots labeled A (1st order Gaussian filter GF1), B (2nd order Gaussian filter GF2), and C (3rd order Gaussian filter GF3) are for Q values in (dB) with filter bandwidth (GHz) plotted against frequency offset (GHz) for 16dB OSNR of a 42.7Gb/s RZ-DQPSK system.

The trend as observed in the above contour plots labeled A-GF1, B-GF2, and C-GF3 are for Q value in (dB) with optical filtering bandwidth (20 to 50GHz) plotted against frequency offset (0 to 40GHz) for 16dB OSNR of a 42.7Gb/s RZ-DQPSK system. As observed from the offset filtering plot labeled GF1 which is for a 1st order Gaussian filter, it is seen that there is minimal induced performance penalty from band-limited filtering reductions from 50GHz to 20GHz OBPF. Importantly the performance seen here is also in agreement with [4] for the case of 50GHz OBPF. There is a progressive 1dB Q value performance penalty for every 10GHz centre frequency displacement for the range of filtering bandwidths for 20 to 50GHz OBPF.

The second plot above labeled B (i.e. 2nd order Gaussian filter), illustrates the performance offset filtered 42.7GB/s RZ-DQPSK system from 20 to 50GHz OBPF. It is evident from this plot that performance of narrow band limited filters i.e. 20 to 30GHz OBPFs do suffer 1dB Q value penalty as compared to higher band pass filters 35 to 50GHz.

The situation with offset filtering shows a progressive 1dB Q value penalty as the filter centre frequency is displaced progressively by every 10GHz. But as the filtering offset increases further away from the 0 offset (i.e. around the 75% filter bandwidth) the performance penalty of the 2nd order Gaussian filter increases more compared to the performance of the 1st order Gaussian OBPF.

Thus it is obvious that the steepness of the OBPF skirts do affect the performance of a DQPSK system in an ASE noise dominated regime. The lesser the steepness of the OBPF the better the robustness to band limited and offset filtering in the presence of ASE noise.

The level of performance penalties of the offset filtered 42.7 RZ-DQPSK is influenced by the particular bandwidth and the level of filtering asymetricity. As obvious in the subsequent plots GF3 and GF4 (3rd and 4th order Gaussian filters), the performance penalties increases as the order of Gaussian filters increase; for the case of the 3rd order Gaussian filter the (50 to 35GHz) OBPF have the same performance as 0 centered filtering. These results are different from the 1st order Gaussian filter performance of the 42.7GB/s RZ-DQPSK in plot 1 (GF1) where there is no performance penalty from (50 to 20GHz) OBPF for the 0 centered filtering.

The results in figure 4.6 show that the shape and bandwidth of OBPF is very influential in choice of any optimization scheme. The analysis of 42.7Gb/s RZ-DQPSK system under the impact of narrow OBPF and offset filtering cannot be complete without a comparative evaluation with the performance of 42.7Gb/s RZ-DPSK system, in the figure 4.7 below plots the penalties induced by offset filtering in a 35GHz OBPF 42.7Gb/s RZ (DQPSK and DPSK) systems are shown.

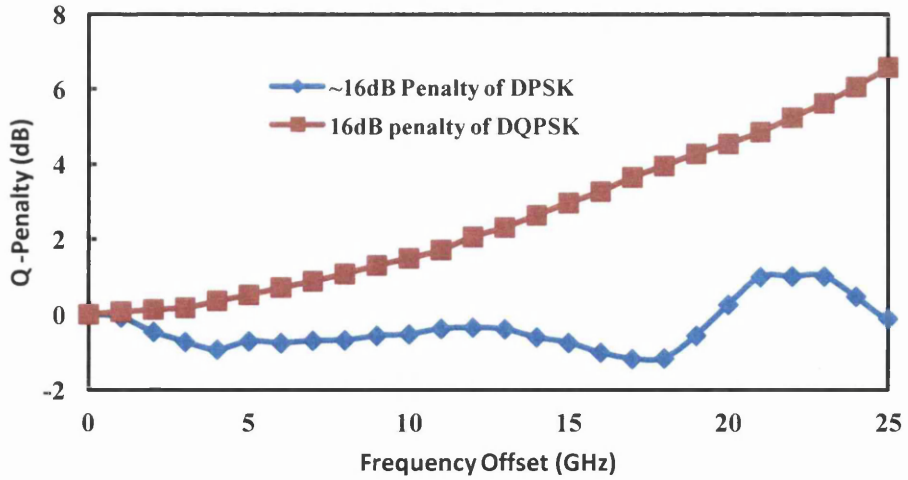

Figure 4.7 ; The plot of Q-Penalty in (dB) for 35GHz OBPF plotted against frequency offset (GHz) for 16dB OSNR of 42.7Gb/s RZ-DQPSK and 42.7Gb/s RZ-DPSK system.

The above figure 4.7 shows the performance penalty from offset filtering from (0 to 30GHz) offset of 35GHz OBPF 42.7GHz RZ-DQPSK and RZ-DPSK system for an OSNR of 16dB for both 3rd order Gaussians filter. As illustrated in the plot above the penalty induced from the performance of 42.7Gb/s RZ-DQPSK system increases from (0 to 25 GHz) frequency offset with penalties ranging from (0 to 7) dB unlike the performance of the same osnr DPSK system where the maximum penalty is ~1dB for 22dB offset of the 35GHz OBPF.

Also as already explained in the former chapter 3 the performance of the DPSK system tends to reach a peak in performance penalty around half the filter bandwidth for a strongly filtered system. The gradually decline in performance (increase in penalty) as seen in the DQPSK performance, is what is expected for most modulation schemes. But the narrow filtered 42.7 Gb/s DPSK is different due to its partial response signaling at the demodulator and simplicity of the symbol modulation enhances better tolerance to offset filtering than DQPSK system.

We would expect the performance improvement as seen in DPSK systems [1,] to be scaled in DQPSK systems but unfortunately the case is not the same [9]. Although it has been shown that DQPSK system suffers more performance penalty compared to DPSK system for the same symbol rates [19]. This alone will justify the sensitivity of the DQPSK systems to asymmetric filtering. In [1,2,3] it was reported that the DPSK system has a 600% better tolerance to offset filtering (laser detuning) than the corresponding DQPSK. The justifications for the lesser tolerance of DQPSK to offset filtering are explained below.

1 The higher level signaling with DQPSK was identified as the one of the major reasons for the less tolerance to offset filtering compared to offset filtering with DPSK. The frequency shift in the AMZI can be represented in the below equation.

$$2\pi\nabla f = \frac{\partial\varphi}{\partial T} \quad 4.18$$

Where T represents the time delay in the AMZI, for a perfect system T is equal to $\frac{1}{S_r}$, φ represents the phase error and ∇f is the frequency. Frequency itself can be defined as the rate of change of phase.

$$T \times 2\pi\nabla f = \varphi \quad 4.19$$

The phase error accumulated for 42.7Gb/s DQPSK offset filtering at the output of the MZI is twice the phase error for 42.7Gb/s DPSK by virtue of the above relationship that translates to the below equations for the same frequency offset.

$$\varphi(DQPSK) = 2T \times 2\pi\nabla f \qquad 4.20$$

$$\varphi(DPSK) = T \times 2\pi\nabla f \qquad 4.21$$

From the equations (4.21) above it is obvious that the effect (phase error) of center frequency offset of the OBPF (laser detuning) in DQPSK systems is twice the effect of the DPSK system for the same data rate. The increase in phase error generation of DQPSK will negate the destructive and constructive interferences of the AMZI, which will eventually result in error prone phase demodulation. Imperfect demodulation (phase to intensity conversion) affects the sensitivity of phase modulated system. Therefore the improved sensitivity of DQPSK systems to linear impairment will be lost with laser detuning (or frequency offset of OBPF).

Also in [1] the lesser performance of DQPSK systems with offset frequency (filtering) compared with DPSK as evident in the increased eye closure of DQPSK was attributed to the a higher Multi-level signaling (encoding) and different operational points (phase for detection) at the AMZI. The increased complexity of the encoding and decoding of DQPSK is directly proportional to the performance penalty via offset filtering. Also of great importance is the distance between constellation points of the DQPSK modulation formats which is half the distance between constellation points of the DPSK modulation formats.

Thus constellation points separation difference between both modulation formats been (factor of 2) twice distance of the DQPSK for the DPSK accounts for about 3 times the sensitivity to laser frequency offset for DQPSK. Increased symbol per bit is also a major factor limiting the performance of DQPSK systems in the presence of laser frequency offset or filtering offsets

4.7 Solutions to DQPSK sensitivity to Offset filtering.

The negating impact of AMZI (phase) frequency offsets on 42.7 GB/s DQPSK systems is very high i.e. the effect of detuning the laser or offsetting the optical bandpass filter in DQPSK systems has been qualitatively compared to DPSK systems in [1, 2, 3] as having a sextuple sensitivity relative to DPSK. The impact of DQPSK demodulation impairments (phase error, AMZI delay, and extinction ratio, amplitude imbalance at the BPD

and signal delay at the BPD) was analyzed in [1] and phase error due to AMZI frequency offset was identified as the major drawback for DQPSK systems.

When the performance of DQPSK systems in linear and non linear regimes are also evaluated in conjunction with demodulation impairments, the severity of the impact of frequency detuning on DQPSK is a major standout as also evident in the figure 4.6 above; Where the ASE noise limited and frequency offset performance of a 42.7Gb/s RZ-DPSK and RZ-DQPSK were both modeled for a typical filter bandwidth experienced in a 50GHz grid. For a frequency offset of half the filter bandwidth in figure 4.6 , the DQPSK system experienced a 3.6dB performance penalty while the DPSK system witnessed a 1.1dB penalty reduction. The contrasting performance of the DQPSK system and the DPSK system with offset filtering is very intriguing, being that the difference between both phase modulated systems is a symbol ratio of 2:1.

4.7.1 Impact of an Asymmetric filtered receiver model on 42.7Gb/s 50%RZ-DQPSK

However despite the detailed physical explanations that has been reported in [1,2,3,4], these research which is based on offset filtering of high speed phase modulated signaling still seek to further understand and improve the performance penalty inherent in offset filtered (laser detuned) 42.7 Gb/s DQPSK systems. Thus a novel model similar to the 42.7 Gb/s RZ-DQPSK system modeled in figure 4.2, but with some alterations at the receiver. The motivation for this model comes for the model that was deployed in the chapter 3; The novel asymmetric filtering receiver design was based on particular physical circumstances evident at the outputs of the MZI for a DPSK system (DB and AMI). However the spectra profile of the output ports of MZI for DPSK is different from the spectra profile of the outputs of AMZI for the DQPSK systems. This is due to the intrusion of the IN-phase modulated DQPSK signals into the Quadrature signals and vice versa. Thus this intrusion results in cross talks that reduces DQPSK system performance relative to DPSK for the same symbol rates.

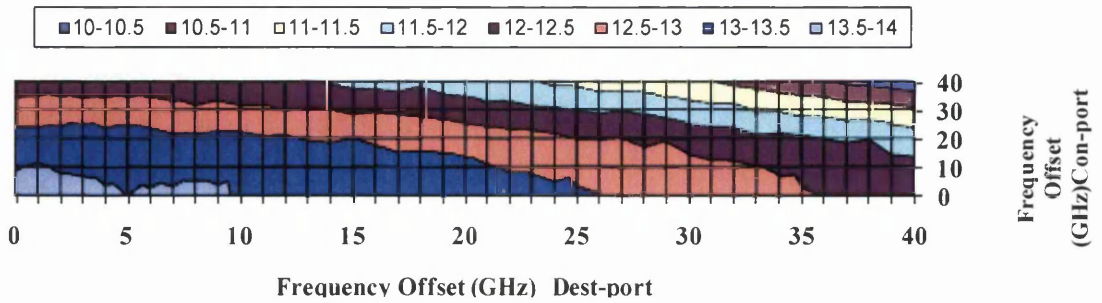

Fig 4.8The contour plot labeled above (1st order 50GHz Gaussian filter), for Q value (dB) plotted against frequency offset of filter at Destructive port –X axis(GHz) and frequency

offset of filter at Constructive port –Y axis(GHz) for 16dB OSNR of a 42.7Gb/s RZ-DQPSK system.

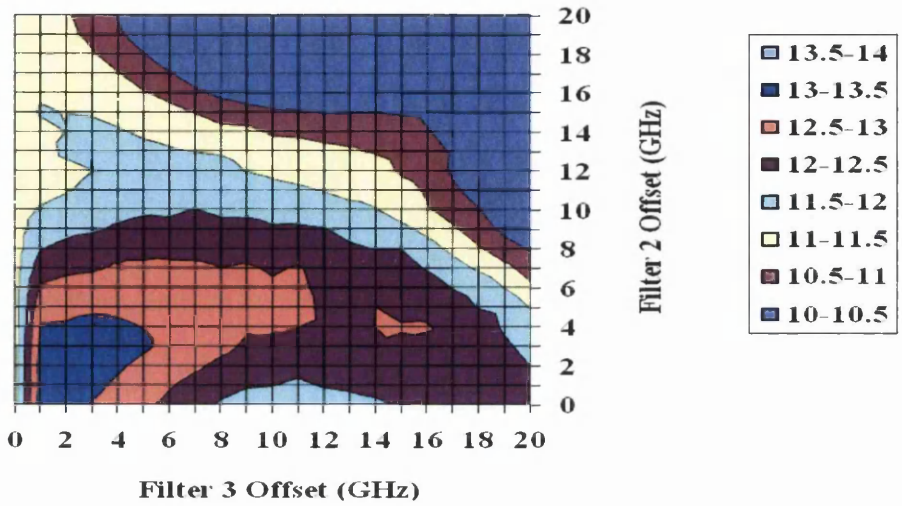

Fig 4.9 The contour plot labeled above (3rd order 35GHz Gaussian filter), for Q value (dB) plotted against frequency offset of filter at Destructive port –X axis(GHz) and frequency offset of filter at Constructive port –Y axis(GHz) for 16dB OSNR of a 42.7Gb/s RZ-DQPSK system.

The contour plots 4.8 and 4.9 are for the performance of a novel filtering design similar to the DPSK model as shown in figure 3.13, but without the filter 1. Thus the motivation for deploying this filter design is to investigate the impact of offset filtering at the two output ports of the AMZI on the performance of a 42.7 Gb/s DQPSK system. The same design was deployed with a DPSK system and it was shown to improve performance by 2dB at low OSNRs (figure 3.15 and figure 3.16). However the result has seen here in figure 4.8 and 4.9 both for different filter bandwidths and shape (figure4.8 -50GHz OBPF 1st order and 4.9 - 35GHz OBPF 3rd order Gaussian filters). The aim of choosing different bandwidths and filter shape is to characterize the impact of the novel filtering design on DQPSK systems and compare with conventional filtering design.

But the results as seen in 4.8 and 4.9, does not show any performance improvement of novel filtering design with a 50GHz OBPF but interestingly improves the performance of the 35GHz OBPF by about 1 dB. The different performances of the novel filtering design with a DQPSK system via different bandwidths can be compared to the performance of asymmetric filtered DPSK systems with different filter bandwidths, where wider filter bandwidths do witness the same level of performance improvements as seen in strongly filtered regime. The absence of significant performance improvements in a DQPSK system via the novel filtering design can be attributed to the level of cross talk between both tributaries. It is well known

that the duobinary signal at the constructive port of a balanced detected DPSK system is very tolerant to tight filtering and the AMI at the complementary output port of the AMZI is very sensitive to narrow filtering. But the results here with the novel DQPSK contour plot above shows an almost equal response of the two output ports as seen on the axis of the contour. The results here does show a marginal performance improvement for the 42.7 Gb/s DQPSK with a 3rd order Gaussian 35 GHz OBPF, this gives some insights on the inherent performance improvement potentials available at the DQPSK demodulator. Thus more extensive investigations are desirable with different filter bandwidths, filter shapes and signal formats so that a comprehensive impact evaluation of the novel filtering design on a 42.7 Gb/s DQPSK systems can be achieved. .

4.8: Impact of offset filtering on 42.7Gb/s DQPSK system in ultra narrow optical filtering regime.

Considering the symbol rate of a 42.7 Gb/s DQPSK which is dual 21.34Gb/s, thus a 35GHz OBPF does not necessarily represent a strong filtering regime for a 42.7 Gb/s DQPSK system. Herein a very strong (17.5GHz OBPF) optical filtering is deployed at the receiver to investigate the extent of the tolerance of the DQPSK system to very narrow filtering.

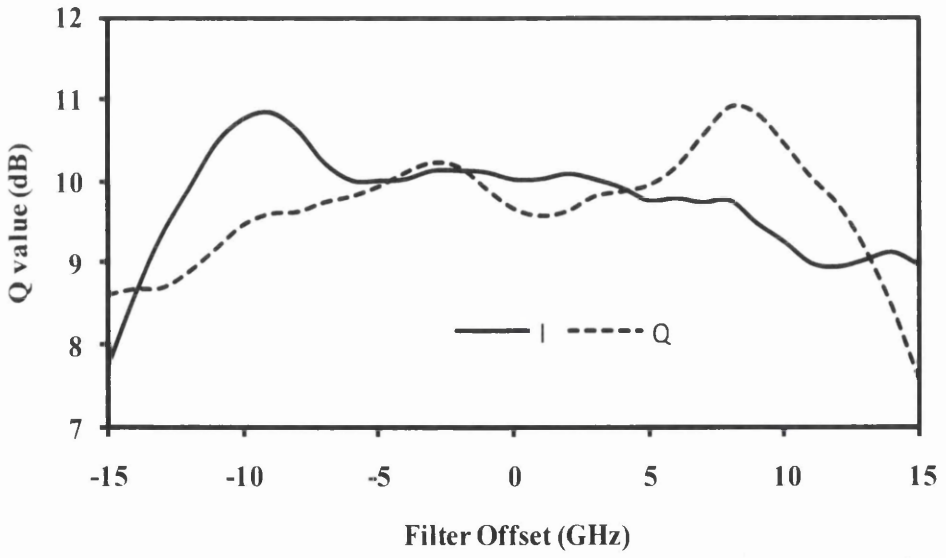

Fig 4.10: Q value (dB) vs frequency offset of filter of a 42.7Gb/s RZ-DQPSK system 3rd 17.5GHz OBPF for 20dB OSNR (dashed lines for quadrature receiver and continuous line for the in phase receiver performance).

The figure 4.9 above shows the Q value in dB plotted against filter offsets in GHz for a 3rd order 17.5 GHz OBPF for a 42.7 Gb/s 50%RZ –DQPSK system. The dash line represents the performance of the quadrature receiver and continuous line represents the performance of the in-phase receiver. The performance shows that at half filter width the performance of the system is improved by around 1dB in calculated Q values as compared to the symmetric filtered case.

Although if the in-phase receiver is considered the filter has to be displaced from carrier frequency by around 8GHz offset to the negative axis, offsetting to the positive axis leads to performance penalty. Vice versa is true for the performance of the quadrature receiver. Thus the result here shows that tolerance of the DQPSK system to offset filtering (laser detuning) is significantly improved in a very narrow filtering regime. If the results here are compared with results in chapter 3 for DPSK system, there is a performance penalty of more than 3dB.

The remarkable feature of the result here is that offset filtering could enhance the performance of 42.7Gb/s DQPSK system in a 25GHz grid.

4.9: Summary on Chapter 4

The impact of band limited filtering, different filter shapes, chromatic dispersion and offset filtering on 42.7 Gb/s DQPSK system has been examined in this chapter. The 42.7Gb/s DQPSK modulation format is very tolerant to strong optical filtering most especially within a 50GHz grid, it offers a better tolerance to chromatic dispersion than an equivalent DPSK system at the same data rate.

Comparing figure 3.2 and figure 4.3 using the performance of a 35GHz optical band pass filter (representative of actual bandwidth available in a 50GHz due to concatenation of several filters) as an indicator, the DQPSK system offers 2dB penalty via best and worst performance of the different filter shapes as opposed to ~6dB performance penalty inherent with an equivalent DPSK system. Thus a DQPSK system is more robust to variations in filter shapes.

Despite the numerous merits of a DQPSK system relative to a DPSK system, an outstanding performance limitation is the performance in the presence of laser detuning (filter offset) or phase error. In the presence of offset filtering the performance of a DQPSK system becomes a performance penalty. In this chapter different receiver designs have been modeled to address this problem and the impacts have been marginal compared to the performance of DPSK systems in the presence of offset filtering. This is largely due to the lesser symbol spacing inherent in a DQPSK systems, which enhances crosstalk from the opposite tributaries.

4.10: Chapter4-References

[1] H. Kim and P. J. Winzer, "Robustness to laser frequency offset in direct detection DPSK and DQPSK systems," *J. Lightw. Technol.*, vol. 21, no. 9, pp. 1887–1891, Sep. 2003.

[2] K.-P. Ho, "The effect of interferometer phase error on direct-detection DPSK and DQPSK signals," *IEEE Photon. Technol. Lett.*, vol. 16, no. 1, pp. 308–310, Jan. 2004.

[3] G. Bosco and P. Poggiolini, "On the Joint Effect of Receiver Impairments on Direct-Detection DQPSK Systems" *J. Lightw. Technol* , vol. 24, no. 3, March 2006.

[4] M. Serbay, et al. "Experimental Investigation of Asymmetrical filtered 43 Gb/s RZDQPSK" *IEEE/ LEOS* annual meeting 2006, paper WH5

[5] V. Mikhailov, R.I. Killey, and P. Bayvel "Experimental investigation of partial demodulation of 85.3 Gb/s DQPSK signals" in *OFC 2007*.

[6] Bhandare, S.; Sandel, D.; Abas, A.F.; Milivojevic, B.; Hidayat, A.; Noe, R.; Guy, M.; Lapointe, M.; "2×40 Gbit/s RZ-DQPSK transmission with tunable chromatic dispersion compensation in 263 km fibre link" *Electronics Lett*, vol 40 Issue:13 pp: 821 – 822. Jun 2004

[7] P. J. Winzer and R. J. Essiambre, "Advanced modulation formats for high-capacity optical transport networks," *J. Lightwave Technol.*, vol. 24, pp. 4711-4728 (2006).

[8] P. S. Chao, V.S. Grigoryan, Y. A. Godin, A. Salamon, and Y. Achiam, "Transmission of 25 Gb/s RZ-DQPSK Signals with 25 GHz Channel Spacing over 1000 km of SMF-28 Fiber", *IEEE Photonics Technology Letters,* vol. 15, (2003), 473–475.

[9] D. Penninckx, H. Bissessur, P. Brindel, E. Gohin, and F. Bakhti, "Optical differential phase shift keying (DPSK) direct detection considered as a duobinary signal," in "*Proc"ECOC*, vol. 3, pp. 456–457, 2001.

[10] C. Chien, Y. Wang, I. Lyubomirsky, and Y. K. Lizé, "Experimental Demonstration of Optical DQPSK Receiver Based on Frequency Discriminator Demodulator" *J. Lightw. Technol,* vol 27,Issue 19, Oct 2008.

[11] F. Vacondio, A. Ghazisaeidi, A. Bononi, and L. A. Rusch, "DQPSK: When Is a Narrow Filter Receiver Good Enough?" *J. Lightw. Technol*, vol. 27, no. 22, Nov 15, 2009.

[12] S. Haykin "Communication Systems 4Th Edition" 2001.

[13] G. Bosco and P. Poggiolini, "On the Joint Effect of Receiver Impairments on Direct-Detection DQPSK Systems" *J. Lightw. Technol*, vol. 24, no. 3, Mar 2006.

[14] D. van den Borne, S. L. Jansen, E. Gottwald, G. D. Khoe, H. de Waardt, "Optical Filtering tolerances of 42.8-Gbit/s RZ-DQPSK Modulation" in "Proc". *OFC* (2006).

[15] L. Zong, J. Veselka, H. Sardesai, and M. Frankel "Influence of Filter Shape and Bandwidth on 44 Gb/s DQPSK Systems", in "Proc" *OFC 2009*- post deadline papers, OFC 2009.

[16] P.J. Winzer and Rene-Jean Essiambre "Optical Receiver Design Trade-Offs" in "Proc" *OFC*, Technical Digest (Optical Society of America, 2003), paper ThG1.

[17] K. Kikuchi, "Phase-Diversity Homodyne Detection of Multilevel Optical Modulation With Digital Carrier Phase Estimation" *IEEE J. Select. Topics Quantum Electron*, vol. 12, no. 4, July 2006.

[18] P. S. Chao, V.S. Grigoryan,Y. A. Godin, A. Salamon, and Y. Achiam, "Transmission of 25 Gb/s RZ-DQPSK Signals with 25 GHz Channel Spacing over 1000 km of SMF-28 Fiber", *IEEE Photonics Technology Letters*, vol. 15, (2003), 473–475.

[19] C. Wree etal "Linear electrical dispersion compensation of 40Gb/s polarization multiplex DQPSK using coherent detection" *IEEE/LEOS* Summer Topical Meetings, 2008 Digest

[20] A.H. Gnauck, P.J. Winzer, S. Chandrasekhar, "Hybrid 10/40-G transmission on a 50-GHz grid through 2800 km of SSMF and seven optical add-drops" *Photon.Technol. Lett.*, vol 17 Issue: 10 2005.

[21] G. Charlet, P. Tran, H. Mardoyan, M. Lefrancois, T. Fauconnier, F. Jorge and S. Bigo, "151 x43Gb/s transmission over 4,080km based on Return-to-Zero-Differential Quadrature Phase-Shift Keying" in "Proc" *ECOC* 2005.

[22] G. Agrawal, "Nonlinear Fiber Optics, Third Edition"

[23] Y. Cai, J. Cai, A. Pilipetskii, G. Mohs, and N. S. Bergano "Spectral efficiency limits of pre-filtered modulation formats" Vol. 18, No. 19 / *Opt Express*, 13 Sept 2010.

[24] O.A Olubodun and N.J. Doran, "Performance Improvement of Asymmetrical Filtered 40Gb/s RZ-DPSK Receiver Design -Strong Filtering Considerations" *IEEE/NOC* July 2011.

[25] D. Penninckx, H. Bissessur, P. Brindel, E. Gohin, and F. Bakhti, "Optical differential phase shift keying (DPSK) direct detection considered as a duobinary signal," in "Proc". *ECOC2001*, vol. 3, pp. 456–457.

[26] D.V. Borne "Robust Optical Transmission Systems/Modulation and Equalization" PhD Thesis page 95-96 (2008).

[27] N. Yoshikane and I. Morita, "160 percent Spectrally-Efficient 5.12 Tb/s (64 x 85.4 Gb/s RZ-DQPSK) Transmission without Polarisation Demultiplexing," in "Proc". *ECOC 2004*, Stockholm, Sweden, Sep. 2004, post-deadline paper Th4.4.3.

CHAPTER 5:

5.1 Optical Coherent Binary Phase Shift Keying (BPSK) modulation format in 50GHz Grid.

This chapter describes the optical coherent phase shift keying modulation (BPSK) within the context of tight optical filtering, most especially the impact of offset filtering within a 50GHz grid. However, having described the contribution of this research investigations to enhancements of DPSK demodulation on a 50GHz grid with offset filtering in chapter 3, and the performance penalty reduction impact of offset filtering on a 42.7Gb/s DQPSK in chapter 4, it becomes imperative to investigate the impact of offset filtering on a coherent detected 42.7Gb/s BPSK system. By comparing DPSK and BPSK signalling in terms of phase referencing, it could be envisaged that the impact of offset filtering on a BPSK system in a tight optical filtering regime might be more beneficial than the an equivalent DPSK systems.

The exact phase referencing with BPSK detection as compared to relative self referencing between successive bits with DPSK might be the key factor determining better performance between the two modulation/demodulation formats. Chapter 5 is composed of the following: the impact of band-limited filtering on BPSK systems, impact of filter shapes, impact of offset filtering and impact of chromatic dispersions all on an optical BPSK modulation format within a 50GHz grid.

5.2 Impact of band limited filtering on coherent BPSK

Coherent BPSK detection has been identified as having about 4 dB improved sensitivity in the presence of ASE noise over the IMDD, also about 2dB improved sensitivity over DPSK detection. The performance analysis of both DPSK and Coherent BPSK is that of mixed merits and demerits, because despite the reported performance improvement of coherent BPSK over other modulation formats, inherent linewidth increase limitation and phase locking requirement are difficult to implement in practise, thus until this impairment is addressed in coherent BPSK i.e. by designing phase lock loops or improving the robustness of coherent homodyne detection to increase laser linewidth it may be difficult to actualize the vast benefits of coherent BPSK.

Notwithstanding it is still relevant to analyse the impact of optical band-limiting filtering on the PSK signals in the presence of ASE noise. The generation of ASE noise is one of the major drawbacks in the transmission of different modulation formats. In the presence of shot

noise the performance of coherent BPSK has been reported in [5] to achieve the best receiver sensitivity of all modulation formats via its lesser number of photons per bit requirement for detection.

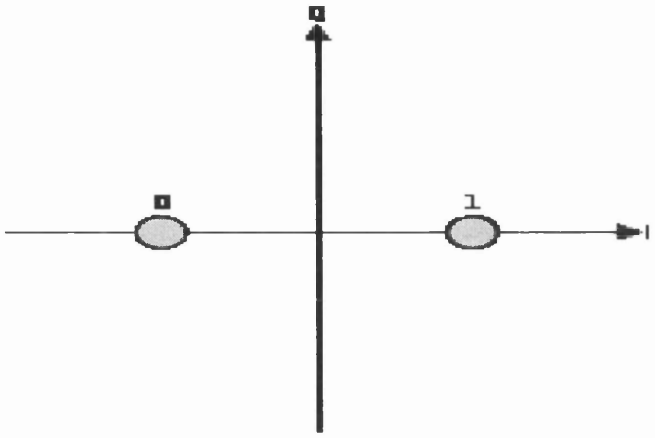

Fig 5.1 BPSK constellation diagram

It is important to note that employing strong OBPF generally results in performance penalty for strongly filtered formats. But the use of narrow filters becomes inevitable particularly on a 50GHz grid which is within the context of this research. The ASE rejection by narrow filtering, the performance of duobinary signalling inherent BPSK formats (constructive port) and the exact phase exaction due to the BPSK signal mixing with the local oscillator's signal, alleviate the performance penalties of strongly filtered PSK modulation formats.

The performance of BPSK modulation formats in the presence of strong filtering will be modelled in this chapter in order to make comparative analysis of BPSK and DPSK formats. The tolerance of DPSK format to tight optical filtering has been reported in [10]. In these analyses wide and narrow bandpass filters have been employed via numerical analysis to characterize the performance of homodyne BPSK detection.

It is important to examine the influence of optical bandpass filters on the performance of Homodyne PSK detection as would be encountered via concatenation of several filters (in practical systems) is inevitable and most importantly on a 50GHz grid.

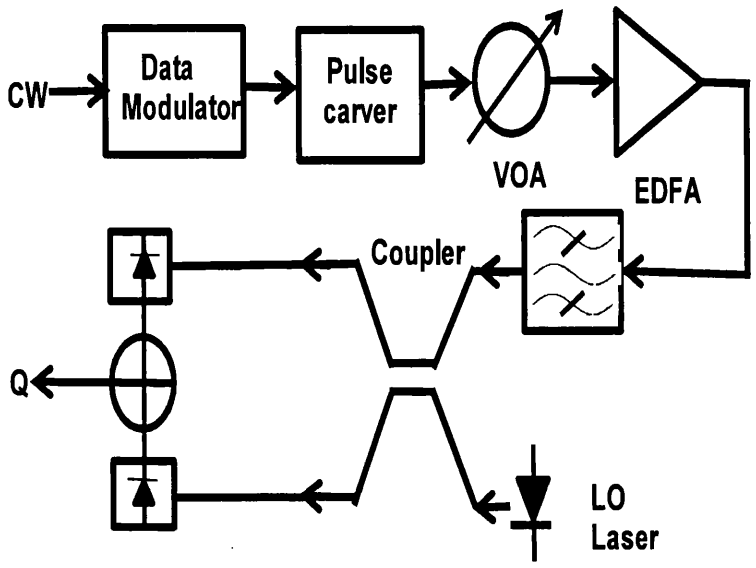

Figure 5.2: Schematic diagram of Coherent BPSK model.

This examination is firstly initiated by mixing the received PSK signal with a local osciillator signal via a bidirectional coupler. The system used in the simulations, illustrated in Fig 5.2 above, is as follows; a 27 PRBS is used to drive a Mach-Zehnder modulator (MZM) to produce a 42.7 Gb/s PSK optical signal. We confirmed that increase in length of PRBS does not result in any significant change in observed trends. A pulse carving MZM is used to generate a 50% RZ signal. Noise is then added using the VOA/amplifier combination. At the receiver, the PSK signal is fed through an optical bandpass (OBPF) filter then to the 1st input arm of a 3dB coupler. The other input of the 3dB coupler is fed with a local oscillator signal.

The local oscillator phase is varied to establish the best performance [4]. The output of the coupler (left arm of the mixer) couples the in-phase PSK signal with the in–phase local oscilllator's signal, the right arm of the mixer couples the out-of-phase PSK signal with the out-of-phase local oscillator signal. A balanced detection model is used to generate the calculated 'Q's. The outputs of the mixer constructive and destructive ports are fed to two photodetectors.

The OSNR at the receiver for the investigation was varied from 15dB to 25dB. The filter at the receiver was generally taken between 80 to 40GHz, although narrow bandpass filtering performance is the major focus of this investigation. It is important to understand the performance trend of PSK homodyne detection from wide filtering regions to narrow filtering regions. A 30GHz bandwidth 5th order Bessel electrical filter (~70% of the optical

bandwidth) was used following the receiver. In the following the Q-values were calculated assuming Gaussian statistics.

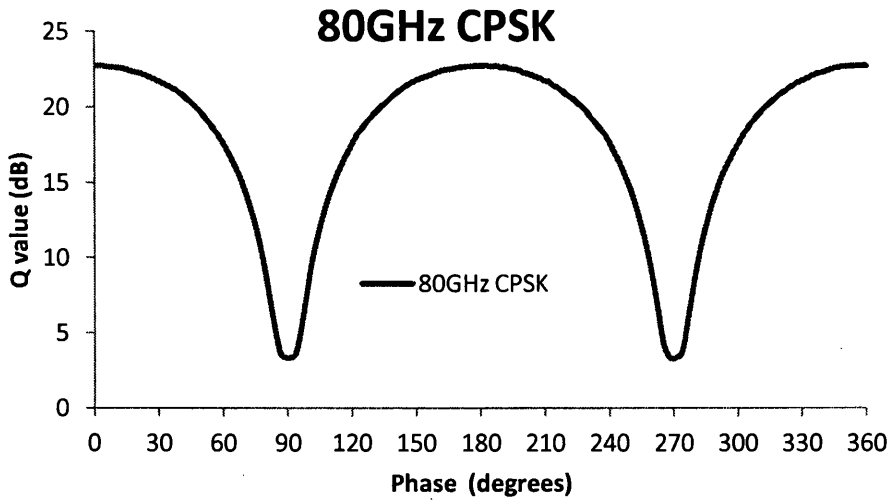

Figure 5.3 The Q values in (dB) for a 80 GHz OBPF Homodyne 42.7Gbps coherent BPSK system plotted against local oscillator phase (Degrees).

Figure 5.3 above shows the performance of an 80GHz OBPF Homodyne 42.7Gbps BPSK system plotted against local oscillator's signal phase (degrees). This result shows that the performance of a Homodyne 50%-RZ PSK system (80GHz OBPF) exhibits a periodicity of 180 degrees at the detector which is consistent with the phase separation of the modulated symbols at the transmitter.

The plot also highlights the significance of phase locking of the homodyne BPSK detection, without which the inherent benefits of the homodyne detection is not optimized. The difficulty in achieving phase locking practically is also shown here with the maximum performance of the homodyne detection is only achieved when the local oscillator's signal is aligned to the phase of the data signal and at ± 90 degree phase alignment the performance of the PSK system is at a minimum. The intermediate frequency of the homodyne PSK is null, due to the frequency alignment of the carrier frequency and local oscillator laser's frequency. The phase periodicity shown here confirms an inherent attribute of phase alignment of a perfect homodyne PSK detection.

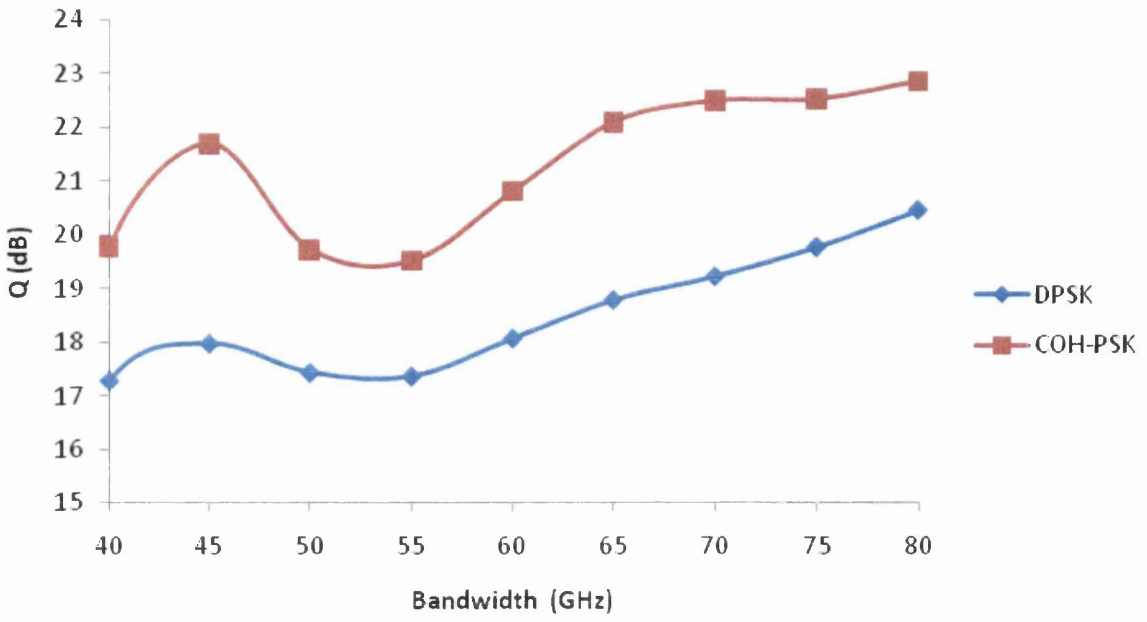

Figure 5.4: The Q values in (dB) plotted against Optical bandwidth (GHz) for a 40 to 80 GHz OBPF Homodyne 20dB 42.7Gbps 50%RZ-PSK and DPSK systems

The figure 5.4 above illustrates the performance of 50%-RZ BPSK and DPSK systems for a 42.7Gb/s data rate. The figure shows the performance of optical band-limited filtering for both DPSK and PSK modulation formats. As seen above there is ~2dB improvement in performance of the coherent PSK system for 40 to 80GHz OBPF over a corresponding DPSK system. The better baseband extraction of the coherent PSK is responsible for the improved sensitivity over the DPSK version, in this case the better (exact) phase extractions of the local oscillator and received signal mixing over the self referencing of the DPSK accounts for the improved sensitivity.

Thus in the presence of ASE noise limited back-to-back transmission of phase modulated formats the PSK achieves ~2dB improvement in Q performance for an OSNR of 20dB over the DPSK format within wide to narrow optical filtering regimes. In view of the OSNR employed in the simulations (20dB) this result is consistent with reported investigations in [7,11] where PSK has been shown to record best receiver sensitivity. Although in some related context the performance of DPSK has been comparable to the synchronous heterodyne systems due to similar photon/bit requirement of the receiver (i.e. 21.9 and 20

photon/bit). It must be noted that in the absence of pre-amplification the sensitivity of the coherent homodyne detection can be as much as 20dB improvement over the direct detected case. This also strengthens the popularity of the DPSK modulation in pre-amplified systems where the receiver sensitivity is greatly improved due to the dominance of the ASE noise over the shot noise.

In terms of the strong filtering regimes which is the main scope of this investigation there is need to explore the inherent signal amplification and baseband information extraction of the PSK over the DPSK modulation format for performance improvement on a 50GHz grid, despite the performance improvement seen with band-limited filtering of BPSK over DPSK. We shall also be investigating the impact of filter shape, tolerance to laser offset (optical offset filtering) and other related linear impairments (dispersion).

5.3 Impact of filter shape on Homodyne coherent detected 42.7Gb/s BPSK

The relevance of optical filter shape and bandwidth in coherent detection of BPSK systems needs to be investigated to understand its implication on multiplexing and demultiplexing (mux/demux) so as to envisage the inherent constraints in the presence of filter concatenation in WDM transmission for a 50GHz or 100GHz channel spacing. The model used in this investigation is the same model deployed in figure 2. In the simulation the OBPF used emulate a DEMUX, whereby the order of the filters is set from 1 through 4 respectively.
The transfer function of Gaussian filter as defined in equation 2.48:

The figure 5.5 shows a plot of Q in (dB) for several other Gaussian filters for specific bandwidths ranging from 35GHz to 80GHz OBPF for a 42.7Gb/s 50% RZ-BPSK 20dB (OSNR) .

It is evident from above results that for wider bandwidths i.e. 45GHz and above that the penalties accruable from deploying higher other filters reduce. This is in contrast to narrower filters where the performance of the BPSK in strongly filtered regimes shows some heavy penalty. But interestingly the performance of BPSK with a 1st order Gaussian filter is more resilient to narrow filtering penalties as compared to higher order Gaussian filters.

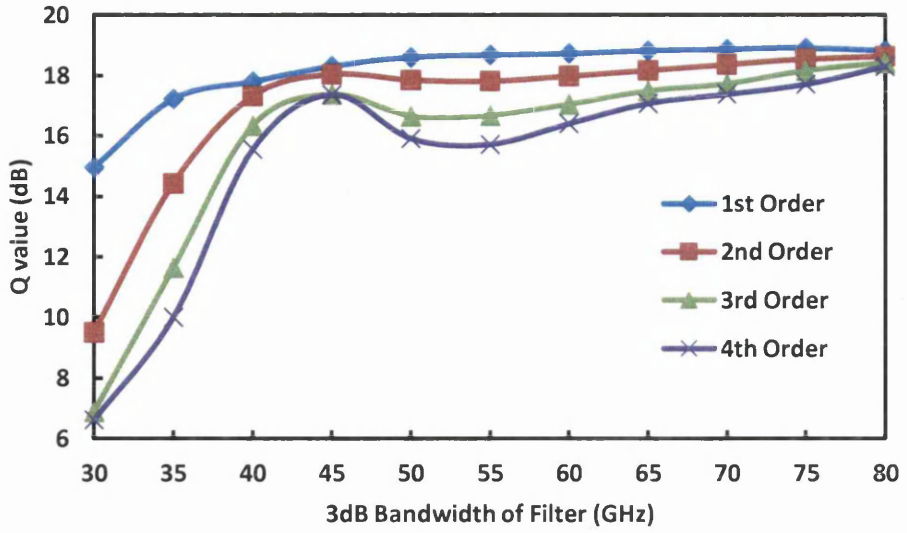

Figure 5.5: The Q values in (dB) plotted against different orders of Optical Gaussian filter bandwidths (GHz) from 30 to 80 GHz OBPF Homodyne 20dB 42.7Gbps 50%RZ-BPSK systems.

It is true that DPSK modulation formats due to the duobinary signal (constructive interference) characteristics have strong tolerance to narrow filtering. This can be derived by deploying narrow filters in single ended detection or by increasing the free spectral range in the MZI (PDPSK) [3].

Thus it will be of interest to seek an alternative performance improvement strategy with BPSK modulation format in narrow filtering regimes. Because the difference between DPSK and PSK is the replacement of phase referencing at demodulator with PSK signal mixed with a pure coherent local oscillator signal, it would be anticipated that the narrow filtering performance of Homodyne BPSK detection should be better than DPSK performance. The baseband extraction by the BPSK detection is thus better as had been shown with the excellent use of DSP to recover the imaginary and real components of detected phase modulation formats [1, 5].

The main focus of this thesis is to investigate strategies for improving analogue transmission of optical phase modulated systems. The performance improvement of DSP, i.e. via electronic dispersion equalization (compensation) has been described as overestimated by [16] as seen in [14, 15]. Also important is to consider the impact of memory modulation formats i.e. combining phase and intensity modulation in improved tolerance to specific impairments [17]. This memory modulation can be induced by pre-filtering (offset filtering) of the memory-less modulation formats [17, 18].

This induced memory modulations as will be seen in the next section can further enhance the performance of BPSK in tight filtering regime. Here in the performance limit of optical coherent BPSK system is investigated without DSP or optical signal processing. Offset filtering and Single side band filtering [12,13] potential strategies that would be explored in the process of improving the sensitivity of Homodyne PSK detection in a 50GHz grid, analogous to the fact that with DPSK, PDPSK has shown performance improvement over conventional DPSK demodulation.

5.4 Impact of Offset filtering on 40 Gb/s coherent BPSK within Strongly filtered regimes

In this section the impact of tight filtering on simple BPSK modulation will be modelled with the aim of evaluating its deployment at 40 Gb/s or at 50Gb/s which with polarization multiplexing could provide a simple route to 100Gb/s transmission. The prospect of deliberately offsetting the filter far from the channel centre to improve performance will be explored. In an earlier work on CSRZ-DPSK [13] it was shown that offset filtering offered ~1 dB improved performance in the presence of ASE noise as compared to symmetric filtering.

The filtering (45 GHz) used in that work was rather wide and may not be fully representative of filtering that can be encountered on a 50GHz grid having several concatenated filters. Here the consideration is for a rather different format of BPSK and will consider the tightly filtered case.

Thus the impact of offset filtering on 42.7 Gb/s coherent BPSK using filter bandwidths in the region of 35GHz will be examined here. It will be shown here that asymmetric filtered 42.7 Gb/s coherent BPSK has an excellent robustness to strong filtering induced penalties compared to the symmetric filtered case. The focus of this section is the improvement of the asymmetric filtered BPSK, that suggests that detuning the transmit laser could result in an exceptional performance improvement in a narrow optical filtering scenario in a 50GHz spaced PSK systems.

The model used in figure 5.2 is also deployed in this section for investigating the impact of offset filtering on a strongly filtered 42.7 Gb/s 50%RZ- BPSK system.

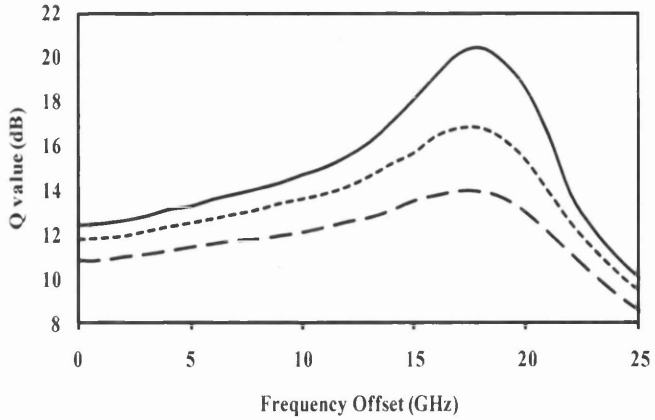

Fig. 5.6 Q values (dB) as function of offset in (GHz) of 42.7Gb/s 50% RZ-PSK 35GHz OBPF for three values of OSNR (dashed-13dB,dotted-16dB continuous-20dB)

The figure 5.6 above illustrates the calculated Q in dB as function of frequency offset of a 35GHz OBPF for three different values of OSNR (13, 16 and 20dB). In all three cases the Q-value rises steadily from zero offset to a peak at ~18GHz and then the performance declines as would be expected. With all three OSNRs the best performance is found with an offset of ~18GHz which is half the filter bandwidth. However when a wider bandpass filter (40GHz) in figure 5.7 is considered the performance trend changes, as compared to the 35GHz OBPF above.

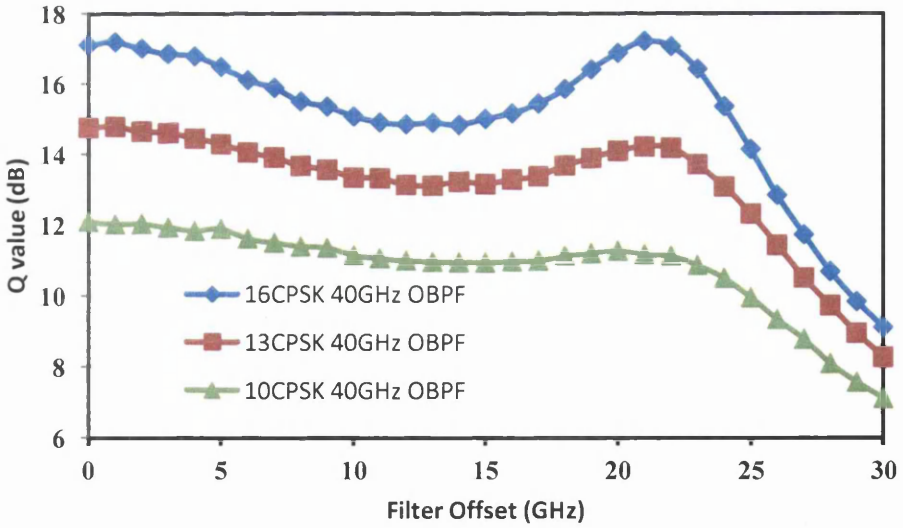

Fig. 5.7 Q values (dB) as function of offset in (GHz) of 42.7Gb/s 50%RZ-BPSK 40GHz OBPF for three values of OSNR (dashed-13dB,dotted-16dB continuous-20dB)

It should be noted that this also a very large fraction of the signal bandwidth. This plot indicates that for a 18GHz offset of a PSK 42.7Gb/s-35GHz OBPF the performance is

significantly improved as compared to the symmetric filtering. The size of the improvement by ~3, 5 and 8 dB for an OSNR of 13, 16 and 20dB respectively is very large and clearly significant. But for a wider filter (40GHz) OBPF the performance of the peak filter offset (around half filter width) becomes more of a performance recovery.

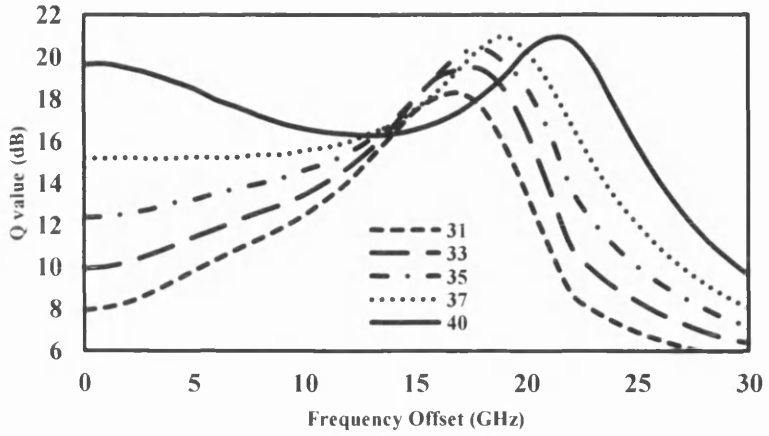

Fig. 5.8 Q value as function of offset in (GHz) for different bandwidths of 42.7 Gb/s 50%RZ-PSK system 20dB OSNR.

The figure 5.8 shows a plot of Q value in dB as a function of frequency offset for a range of filters for an OSNR of 20dB. Of course, in this model, filter bandwidth and data-rate exactly track each other so that stronger values for filtering correspond with what would be expected in a higher data-rate system, e.g. increasing data-rate to 50Gb/s is equivalent to ~25% reduction in filter width.

The different strongly filtered bandwidths show a general trend in performance improvement as the centre frequency of the filter is displaced from the carrier. The peak for the listed OBPFs offsets coincides with half the optical filtering bandwidths. The corresponding performance in Q values (relative to the centre filter Q) for the optimized offsets range from 10dB to 1.23dB improvement for the narrowest to the widest filter used in the calculation. Figure 5.8 shows clearly the decrease in the magnitude of the Q improvement as the filtering bandwidth is increased.

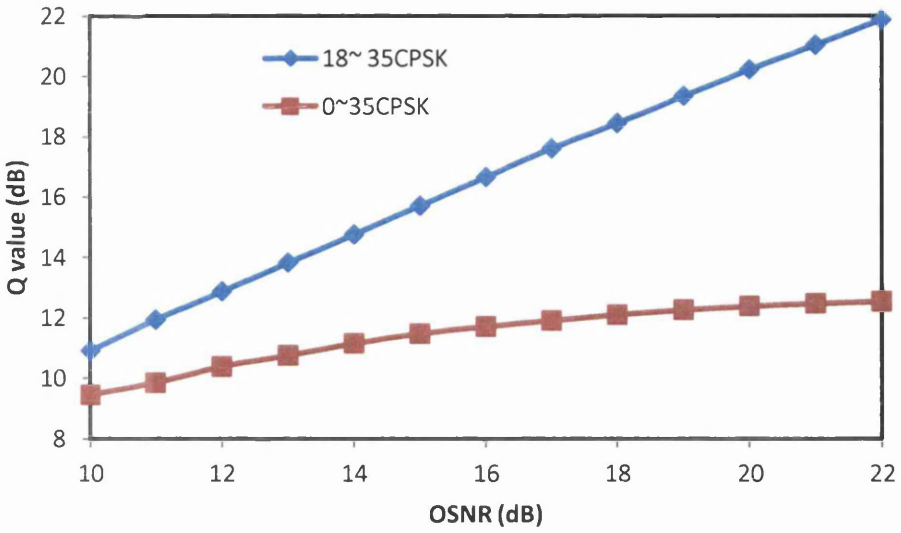

Fig. 5.9 Q value as function of OSNR in (dB) for conventional (square-marker) and 18GHz offset (diamond – marker) for 35GHz of 42.7Gb/s 50%RZ-BPSK system.

These results can be better appreciated by the plots in figure 5.9 which shows the performance improvement of a 35GHz bandwidth for the centred filtered and optimized offset filtering(35GHz-OBPF) for 42.7Gb/s RZ-PSK for 20dB OSNR. For the higher OSNR, the performance improvement is as much as 9dB and the performance diminishes to about 3dB in calculated Q for lower OSNRs.

The initial report of performance improvement by offsetting the filter in phase modulated systems was first reported in [13] for DPSK where relatively wide filtering was used and the improvement observed was modest. By contrast here we have observed a larger performance improvement of PSK with tight offset filtering. The improvement referred to here should be understood to be in effect a recovery from the impact of the tight filter so that the narrower the filter the greater the potential for recovery.

In figure 5.8 it can be seen that an almost full recovery is possible for the case of an ASE limited system if an offset of half the filter bandwidth is achieved. Thus this is why the very large improvements are seen for the narrowest filters [12, 19].

Thus the actual physical reason for the improvements as seen with offset filtering is better analysed with the corresponding eye diagrams in figure 5.10, which compares the received (balanced) eyes at zero offset (5.10A) and that at the half filter bandwidth offset (5.10B). The wider eye opening seen in the offset case (5.10B) is due to pulse width reduction occasioned by an induced memory modulation from offset filtering at half filter bandwidth [17]. The offset filtering at half filter bandwidth (18GHz) clearly introduces side-band

suppression (VSB filtering) and the VSB filtering enhances improved performance over centred filtered case [12, 20, 21] in a tightly filtered regime due to better ASE-noise rejection. More importantly offset filtering (prefiltering) has been identified to induce memory modulation in a memory-less modulation format [18] and memory modulation formats have an inherent better tolerance to specific impairments (tight filtering induced penalties) due to the correlative nature of the memory modulation format [17, 18]. Thus the improved performance of 18GHz offset filtered (VSB) coherent PSK system (memory modulation) over the centred filtered case (memory-less) is due to the additional degree of freedom gained by the offset filtering induced symbol correlations. However the level of the memory modulation induced in a tightly filtered regime is more enhanced with coherent 42.7Gb/s PSK system than as seen with a 42.7Gb/s DPSK system [13, 19] due to a better phase extraction as opposed to the self phase referencing of sequential bits in the DPSK system.

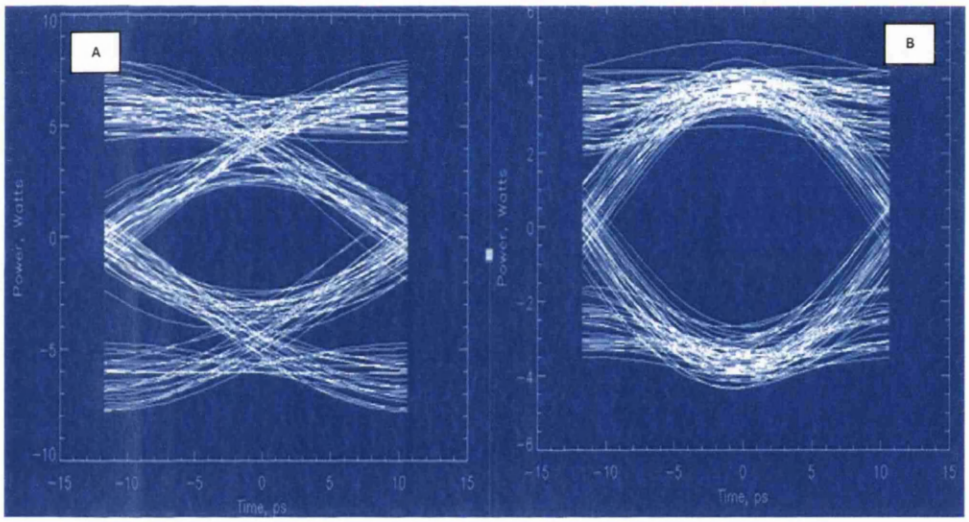

Fig. 5.10 Eye diagrams for 42.7Gb/s BPSK for a centered filtered (A) and 18GHz offset filtered (B) for 35GHz filter (20dB OSNR)

5.5 Chromatic Dispersion performance of Coherent Detected 42.7Gb/s BPSK system

The performance of coherent BPSK systems in the presence of chromatic dispersion has been reported by several papers [1,2] compared to the DPSK, coherent BPSK has been described to a large extent as largely degraded. This leads to the largely popular DSP used in processing of coherent detected signals, by equalizing the baseband at the electrical end for the chromatic dispersion penalties [3,4]. But a paper [16] reported on the resilience of 10 Gb/s coherent NRZ-BPSK to chromatic dispersion induced ISI, this was achieved by phase

rotation of the local oscillator signal. The lesser penalty induced by phase rotation of local oscillator (phase lock loop PLL) in this paper compared to without phase rotation and a similar DPSK system is quite convincing (NRZ in 10Gb/s Coherent PSK system).

In view of RZ receiver designs outperforming NRZ receiver designs in the presence of linear and non-linear impairments, the tight filtering scenario encountered in 50GHz grid and severity of the chromatic dispersion impact on 40Gb/s PSK signals: It becomes inevitable to investigate the impact of residual dispersion on strongly filtered 42.7Gb/s RZ-PSK systems.

The impact of chromatic dispersion on 42.7Gb/s PSK is 16 times the impact on 10Gb/s PSK. The magnitude of the performance improvement seen here within a strong filtering regime via phase rotation of local oscillator's signal in 42.7Gb/s RZ-coherent PSK is significantly higher than reported in [16].

The 42.7Gb/s PSK and DPSK (without phase rotation) performance in the presence of chromatic dispersion are lesser than PSK with PLL. Thus failing to justify the overall potential of the homodyne 42.7Gb/s coherent detected PSK in presence of residual dispersion without (PLL) phase rotation in narrow filtering regimes may lead to overvaluation of the impact of DSP.

5.5.1 Results of chromatic dispersion performance of 42.7Gb/s 50%RZ-PSK.

In this section the unusual performance improvement of 42.7Gb/s coherent BPSK in the presence of residual dispersion will be presented, by actually quantifying the impact of tight optical filtering with 35GHz OBPF.

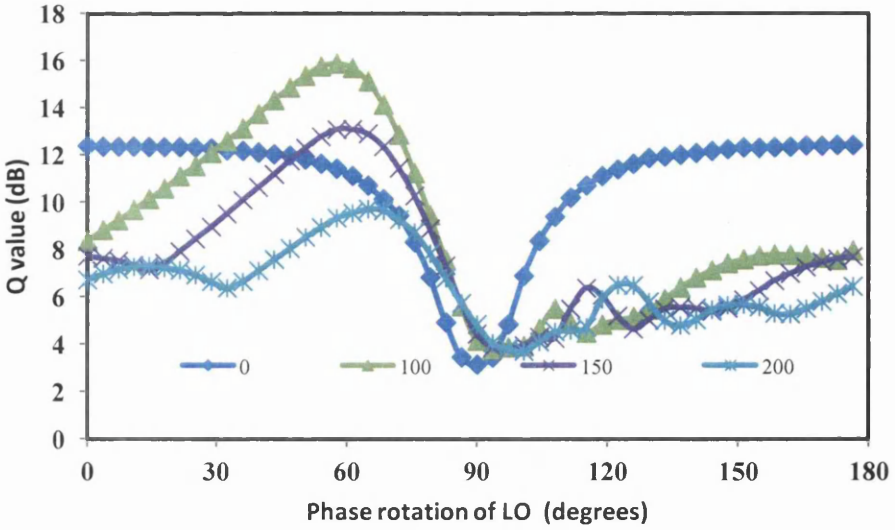

Figure 5.11: The Q values in (dB) plotted against Optical bandwidth (GHz) for a 35GHz OBPF Homodyne 20dB 42.7Gbps 50%RZ-PSK and DPSK systems in the presence of 0,100,150 and 200 ps/nm.

These results suggest that via coherent PSK detection in tight filtering regimes that the optimum performance is achieved in the presence of some residual dispersion as opposed to zero dispersion. The system model is similar to the model in figure 5.2, but for the addition of some chromatic dispersion as a function of fibre lengths.

The figure 5.11 plots the Q values in dB against the LO`s phase rotations in degrees for a balanced detected 42.7 Gb/s PSK system. It can be seen that the performance of the system in the presence of 100ps/nm chromatic dispersion outperforms the zero dispersion performance. However the system performance becomes degraded in presence of 200ps/nm chromatic dispersion relative to the zero dispersion performance.

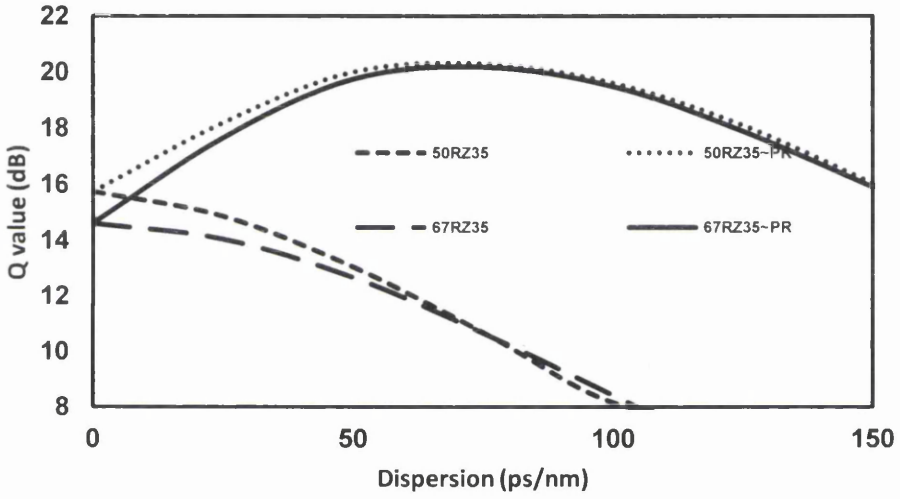

Figure 5.12: The Q values in (dB) plotted against chromatic dispersion in ps/nm for 35GHz OBPF Homodyne 20dB OSNR for 67% and 50% RZ for 42.7Gbps-PSK and DPSK systems.

The Figure 5.12 shows a plot of Q value in dB against chromatic dispersion in ps/nm for a 35GHz OBPF 42.7 Gb/s BPSK OSNR of 20dB (for both 50% and 67% RZ). The dotted line, smaller dashed line, longer dashed line and continuous line represents 50% RZ with phase rotation in local oscillator, 50% RZ without phase rotation, 67% RZ without and with phase rotation in the local oscillator. Figure 5.12 shows that the performance of 42.7 Gb/s RZ-BPSK (no PLL) declines in the presence of dispersion, but with an efficient PLL performance increases with dispersion to a peak of around 75 ps/nm before the performance starts to decline, thereby showing a performance improvement of 9.52 dB (calculated Q) in the presence 75 ps/nm with PLL, as opposed to the performance without a PLL.

This result is more interesting considering the fact that the performance of a strongly filtered 42.7Gb/s RZ-PSK in the presence of some chromatic dispersion (75 ps/nm) actually outperforms the performance without any chromatic dispersion by ~4.5 dB. Thus we carried out the same investigations with the same configuration used in figure 1 but with an OSNR of 15dB and we still noticed the same trend in performance of a strongly filtered 42.7Gb/s RZ-BPSK with PLL, i.e. ~6 dB improvement in the presence 75 ps/nm chromatic dispersion with PLL that also show ~2 dB improvement over zero dispersion performance.

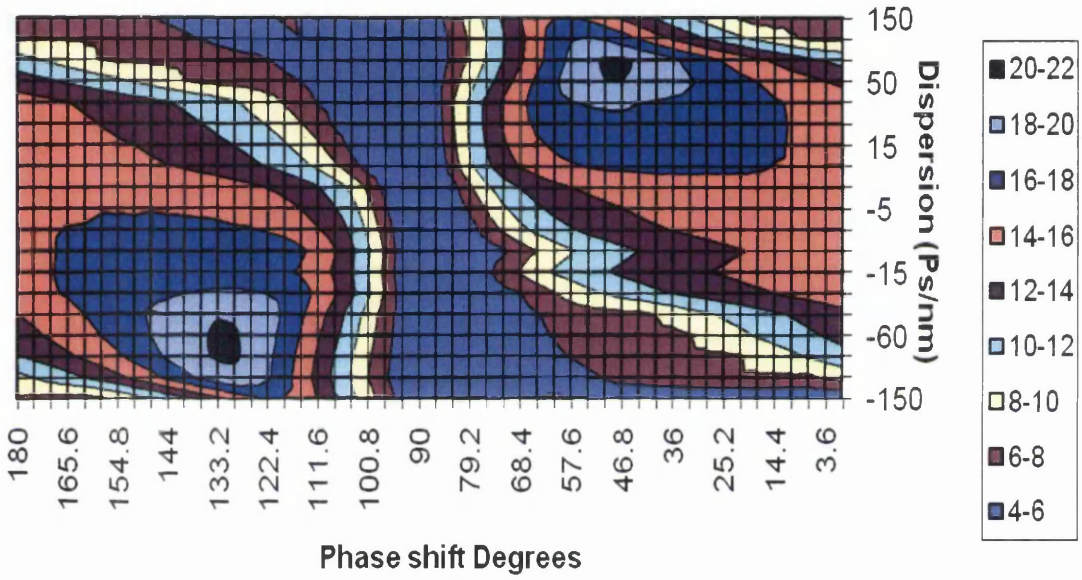

Fig 5.13: Contour plot of Q^2 value in (dB) for chromatic dispersion (ps/nm) against phase rotation of local oscillator (degree) for 42.7Gb/s 50%RZ BPSK for strongly filtered 35GHz OBPF.

The contour plot in figure 5.13 enhances a better understanding of the performance of homodyne Coherent PSK with PLL in the presence of residual dispersion. The contour plot show the plot of residual dispersion (-150 to 150 ps/nm) on the vertical and phase rotation in (degrees) on the horizontal axis. The plot shows that the performance of a strongly filtered 42.7Gb/s 50%RZ-PSK reaches a peak at ~ -75 and 75ps/nm with corresponding LO phase rotations of ~135 and 45 degree relative to zero dispersion performance.

It is a known theoretical fact that phase change due to dispersion in optical transmission is directly proportional to GVD, angular frequency and distance i.e.

$$U(z,\omega) = U(0,\omega)\exp\left(-\frac{i}{2}\beta_2\omega^2 z\right). \qquad 5.1.$$

where $U(z,\omega)$, β_2, ω *and* z represents Fourier transform of the optical field, GVD, angular frequency and distance of fiber. The phase change with a Gaussian pulse in the PSK system itself can be represented as

$$\emptyset(z,T) = -\frac{sgn(\beta_2)(z/L_D)}{1+(z/L_D)^2}\frac{T^2}{2T_0{}^2} + \frac{1}{2}\,tan^{-1}\left(\frac{z}{L_D}\right) \quad 5.2.$$

where $\emptyset(z,T)$, L_D, T_0 *and* T are the time-dependent phases, dispersive length, initial pulse width, and pulse-width after distance Z respectively. From 5.2 it can be seen that first part of the equation has a negative sign that justifies the performance in figure 5.13 where in the presence of +75ps/nm dispersion the phase change in local oscillator is complementary of the phase change for -75ps/nm dispersion, i.e. 45 and 135 degree. Thus dispersion imposes linear frequency chirp that are of opposite signs for $\beta_2 > 0$ (-) and $\beta_2 < 0$ (+).

In the equation 5.2 above the first part shows the time dependent phase shift inherent in the presence of chromatic dispersion and the direction of the phase rotation depends on the sign of the β_2

$$-\frac{sgn(\beta_2)(Z/L_D)}{1+(Z/L_D)^2}\frac{T^2}{2T_0{}^2} \qquad \mathbf{5.3}$$

And the second part shows the constant time constant phase shift that depends on distance and pulse width.

$$+\frac{1}{2}\,tan^{-1}\left(\frac{Z}{L_D}\right) \quad \mathbf{5.4}$$

For a positive chromatic dispersion, a negative phase shift is induced on the PSK system by the combination of the constant phase shift (5.4) and time dependent phase shift (5.3). The two different phase shifts are in opposite directions, but the magnitude of (5.3) exceeds the

magnitude of (5.4), such there is a net negative phase shift induced by the presence of a positive chromatic dispersion in the scenario in the contour plot above. The impact of the local oscillator phase rotation which can be seen from the figure 5.13 shows and justifies the positive phase rotation of +~50° for the local oscillator to compensate for the net negative phase shift due to chromatic dispersion and the OBPF.

The reverse is the case for a negative chromatic dispersion, a net positive phase shift is induced on the BPSK system by the combination of the constant phase shift (5.4) and time dependent phase shift (5.3). The two different phase shifts are in opposite directions, but the magnitude of (5.3) adds up to the magnitude of (5.4), such there is a net positive phase shift induced by the presence of a negative chromatic dispersion in the scenario in the contour plot above. The impact of the local oscillator`s phase rotation which can be seen from the figure above (5.13) shows and justifies the negative phase rotation of -~130° for the local oscillator to compensate for the net positive phase shift due to a negative chromatic dispersion.

5.6 Chapter 5 Summary

1 In this chapter it has been shown, via numerical simulation, that the impact of tight optical filtering in high-speed coherent PSK systems can be greatly reduced by offsetting the OBPF (equivalent to laser detuning). Impact as large as 10dB is reported for very tight filtering. A simple local oscillator system has been modelled for coherent detection of 42.7 Gb/s PSK signal with strong offset filtering. The results show that the performance of strongly filtered PSK system can be greatly improved by offsetting the filter (or equivalently detuning the transmit signals) by around one half the filter bandwidth. For low OSNR (13dB) an improvement of up to 3dB and by up to 10dB for a high OSNR has been reported in this chapter for coherent PSK. The improvement seen here is quite general and, for example, could enable simple, but high performance, PSK coherent 40Gb/s systems compatible within a 50GHz grid.

2 The effect of coherent detection (PSK) in a strongly filtered regime on the chromatic dispersion performance of 42.7Gb/s 50%RZ-PSK systems was modeled and it was shown that system performance can be improved by rotating the phase of the local oscillator signal to align with phase of the dispersed PSK signal. The eye opening penalty of coherent Detected PSK signal can be reduced by as much 8 dB in the presence of chromatic dispersion.

5.7 References:

[1] J. M. Kahn "Modulation and Detection Techniques for Optical Communication Systems" Stanford University, Department of Electrical Engineering, 372 Packard Building, 350 Serra Mall, Stanford, CA 94305-9515 USA.

[2] D. Ly-Gagnon, S. Tsukamoto, K. Katoh, and K. Kikuchi "Coherent Detection of Optical Quadrature Phase-Shift Keying Signals With Carrier Phase Estimation" *J. Lightw. Technol.*, vol 24 Issue: 1, pp: 12 – 21, Jan. 2006.

[3] D. S. Govan and N. J. Doran, "An RZ DPSK receiver design with significantly improved dispersion tolerance," *Opt. Express*, vol. 15, no 25, pp. 16916-16921, 2007.

[4] X. Li, F. Zhang, X. Zhang, D. Zhang, Z. Chen, and A. Xu "Free spectral range optimization of return-to-zero differential phase-shift keyed demodulation in 40 Gbit/s nonlinear transmission" *Opt. Express*, vol. 16, no 23, pp. 2056-2061, 2008.

[5] L. G. Kazovsky, G. Kalogerakis, W. T. Shaw, "Homodyne Phase-Shift-Keying Systems: Past Challenges and Future Opportunities" *J. Lightw. Technol.* vol: 24 , Issue: 12 , pp: 4876 – 4884, 2006.

[6] S. Camatel ; V. Ferrero ; "Homodyne coherent detection of ASK and PSK signals performed by a subcarrier optical phase-locked loop" *IEEE Photon. Technol. Lett.*, vol 18, Issue:1 Jan. 1, 2006.

[7] K. P. Ho "Phase-modulated optical communication systems" Springer, 30 Jun 2005 - Technology & Engineering.

[8] L. G Kazovsky, "Performance analysis and laser linewidth requirements for optical PSK heterodyne communications systems," *J. Lightw. Technol.*, vol. Lt-4, no. 2, pp. 415–425, Apr. 1986.

[9] K. Kikuchi et al, "Degradation of bit-error rate in coherent optical communications due to spectral spread of the transmitter and the local oscillator," *J. Lightw. Technol.*, vol. Lt-2, no. 6, pp. 1024–1033, Dec. 1984.

[10] P. J. Winzer and R. J. Essiambre, "Advanced modulation formats for high-capacity optical transport networks," *J. Lightwave Technol.*, vol. 24, pp. 4711-4728 (2006).

[11] O. K. Tonguz and R. E. Wagner "Equivalence between Preamplifier Direct Detection and Heterodyne Receivers" *IEEE Photon. Technol. Lett.*, vol. 3, no 9, Sept 1991.

[12] T. Tsuritani, A. Agata, I. Morita,, K. Tanaka, , and N. Edagawa, "Performance comparison between DSB and VSB signals in 20Gbit/s – based ultra-long-haul WDM systems," in "Proc" *OFC* 2001, OSA paper MM5.

[13] K. Tanaka, I Morita and N. Edagawa, "Study on optimum pre-filtering condition for 42.7Gbit/s CS-RZ DPSK signal" in "Proc" *OFC* 2004., vol 1, OFC 23-27 Feb. 2004.

[14] A.-E. Elrefaie, R.-E. Wagner, D.-A. Atlas, and D.-G. Daut, "Chromatic dispersion limitations in coherent lightwave transmission systems," *J. Lightwave Technol.*, vol. 6, no. 5, pp. 704–709, May 1988.

[15] S. Betti, G. de Marchis, and E. Iannone, Coherent Optical Communication Systems. New York: John Wiley & Sons, 1995.

[16] K. P. Ho and H. Wang, "Effects of Chromatic Dispersion on Optical Coherent-Detection Systems" *IEEE Transaction on Communications*, vol. 56, no. 9, Sept 2008

[17] P. J. Winzer and R. J. Essiambre, "Advanced modulation formats for high-capacity optical transport networks," *J. Lightwave Technol,* vol. 24, pp. 4711-4728 (2006).

[18] Y. Cai, J. Cai, A. Pilipetskii, G. Mohs, and N. S. Bergano "Spectral efficiency limits of pre-filtered modulation formats" *Opt Express*, vol. 18, No. 19 / 20273/13 September 2010.

[19] O.A Olubodun and N.J. Doran "Performance Improvement of Asymmetrical Filtered 40 Gb/s RZ-DPSK Receiver Design -Strong Filtering Considerations" *IEEE/NOC* July 2011.

[20] N. B. Pavlovic´ and A. V. T. Cartaxo "Single-Sideband Differential Phase-Shift Keying Asynchronous Carrier-Suppressed Return-to-Zero – A Novel Signalling Format Optimized for Long-Haul UDWDM Systems" *J. Lightw. Technol.*, vol. 27, no. 12, June 15, 2009

[21] N. B. Pavlovic´ and A. V. T. Cartaxo "Influence of Tight Optical Filtering on Long-Haul Transmission Performance of Several Advanced Signalling Formats," *J. Lightwave Technol*, vol 26, pp. 1339-1348 June 2008.

CHAPTER 6

6.1 Optical Coherent Quadrature Phase Shift Keying (QPSK) modulation format in 50 GHz Grid.

The impact of offset filtering on 42.7 Gb/s DPSK, DQPSK and BPSK systems on a strongly filtered regime (50GHz grid) has been investigated and reported in chapters 3, 4 and 5. However, despite the inherent performance improvements of the 42.7 Gb/s DSPK and BPSK systems in a strongly filtered regime due to offset filtering as opposed to the performance penalty inherent with in 42.7 Gb/s DQPSK system with offset filtering, it will be of great interest to characterise the optical (analogue) performance of 42.7 Gb/s QPSK systems in a 50 GHz grid.

The performance of DQPSK systems is largely degraded with frequency offsets due to lesser symbol spacing ($\pi/2$) between bits as opposed to π phase difference between DPSK and BPSK bits, higher induced phase error, and higher number of optical phase symbols and (AMZI) operating points (leads to higher eye closure). Nevertheless, the performance penalty inherent with offset filtering of the 42.7 Gb/s DQPSK systems within a 50GHz grid is not the main highlight of this multi-level signalling format; its compatibility with a 50GHz grid via narrow band-limited filtering is the reason for its prominence.

The investigations on coherent 42.7 Gb/s QPSK performance in a TOF regime will be presented in this chapter by describing the modulation and demodulation in section 6.2. The next sections 6.3, 6.4, 6.5 and 6.6 will be focused on the modelled performance of a coherent 42.7 Gb/s QPSK system in a narrow filtering regime, its impact with different filter shapes, its performance with asymmetric filtering, and the performance of a 42.7 Gb/s QPSK system in the presence of chromatic dispersions. The section 6.7 conclusion section compares the results generated with QPSK under different applications scenario with an equivalent DQPSK system.

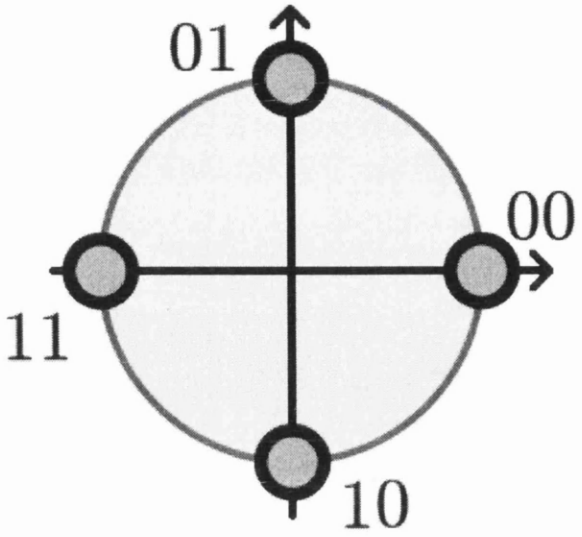

Figure 6.1: QPSK symbol spacing

The figure above shows the constellation diagram of a QPSK system, which has the same constellation diagram as an optical DQPSK system. Optical coherent quadrature phase-shift keying (CQPSK) modulation and demodulation is of great importance, because despite the inherent sensitivity advantages of coherent binary phase shift keying (CBPSK), there are mitigations to its implementations in real systems. Some of these inherent CBPSK mitigations like chromatic dispersion, tolerance to optical filtering and polarisation mode dispersion [1,2] can be greatly relaxed via multi level signalling formats such as QPSK, DQPSK, 8PSK and higher level signalling format.

However, these higher-level (multi-level) modulation formats also have their own inherent limitations such as higher OSNR sensitivity, higher cost and complexity of the local oscillator in coherent detection. The foremost modulation formats that can enhance 100Gb/s data rate deployment in a 50GHz grid are 50Gb/s DQPSK and QPSK with polarised division multiplexing (PMX) [2,3]. The limitation imposed by the available electrical bandwidth is a real barrier to the efficient deployment of a simpler modulation format (DPSK/CBPSK) despite its improved OSNR sensitivity. However, this research seeks to investigate available alternatives to 40 Gb/s PDPSK (partial DPSK) in a 50 GHz grid or 50 Gb/s DQPSK with PDM in a 50GHz grid. It is imperative to evaluate the pros and the cons of QPSK over DQPSK.

A better understanding of the modulation and demodulation of 40Gb/s QPSK in tight filtering regimes (50GHz grid) can lead to a better understanding of the physical reasons for its performances, and strategies for improving the performance of QPSK systems at higher data rates (i.e. >100Gb/s). For example, chromatic dispersion is known to increase by a

quadratic factor with an increase in data rates, thus the impact of chromatic dispersion will be more severe as data rates increase, especially in the context of a narrow filtering scenario. Coherent detection of optical systems is inevitably the technology of the next generation, due to the higher sensitivity of coherent detection over the differential detection and in conjunction with digital signal processing (DSP), thereby compensating and equalising the inherent linear impairment [4, 5, 6, 7, 8, 9, 10]. In the numerical model, a coherent QPSK system with different optical filter shapes (orders of Gaussian filters), optical filter bandwidths and optimised electrical filtering (5^{th} order Bessel filters) at the receiver in a back-to-back transmission are modelled.

The low tolerance of DQPSK systems to laser frequency detuning has been reported in [11, 12] and it presents itself as major mitigation to the performance of DQPSK systems. Just as polarised multiplexing can be implemented with DQPSK systems, it can also be implemented with QPSK to further improve the spectral efficiency of optical communication systems. QPSK is essentially 4PSK, meaning that two 2PSK signals are simultaneously encoded in one bit, thus having the same BER error rate as PSK but a different (lower) symbol error rate.

This is because the QPSK requires twice the amount of power to modulate a CBPSK. The spectra efficiency (SE) of phase-modulated formats can thus be improved by deploying QPSK/DQPSK, thereby increasing the SE by a factor of 2 and another factor of increase in spectral efficiency by virtue of polarised multiplexing. Unlike the optical DQPSK system where a precoder is desirable in order to demodulate the quadrature phase-encoded shift-keying format, the demodulation here is thus implemented by virtue of the phase separation of the two tributaries that are ninety degrees apart.

Importantly, the impact of DSP on coherent detection is one of the major drivers for the resurgence in the demand for coherent detection, due to the excellent impact of LE (linear equalisation), non-linear cancellation and maximum likelihood sequence (MLSE) on ISI. But aside from the cost of the coherent detection via the addition of extra lasers (local oscillator) for the mixing of the received signal, there is also an additional cost in deploying DSP. All these additional costs make coherent QPSK slightly unattractive in terms of its performance relative to DQPSK modulation format's performances in the presence of ISI: QPSK far outperforms DQPSK, especially with polarised multiplexing. As noted in [8] for unequalised systems, it is important to investigate the full potential of the analogue system (optical coherent detection) especially in the presence of strong filtering (50GHz grid) as it is the focus of this research.

6.2 QPSK Demodulation

The demodulation of an encoded QPSK modulation format is via mixing of the transmitted QPSK signal at the (receiver) output of the optical bandpass filter with a local oscillator signal. This mixing is implemented on a linear regime thereby enhancing an exact phase extraction, unlike the DQPSK modulation where an asymmetric MZI is deployed in realising self phase-referencing by delaying the DQPSK signal and interfering the delayed signal with the signal itself at the output of the AMZI.

The simplicity of the DQPSK demodulation is an advantage in terms of the cost of the AMZI, but the drawback is that the phase extraction of the process is not precise when compared to the QPSK demodulation. The QPSK demodulator can employ one LO (laser), but with a 90^0 phase shift for each of the tributaries. Thus one LO is deployed to save the cost of having two separate lasers for each receiver. Thus for demodulation of the tributaries, a 3dB/180^0 coupler is deployed after the OBPF and the local oscillator, thereby mixing the in-phase signal of the QPSK signal (received QPSK signal) with the in-phase signal of the local oscillator (laser with 0 degree phase alignment). Also, the out of phase component of the QPSK signal (out of phase) is mixed with the out of phase component of the local oscillator (laser with 90 degree phase alignment).

However, four single ended detections can also be deployed at both the constructive and destructive output ports of the LO`s system.

But balanced detection offers better performance than the single-ended detection due to the cross talk originating from each of the tributaries, thus leading to interferences at the output ports of the two separate mixers, and in the process reducing the sensitivities of the two single-ended detections. The balanced detection forms an electrical decision variable from the subtraction of the signals (current) at the constructive and destructive ports.

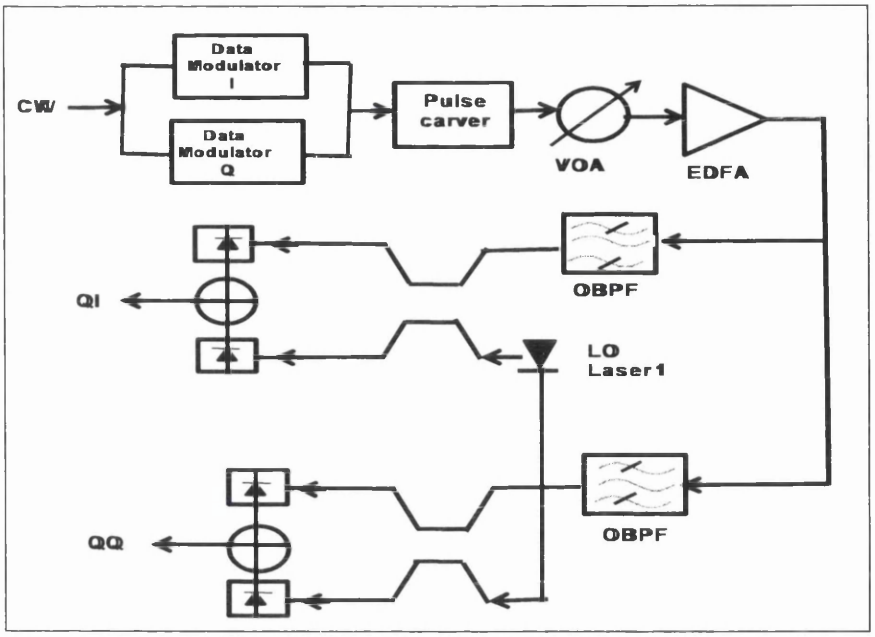

Figure 6.2: Schematic diagram of Coherent QPSK model.

Figure 6.2 above is the diagram for a QPSK back-to-back transmission and detection, where there are two coherent demodulators (in-phase and quadrature). The local oscillator deployed in the mixing with the QPSK signal is a perfect local oscillator with zero linewidth, and phase locking is not implemented in any of the simulations. However, actual phase displacement is implemented to align the phase of the received signal. This is of course difficult to implement in practice because the phase matching in the field is subject to time variants. For all the cases of coherent detection in this chapter, homodyne detection was modelled in the simulations, thus the frequency of the local oscillator signal is assumed to be 0 GHz.

The focus of the coherent QPSK investigation here is based on homodyne rather than heterodyne due to the performance improvement (smaller photon per bit requirement for detection) and narrower receiver optical bandwidth compared to heterodyne coherent detection (larger bandwidth) [7,13] Although a homodyne coherent system requires optical phase-lock loop, the phase locking by a heterodyne system is implemented at the electrical stage. Also, the line width requirement of the heterodyne coherent system is more tolerant to increases in linewidth of the local oscillator laser [10, 14, 15].

6.3 Impact of band-limited filtering on coherent QPSK

Coherent QPSK detection has been identified as having at least 2dB-improved performance over the DQPSK. The performance analysis of both DQPSK and coherent QPSK is of mixed merits and demerits, because despite the reported performance improvement of coherent BPSK over other modulation formats, inherent linewidth increases limitations, and phase-locking requirements are difficult to implement in practice. Thus, until these impairments are addressed in a practical coherent PSK [16], i.e. until perfect lock (phase) loops are designed or the robustness of coherent homodyne detection is improved to increase in laser linewidth, it may be difficult to actualise the vast benefits of coherent PSK or QPSK because practical voltage controlled oscillators 'VCO' operating in the optical domain are not available.

Therefore, QPSK is expected to suffer more from linewidth-induced impairments due to its higher symbol rate over BPSK (factor of 2). Notwithstanding this, it is still relevant to analyse the impact of optical band limiting filtering on the QPSK systems in the presence of ASE noise. This is due to the vast inherent advantages of QPSK modulation, such as an increase in spectra efficiency, improved tolerance to chromatic dispersion, polarised mode dispersion, polarised multiplexing (from which a data rate of X-Gb/s can be achieved with a symbol rate of X/4-Gb/s) [17] and transmission impairments' reduction from DSP. The generation of ASE noise is a setback for any modulation scheme because in the process of amplifying optical signals over transmission links this (ASE), noise will be added to the signals and it impacts on the optical signal to noise ratio. The performance of QPSK systems in a back-to-back transmission is more sensitive than DQPSK [17]

It is important to note that deploying OBPF generally results in performance penalties for strongly-filtered modulation formats. But the use of narrow filters becomes inevitable, particularly in a 50GHz grid, which is within the concentration of this research. The ASE rejection by narrow filtering, the performance of duobinary signalling inherent QPSK formats (constructive port) and the exact phase exaction due to the QPSK signal mixing with the local oscillator's signal, alleviate the performance penalties of strongly-filtered QPSK modulation formats. We shall be investigating the performance of the QPSK format in the presence of strong filtering in order to establish a comparative analysis of QPSK and DQPSK formats. The tolerance of DQPSK format to optical filtering has been reported in [18], and as expected the tolerance of 43Gb/s DQPSK format is within less than one dB penalty for a 30GHz imposed optical filtering. With better phase referencing of QPSK demodulation (on a linear regime, thus enhancing better base band extraction) one can envisage an improved

performance and better tolerance optical filtering for QPSK [17]. In these analyses wide and narrow band pass filters have been deployed via numerical analysis to characterise the performance of homodyne PSK detection.

It is important to examine the influence of optical band pass filters on the performance of Homodyne QPSK detection. In a comparison of QPSK to BPSK, there is the advantage of reducing the optical filter bandwidth for the same data rate deployed with BPSK (half symbol rate for QPSK). This examination is firstly initiated by mixing the received QPSK signal with a local oscillator signal via a bi-directional coupler. The system used in the simulations, illustrated in Fig 1, is as follows: a 2^9 PRBS is used to drive a Mach-Zehnder modulator (MZM) to produce a 42.7 Gb/s QPSK optical signal. A pulse-carving MZM is used to generate a fifty percent RZ signal. Noise is then added using the VOA/amplifier combination. At the receiver, the two separate PSK signals are demodulated with a ninety degree phase difference in the two deployed local oscillators for the mixing of the QPSK signals, and the QPSK signal (In-phase) is fed through an optical band pass (OBPF) filter to the first input arm of a 3dB coupler.

The other input of the 3dB coupler is fed with a local oscillator signal while the quadrature QPSK signal is mixed with the same local oscillator signal at a ninety-degree phase displacement to the in-phase QPSK local oscillator signal. The local oscillator phase is varied to establish the best performance [7]. The output of the first coupler couples the in-phase QPSK signal with the in–phase local oscillator in the first leg of the output 3dB coupler. The second leg couples the out of phase QPSK signal with the out of phase local oscillator signal. Two separate balanced detection models are used to generate the calculated 'Q's. The output of the mixer is fed to another 3dB coupler that is eventually fed to two photodetectors. The OSNR at the receiver for the investigation varied from 16dB. The filter at the receiver was generally taken between 80 to 30GHz, although narrow bandpass filtering performance is the major focus of this investigation. It is important to understand the performance trend of QPSK homodyne detection from wide filtering regions to narrow filtering regimes. A 30GHz bandwidth fifth order Bessel electrical filter was used following the receiver. In the following the Q-values were calculated assuming Gaussian statistics.

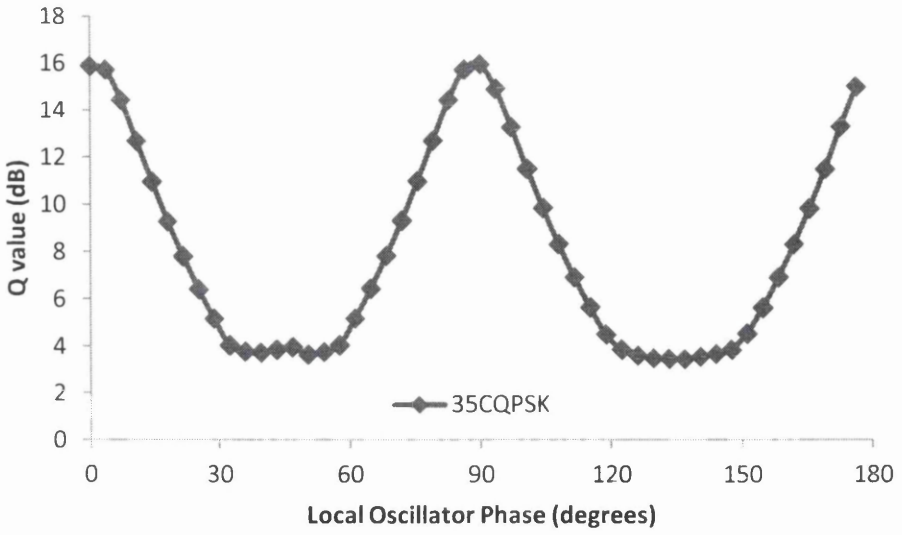

Figure 6.3: The Q values in (dB) for an 80 GHz OBPF Homodyne 42.7Gbps QPSK system plotted against local oscillator phase (Degrees).

Figure 3 above shows the performance of an 80GHz OBPF Homodyne 42.7Gb/s QPSK system plotted against the local oscillator signal's phase (Degrees). This result shows that performance of a Homodyne 50%-RZ QPSK system (80GHz OBPF) exhibits a periodicity of ninety degrees at the detector, which is consistent with the phase separation of the modulated symbols at the transmitter. The plot also highlights the significance of phase locking of the homodyne QPSK detection, without which the inherent benefits of homodyne detection are not optimised.

The difficulty in practically achieving phase locking is also shown here, as the maximum performance of the homodyne detection is only achieved with a local oscillator's signal aligned to the phase of the data signal. The ninety degree phase separation between the in-phase and quadrature QPSK tributaries at the transmitter is highlighted by the plot above, unlike the plot for the periodicity of the local oscillator's phase for the PSK (figure 5.3 of chapter 5) with a 180 degree periodicity. The main difference between the periodicity plot for the QPSK and the PSK is that of interference witnessed in each tributary (in-phase symbol) due to the crosstalk from the opposite (quadrature symbol) and vice versa. The intermediate frequency of the homodyne PSK is null due to the frequency alignment of the carrier frequency and local oscillator laser's frequency. The phase periodicity shown here confirms an inherent attribute of phase alignment of a perfect homodyne QPSK detection. Without the phase alignment of the local oscillator to the received QPSK signal, the performance of the

Homodyne QPSK system is greatly impaired due to the sensitivity of QPSK signals to laser frequency offsets [11].

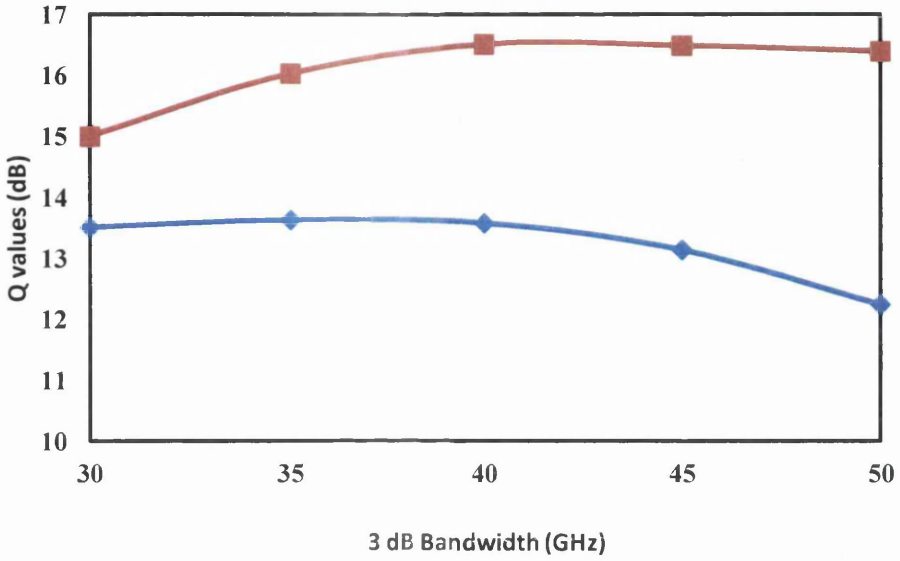

Figure 6.4: The Q values in (dB) plotted against optical bandwidth (GHz) for a 30 to 50 GHz OBPF (3rd order OBPF) Homodyne 16dB 42.7Gbps 50%RZ-QPSK-red line and DQPSK-blue line systems

Figure 4 above illustrates the performance of 50%-RZ QPSK and DQPSK systems for a 42.7Gb/s data rate. The diagram shows the performance of optical bandlimited filtering for both DQPSK and QPSK modulation formats for an OSNR ~16dB. As seen above, there is >2dB improvement in the performance of the coherent QPSK system for 30 to 50GHz OBPF over a corresponding DQPSK system. The better base band extraction of the coherent QPSK is responsible for the improved sensitivity over the DQPSK version. In this case, the better (exact) phase extractions of the local oscillator and received signal mixing over the self referencing via the asymmetric MZI of the DQPSK accounts for the improved sensitivity.

Thus, in the presence of ASE noise-limited back-to-back transmission of phase-modulated formats, the QPSK achieves >2dB improvement in Q performance for an OSNR of 16dB over the DQPSK format within wide to narrow optical filtering regimes. In view of the OSNR deployed in the simulations (16dB) this result is consistent with reported investigations in [ ] where PSK has been shown to record the best receiver sensitivity. However, the heterodyne QPSK systems have a similar performance with the homodyne QPSK due to the presence of cross talks in each of the tributaries, because of the presence of the other out-of-phase signals in the demodulation of in-phase signals. In terms of strong filtering regimes, which are the main scope of this investigation, there is a need to explore the inherent signal amplification and base band information extraction of the QPSK over the

DQPSK modulation format for performance improvement in a 50GHz grid, despite the performance improvements shown with band limited filtering of QPSK over DQPSK. We shall also be investigating the impact of filter shape, tolerance to laser offset (optical offset filtering) and other related linear impairments (dispersion) in the performance of QPSK systems in this chapter.

6.4 Impact of filter shape on homodyne coherent detected 42.7Gb/s QPSK.

The relevance of optical filter shape and bandwidth in coherent detection of QPSK systems needs to be investigated to understand its implication on multiplexing and demultiplex (mux/demux) so as to envisage the inherent constraints in the presence of filtering concatenation in a WDM transmission for a 50GHz or 100GHz channel spacing. As would be expected for a 42.7Gb/s QPSK/DQPSK modulation format in a 50GHz grid, a symbol rate of 21.35Gb/s will be significantly tolerant to 50GHz imposed optical filtering limits. Thus, these investigations on the performance of 42.7Gb/s QPSK modulation format are based on characterising the performance of different filter shapes and bandwidths in a 50GHz grid.

Understanding the optical filtering performance of 42.7Gb/s QPSK in a 50GHz can enhance the design and deployment of polarised multiplex >100Gb/s QPSK modulation in a 50GHz grid. These can be justified by the different performances of different modulation formats with changes in steepness of the filter edges.

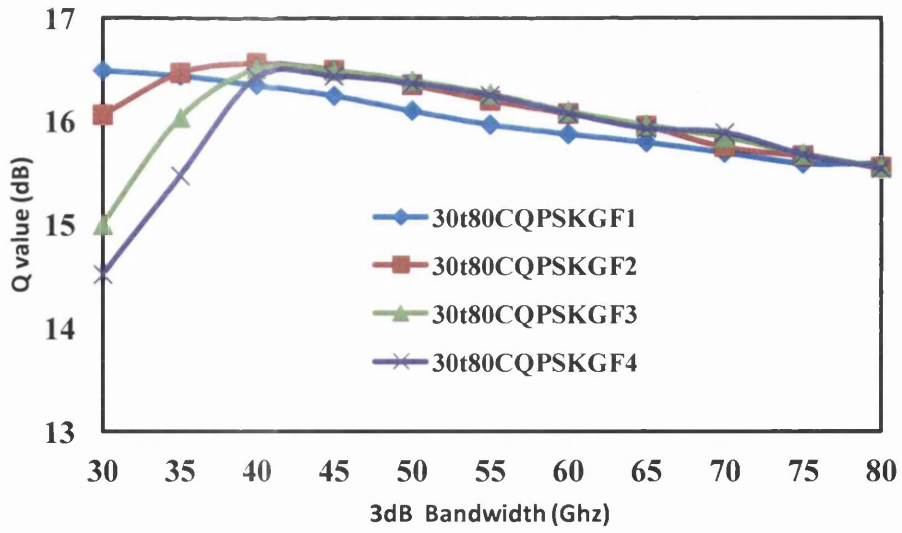

Figure 6.5: The Q values in (dB) plotted against different orders of Optical Gaussian filter bandwidths (GHz) from 30 to 80 GHz OBPF Homodyne 16dB 42.7Gbps 50%RZ-QPSK systems.

Figure 6.5 above shows a plot of Q in (dB) for several orders of Gaussian filters for specific bandwidths ranging from 30GHz to 80GHz OBPF for a 42.7Gb/s %50RZ-QPSK 16dB (OSNR). It is evident from the above results that for the filtering bandwidths > 40GHz, the order (steepness) of the filter does not impact negatively on the performance of homodyne QPSK systems. I.e. the performance of the Gaussian filters from first order to third order for narrow optical filtering (<40GHz) in the presence of ASE noise is similar for wider bandpass filters (i.e. ~1dB penalty is imposed for narrow filtering regimes <40GHz for the different orders of the Gaussian filters). But in the presence of strong filtering, the impact of the steepness of the optical filters is significant. As shown in figure 5 above for filtering bandwidths less than the bit rate, the 1st order Gaussian filters for a 50%RZ 42.7Gb/s QPSK (homodyne) systems, outperforms the super Gaussian filters. Also evident in the strong filtering region is that as the order of the super Gaussian filter increases the performance of the system, it becomes slightly degraded. For the case of 30GHz OBPF the fourth order filter has a 2 dB performance penalty relative to the first order OBPF. This could have performance implications in view of the deployments of QPSK systems in a 50GHz grid where the available bandwidths are very limited, and of course the choice of filters could reduce the performance penalties accruable from strong filtering. There have been recent advancements in the design of OBPF for optical communication, such that optical signal spectrum could be shaped to suit the filtering aspiration of the network provider or service engineer [18].

6.5 Impact of offset filtering on 40 Gb/s coherent QPSK within 50GHz grid

The most important objective of any optical communication research is the need to increase data rates, while increasing the spectra efficiency simultaneously. Another important consideration while investigating the several techniques to improve performance (extending the reach of the optical communication system) is primarily the channel spacing limitations of the 50GHz grid imposed by already-installed capacities (OOK). QPSK/DQPSK offers increased SE, although it has higher OSNR sensitivity than BPSK/DQPSK for the same bit error rate. The increased SE of QPSK/DQPSK when combined with polarised multiplexing makes quadrature phase modulation formats a viable candidate for 100Gb/s data rate systems within a 50GHz grid. The deployment of a 50Gb/s data rate on a simpler BPSK/DPSK is limited by the non-availability of the electronics despite the improved OSNR performance

over 50Gb/s QPSK/DQPSK modulation. The performance of QPSK systems over DQPSK systems make QPSK more attractive for >100Gb/s [2].

The fact that mixing of the local oscillator signal can be accomplished in a linear regime (optoelectronic conversion) thus ensures better phase extraction in QPSK systems rather than DQPSK systems (self-phase referencing). DSP (Digital Signal Processing) can relax some laser line width requirements of PSK/QPSK systems. We shall consider the purely optical realisation of coherent QPSK. The performance of phase modulated formats in the presence of offset filtering has been reported in several papers [11, 12, 20, 21, 22, 23, 24, 25], but although the impact was analysed by experimentation, simulation and semi-analytic techniques, the impact of frequency offsets was discussed from different locations in the transmission mission systems. At the transmitter, the offset filtering was analysed as prefiltering or laser detuning [20, 21], frequency offset between the transmitter and the demodulator was used in [11, 23, 26], while phase error was used to capture the impact of frequency drift on demodulator [24, 25].

From all the papers mentioned above, what is consistent is the fact that binary-phase modulated formats are more tolerant to offset filtering (as has been confirmed in chapters 5 and 6) while the sensitivity DQPSK had to offset filtering was quantified as six times the sensitivity of DPSK. The lesser tolerance to offset filtering in quadrature-phase modulation format rather than phase modulation format is due to the higher number of symbol-phases, lesser symbol rate (higher phase error in DI), faster eye diagram closure due to frequency offsets, and lesser efficiency of the AMZI in conversion from phase to intensity modulation at detector. However, it has been established in chapters 3 and 4 that phase modulated formats (40Gb/s DPSK and BPSK) can actually benefit from asymmetrical filtering in a strongly filtered regime [27, 28]. We also investigated the impact of offset filtering on 40Gb/s DQPSK systems and confirmed, as had previously been reported [26], the high sensitivity of the 40GB/s DQPSK system to offset filtering.

Imperatively, it would be of great interest to investigate the performance of 40Gb/s QPSK in the presence of offset filtering, despite the improved performance of QPSK over DQPSK with band limited filtering as seen in fig. 5. Characterising the performance of QPSK with offset filtering at receiver should be paramount, because asymmetric filtering has been identified as a major mitigation to the performance of DQPSK systems [29]. In QPSK detection there are no DI as opposed to DQPSK demodulation, thus the net filtering effect of the OBPF and AMZI can still be modelled with the QPSK systems because the OBPF and MZI both operate in a linear regime.

In this work the impact of offset filtering on a simple QPSK modulation is explored with the aim of evaluating its deployment at 40Gb/s or 50Gb/s, which with polarisation multiplexing provides a route to 100Gb/s transmission. Here we will explore the prospect of deliberately offsetting the filter from the channel centre to characterise the performance 42.7Gb/s RZ-QPSK modulation. Thus we will investigate the impact of offset filtering on 42.7Gb/s coherent QPSK using filter bandwidths in the region of 35GHz. We will compare the performance of asymmetric-filtered 42.7Gb/s coherent QPSK to the symmetric-filtered case. The focus of this section is to model offset filtering at the receiver in a 50GHz grid for a 42.7Gb/s QPSK, which has the same effect as detuning the transmit laser.

Also in this section the tolerance of QPSK systems via OBPF (>35GHz) to offset filtering (transmit laser detuning) is examined. The effect of offset filtering (laser offset) can also be envisaged to occur due to non-ideal frequency drifts between the transmitter and receiver. The understanding of the performance of the QPSK systems in the presence of this frequency offsets, either at transmitter or at receiver, is essential as higher data rates and polarised multiplexing will be deployed in the nearest future. The model used in the simulation is shown below and the difference between this model and the model used in section 6.2 is that frequency offsets are implemented at the OBPF, as opposed to band-limiting filtering.

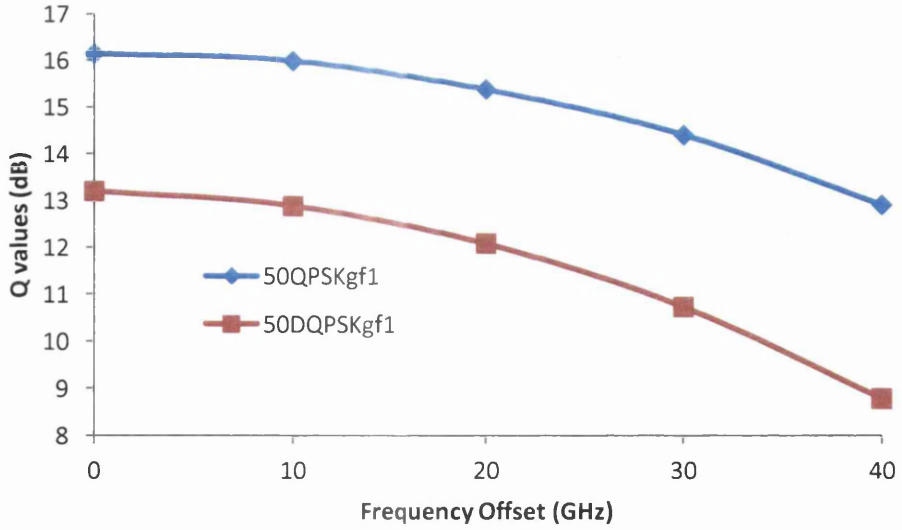

Figure 6.6: Q value in (dB) against Filter frequency offset (GHz) blue line for QPSK and red line for DQPSK system.

Figure 6.6 above illustrates the Q value (dB) against filter frequency offset in (GHz): the red line is for 42.7Gb/s 50%RZ-DQPSK system and the blue line for 42.7Gb/s 50%RZ-

QPSK system. Both for an OSNR 16dB, 50GHz OBPF frequency offsets from 0 to 40GHz. The result as shown with the red line (DQPSK) is consistent with results reported in [26]. The blue line indicates that the performance of 42.7Gb/s QPSK system, 50GHz OBPF has improved performance compared to the equivalent DQPSK.

The level tolerance of 50% RZ-QPSK system to offset filtering as shown in figure 6.6 is illustrated with a corresponding 0.15, 0.76, 1.74 and 3.5dB penalties for 10, 20, 30 and 40GHz filter offsets, while there are corresponding 0.3, 1.2, 2.48 and 4.43dB penalties for the same filter offsets relative to 0 GHz filter offset performance. It is obvious that QPSK is slightly more tolerant to offset filtering compared to DQPSK systems, although there is 2.8dB performance improvement of the QPSK system over the DQPSK system via 50GHz OBPF first order Gaussian filter, 30GHz fifth order Bessel filter (electrical bandwidth).

The performance improvement of the QPSK system over the DQPSK system, as seen with the simulation above, gives an insight into the significance of offset filtering as a major mitigation factor that can degrade the performance of the very attractive QPSK modulation formats. The choice of optical filter bandwidth, signal formats and electrical filtering can influence the performance of different modulation formats based on application scenarios [29], thus the results as seen here with 42.7Gb/s 50%-RZ-QPSK system over the equivalent DQPSK give an insight into the slightly improved tolerance of QPSK modulation to offset filtering or transmit laser detuning. Also, for better comparison it is relevant to stress that the impact of the better phase referencing of the QPSK from the mixing of the local oscillator's signal with the transmitted QPSK signal does not have much effect on improving the tolerance of QPSK systems to offset filtering.

The higher number of symbol phases (4) increased phase error due to the resultant impact of the QPSK symbol period on frequency offsets ($\varphi(QPSK) = 2T \times \nabla f$) as opposed to phase error from PSK symbol period on frequency offset ($\varphi(PSK) = 2T \times \nabla f$). Most importantly it is essential to note that in the demodulation of QPSK/DQPSK systems for either the in-phase or quadrature tributaries, there is the presence of the quadrature phase-modulated signal in the in-phase tributary and the opposite is true; this is responsible for the ghost pulses as seen in the DQPSK/QPSK eye diagrams. In chapter 4 the penalties induced by offset filtering on DQPSK systems were reduced by a novel filtering design, the same novel design has been investigated on QPSK systems and the performance did not significantly impact on the system here, thus showing that the novel design was not necessarily suitable for efficient systems.

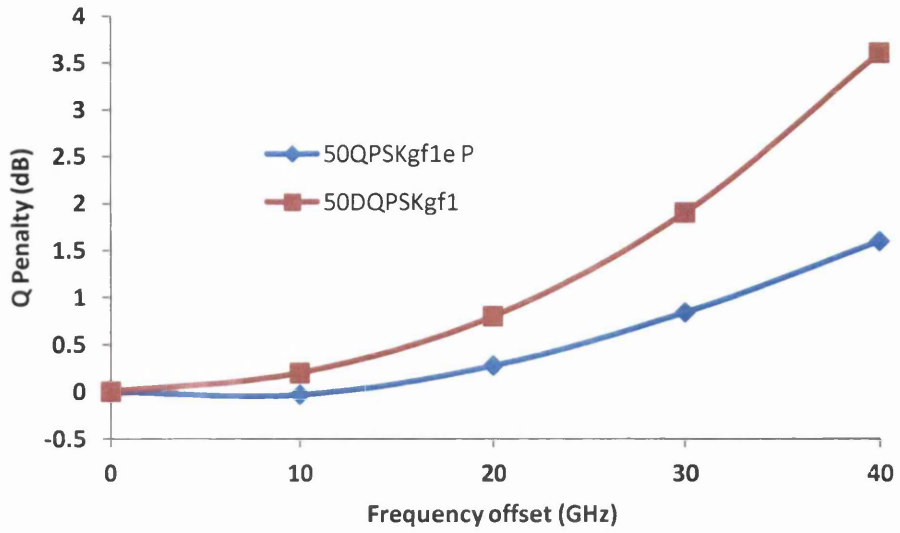

Figure 6.7: Q penalty in (dB) against Filter frequency offset (GHz) blue line for QPSK and red line for DQPSK system.

Figure 6.7 above illustrates the Q penalty (dB) against filter frequency offset, with a blue line for QPSK and red line for DQPSK. The simulation model used in figure 6.7 is essentially the same as figure 6 except that the fifth order electrical filtering bandwidth is now optimised for both QPSK and DQPSK. Thus we see from the Q penalty plotted above that the sensitivity of QPSK to offset filter is about two times less sensitive than DQPSK: i.e. for a 40GHz offset in a 50GHz OBPF there is a 1.6 and 3.6 dB performance penalty for both 42 Gb/s 50% DQPSK and DQPSK systems.

6.6 Chromatic Dispersion Performance of Coherent Detected 42.7Gb/s QPSK System

In this section the performance results of coherent 42.7 Gb/s QPSK will be presented in the presence of chromatic dispersion in a strongly-filtered regime (50GHz grid). The performance of the coherent QPSK will be examined relative to the performance of DQPSK in the presence of some chromatic dispersion. QPSK is very prominent for high-speed modulation formats due to its improved tolerance to linear and non-linear impairment, largely due to the success of different DSP strategies or electrical equalisations. However, in all the results that will be presented in this section, the impact of PDM, DSP or electrical equalisation will not be considered. The aim of these investigations into the performance of

coherent 42.7Gb/s QPSK in a 50GHz grid, and especially in the presence of chromatic dispersion, is to understand and characterise the limits of 42.7Gb/s QPSK in a dispersive regime.

The performance of a coherent 42.7Gb/s QPSK will further be examined relative to coherent 42.7Gb/s PSK in a 50GHz grid, largely due to the inherent OSNR advantages of the PSK systems. This is what was identified in chapter 5 with the performance of digital coherent PSK, where it was shown that the performance of coherent phase-modulated systems is largely exaggerated with DSP if the LO's phase rotation is not optimised [7]. Theoretically, implementing a phase lock loop (PLL) for coherent detected signals is simple compared to the complications that set in for the special cases of 90° couplers desirable for QPSK detection, which are lossy due to the combination of beam splitters and polarisation controllers. And most importantly for conventional balanced PLL, the transmission of residual carrier is also a limiting factor, especially in combination with an optical amplifier [29]. Additional phase modulation could also be implemented at the transmitter to enhance the phase-locking attributes of the LO [30, 31]. Thus, implementing an efficient LO is difficult to actualise in real systems.

6.6.1: 42.7Gb/s QPSK chromatic dispersion results

In this section, the investigated results via the QPSK model will be presented and discussed in the presence of chromatic dispersion. The model deployed in the simulation here is essentially the same as the model deployed in [6.2] for the dispersion, which is added as a function of fibre lengths before the OBPF. The same parameters are maintained in these simulation investigations for the 42.7 Gb/s 50%RZ-QPSK systems (bit sequence, OSNR, optical band pass filter and electrical filter).

The impact of chromatic dispersion on 42.7 Gb/s QPSK is sixteen times the impact at 10Gb/s PSK. The magnitude of the performance improvement seen here within a strong filtering regime (350GHz OBPF) in the presence of chromatic dispersion via phase rotation of the local oscillator's signal in 42.7Gb/s RZ-coherent PSK is very significant compared with the same system that does not optimise the phase rotation of the local oscillator.

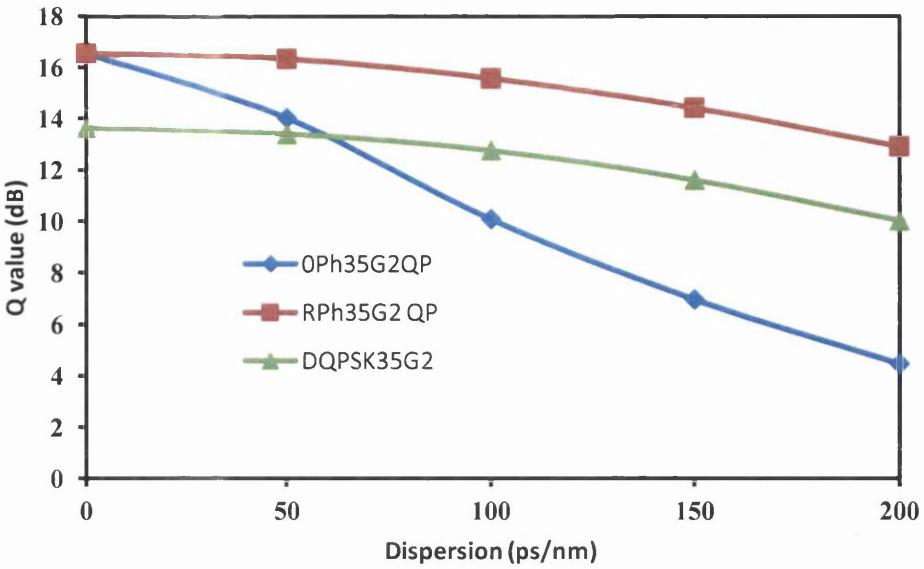

Figure 6.8: Q penalty in (dB) against chromatic dispersion (ps/nm) for 35GHz OBPF-42.7Gb/s 50%RZ-QPSK system, (red line represents the performance of the QPSK with optimized phase rotation of the LO, blue line represents QPSK performance with no phase rotation of the LO and green line represents the equivalent DQPSK performance) for an OSNR of 17dB.

The plot in figure 6.8 above represents the performance of a strongly-filtered 35GHz OBPF, which is representative of actual bandwidth in a 50GHz grid due to several concatenations of several filters for a 42.7Gb/s 50%RZ QPSK system in the presence of some dispersions. The Q value in dB was plotted against chromatic dispersion in ps/nm from 0 to 200ps/nm. Thus, from the plot above, which shows the performance of just one of the individual receivers (either in-phase or out of phase, due to the similar performances of both receivers), it is obvious that the QPSK system (red line) with phase rotation of the LO is around 2dB better than the DQPSK system (green line) in the presence of chromatic dispersion, as represented by the 35GHz OBPF.

Interestingly, if the phase rotation of the LO is not optimised (which has been described as difficult to implement in real systems) then the performance of the QPSK system (blue) is only seen to be better than the DQPSK system (green) for zero dispersion, and in the presence of some chromatic dispersion, the performance of the DQPSK system (green) seems better than the QPSK system (blue line). Another significant highlight of the plot above shows that without optimised phase rotation of the local oscillator there is no penalty for no chromatic dispersion, a 2.3dB penalty in the presence of dispersions of 50ps/nm, and as much as a 7.5dB penalty in the presence of 200ps/nm chromatic dispersion. Thus, the graph above shows the magnitude of the impact of an efficient LO-PLL to the performance of high-speed QPSK systems.

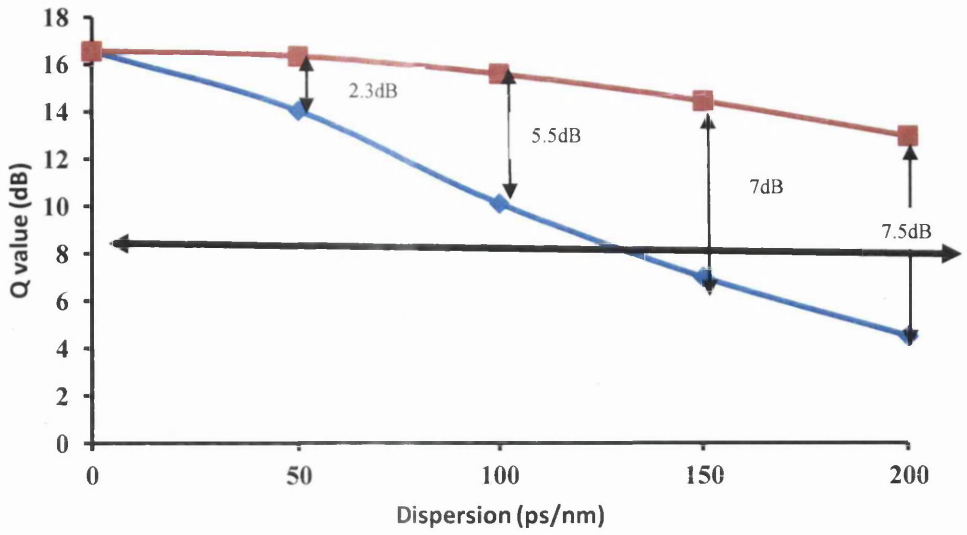

Figure 6.9: Q penalty in (dB) against chromatic dispersion (ps/nm) for 35GHz OBPF-42.7Gb/s 50%RZ-QPSK system, (red line represents the performance of the QPSK with optimized phase rotation of the LO and blue line represents QPSK performance with no phase rotation of the LO) for an OSNR of 17dB.

Figure 6.9 above further shows the performance improvement that is inherent with a perfect PLL for a coherent QPSK system, showing 2.3, 5.5, 7 and 7.5dB for 50, 100, 150 and 200ps/nm respectively, compared to performances in the presence of chromatic dispersions with deploying a PLL. Thus, as was shown in [7] without optimising the performance of the LO, it may seem quite easy to overestimate the performance of DSP in coherent detected systems when compensating for linear impairments. However, this is not to say that an efficient analogue system would outperform the digital systems (MLSE, MAP, etc.) both by optimising the performance of the LO the performance of the DSP could be further enhanced. The horizontal black line on the plot above shows an 8dB limit below which calculated Q values are not reliable.

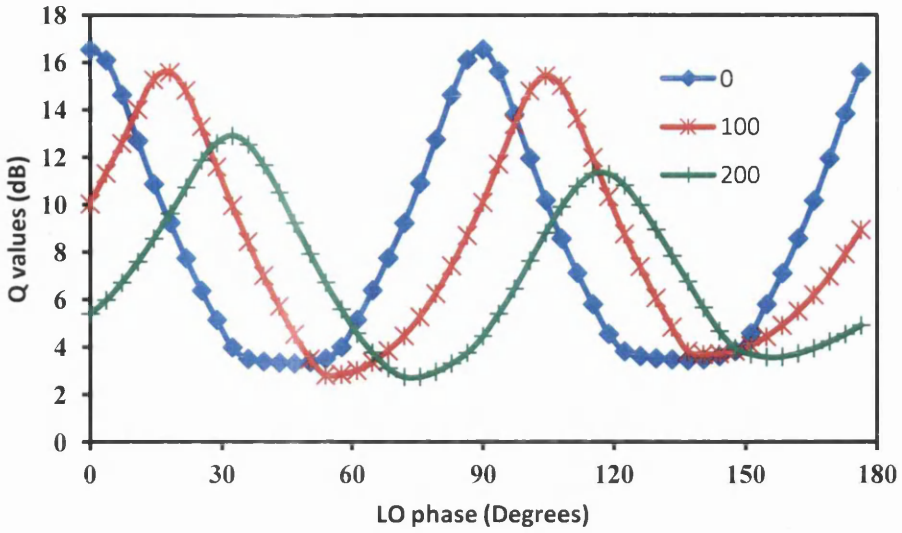

Figure 6.10: Q penalty in (dB) against LO`s phase rotation (Degrees) for 35GHz OBPF-42.7Gb/s 50%RZ-QPSKsystem, (blue line represents the performance of the QPSK with for 0 ps/nm, red line represents QPSK performance with 100 ps/nm, and green line represents QPSK performance with 200 ps/nm for an OSNR of 17dB.

Figure 6.10 above represents the performance of a 42.7Gb/s QPSK system under strong filtering (35GHz OBPF) for the LO`s phase rotation in the presence of some dispersion. Three different chromatic dispersion values are present so that the analysis of the QPSK performance could be better profiled, as opposed to having more chromatic dispersion points in the plots. As illustrated in the plots above it can be seen that for 0ps/nm dispersion, the performance of the rotation of the local oscillator is seen to be optimised at 0, 90 and 180 degrees.

The 90 degrees difference is occasioned by the presence of the two tributaries for each of the demodulations. Thus, two tributaries display the same periodicity, and the performance of the first tributary (in-phase) can be taken as zero phase, and the out of phase tributary at 90 degrees. But importantly, for a performance in the presence of chromatic dispersion of 100ps/nm, the phase of the LO has to be rotated by 18 and 108 degrees for both tributary and for 200ps/nm the phase of the LO has to be rotated by 36 and 126 degrees for the optimum performance. For negative dispersions -100 and -200ps/nm, the LO`s phase is rotated in the reverse direction but with same phase displacement (phase rotation is complementary of the positive phase rotation). The results here suggest that via coherent QPSK detection in tight-filtering regimes, the optimum performance for the amount of chromatic dispersion is directly proportional to the phase rotation of the LO`s signal.

6.7: Summary to Chapter 6

The performance of a coherent QPSK system has been examined at a data rate of 42.7Gb/s in a tight optical filtering regime (50GHz grid), and the results here show that coherent QPSK is very tolerant to optical filtering. The narrow optical filtering tolerance shown by the coherent QPSK signal surpasses all the investigated phase modulated formats, thus making it a very suitable cardidate for >100Gb/s data rate deployment via polarised multiplexing.

The tolerance of a 42.7Gb/s QPSK system to optical filter offsets or laser detuning was also investigated without the impact of DSP, and the results show that the although the QPSK is slightly more tolerant to laser detuning or OBPF frequency offset than an equivalent 42.7Gb/s DQPSK system, it is still more sensitive compared to a 42.7Gb/s DPSK/PSK.

The chromatic dispersion performance of a 42.7Gb/s QPSK system was investigated in this work without considering the impact of DSP, and the results shown here indicate that without a perfect phase-lock loop, the performance of a strongly-filtered QPSK system in the presence of some chromatic dispersion may seem to be less tolerant compared to an equivalent DQPSK system. But if perfect phase-tracking is deployed with the local oscillator, then the QPSK system clearly outperforms the DQPSK in the presence and absence of chromatic dispersion by more than 2dB in calculated Q values.

6.8: Chapter 6: References

[1] D.S. Ly-Gagnon, S. Tsukamoto, K. Katoh, and K. Kikuchi, "Coherent Detection of Optical Quadrature Phase-Shift Keying Signals With Carrier Phase Estimation," *IEEE J. Lightwave Technol*, vol. 24, no. 1, , pp. 12-21, Jan 2006.

[2] J. Renaudier, "Coherent-based systems for high capacity WDM transmissions" in "Proc" *OFC*, Feb 2008.

[3] D. Chang, F. Yu, Y. Huang, B. Mao, Y. Fang, L. Zeng and Q. Xiong "Analysis of OSNR margin improvement in beyond 100Gb/s PDM-DQPSK systems due to FEC (Proceedings Paper)" DOI: 10.1117/12.852189 SPIE 2009.

[4] M.G. Taylor "Coherent detection method using DSP for demodulation of signal and subsequent equalization of propagation impairments" *IEEE Photon. Technol. Lett* , pp; 674-676, 2004

[5] E. Torrengo, V. Ferrero, S. Camatel, "A 20-Gb/s Quadrature Phase-Shift-Keying Real-Time Coherent System Based on a Subcarrier Optical Phase-Locked Loop" *IEEE Photon. Technol. Lett.* vol. 21, no. 18 Sept 15 2009.

[6] S. Camatel, V. Ferrero, R. Gaudino and P. Poggiolini "Optical phase-locked loop for coherent detection optical receiver" *Electronics Letters* 18th March 2004 Vol. 40 No. 6.

[7] K. Ho and H.-Cheng "Effects of Chromatic Dispersion on Optical Coherent-Detection Systems" *IEEE Transaction on Communications*, vol. 56, no. 9, Sept 2008.

[8] B. Glance "Performance of homodyne detection of binary PSK optical signals" *J. Lightw Technol* vol.4, no. 2, Feb 1986.

[9] J. Renaudier, G. Charlet, M. Salsi, O.B. Pardo, H. Mardoyan, P. Tran, S. Bigo, " Linear Fiber Impairments Mitigation of 40-Gbit/s Polarization-Multiplexed QPSK by Digital Processing in a Coherent Receiver" of *J. Lightw. Technol,* vol 26, Issue:1, Jan.2008.,

[10] U. Koc, A. Leven, Y. Chen and N. Kaneda, "Digital Coherent Quadrature Phase-Shift-Keying (QPSK)" in "Proc" *OFC 2006*.

[11] H. Kim and P. J. Winzer, "Robustness to laser frequency offset in direct detection DPSK and DQPSK systems," *J. Lightw. Technol.*, vol. 21, no. 9, pp. 1887–1891, Sep. 2003.

[12] K. Ho, "The effect of interferometer phase error on direct-detection DPSK and DQPSK signals," *IEEE Photon. Technol. Lett.*, vol. 16, no. 1, pp. 308–310, Jan. 2004.

[13] L. G. Kazovsky, G. Kalogerakis, Shaw, W. T., "Homodyne Phase-Shift-Keying Systems: Past Challenges and Future Opportunities" *J. Lightw. Technol*: vol 24 , Issue: 12 , Page(s): 4876 – 4884, 2006.

[14] L. G. Kazovsky, "Performance analysis and laser linewidth requirements for optical PSK heterodyne communications systems," *J. Lightw. Technol.*, vol. LT-4, no. 2, pp. 415–425, Apr. 1986.

[15] K. Kikuchi et al., "Degradation of bit-error rate in coherent optical communications due to spectral spread of the transmitter and the local oscillator," *J. Lightw. Technol.*, vol. LT-2, no. 6, pp. 1024–1033, Dec. 1984.

[16] T. Okoshi and K. Kikuchi, Coherent Optical Fiber Communications. Boston, MA: Scientific Publishers/Tokyo/ Kluwer Academic Publishers, 1988.

[17] T. Schmidt et al. "Mitigating channel impairments in high capacity serial 40G and 100G DWDM transmission systems", *IEEE LEOS*, Summer Topical 2008.

[18] L. Zong, J. Veselka,. H. Sardesai,. And M. Frankel, M. "Influence of filter shape and bandwidth on 44 Gb/s DQPSK systems" in "Proc" *OFC 2009*, 22-26 March 2009 .

[19] E. A. Swanson, J. C. Livas, and R. S. Bondurant, "High Sensitivity Optically Preamplified Direct Detection DPSK Receiver with Active Delay-Line Stabilization" *IEEE Photon. Technol. Lett.*, Vol. 6, pp.263-265, Feb 1994.

[20] T. Tsuritani, A. Agata, I. Morita,. K. Tanaka, , and N. Edagawa, "Performance comparison between DSB and VSB signals in 20Gbit/s – based ultra-long-haul WDM systems." in "Proc" *OFC* 2001, OSA paper MM5, 2001.

[21] K. Tanaka, I Morita and N. Edagawa, "Study on optimum pre-filtering condition for 42.7Gbit/s CS-RZ DPSK signal" in "Proc" *OFC'2004*, 2004., vol 1, OFC 23-27 Feb. 2004.

[22] G. Bosco and P. Poggiolini, "An analysis of the impact of receiver imperfections on the performance of optical DQPSK systems," *Electron. Lett.*, vol. 40, no. 18, pp. 1147–1149, Sep. 2004.

[23] F. Vacondio, A. Ghazisaeidi, A. Bononi, and L.A Rusch, "DQPSK: When Is a Narrow Filter Receiver Good Enough?" *J. Lightw. Technol.* vol: 27, pp5106-5114,2009.

[24] G. Bosco and P. Poggiolini, "The impact of receiver imperfections on the performance of optical direct-detection DPSK," *J. Lightw. Technol*, vol. 23, no. 2, pp. 842–848, Feb. 2005.

[25] G. Bosco and P. Poggiolini, "On the Joint Effect of Receiver Impairments on Direct-Detection DQPSK Systems" *J. Lightw. Technol.* vol. 24, NO. 3, March 2006.

[26] M. Serbay, J. Leibrich, W. Rosenkranz, T. Wuth, and C. Schulien "Experimental Investigation of Asymmetrical filtered 43 Gb/s RZDQPSK" *IEEE/LEOS*, Annual meeting 2006, paper WH5.

[27] O. Olubodun and N.J. Doran "Performance Improvement of Asymmetrical Filtered 40GB/s RZ-DPSK Receiver Design -Strong Filtering Considerations" *IEEE/NOC2011*.

[28] O. Olubodun and N.J. Doran "Performance Impact of Offset Filtered 40Gb/s RZ-DPSK-Strong Filtering Considerations" *IEEE/ICBEIA* 2011.

[29] F. Herzog, K. Kudielka, D. Erni, and W. Bachtold, "Optical Phase Locking by Local Oscillator Phase Dithering" *IEEE J. Select. Topics Quantum Electron*, vol. 42, no. 10, Oct 2006.

[30] W. Glatt, M. A. Schreiblehner, C. Haider, and W. R. Leeb, "Optical PSK homodyne system using a switched residual carrier for phase synchronisation," *Electron. Lett.*, vol. 32, no. 15, pp. 1386–1387, Jul. 1996.

[31] C. Rapp, "Modulated residual carrier method with envelope processing: A novel phase synchronisation method for optical homodyne transmission," *J. Commun. Res. Lab.*, vol. 46, no. 3, pp. 321–325, Nov. 1999.

Chapter 7

Transmission and Experimentation

7.1 Offset Filtering Transmission of Strongly Filtered 40 Gb/s DPSK system and Research Conclusions

In this chapter the longhaul transmission of a strongly filtered 42.7Gb/s 50%RZ-DPSK system via offset filtering will be presented, as the main core of these investigations were based exclusively on a linear regime. Thus the transmission results could enhance an estimation of the impact of the various contributions of these research investigations on a longhaul optical transmission with other modulation formats (DQPSK, PSK and QPSK) in a 50GHz grid.

The remaining part of this chapter will be based on the conclusions for the research results that were presented in chapter 3 to chapter 6. It is important to draw a conclusive view on the different performances of offset filtering of phase modulated formats in a 50GHz grid, while projecting on the impact of the results presented in this investigations on practical systems and even higher data rate deployments (>100Gb/s).

7.2 Transmission of Strongly Filtered Asymmetrical 42.7Gb/s RZ-DPSK over 1000 km

The impact of offset filtering has been investigated extensively in these researches based on ASE noise limited regimes and dispersive regimes, with different phase modulated formats. However, despite the very encouraging (positive) results that have been achieved here [1, 2, 3, 4], it is important to understand that optical fiber transmission is not only impaired by linear limitations. The impact of fiber nonlinearity will become significant as the transmission distances increase and as data rates increase. The DPSK modulation format is popular due to its improved OSNR sensitivity and improved tolerance to fiber nonlinearity [5]. Also in [6,7] penalty reductions in the presence of ASE noise, dispersion and fiber nonlinearity were reported via pre-filtering of 42.7Gb/s CSRZ-IMDD/CSRZ-DPSK system via simulation and experimental investigations.

Herein the investigation of the impact of asymmetric filtering will be implemented with a strongly filtered 42.7Gbits/s 50%RZ-DPSK transmission over 1000km, with narrow filtering at the receiver with 35GHz OBPF via carrier wavelength displacement. The difference between this transmission investigations and the transmission result in [6] is that

the context in which the investigation of the paper was carried out was for ultra longhaul transmission (submarine installation) but our investigation is based on typical bandwidths available in a 50GHz grid and for long distances (longhaul). Also the bandwidth utilized in our investigation is a 35GHz OBPF as opposed to 45GHz OBPF which was deployed in [6]. In terms of spectral efficiency our effective bandwidth for the investigation is around 17 GHz to 20GHz offset of a 35GHz OBPF as opposed to 7.5 GHz offset of 45GHz OBPF. Thus the investigation here is similar to single sideband modulation (net bandwidth of 17 GHz bandpass) as compared to a slight vestigial sideband (net bandwidth of ~37.5 GHz) in the reported investigations [6, 7]. With an optimized frequency offset in the numerical model, an average of 2dB improvement performance was achieved over the conventional symmetric filtered system (0 offset of 35GHz OBPF) for a range of average power between -3 to 3 dBm.

7.2.1: Modeled 1000km Transmission system.

Figure 7.1 shows a 42.7 Gb/s 50% RZ-DPSK transmission setup. The transmitter employs a 2^7 PRBS used to drive a Mach-Zehnder modulator (MZM) to produce 42.7 Gb/s DPSK optical signal, which is followed by pulse carver MZM for the 50% RZ-DPSK duty cycle, with a 23.4ps delay for average transmission powers ranging from -3 dBm to 3 dBm. The transmitted signal is propagated through a system of 13 spans (82.5 km of SMF), 5 times over. The span consists of SMF having a dispersion of 16.5ps/nm, dispersion slope of 0.055 ps/nm^2/km, a loss coefficient of 0.25dB/km and an effective area of 80 μm^2. The dispersion compensating fiber (DCF) has a dispersion of -123 ps/nm, dispersion slope of -0.33 ps/nm^2/km, loss coefficient of 0.75 dB/km and effective area of 25 μm^2.

The DCF lengths for the pre-chirp and post-chirp were varied in each simulation run with an inline average dispersion of 0.43 ps/nm/km, an inline average dispersion of 0.95 was also deployed to compare the simulations here with [8] but the difference here was that lesser pre-compensation and inline compensation were deployed here. Whereas in [8] a pre-compensation of ~10 km of DCF was deployed as opposed to 1 km to 3 km DCF deployed here, also in [8] the inline dispersion compensation was close to 100% as opposed to the 43% compensation deployed here. The gain of the main amplifier is 15dB with a noise figure of 5.7dB and the number of points per bit is 64 for the single channel propagation.

At the receiver, the DPSK signal is received with a narrow optical bandpass filter (35GHz OBPF 3rd order Gaussian filter) with central frequency of the filter displaced from 0 to 30GHz offset away from the signal wavelength. Followed by a Mach-Zehnder

interferometer (MZI) with a 1 bit delay followed by a balanced receiver. The OSNR at the receiver is ~16dB. The electrical filter used was a 30GHz bandwidth 5th order Bessel electrical filter. The Q-values were calculated assuming Gaussian statistics.

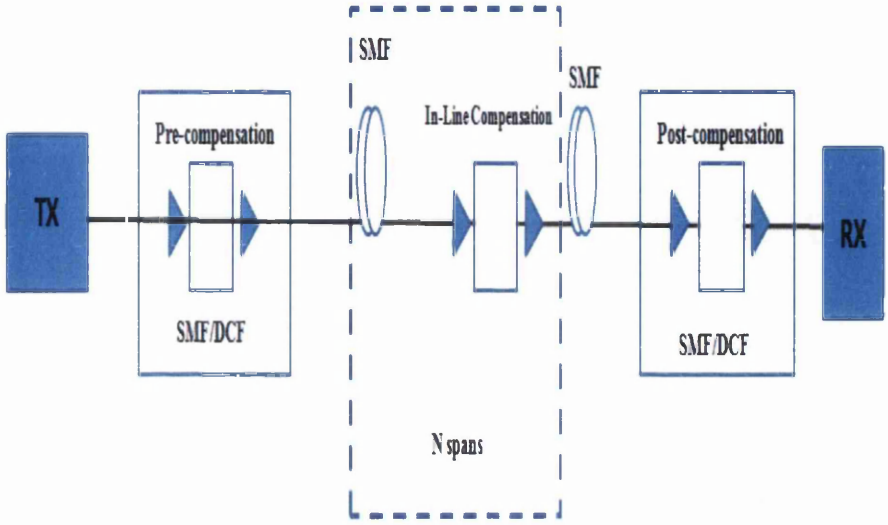

Fig. 7.1: Transmission Model for Long Haul 42.7Gb/s DPSK System

7.3: Transmission results of a 42.7Gb/s 50%RZ-DPSK system with offset filtering of 35GHz OBPF

The results in figure 7.2 below shows the Q-value in dB for 50%-RZ-DPSK signals filtered at the receiver with a 35GHz OBPF at the receiver for the transmission setup for both conventional and optimized offset filtered DPSK system. The Q values for the blue represents the symmetrical filtered case and the red line represents the optimized offset filtered case. The plot shows an improvement of ~2dB in the Q-values of the offset filtered 42.7Gb/s DPSK transmission system over conventional filtered case.

The performance improvement of the optimized offset filtered 1000km transmission ranges from around 2dB improvement for an average power of -3dBm to 0dBm and an improvement of ~3dB for an average transmit power of 4dBm over the symmetric filtered case. The performance of both the conventional and offset filtered transmission systems can further be evaluated in the figure 7.3, via the eye diagrams. Although there is an evident performance penalty due to the impact of narrowband filtering, figure 7.3a shows the eye diagram of the symmetric filtered 35GHz OBPF 42.7 Gb/s DPSK system for 0dBm transmit

power for a 1000km transmission and the figure 7.3b the eye diagram for 0dBm power for an optimised offset filtered system at ~20GHz offset of the 35GHz OBPF at the receiver.

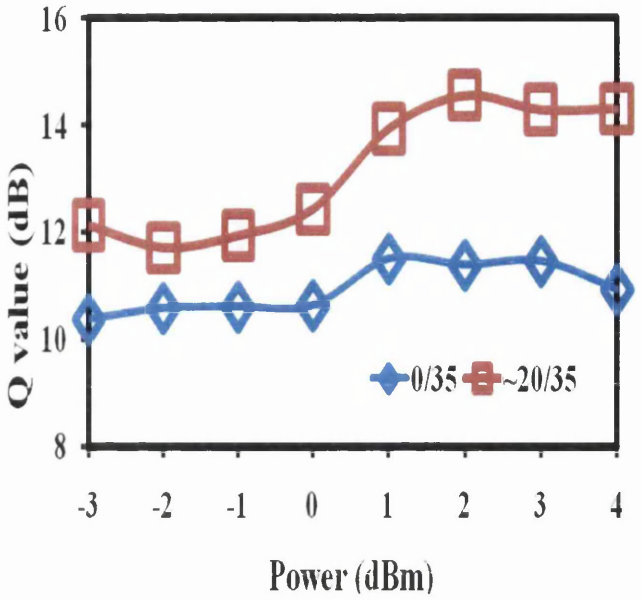

Fig 7.2: Q-value in dB vs. Power in dBm for 35GHz OBPF, 0/35 represents conventional filtered 42.7Gb/s DPSK transmission system and 20/35 represents optimized offset filtered 42.7Gb/s DPSK transmission system over 1000km.

The comparison of the two eye diagrams shows a better eye opening in width and length for the figure 7.4b eye diagram of offset filtered system as compared to the first eye diagram for the conventional filtered system. The difference in the opening of the two eye diagrams can be attributed to the high amplitude imbalance due to the symmetric filtering of a strongly filtered 42.7Gb/s DPSK system as opposed to the lesser amplitude imbalance due to the offset filtered system. Importantly vestigial sideband filtering has been identified to offer better performance over double sideband filtering in a strongly filtered regime [9] due to better ASE noise rejection of the narrowed spectrum of the VSB.

Offset filtering of any memory modulation format (i.e. intensity, phase and frequency modulation format) induces a memory modulation format which by its inherent attribute of using three optical symbols $\{0, \mp|E|\}$ in detecting two electrical symbols$\{0, |E|^2\}$. Thus the additional degree of freedom gained by extra phase modulation enhances a beneficial spectral shaping in the presence of a particular optical fiber impairment (both linear and nonlinear) [10]. Conventional filtering of a DPSK system results in a duobinary signal and alternate mark inversion signal at both the constructive and destructive port of the MZI [1, 10].

However offset filtering at the OBPF will result in VSB-DB and VSB-AMI at the constructive and destructive port of the MZI [1, 2, 3, 4]. The VSB-DB has an improved

tolerance to fiber nonlinearity and VSB-AMI has an improved tolerance to linear impairment relative to their initial DSB formats. Thus the signals at the two ports of the conventional filtered system are now more severed via the longhaul transmission, compared to the offset filtered system in which the spectrum at the ports are now like a VSB signalling i.e. leading to the alternate mark inversion signal been offset filtered to VSB-AMI now being located at the destructive port and the duobinary signal been offset filtered to SSB-DB.

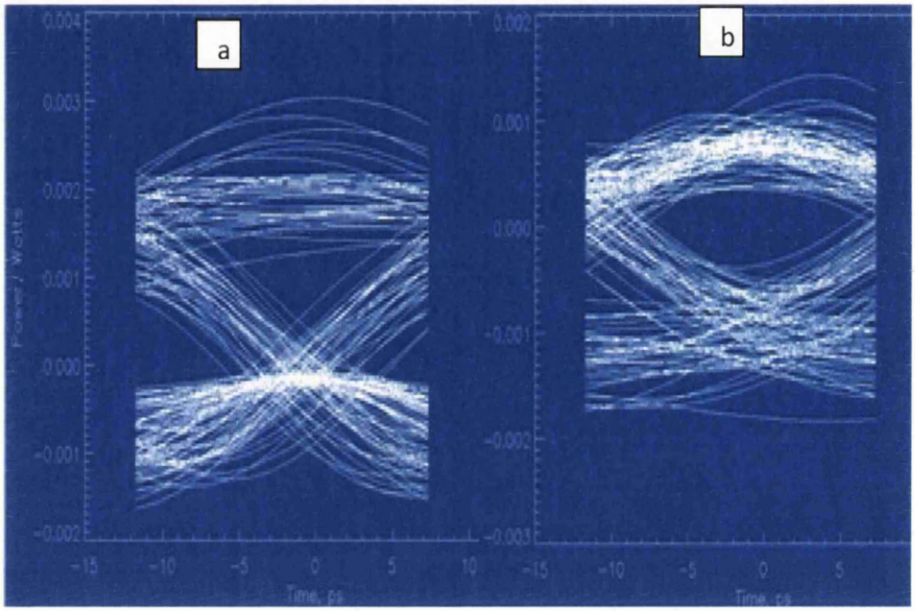

Figure 7.3: Power in (watts) vs. Time in (ps) , 7a~ Conventional filtered 35GHz system and 7b~optimized offset (~18GHz) filtered system.

7.4 Experimental Investigation on impact of offset filtering on the performance of strongly filtered 42.7Gb/s 67%RZ DPSK system.

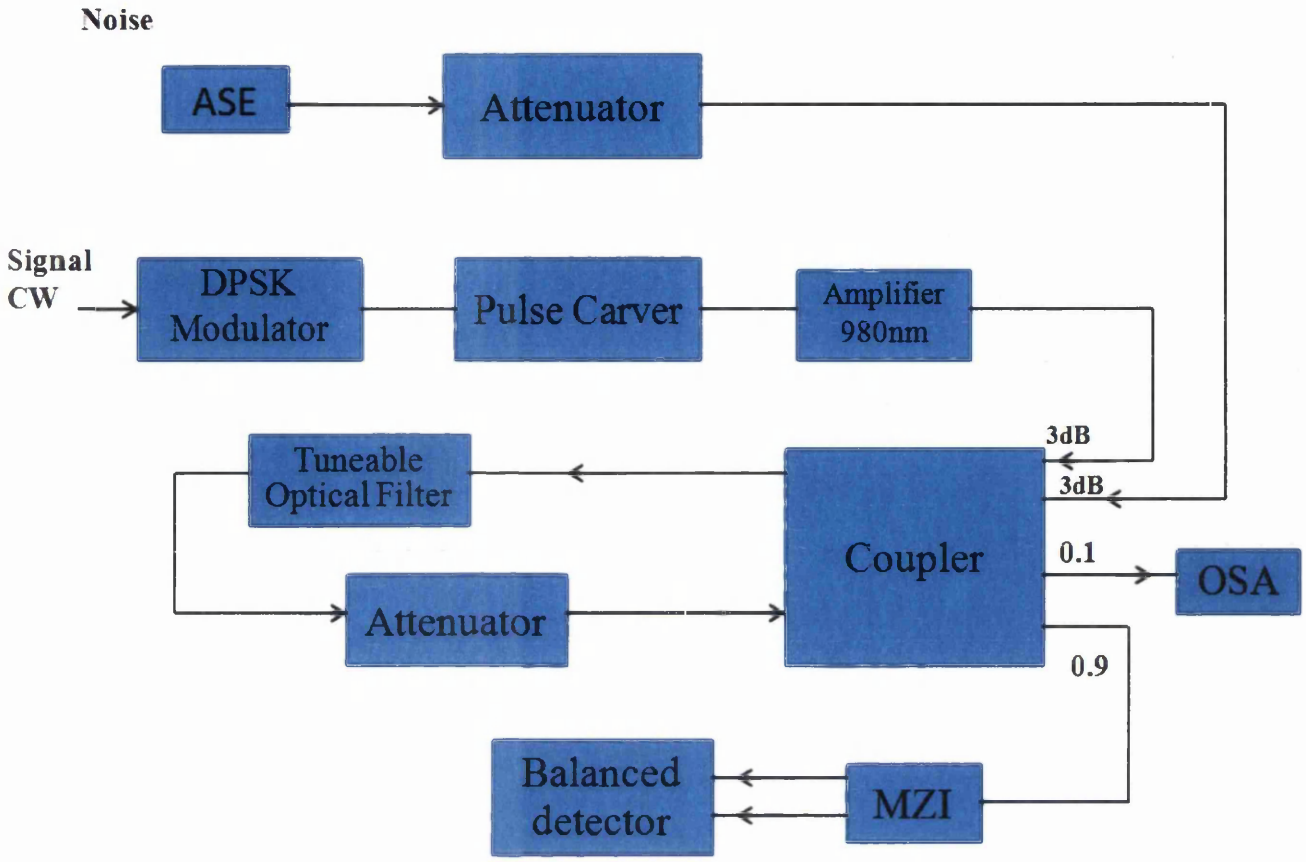

Figure 7.4. The system used to implement the experiment.

The system used to carry out the experiment is shown in Figure 6. This consists of a pattern generator which drives a Mach-Zehnder modulator with 2^{31-1} PRBS followed by a pulse carving MZM to generate a 67% RZ DPSK signal at 42.7 Gbit/s. Noise is then added to the optical signal and the resultant signal plus noise passes through a tuneable optical band pass filter.

The signal is then filtered, goes through the MZI and is finally received using a balanced detector. The system described above was investigated with several filter widths. In other to measure the impact of large offsets in a strongly filtered regime using strong filtering bandwidth, the OSNR was set to 20.8dB (in a 0.1nm bandwidth) and the signal power at the receiver was kept at -8dBm. Measurements were taken for two values of filter centre frequency offsets of 0 and 17GHz. The MZI delay was fixed at100% of a bit period. The impact of the symmetric filtering and the large asymmetric filtering can be seen in the plots in Figure 7.5. The figure 7.5 above shows a plot of power penalty in dB against optical filter bandwidths in nm. The 0 GHz (diamond-marker) and 17GHz offset were plotted for the

different filter widths. The choice of 17GHz offset is influenced by the results as shown in the simulation investigations. The plot shows a significant penalty reduction for the 17GHz offset as the filter bandwidths increases (i.e. approaches half filter bandwidth). Thus for a 0.28 nm (35GHz) in figure 7.5 there is a 0.45 dB penalty, which shows an excellent agreement with the simulated results of the 3rd order Gaussian filter in figure 7.6 (0.49 dB penalty for ~ half filter width).

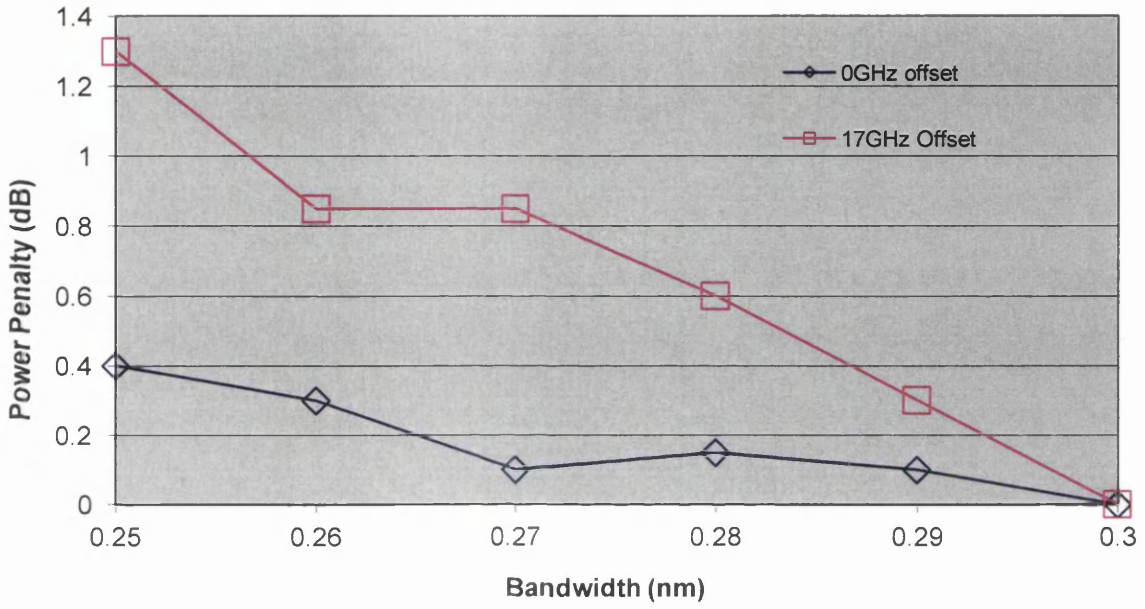

Figure 7.5 Q penalty (dB) against filter bandwidths (GHz) (diamond marker for 0 GHz offset and square marker for the 17GHz offset) for the experimental investigations.

Although the filter deployed in the experiment is a flat top filter shape with steep filter flanks as opposed to the Gaussian filter shapes deployed in the simulation investigations, a one to one comparison of both investigations is not possible. However, the penalty reductions for large filter offset in a strongly filtered regime as shown in figure 7.5 was confirmed.

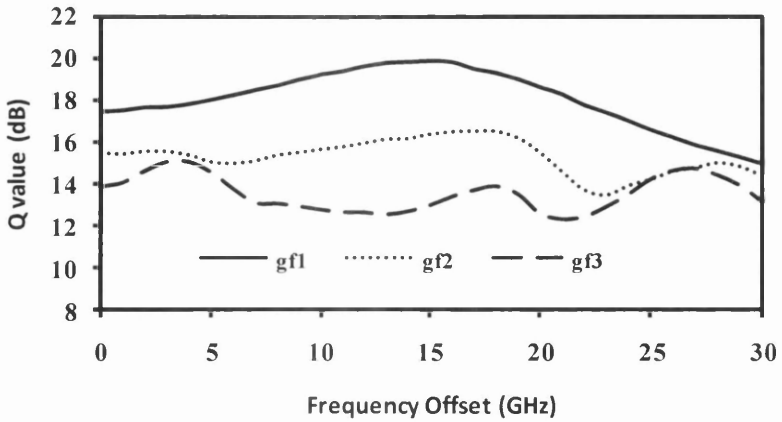

Figure 7.6. Q value as a function of different filter shapes for 1st, 2nd and 3rd order Gaussian filters for 35GHz OBPF 42.7Gb/s DPSK system.for an OSNR of 20dB.

Importantly the 17GHz filter offset performance penalty is also completely eliminated for a bandwidth of 0.3 nm (37.5 GHz). A better agreement can be anticipated between the simulated results here and experimental investigations where replica filter shapes [16] are deployed.

7.5: Chapter 7 -References:

[1] O. A Olubodun and N. J Doran., "Characterization of Asymmetric Filtered 40Gb/s RZ-DPSK System-Strong Filtering Considerations", *Optics Communication Journal,* July 2011.

[2] O.A Olubodun and N.J. Doran "Performance Improvement of Asymmetrical Filtered 40GB/s RZ-DPSK Receiver Design -Strong Filtering Considerations" *IEEE/NOC* July 2011.

[3] O.A Olubodun, M. Jamshidifar and N.J. Doran "Performance Impact of Offset Filtered 40Gb/s RZ-DPSK-Strong Filtering Considerations" *IEEE/ICBEIA* June 2011.

[4] O.A. Olubodun, D.S. Govan, N.J. Doran "Performance Recovery of 42.7 Gb/s DPSK System Due to Offset Filtering" *OFMC* Sept 2009.

[5] A. H. Gnauck et al., "2.5Tb/s (64x42.7Gb/s) Transmission over 40x100-km NZDSF using RZ-DPSK format and all-Raman –amplified spans", OFC 2002, Paper FC2, 2002.

[6] K. Tanaka, I Morita and N. Edagawa, "Study on optimum pre-filtering condition for 42.7Gbit/s CS-RZ DPSK signal" in "Proc" OFC 2001.

[7] A. Agata, I Morita, T. Tsuritani, and N. Edagawa, "Characteristic of Asymmetrically Filtered 40Gbit/s CS-RZ signals" in "Proc" *OFC* 2001.

[8] N. B. Pavlovic′, N.M.S. Costa, and A. V. T. Cartaxo, "Single-Sideband Differential Phase-Shift Keying Asynchronous Carrier-Suppressed Return-to-Zero – A Novel Signaling Format Optimized for Long-Haul UDWDM Systems" *J. Lightw. Technol*, vol. 27, no. 12, June 15, 2009.

[9] T. Tsuritani, A. Agata, I. Morita, K. Tanaka, , and N. Edagawa, "Performance comparison between DSB and VSB signals in 20Gbit/s – based ultra-long-haul WDM systems," in "Proc" *OFC* 2001, OSA paper MM5.

[10] P.J Winzer, P.J and R.J Essiambre. "Advanced modulation format for high-capacity optical transport network", *J. Lightwave Technol*,vol 24, pp. 4711–4728 2006.

[11] P.M.A. Charrua, and A.V.T Cartaxo, "Performance analysis of AMI-RZ single-sideband signals in 40 Gbit/s transmission systems" *IEE "Proc".-Optoelectronic.*, vol. 153, No. 3, June 2006.

[12] Y Cai, J. Cai, A. Pilipetskii, G. Mohs, and N. S. Bergano "Spectral efficiency limits of pre-filtered modulation formats" *Opt Express* , vol. 18, No. 19 / 20273/13 September 2010.

[13] M. Sjödin, P. Johannisson, M. Karlsson, Z. Tong, and P. A. Andrekson "OSNR Requirements for Self-Homodyne Coherent Systems" *IEEE Photonics Tech Lett*, vol. 22, no. 2, Jan 15, 2010.

[14] L.G. Kazovsky, G. Kalogerakis, W. T Shaw, "Homodyne Phase-Shift-Keying Systems: Past Challenges and Future Opportunities" *J. Lightw. Technol*, vol: 24 , Issue: 12 , Page(s): 4876 – 4884. 15, 2006.

[15] L.G. Kazovsky, R. Welter, A.F. Elrefaie, "Wide-linewidth phase diversity homodyne receivers" *J. Lightw. Technol* vol: 6,Issue:10 page(s): 1527-1536, Oct 1988 .

[16] S. Poole, S. Frisken, M. Roelens, C. Cameron "Bandwidth-flexible ROADMs as Network Elements" in "Proc" OSA/OFC/NFOEC 2011.

Chapter 8

Conclusions and Recommendations

8.1: Conclusions on the improved performance of 40Gb/s DPSK system in a 50GHz grid

The impact of offset filtering (asymmetric filtering) of a 42.7Gb/s DPSK system has been investigated in a strong optical filtering environment dominated by ASE noise (50GHz grid). The results show that the performance of the strongly filtered DPSK system can be improved by ~1dB at low OSNR (15dB) and by up to 1.5dB for an OSNR of 20dB by detuning the laser frequency and thus it shows that with higher OSNRs the performance improvement of offset filtering in a strongly filtered regime can be comparable to results achieved with PDPSK.

The different performance trends (peaks) of the balanced, constructive and destructive single ended detections in the presence of offset filtering of a strongly filtered DPSK, thus provides further potentials to improve the performance of the strongly filtered system, by optimizing the spectral shapes at the output ports of the MZI.

The performance improvements seen here are not filter shape dependent, i.e. ranging from 1st order Gaussian filter to 4th order Gaussian filters the performance improvements of the offset filtered DPSK system are evident irrespective of the shape of the filter in a strongly filtered regime.

The precise offset of 42.7Gb/s DPSK system required for improved performance in strongly filtered DPSK systems is filter bandwidth dependent. But in a WDM system the impact of offset filtering will lead to significant crosstalk penalties. However several optical strategies have been deployed to mitigate the impact of crosstalk in WDM systems [10].

The impact of offset filtering on a 42.7Gb/s DPSK system was also investigated in the presence of some chromatic dispersion. The results suggest that symmetrical filtering has better chromatic dispersion tolerance than the offset filtered systems. However in presence of 0 to 50ps/nm chromatic dispersion the performance of the optimized offset filtered DPSK system tends to have performance improvement over the symmetric filtered system. This could have implications as to the level of the chromatic dispersion compensations that would be deployed in a longhaul or ultra longhaul transmissions. A novel DPSK receiver design was conceptualized as a result of the very interesting performance of offset filtering of a strongly filtered DPSK system with balanced and the two single ended detections. Thus this novelty

resulted in > 2dB performance improvement in calculated Q over the conventional filtered model at low OSNRs.

The experimental results reported in [6] is a good indication as to the practicality of the performance improvement seen with offset filtering. There is still need for further intensive experimental confirmation of the improvement (penalty reductions) seen here with a 35GHz OBPF and neighboring OBPF with different duty cycles.

8.2. Recommendations for improved performance of 40Gb/s DPSK system in a 50GHz grid:

The performance improvement inherent with offset filtering in a strongly filtered regime is around 1 to 2 dB improvements over the conventional filtering performance, thus from the different performance peaks that were seen with the different detections (constructive and destructive), further optimization of the inherent signals at the outputs of the MZI could significantly improve the performance of 42.7Gb/s DPSK system in a 50GHz grid. This optimization strategy has been investigated and reported in this research. Further work will be needed to investigate its impact on different signal formats, optical bandwidths and filter shapes.

The impact of different filter shapes on offset filtering of a strongly filtered DPSK system were investigated, but Nyquist filtering was not considered in the investigations. Thus further performance improvement of the strongly filtered DPSK system might be inherent with Nyquist filtering (asymmetric Nyquist filtering).

The investigations here were implemented on a single channel system, the impact of crosstalk in a WDM or Hybrid system will degrade the system performance without additional innovative strategy to reduce the crosstalk. However in [8] SSB filtering was deployed at transmitter for 3 channel systems, and crosstalk penalty was significantly reduced. It will be essential to further investigate the impact of offset filtering in a strongly filtered WDM regime with a similar strategy as deployed in [8] and for hybrid systems. The impacts of the novel filtering design on residual chromatic dispersions performance of a DPSK system within a WDM environment could also be of high interest.

Experimental investigations will also be needed to reaffirm the performance improvements of asymmetric filtered 42.7Gb/s DPSK systems and the performance enhancements of the novel filtering design as seen here via numerical investigations. Thus offset filtering of DPSK signals in a 50GHz grid could provide a simple alternative to achieving 50Gb/s DPSK systems and/or 100Gb/s with polarization multiplexing.

8.3: Conclusions and recommendations for improved performance of 40Gb/s DQPSK system in a 50GHz grid

The impact of band limiting filtering, different filter shapes for a DQPSK system has been presented in this research and the results show that 40Gb/s DQPSK system is very tolerant to strong filter induced penalties. Thus compared to an equivalent DPSK system the impact of very narrow optical filters is as comparable to wide filters due to the symbol rate of the DQPSK systems. The chromatic dispersion performance of a 40Gb/s DQPSK system was investigated and the results showed a better tolerance compared to 40Gb/s DPSK system.

However the impact of offset filtering of 40Gb/s DQPSK system was also presented in chapter 4, the results showed a performance penalty as the filter central frequency is displaced away from the carrier frequency of the channel. The offset filtering or laser frequency detuning was identified as one of the major drawbacks of the 40Gb/s DQPSK system, in that the system can suffer a 3dB penalty for an offset of half the filter bandwidth for a typical 35GHz OBPF as compared to a performance improvement of an equivalent DPSK system.

Thus aside from the relative OSNR penalty of the DQPSK to a DPSK system, offset filtering of the OBPF or laser detuning could easily degrade the system performance despite the tolerance to DQPSK system to linear impairments and its improved spectral efficiency. Thus a novel offset filtering receiver design (same as the design in chapter 3) was deployed to investigate the impact of offset filtering on 42.7 Gb/s DQPSK. The result showed a marginal penalty reduction as compared to the conventional DQPSK model.

8.4: Recommendations for 40Gb/s DQPSK systems in a 50GHz grid

The impact of offset filtering on a 40Gb/s DQPSK system is not as interesting as the performance improvement seen with 40Gb/s DPSK system in a 50GHz grid. However a slightly modified novel receiver design showed some very significant performance penalty reductions which would need further comprehensive simulations and experimental work to confirm the results for several optical filter bandwidths. The performance of 40 Gb/s DQPSK system as shown in figure 4.3 thus shows with optimized Nyquist filtering that performance of a very narrow filtered 42.7Gb/s DQPSK system could suffer lesser than 1dB penalty with filter bandwidths lesser than symbol rate. Thus it could enhance 100Gb/s data rate at reduced symbol rates for a DQPSK systems through polarization multiplexing.

8.5: Conclusions and recommendations for improved performance of 40Gb/s Coherent PSK system in a 50GHz grid

Optical coherent 40Gb/s PSK systems have been investigated with different filter shapes and bandwidth, and the results show a performance improvement over the 40Gb/s DPSK system (~2dB improvement) for medium to wider filters. But in the presence of very strong filtering the performance of both systems are very similar. PDPSK and offset filtering have been shown to improve the performance of DPSK in strongly filtered regimes; consequently the impact of offset filtering has been investigated in this research to seek for better tolerance to strong filtering imposed penalties in a 50GHz grid.

The offset filtering impact on strongly filtered 40Gb/s PSK shows performance improvements over the symmetric filtered case. This is not surprising as offset filtering has been shown to improve the performance of different modulation formats ranging from OOK [7] to DPSK [1, 2, 3, 6] systems in a strongly filtered regime. The exciting results with offset filtering of a strongly filtered 42.7Gb/s PSK system i.e. with ~5dB improvement in calculated Q values over the symmetric filtered case for an OSNR of 16dB, is the main result for the performance of strongly filtered PSK systems. Thus offset filtering of a memory-less modulation format induces a memory modulation [12]. This process is not restricted to coherent PSK modulation format but as seen in [1, 2, 3, 6, 7] from different modulation formats that offset filtering leads to performance improvements over the conventional filtered modulation format, but this memory modulation is more enhanced via coherent detection PSK signals.

The impact of chromatic dispersion was also investigated in a strongly filtered (35GHz) 42.7Gb/s PSK systems and the results shows that contrary to the major investigated reports that the performance of an homodyne PSK offers better tolerance to chromatic dispersion compared to 42.7Gb/s DPSK systems. The result was presented with phase rotation of the local oscillator's signal and without phase rotation of the local oscillator's signal, thus the performance of system with phase rotation showed significant performance improvement over the case without phase rotation and most importantly the optimized performance of a strongly filtered PSK system is in the presence of some chromatic dispersion rather than what is obtainable in most modulation formats where the zero dispersion performance is always the best performance compared to the performance in the presence of chromatic dispersion.

This interesting results show the need for an efficient phase tracking in homodyne detection (which is quite difficult to implement in practical systems without transmission of the residual carrier) and that there is a mutual compensation of the filtering induced penalties

in the presence of some chromatic dispersions. This is accomplished by the phase rotation of the local oscillator's signal being synchronised with the PSK signal and in the process compressing the broadened pulse due to dispersion, thus eventually compensating for the filtering induced ISI.

Interestingly the performance impact of offset filtering on coherent PSK with balanced detection, constructive and destructive single-ended detection were further analysed in the presence of ASE noise and chromatic dispersion. The result thus shows that for offset filtering the three detections offer similar performances, but in the presence of chromatic dispersion the performance of balanced detection largely outperformed the two single-ended detections.

8.6: Recommendations for 40Gb/s Coherent PSK systems in a 50GHz grid

The performance improvement evident in a strongly filtered 42.7Gb/s PSK via offset filtering could enhance the performance of 50Gb/s DPSK in a strongly filtered regime despite the inherent limitations presented by the limited electrical bandwidths. Thus a numerical investigation will be needed to confirm the performance of a strongly filtered 50Gb/s PSK system in a 50GHz grid, with Nyquist filtering and via polarization multiplexed 100 Gb/s PSK system within a 50GHz grid.

Some experimental investigations will be essential to confirm the performance trend of the offset filtered 42.7Gb/s PSK system as presented in this research with numerical investigations. The improved performance of strongly filtered coherent PSK systems in the presence of chromatic dispersion as presented here via numerical investigations calls for experimental confirmations. Importantly WDM transmissions over longhauls will be required with numerical and experimental investigations to quantify the impact of offset filtering on WDM channel crosstalk and alternative techniques to minimize the crosstalk penalty will be required.

8.7: Conclusions and recommendations for improved performance of 40Gb/s Coherent QPSK system in a 50GHz grid

The performance of coherent QPSK system has been examined at a data-rate of 42.7Gb/s in a tight optical filtering regime (50GHz grid). The results, presented in chapter 6, show that coherent QPSK is more tolerant to optical filtering than DQPSK systems. The narrow optical filtering tolerance shown by the coherent QPSK signal makes it a very suitable candidate for >100Gb/s data rate deployment via polarized multiplexing. Although the

homodyne detection was deployed in this research investigation, the stringent requirement for hyrid phase lock loops (i.e. 90°) difference between the two demodulating local oscillator makes difficult to realise the fully improved performance benefit of the system.

The tolerance of a 42.7Gb/s QPSK system to optical filter offsets/laser detuning was also investigated without the impact of DSP and the results show that the although the QPSK is slightly more tolerant to laser detuning/ frequency offset than an equivalent 42.7Gb/s DQPSK system, it is still more sensitive compared to 42.7Gb/s DPSK/PSK where performance improvements were realised above the conventional filtered case.

The chromatic dispersion performance of a 42.7Gb/s QPSK system was investigated in this work without considering the impact of DSP, and the results here shows that without a perfect phase lock loop the performance of a strongly filtered QPSK system in the presence of some chromatic dispersion may seem to be less tolerant compared to an equivalent DQPSK system. But if a perfect phase tracking is deployed with the local oscillator, then the performance of the QPSK system clearly outperforms the DQPSK in the presence and absence of chromatic dispersion by more than 2dB in calculated Q values.

8.8: Recommendations for 40Gb/s Coherent QPSK systems in a 50GHz grid

Further simulation work will be required to investigate the limits of the homodyne detection of QPSK system relative to heterodyne detections within a strongly filtered regime. The impact of Nyquist filtering on Coherent QPSK in a strongly filtered regime seeks for numerical investigations relative to the performance of bandpass filtering most especially in relations to offset filtering.

Also phase diversity homodyne QPSK system would be investigated within the context of strongly filtered system. This is particularly attractive due to the fact that the phase diversity system does not require a phase lock loop compare to conventional homodyne system [14,15] and a smaller bandwidth relative to the heterodyne detection.

The phase-diversity homodyne system deploys a hybrid 120 degrees at the LO coupler relative to 90 degrees deployed for the conventional coherent QPSK, thus requiring a three branch balanced detection. Comprehensive experimental investigations are desirable within the context of longhaul transmission for 42.7Gb/s QPSK system or higher data rates within a very narrow filtering regime (25GHz grid). Also the performance impact of high multi-level signalling (6PSK, 8PSK, 12PSK etc) will also be investigated to seek for strategies that can enhance the inherent OSNR penalty.

8.9: Chapter 8 -References:

[1] O. A Olubodun and N. J Doran., "Characterization of Asymmetric Filtered 40Gb/s RZ-DPSK System-Strong Filtering Considerations", *Optics Communication Journal,* July 2011.

[2] O.A Olubodun and N.J. Doran "Performance Improvement of Asymmetrical Filtered 40GB/s RZ-DPSK Receiver Design -Strong Filtering Considerations" *IEEE/NOC* July 2011.

[3] O.A Olubodun, M. Jamshidifar and N.J. Doran "Performance Impact of Offset Filtered 40Gb/s RZ-DPSK-Strong Filtering Considerations" *IEEE/ICBEIA* June 2011.

[4] O.A. Olubodun, D.S. Govan, N.J. Doran "Performance Recovery of 42.7 Gb/s DPSK System Due to Offset Filtering" *OFMC* Sept 2009.

[5] A. H. Gnauck et al., "2.5Tb/s (64x42.7Gb/s) Transmission over 40x100-km NZDSF using RZ-DPSK format and all-Raman –amplified spans", OFC 2002, Paper FC2, 2002.

[6] K. Tanaka, I Morita and N. Edagawa, "Study on optimum pre-filtering condition for 42.7Gbit/s CS-RZ DPSK signal" in "Proc" OFC 2001.

[7] A. Agata, I Morita, T. Tsuritani, and N. Edagawa, "Characteristic of Asymmetrically Filtered 40Gbit/s CS-RZ signals" in "Proc" *OFC* 2001.

[8] N. B. Pavlovic′, N.M.S. Costa, and A. V. T. Cartaxo, "Single-Sideband Differential Phase-Shift Keying Asynchronous Carrier-Suppressed Return-to-Zero – A Novel Signaling Format Optimized for Long-Haul UDWDM Systems" *J. Lightw. Technol*, vol. 27, no. 12, June 15, 2009.

[9] T. Tsuritani, A. Agata, I. Morita, K. Tanaka, , and N. Edagawa, "Performance comparison between DSB and VSB signals in 20Gbit/s – based ultra-long-haul WDM systems," in "Proc" *OFC* 2001, OSA paper MM5.

[10] P.J Winzer, P.J and R.J Essiambre. "Advanced modulation format for high-capacity optical transport network", *J. Lightwave Technol*,vol 24, pp. 4711–4728 2006.

[11] P.M.A. Charrua, and A.V.T Cartaxo, "Performance analysis of AMI-RZ single-sideband signals in 40 Gbit/s transmission systems" *IEE "Proc".-Optoelectronic.*, vol. 153, No. 3, June 2006.

[12] Y Cai, J. Cai, A. Pilipetskii, G. Mohs, and N. S. Bergano "Spectral efficiency limits of pre-filtered modulation formats" *Opt Express* , vol. 18, No. 19 / 20273/13 September 2010.

[13] M. Sjödin, P. Johannisson, M. Karlsson, Z. Tong, and P. A. Andrekson "OSNR Requirements for Self-Homodyne Coherent Systems" *IEEE Photonics Tech Lett*, vol. 22, no. 2, Jan 15, 2010.

[14] L.G. Kazovsky, G. Kalogerakis, W. T Shaw, "Homodyne Phase-Shift-Keying Systems: Past Challenges and Future Opportunities" *J. Lightw. Technol*, vol: 24 , Issue: 12 , Page(s): 4876 – 4884. 15, 2006.

[15] L.G. Kazovsky, R. Welter, A.F. Elrefaie, "Wide-linewidth phase diversity homodyne receivers" *J. Lightw. Technol* vol: 6,Issue:10 page(s): 1527-1536, Oct 1988 .

[16] S. Poole, S. Frisken, M. Roelens, C. Cameron "Bandwidth-flexible ROADMs as Network Elements" in "Proc" OSA/OFC/NFOEC 2011.